

# miRNAs and their role in neural crest development

**Nicole J Ward**

Thesis submitted for the degree of Doctor of  
Philosophy

University of East Anglia  
School of Biological Sciences  
Norwich  
United Kingdom

July 2017

Word count: 59,157

© This copy of the thesis has been supplied on condition that anyone who consults it is understood to recognise that its copyright rests with the author and that use of any information derived there from must be in accordance with current UK Copyright Law. In addition, any quotation or extract must include full attribution

## **Abstract**

The neural crest (NC) is a multipotent, migratory cell population that is unique to vertebrate embryos and gives rise to many derivatives, such as the craniofacial skeleton, sensory neurons and pigment cells. A complex gene regulatory network underlies the process of NC formation, which involves the early induction of the neural plate border (NPB), specification of the NC, migration of the NC away from the neural tube along distinct pathways and differentiation into diverse cell types. microRNAs (miRNAs) are a class of non-coding regulatory genes, which act post-transcriptionally to regulate gene expression. They are of widespread significance and have been implicated in many biological processes. Many miRNAs have now been identified, however, as of yet, they have not been shown to have any direct roles in early NC development. Using various molecular techniques this study has placed specific miRNAs within the complex NC gene network. These miRNAs are miR-196a and miR-219. SRNA sequencing of induced *Xenopus* NC tissue generated a miRNA expression profile which in combination with whole mount *in situ* hybridisation (*WISH*) revealed multiple candidate miRNAs expressed in NC. Using knockdown (KD) experiments, the depletion of miR-196a and miR-219 resulted in aberrant NC development including abnormal craniofacial cartilage development. Using luciferase assays, this study shows for the first time that miR-219 directly targets the transcription factor *Eya1 in vitro*. This gene lies directly upstream of the NPB marker *Pax3*. When miR-219 is knocked down, *Pax3* expression is expanded across the surface ectoderm of the embryo suggesting the miR-219 serves to inhibit the *Pax3* domain. To begin to understand the molecular mechanisms behind both this phenotype and why the NC is lost, RNA sequencing on dissected NC tissue was employed. Results from this sequencing data demonstrated that following miR-219 KD the NPB and the placodes form whilst the NC is lost. This indicates that miR-219 is playing a role in ensuring the correct specification of NC. In comparison, following miR-196a KD the NPB development is impaired and derivatives are lost (placode and NC). This implies miR-196a has an earlier role in ensuring the correct induction of the NPB possibly through fine-tuning early inducing signals such as BMP and Notch. Using the data presented in this study, the first models of how specific miRNAs could function in NC development have been formulated.

# Content

## Table of Contents

Abstract .....	II
Content .....	III
Figure Index .....	IX
Table index.....	XII
Appendices Index.....	XIII
Abbreviations.....	XIV
Acknowledgements.....	XVIII
<b>Chapter 1: Introduction .....</b>	<b>1</b>
<b>1. Neural crest – a vital cell population for development .....</b>	<b>4</b>
<b>1.1. Induction and formation of the NPB .....</b>	<b>4</b>
1.1.1. Challenging the working model of neural crest cell induction.....	7
<b>1.2. Specification of the neural crest.....</b>	<b>8</b>
<b>1.3. Neural crest migration .....</b>	<b>12</b>
<b>1.4. Neural crest differentiation.....</b>	<b>15</b>
<b>2. miRNAs and their role in development.....</b>	<b>17</b>
<b>2.1. Biogenesis and mechanism of miRNAs .....</b>	<b>17</b>
<b>2.2. miRNAs in development .....</b>	<b>18</b>
<b>2.3. miRNAs regulate pluripotency and cell migration in many systems.....</b>	<b>20</b>
<b>2.4. The role of miRNAs in neural crest cell development .....</b>	<b>21</b>
<b>3. Rationale .....</b>	<b>22</b>
<b>Chapter 2: Materials and methods .....</b>	<b>24</b>
<b>4. Husbandry .....</b>	<b>24</b>
<b>4.1. Obtaining embryos .....</b>	<b>24</b>
4.1.1. Fixing embryos .....	25
<b>5. Whole mount <i>in situ</i> hybridisation (WISH) .....</b>	<b>25</b>
<b>5.1. mRNA probe synthesis.....</b>	<b>25</b>
5.1.1. Preparation of competent cells .....	25
5.1.2. Transformation .....	26
5.1.3. DNA mini prep.....	26
5.1.4. DNA midi prep.....	26
5.1.5. DNA and RNA quantification.....	26
5.1.6. Probe synthesis .....	26
5.1.7. Purification of probes .....	27

<b>5.2.</b>	<b>WISH.....</b>	<b>27</b>
5.2.1.	Double WISH: .....	28
5.2.2.	Cryosectioning of WISH embryos.....	29
<b>6.</b>	<b>Alcian blue staining .....</b>	<b>30</b>
<b>7.</b>	<b>Microinjection.....</b>	<b>30</b>
<b>8.</b>	<b>Animal cap assay for sRNA sequencing.....</b>	<b>31</b>
8.1.1.	Capped RNA synthesis .....	31
<b>8.2.</b>	<b>RNA extraction for sRNA sequencing .....</b>	<b>33</b>
8.2.1.	RNA Quantification .....	34
<b>8.3.</b>	<b>Semi-quantitative mRNA PCR to validate animal cap tissue induction.....</b>	<b>34</b>
8.3.1.	Reverse Transcription .....	34
<b>9.</b>	<b>sRNA library construction for Next Generation Sequencing.....</b>	<b>34</b>
9.1.1.	HD adapter synthesis .....	34
<b>9.2.</b>	<b>Illumina sRNA preparation.....</b>	<b>38</b>
9.2.1.	3' adapter ligation .....	38
9.2.2.	RNA clean up.....	38
9.2.3.	Deadenylation and removal of 3' adapters.....	38
9.2.4.	5' HD adapter ligation .....	39
9.2.5.	Di-Tagged RNA purification.....	40
9.2.6.	Reverse transcription.....	40
9.2.7.	Polymerase chain reaction.....	41
9.2.8.	8% PAGE Gel and library band recovery .....	42
<b>10.</b>	<b>Bioinformatic analysis .....</b>	<b>42</b>
10.1.1.	Raw sequence mapping and filtering.....	42
10.1.2.	Profiling of mapped reads to miRBase.....	43
10.1.3.	Differential Expression Analysis .....	43
10.1.4.	Novel miRNA predictions .....	43
<b>11.</b>	<b>Validation of sRNA sequencing.....</b>	<b>44</b>
11.1.1.	Quantitative miRNA qRT-PCR .....	44
<b>12.</b>	<b>Experimental evaluation of putative miRNA targets.....</b>	<b>44</b>
<b>12.1.</b>	<b>Generation of miRNA sensing luciferase construct .....</b>	<b>44</b>
<b>12.2.</b>	<b>Generating a mutant pGL3-EYA1 construct .....</b>	<b>44</b>
12.2.1.	Mutagenesis PCR of pGL3-EYA1 construct.....	44
<b>12.3.</b>	<b>Luciferase assays of PGL3-EYA1 construct .....</b>	<b>47</b>
12.3.1.	Cell culture .....	47
12.3.2.	Cell transfection .....	47
12.3.3.	Luciferase assay .....	48
12.3.4.	Normalisation of luciferase assay data .....	48
<b>13.</b>	<b>Microsurgical removal of cranial neural crest tissue for RNA sequencing.....</b>	<b>49</b>

13.1.1.	Total RNA purification for RNA seq.....	49
13.1.2.	Bioanalyser.....	50
13.1.3.	Reverse transcription.....	50
13.1.4.	PCR Amplification.....	51
13.1.5.	RNA sequencing.....	51

### **Chapter 3: Identification of miRNAs in neural crest cells..... 53**

#### **The XenmiR database; a candidate approach ..... 53**

#### **13.2. Introduction.....53**

13.2.1.	The XenmiR database .....	53
13.2.2.	Expression analysis using WISH .....	54

#### **13.3. Results.....54**

13.3.1.	Expression profiling of 180 miRNAs reveals diverse expression patterns throughout various developing organs and tissues .....	54
13.3.2.	LNA WISH on potential neural crest miRNAs.....	55
13.3.3.	Co-expression analysis of candidate miRNAs with the NC marker <i>Sox10</i> .....	58
13.3.3.1.	miR-196a and miR-302 expression overlaps with the NC marker <i>Sox10</i> .....	58
13.3.3.2.	Sectioned double WISH clearly demonstrate the overlap between miR-196a and miR-302 with the NC marker <i>Sox10</i> .....	58

#### **Next generation sequencing of sRNAs in induced neural crest and neural tissue ..... 61**

#### **13.4. Introduction.....61**

13.4.1.	Techniques for assessing miRNA expression .....	61
13.4.2.	NGS library preparation and sequencing.....	62
13.4.3.	Are miRNAs the key regulators in the maintenance of NC pluripotency? .....	64

#### **13.5. Results:.....65**

13.5.1.	Induction of both NC and neural animal cap tissue.....	65
13.5.1.1.	Collection of tissue types using the <i>Xenopus</i> animal cap assay .....	65
13.5.1.2.	PCR expression profile of neural and NC markers.....	65
13.5.1.3.	WISH of induced animal cap tissue .....	66
13.5.1.4.	Quality control of sRNA sequencing.....	66
13.5.2.	SRNA libraries gave two closely sized bands and minimal adapter-adapter binding.....	66
13.5.3.	Libraries were enriched for both 23 nt and 29 nt sequences .....	69
13.5.4.	Blastula peak shift is not caused by piRNAs.....	72
13.5.5.	miRNA annotation across the four samples .....	73
13.5.5.1.	Annotated miRNAs.....	73
13.5.5.2.	Novel miRNAs.....	73
13.5.6.	Global miRNA populations within each tissue type are dominated by miR-427 .....	73
13.5.7.	miRNA expression profile over the samples .....	74
13.5.8.	Several miRNA hairpins are differentially expressed between neural tissue and NC tissue	76

13.5.9.	miR-338 and miR-301a are expressed in both neural crest and blastula samples ...	79
13.5.10.	Validation via qRT-PCR.....	79
<b>13.6.</b>	<b>Discussion.....</b>	<b>82</b>
13.6.1.	miR-196a and miR-302 are co-expressed with <i>Sox10</i> in the developing NCC .....	82
13.6.2.	Libraries were enriched for both 23 nt and 29 nt sequences .....	86
13.6.3.	Global miRNA populations within each tissue type are dominated by miR-427 .....	87
13.6.4.	miRNA expression profile over the samples .....	88
13.6.5.	Several miRNA hairpins are differentially expressed between the neural and NC samples	90
13.6.6.	miR-338 and miR-301a are expressed in both NC and blastula samples.....	91
<b>Chapter 4: Functional analysis of candidate miRNAs.....</b>		<b>94</b>
<b>13.7.</b>	<b>Introduction.....</b>	<b>94</b>
<b>13.8.</b>	<b>miRNA knockdown .....</b>	<b>94</b>
<b>13.9.</b>	<b>Results.....</b>	<b>95</b>
13.9.1.	Preliminary MO injections .....	95
	qRT-PCR validation of MO knock down .....	98
13.9.2.	MiR-302 KD results in defective neural development .....	98
13.9.2.1.	miR-302 KD results in an abnormal eye development.....	99
13.9.2.2.	<i>Sox2</i> is miss-expressed in miR-302KD embryos .....	99
13.9.3.	Full characterisation of miR-219 and miR-196a knock down .....	101
13.9.3.1.	Effect of miRNA KD on craniofacial cartilage development .....	101
13.9.3.2.	Analysis of key NC and NPB genes effected by miRNA knockdowns using WISH	103
	miR-196a .....	103
<b>13.10.</b>	<b>Discussion .....</b>	<b>109</b>
13.10.1.	MiR-302 KD impairs development of neural tissue .....	109
13.10.2.	miR-196a and miR-219 KD result in an inhibition of NC development .....	110
13.10.2.1.	miR-196a .....	110
13.10.2.2.	miR-219 .....	112
<b>Chapter 5: Downstream target analysis of miR-196a and miR-219.....</b>		<b>114</b>
<b>Approach one – Computational miRNA target prediction .....</b>		<b>114</b>
<b>13.11.</b>	<b>Introduction .....</b>	<b>114</b>
13.11.1.	miRNA-mRNA interactions.....	114
13.11.2.	Computational miRNA target prediction .....	117
13.11.2.1.	miRanda.....	117
13.11.2.2.	TargetScan.....	117
<b>13.12.</b>	<b>Results and discussion .....</b>	<b>118</b>
13.12.1.	Predicted targets for miR-196a include various HOX genes .....	119

13.12.2.	Predicted targets for miR-219 include the co-factor Eya1 .....	120
13.12.3.	Validation of Eya1 as a target of miR-219 using luciferase assays .....	121
13.12.3.1.	miR-219 targets Eya1 3'UTR .....	124
<b>Approach two: Transcriptomic analysis of neural crest tissue following knockdown of miR-219 and miR196a.....</b>		<b>126</b>
<b>13.13.</b>	<b>Introduction .....</b>	<b>126</b>
13.13.1.	Experimental pipeline .....	126
<b>13.14.</b>	<b>Results and discussion .....</b>	<b>127</b>
13.14.1.	Validation of knockdowns using qRT-PCR .....	127
13.14.2.	RNA sequencing results .....	129
13.14.2.1.	Quality control of RNA sequencing .....	129
13.14.2.2.	miR-219 stage 14 .....	134
	GO Analysis of miR-219KD transcriptome .....	134
13.14.2.3.	NC is lost following miR-219 KD .....	136
13.14.2.4.	Pax3 expansion in the superficial ectoderm does not induce expression of its downstream hatching gland specific target Xhe2 .....	137
13.14.2.5.	Multiple genes involved in neural pluripotency were upregulated following miR-219 KD	137
13.14.2.6.	Notch signalling is increased further promoting neural pluripotency.....	139
13.14.2.7.	BMP antagonists are upregulated indicating that BMP signalling is decreased	140
13.14.2.8.	miR-196a .....	144
13.14.2.9.	miR-196a KD results in impaired induction of the NPB and a loss of NC specification	144
13.14.2.10.	Induction of all NPB derivatives are lost.....	148
13.14.2.11.	Cell fate has been changed to neural and this appears to be mediated by an upregulation of the zinc finger protein zic1 .....	149
13.14.2.12.	BMP signalling is attenuated following miR-196a KD which potentially regulates Zic1 induction .....	149
13.14.2.13.	Notch signalling is increased following miR-196a KD possibly promoting neural pluripotency	150
13.14.2.14.	The cell population following miR-196a KD is characterised by high levels of neural 'stemness factors' .....	151
<b>Chapter 6: General discussion and concluding remarks.....</b>		<b>156</b>
<b>13.15.</b>	<b>Study aims.....</b>	<b>156</b>
<b>13.16.</b>	<b>Candidate miRNAs for NC development .....</b>	<b>156</b>
13.16.1.	Multiple miRNAs are expressed in the developing NC .....	156
<b>13.17.</b>	<b>miR-219 and miR-196a KD result in aberrant NC development .....</b>	<b>157</b>
13.17.1.	miR-219 and its role in NC development .....	157

13.17.1.1.	miR-219 KD causes an expansion of Pax3 in the surface ectoderm .....	157
13.17.1.2.	miR-219 directly targets Eya1, a placodal gene directly upstream of Pax3 .....	157
13.17.1.3.	RNA sequencing of miR-219 KD tissue reveals multiple potential models for its role in NC development .....	158
13.17.2.	miR-196a and its role in NC development .....	159
13.17.2.1.	WISH on miR-196a KD embryos revealed a loss of NC specifiers and a gain of neural markers .....	159
13.17.2.2.	KD of miR-196a results in impeded NPB development, a loss of NPB derivatives and an expansion of NP tissue .....	159
13.17.2.3.	miR-196a usually maintains a gradient of BMP signalling ensuring correct patterning of the neuroectoderm .....	160
13.17.2.4.	Absence of miR-196a alters balances of pluripotency and differentiation (via Notch)	160
13.17.3.	miR-301 and miR-338 are candidates for the maintenance of NC pluripotency ....	161
<b>13.18.</b>	<b>Future work.....</b>	<b>164</b>
13.18.1.	WISH .....	164
13.18.1.1.	miR-219 expression .....	164
13.18.1.2.	RNA sequencing validation.....	164
13.18.1.3.	Changes in expression of Eya1 and Xhe2 .....	164
13.18.2.	Can Eya1 KD rescue the expanded Pax3 phenotype?.....	165
13.18.3.	Validating additional NC candidates .....	165
13.18.3.1.	NC specific miRNAs identified from sRNA sequencing .....	165
13.18.3.2.	miR-301 and miR-338 and their role in pluripotency .....	165
13.18.4.	Validation of direct targets of miR-219 and miR-196a .....	165
13.18.5.	Measuring changes in BMP activity following miR-219 and miR-196a KD .....	166
<b>13.19.</b>	<b>Applying these results to regenerative medicine – ‘the bigger picture’ .....</b>	<b>166</b>
<b>Chapter 7: References .....</b>	<b>168</b>	
<b>Appendices .....</b>	<b>XVIII</b>	
<b>Publications .....</b>	<b>XXIX</b>	

## Figure Index

Figure 1: Key stages in NC development.....	3
Figure 2: The gene regulatory network underlying the formation of the various stages of neural crest and the preplacodal region .....	12
Figure 3: miRNA biogenesis and mechanism of action .....	19
Figure 4: A schematic drawing of an animal cap assay. ....	33
Figure 5: HD adapter synthesis .....	37
Figure 6: Luciferase assay protocol used to assess EYA1 as a target of miR-219 .....	46
Figure 7: <i>Xenopus</i> miRNA expression in a diverse number of developing organs and cell types.....	56
Figure 8: LNA WISHs on neurula staged embryos show expression in the neural plate and neural plate border for all candidate miRNAs .....	57
Figure 9: MiR-302 and miR-196a have clear a overlap in expression with the NC marker <i>Sox10</i> .....	59
Figure 10: GNW8, miR-30a-3p, miR-429 and miR-17-5p all show partial overlap in expression with the NC marker <i>Sox10</i> .....	60
Figure 11: Models of NC development .....	64
Figure 12: Neural Crest and neural tissue was sufficiently induced using the animal cap technique .....	67
Figure 13: sRNA libraries gave two closey sized bands and minimal adapter-adapter binding.....	68
Figure 14: Size distribution and clustering of sequenced small-RNA enriched total RNA.....	71
Figure 15: MiR-427 dominates the miRNA reads in all tissue types. ....	75
Figure 16: miRNA expression profiles and heatmap analysis of miRNAs in early <i>Xenopus</i> development. ....	77
Figure 17: Several miRNAs are upregulated in neural crest when compared to neural tissue. ....	78
Figure 18: MiR-338 and miR-301a are expressed in both neural crest and blastula samples. ....	80
Figure 19: Neural crest miRNAs identified by small RNA sequencing were validated using qRT-PCR.....	81
Figure 20: Schematic representation of the structure of the four mammalian HOX gene clusters with the location of the hosted miRNAs. ....	83
Figure 21: Preliminary MO screens show miR-219, miR-196a and miR-302 KDs to	

give a NC phenotype.....	97
Figure 22: qRT-PCR confirms that MOs targetting miR-302, miR-219 and miR-196a cause dose dependent knockdown.....	98
Figure 23: miR-302 KD results in a neural phenotype charactised by an abnormal eye. ....	100
Figure 24: miR-196a and miR-219 KD results in abnormal craniofacial cartilage development. ....	102
Figure 25: MiR-196a kd alters expression of neural crest and neural plate border markers. ....	104
Figure 26: The effect of miR-196a knock down on various markers.....	107
Figure 27: The effect of miR-219 knock down on both neural plate border and neural crest markers.....	108
Figure 28: A schematic representation of various miRNA interactions .....	116
Figure 29: Multiple HOX genes are predicted to be targeted by miR-196a.....	122
Figure 30: Multiple members of the PSED network are predicted to be targeted by miR-219. ....	123
Figure 31: Schematic drawing of the various regions induced during early neural plate development.....	124
Figure 32: EYA1 is a target of miR-219 <i>in vitro</i> . ....	125
Figure 33: Schematic drawing of the steps taken for the RNA sequencing of dissected neural crest (NC) tissue. ....	128
Figure 34: Expression profile of various genes in dissected samples sent for sequencing following KD of miR-196a or miR-219.....	131
Figure 35: PCA plot showing clustering of replicates between MO injected embryos and MM control.....	132
Figure 36: Sample distance heat map showing clustering of replicates between MO injected embryos and MM control.....	133
Figure 37: Gene changes following miR-219 KD.....	135
Figure 38: The top 50 downregulated and upregulated genes following miR-219 KD. ....	142
Figure 39: Model of the potential molecular mechanisms miR-219 uses to prevent neural induction and control neural pluripotency during <i>Xenopus</i> neuroectoderm patterning.....	143
Figure 40: Gene changes following miR-196a KD.....	145
Figure 41: Heat map of gene changes following miR-196a (stage 14) .....	146
Figure 42: Heat map of gene changes following miR-196a (stage 17) KD.....	147
Figure 43: The top 50 downregulated and upregulated genes following miR-196a (stage 14) KD. ....	153

<b>Figure 44: The top 50 downregulated and upregulated genes following miR-196a (stage 17) KD. ....</b>	<b>154</b>
<b>Figure 45: Model of the potential molecular mechanisms miR-196a uses to prevent neural induction and control neural pluripotency during <i>Xenopus</i> neuroectoderm patterning.....</b>	<b>155</b>
<b>Figure 46 A summary of the changes in gene expression following miR-219 KD. ....</b>	<b>162</b>
<b>Figure 47 A summary of the changes in gene expression following miR-196a KD. ....</b>	<b>163</b>

## **Table index**

<b>Table 1: Probe Synthesis.....</b>	<b>27</b>
<b>Table 2: Morpholino sequences.....</b>	<b>31</b>
<b>Table 3: Plasmids used for capped RNA synthesis .....</b>	<b>32</b>
<b>Table 4: Master mix for adapter adenylation .....</b>	<b>35</b>
<b>Table 5: Materials required for 16% (w/v) PAGE urea gel synthesis .....</b>	<b>36</b>
<b>Table 6: Master mix for 3' adapter ligation .....</b>	<b>38</b>
<b>Table 7: Master mix for deadenylation of adapter.....</b>	<b>39</b>
<b>Table 8: Master mix for degradation of adapter of adapter .....</b>	<b>39</b>
<b>Table 9: Master mix for 5' adapter ligation .....</b>	<b>40</b>
<b>Table 10: Master mix for reverse transcription .....</b>	<b>41</b>
<b>Table 11: Master mix for PCR amplification .....</b>	<b>41</b>
<b>Table 12: Materials required for 8% PAGE gel synthesis.....</b>	<b>42</b>
<b>Table 13: Master mix for phusion PCR.....</b>	<b>45</b>
<b>Table 14: Master mix for PCR amplification .....</b>	<b>51</b>
<b>Table 15: Samples collected for RNA sequencing (green boxes). All samples had three replicates except 219MO (stage 14) which had four. 219MO (stage 17) was not sequenced. ....</b>	<b>52</b>
<b>Table 16: A summary of the number of reads obtained from each library and the percentage of these reads that aligned to the genome. ....</b>	<b>70</b>
<b>Table 17: piRNA clustering and transcriptome analysis of sequenced animal cap tissue .....</b>	<b>72</b>
<b>Table 18: Changes in the expression of various HOX genes following miR-196a KD .....</b>	<b>151</b>

## **Appendices Index**

Appendix 1: plasmids used to make RNA probes .....	XVIII
Appendix 2: miRNA primers used for smallRNA sequencing validation.....	XIX
Appendix 3: mRNA primers used for qRT-PCR prior to RNA sequencing .....	XIX
Appendix 4: Number of reads and percentage of mapped reads following RNA sequencing.....	XX
Appendix 5: Structure of novel miRNA hairpins.: .....	XX
Appendix 6: miR-429 KD embryos do not respond during the ‘poke and stroke’ assay. ....	XX
Appendix 7: Top predicted targets of miR-219 using miR-system.....	XXI
Appendix 8: Top predicted targets of miR-196a using miR-system.....	XXII
Appendix 9: Expression profile of various genes detected by qRT-PCR in dissected samples following KD of miR-219. ....	XXIII
Appendix 10: Expression profile of various genes detected by qRT-PCR in dissected samples following KD of miR-196a. ....	XXIV
Appendix 11: PCA plot showing clustering of replicates between MO injected embryos and MM control.....	XXV
Appendix 12: Sample distance heat map showing clustering of replicates between MM control and control.....	XXVI
Appendix 13: An MA-plot of gene changes between MM control and non-injected controls. ....	XXVII
Appendix 14: Differential expression analysis results following RNA sequencing of MO vs MM samples .....	XXVIII

# Abbreviations

**AGO** - Argonaute

**BCIP** – 5-Bromo4-chloro-3indolyl phosphate

**bHLH** – Basic helix-loop-helix

**BLAST** – Basic Local Alignment Search Tool

**BMP** – Bone morphogenic protein

**Bp** – Basepair

**BSA** – Bovine serum albumin

**CaCl<sub>2</sub>** – Calcium chloride

**cDNA** – Complementary DNA

**cRNA** – capped RNA

**CHAPS** – 3-((3-cholamidopropyl) dimethylammonio)-1propanesulfonate

**Chorulon** – Human chorionic gonadotrophin

**CLASH** - Cross-linking, ligation, and sequencing of hybrids

**DACH** - Dachshund-related homeobox

**DEPC** – Diethylpyrocarbonate

**DIG** – Digoxigenin

**DMEM** – Dulbecco's modified eagle medium

**DNA** – Deoxyribonucleic acid

**dNTP** – Deoxynucleotide

**DTT** – Dithiothreitol

**ECM** – Extracellular matrix

**EDTA** – Ethylenediaminetetraacetic acid

**EMT** – Epithelial to Mesenchymal transition

**EtOH** – ethonal

**EYA** – Eyes absent-related homeobox

**FGF** - Fibroblast growth factor

**Fig** – Figure

**FITC** – Fluorescein isothiocyanate

**GFP** – Green fluorescent protein

**GO** – Gene ontology

**H** – Hour

**H<sub>2</sub>O** – Water

**Irx** – Iriquois

**ISH** - *in situ* hybridisation

**KD** – Knock down

**LNA** – Locked nucleic acid

**MAB** – Maleic acid buffer

**MgCL** – Magnesium chloride hexahydrate

**Min** - Minutes

**MiR** – MicroRNA

**miRNA** – MicroRNA

**MM** – mismatch

**MMR** – Marc's modified ringer's

**MnCl<sub>2</sub>** – Manganese chloride

**MO** – Morpholino

**MOPS** – 3-(N-morpholino) propane sulfuric acid

**mRNA** – Messenger RNA

**NaCl** – sodium chloride

**NaOH** – sodium hydroxide

**NBT** – nitroblue tetrazolium

**NC** – Neural crest

**NGS** – Next generation sequencing

**NP** – Neural plate

**NPB** – Neural plate border

**Nt** – Nucleotide

**O/N** – Overnight

**PAX** – paired box

**PBS** – Phosphate buffer saline

**PCR** – polymerase chain reaction

**PPE** – preplacodal ectoderm

**PiRNA** – piwi-interacting RNA

**Pre-miRNA** – precursor microRNA

**Pri-miRNA** – Primary miRNA

**PSED** – Pax/Six/Eya/Dach

**qRT-PCR** – quantitative reverse transcriptase polymerise chain reaction

**RISC** – RNA- induced silencing complex

**RNA** – Ribonucleic acid

**Rpm** – Revolutions per minute

**Sec** – seconds

**SEM** – standard error of the mean

**SHH** – Sonic hedgehog

**SiC** – Control small interfering RNA

**SiteRNA** - small intronic transposable element RNAs

**SIX** – Sine oculis-related homeobox

**sRNA** – small RNA

**SSC** – Saline sodium citrate

**St** – stage

**TM** – Melting temperature

**TF** – Transcription factor

**UTR** – Untranslated region

**WE** – Whole embryo

**WISH** – Whole mount *in situ* hybridisation

**WT** – Wildtype

## Acknowledgements

**Dr. Grant Wheeler** – For being the **best** supervisor ever.

**Prof Andrea Munsterberg and Prof Tamas Dalmay** – For your invaluable suggestions for future experiments and providing a wealth of miRNA knowledge.

**Prof Anne-Helene Monsoro-Burq and Meghane Sittewelle** – For all your help during my time spent at Institut Curie and for making me feel so welcome.

**Dr. Vicky Hatch** – For teaching me everything I know about *Xenopus* and providing a ‘hooge’ amount of entertainment for the lab.

**Danielle Blackwell** – For being one of the most kind hearted / empathetic / motivational people I know, couldn't have done it without you!

**Ines Desanlis** – For always being up for a night out, for your entertainingly angry outbursts and for being the reason I am now fluent in French.

**Katy Saide** – For your sarcastic comments and all the love and affection you give me.

**Dr. Geoff Mok** – For having superb banter.

**Johannes Wittig** – For being an absolute tech genius and pretty much formatting my whole thesis.

**Marta Marin-Barba** – For keeping me company during our over-night animal capping stints.

**Dr. Camille Viaut and Dr. Darrell Green** – For being experts in ‘your thing’ and taking the time to teach me when I needed you.

**Dr. Simon Moxon, Dr. Janet Higgins and Dr. Leighton Folkes** – For all your help with bioinformatic analysis and for being so understanding when I still don't understand what you've done after explaining it three times.

**Dr Adam Hendry and Dr James Mccoll** – For never mentioning the fact you completed an Iron Man.

**The rest of the Wheeler/Munsterberg clan** – For all your help, support and homemade cakes over the past four years.

**Mum, Dad and Kirsty** – For always having faith in me and supporting me in every decision I've ever made. I'll never forget that.

**My friends** – For making me laugh Every. Single. Day. (mostly with memes) and for not having a clue what I do whilst at work (make frogs pregnant?). A special shout out to Charlotte and all members of 2.5.

**Dave and Conor** – For waiting on me hand and foot whilst I've been writing.

**Matty and Harper** – For keeping me sane when things got tough.

# Chapter 1: Introduction

---

The neural crest (NC), often referred to as the “fourth germ layer”, is a transient, multipotent stem cell–like population of highly migratory embryonic cells found exclusively in vertebrates (Hall, 2000). Their derivatives contribute to a wide variety of tissues and organs in the developing embryo. These include, but are not limited to melanophores, enteric ganglia, neuroendocrine cells, neurons, craniofacial cartilage and bone (Le Douarin, 1999). As a defining feature of vertebrates, NC cells have attracted the attention of embryologists for over a century as a model for studying embryonic induction, specification, tissue commitment, migratory potential and cell-fate determination. In addition to their multipotent characteristics, NC cells can regenerate after ablation, with residual neural tube cells and adjacent NC compensating for the missing tissue (Scherson et al., 1993, Hunt et al., 1995). As a result of these defining characteristics, NC cells have spawned wide interest from the scientific community in gaining an understanding of the mechanisms behind NC development as well as using these cells in stem-cell-based therapies (Crane and Trainor, 2006).

During development, NC cells form over a time period that spans from pre-gastrulation to late organogenesis, this is in response to both intrinsic and extrinsic influences (Simoes-Costa and Bronner, 2015, Hoppler and Wheeler, 2015). To initiate NC development a combination of inductive signals emanating from surrounding tissues is required. Fate map studies have demonstrated that presumptive NC cells are in proximity to three different regions: the underlying mesoderm, the neuroectoderm (neural plate) and the non-neural ectoderm (presumptive epidermis) (Liem et al., 1995). It is as a response of signalling from these tissues that the presumptive NC region, namely the neural plate border (NPB) is set up. Once induced, this territory becomes competent to respond to signals specifying *bona fide* NC progenitors (Stuhlmiller and Garcia-Castro, 2012). As neurulation progresses, these precursors come to lie within the elevating neural folds, then, following neural tube closure they come to reside in a domain of the dorsal neural tube from which they will subsequently migrate (**Figure 1**). During this period, NC cells lose cell–cell adhesion and undergo cytoskeletal rearrangements and morphological changes that allow them to

delaminate and emigrate from the neuroepithelium. They acquire a migratory ability, with the acquisition of cell-surface receptors, metalloproteases and adhesion molecules that allow them to respond properly to cell–cell interactions and environmental cues that guide them along their well-defined pathways of migration. After settling in diverse and sometimes distant sites in the periphery, NC cells finish their journey by differentiating into a vast array of derivatives including elements of the craniofacial skeleton and pigment of the skin (Simoes-Costa and Bronner, 2015, Sauka-Spengler and Bronner-Fraser, 2008a). Cell lineage-tracing experiments have identified the various derivatives to be associated with specific NC populations. For example, cranial NC form the facial skeleton, including the upper and lower jaw bones of the neck and various aspects of the cranial ganglia (Couly et al., 1998) whilst the vagal NC form the outflow tract of the heart of enteric ganglia of the gut (Le Douarin and Teillet, 1973, Creazzo et al., 1998). The trunk NC contribute to the ganglia of the sympathetic nervous system (Le Douarin and Smith, 1988).

This complex array of events is guided by a well-orchestrated gene regulatory control network that has been extensively studied and reviewed (Sauka-Spengler and Bronner-Fraser, 2008a, Betancur et al., 2010, Simoes-Costa and Bronner, 2015). This network is comprised of multiple regulatory modules that guide acquisition of specific properties such as multipotency and migratory capacity in NC cells. It involves signalling pathways and transcription factors that are responsible for the induction, specification and differentiation of the NC.

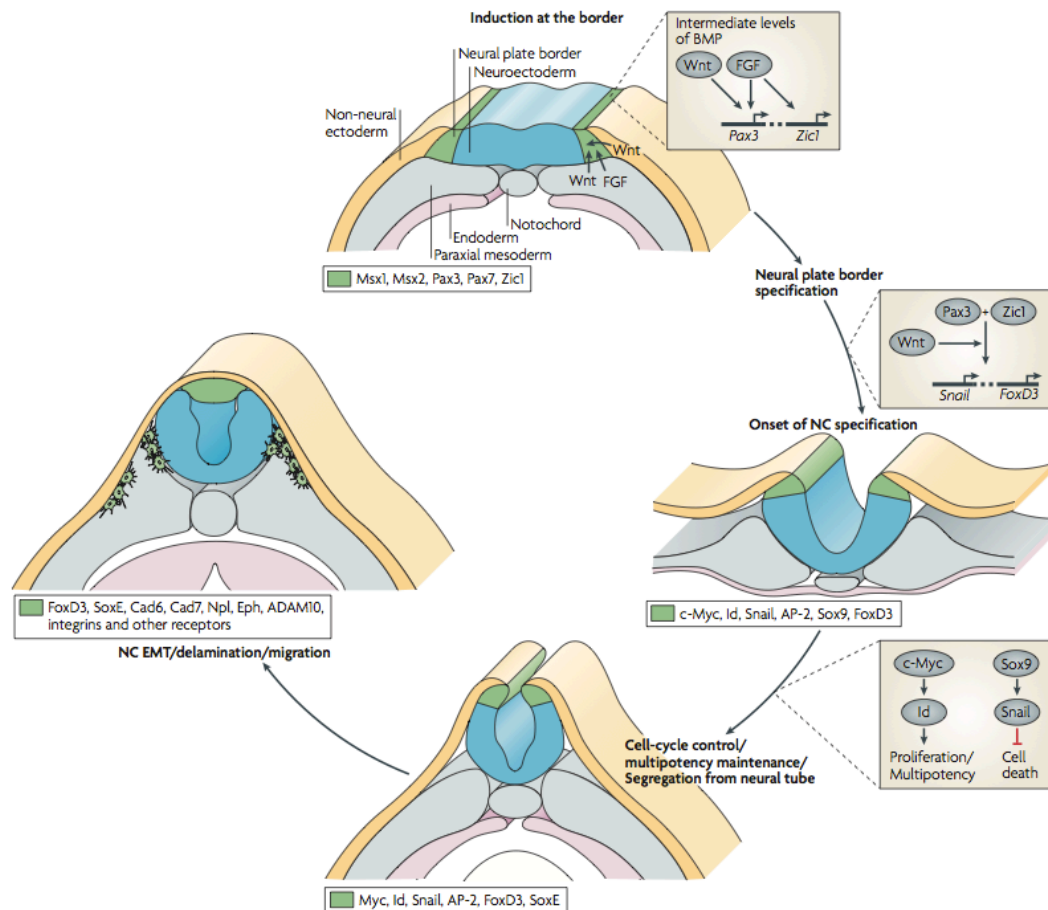


**Figure 1: Key stages in NC development.**

Induction of NC initiates at the NPB and is mediated by signals including FGF, Wnt and BMP. These signals collaboratively induce the expression of a number of NPB specifiers including *Pax3* and *Zic1*. *Pax3* and *Zic1* in turn act synergistically, in a Wnt-dependent manner, to up-regulate NC specifiers such as *Snail* and *FoxD3* in the neural folds. *c-Myc* and *Id* work by mediating cell-fate decisions by controlling the cell cycle, but also may maintain the NC progenitor pool in a multipotent state. *Sox9* confers survival properties to trunk NC precursors through up-regulation of *Snail*, an anti-apoptotic factor. Expression of these early NC specifiers in the NC progenitor population segregates them from the dorsal neuroepithelium, as these genes control the events of cell proliferation, delamination and the onset of the epithelial to mesenchymal transition (EMT). Other NC specifiers, such as *FoxD3* and *Sox10*, persist in delaminating and migrating NC cells, where they control expression of downstream effector genes such as type II cadherin, cadherin-7 (*Cad7*) (Sauka-Spengler and Bronner-Fraser, 2008a)

MicroRNAs (miRNAs) are small non-coding regulatory RNAs that range between 19-25 nucleotides (nt) in length, they are thought to regulate the expression of more than 30 percent of protein-coding genes in mammalian genomes (Filipowicz et al., 2008). By inhibiting target mRNAs through translational degradation, repression or other mechanisms, miRNAs are involved in a number of biological processes including but not limited to cellular differentiation and development (Bartel, 2004). With the tremendous improvement in the ability to identify miRNAs over the last decade, along with the ability to manipulate miRNAs both *in vitro* and *in vivo* with synthetic precursor and inhibitor miRNA molecules, the

understanding of the roles miRNAs play in various cell types has been vastly expanded (Croce, 2009) (Melo and Esteller, 2011). Up to this point, the role of miRNAs in early NC development is yet to be elucidated. The present study sought to investigate the roles of varying miRNAs in early NC development using *Xenopus laevis* as a model organism.

## **1. Neural crest – a vital cell population for development**

### **1.1. Induction and formation of the NPB**

The classical view of NC induction suggested that it occurs during the process of neurulation, as the neural folds elevate. This was thought to be caused by interactions resulting from the juxtaposition of epidermis on the elevating neural plate (NP) (Mancilla and Mayor, 1996, Selleck and Bronner-Fraser, 1995). Following that, findings in frog (Monsoro-Burq et al., 2005) and chicken (Basch et al., 2006) shed light that NC induction is underway much earlier, during gastrulation. During this period, the NPB is established, this region of cells is a broad territory between the future neural and epidermis domains which contains a multi-progenitor cell population. These cells give rise to NC as well as ectodermal placodes and the hatching gland (a gland that releases proteolytic enzymes to enable the tadpole to degrade the vitelline membrane) (Groves and LaBonne, 2014, Hong and Saint-Jeannet, 2007). More recently, it has been suggested that the process of NC induction arises even earlier, prior to gastrulation, this is discussed further in section 1.1.1 (Hoppler and Wheeler, 2015, Buitrago-Delgado et al., 2015).

Induction of the NPB is initiated in response to signalling molecules emanating from adjacent tissues. The “response” that sets future NC cells apart from other border cells requires the activation of a battery of transcription factors that imbues them with multipotency, characteristics of proliferating cells, and the competence to respond to later NC-specifying signals (Groves and LaBonne, 2014). As mentioned previously, fate map studies demonstrate that presumptive NC cells are in proximity to three different regions: the underlying mesoderm, adjacent

neuroectoderm and non-neural ectoderm (Liem et al., 1995, Steventon et al., 2009). These tissues are thought to secrete signalling ligands, including Wingless-type proteins (Wnt), bone morphogenetic protein (BMPs) and fibroblast growth factor (FGFs), that have all been demonstrated as essential for the early induction, maintenance and differentiation of NC (Knecht and Bronner-Fraser, 2002, Groves and LaBonne, 2014).

In *Xenopus*, high levels of BMP have been shown to be necessary for the acquisition of epidermal fate, whereas inhibition of BMP is required for neural induction (LaBonne and Bronner-Fraser, 1998). The current model for both *Xenopus* and zebrafish suggests that an intermediate level of BMP is responsible for the induction of NC. Indeed, loss of BMP signalling activity in the Zebrafish mutants swirl (*swr*)/*bmp2b* and snailhouse (*snh*)/*bmp7* results in the disruption of NC induction (Nguyen et al., 1998, Schmid et al., 2000). It is proposed that this gradient is established through diffusion of secreted BMP originating from the non-neural ectoderm thus creating a dorso-ventral gradient of BMP. Alternatively, it has been suggested that this gradient is achieved through the action of BMP antagonists including Cerberus, Noggin, Chordin, and Follistatins, all of which are ligands secreted by underlying paraxial mesoderm (Sauka-Spengler and Bronner-Fraser, 2008a, Tribulo et al., 2003, Wilson et al., 1997, Marchant et al., 1998). Regardless of the way a BMP gradient is established, intermediate levels of BMP alone are not sufficient to induce expression of NC markers in *Xenopus* or any other vertebrate model organisms (Garcia-Castro et al., 2002, LaBonne and Bronner-Fraser, 1998). BMP signalling is therefore an important initial step but additional signals are required for induction of the NC.

Gain and loss of function experiments in *Xenopus* and Zebrafish have been used to show that the canonical Wnt pathway is required at two time points during NC development (Garcia-Castro et al., 2002, LaBonne and Bronner-Fraser, 1998). Initially, during induction, an early gastrula-dependent Wnt-signal acts in collaboration with BMP antagonists to induce NPB tissue (Groves and LaBonne, 2014). At later neural-stages, Wnt signalling acts in concert with BMP signalling to maintain NC cell fates (Steventon et al., 2009). Throughout the literature, the importance of Wnt signalling in NPB formation has been demonstrated extensively. For instance, overexpression of Wnt ligands or dominant negative forms of LRP6 and TCF proteins perturbed NC induction (Lewis et al., 2004,

Saint-Jeannet et al., 1997, Tamai et al., 2000). Several Wnts have been identified as key players in *Xenopus* NPB induction including Wnt6, Wnt8, Wnt1, Wnt3a and Wnt7b (Saint-Jeannet et al., 1997, Chang and Hemmati-Brivanlou, 1998, LaBonne and Bronner-Fraser, 1998, Schmidt et al., 2007) all of which are secreted from the paraxial mesoderm (Christian et al., 1991, Knecht and Bronner-Fraser, 2002). The downstream frizzled receptors that these Wnts are signalling through have also been characterized and include both Frizzled 3 and 7 (Abu-Elmagd et al., 2006, Deardorff et al., 2001). Another signalling molecule secreted from the paraxial mesoderm that is suggested to participate in defining the NPB is FGF. However, as with Notch signalling, the importance of these molecules varies somewhat between species (Endo et al., 2002, Monsoro-Burq et al., 2003, Yardley and Garcia-Castro, 2012). It has been suggested that Fgf8 acts indirectly, by activating expression of *Wnt8* in the mesoderm, which then induces NC in the overlying ectoderm (Hong et al., 2008). However, recent evidence from *Xenopus* suggests that FGFs can act directly on NC formation through activation of the Stat pathway (Nichane et al., 2010).

Following reception of these “inducing signals” into the NPB territory, a cohort of transcription factors, collectively termed NPB specifiers, are activated. These specifiers work by imbuing the NPB cells with multipotency and competence equipping them with the molecular toolkit to later respond to appropriate signals that bestow NC cell fate. Interestingly, it is the region of overlap of these genes along with the previously maintained transcription factors which are originally characteristic of either the NP or non-neural ectoderm that defines the broad territory of the NPB (Simoës-Costa and Bronner, 2015). Expression of the NPB specifiers is first noted during gastrulation and includes *Msx1*, *Pax3/7*, *Zic1*, *Tfap2a*, *Gbx2*, *Dlx5/6*, *Gata2/3*, *Hairy2* and *Foxi1/2* (Meulemans and Bronner-Fraser, 2004, Nichane et al., 2008b, Khudyakov and Bronner-Fraser, 2009). Studies have shown that once the expression of these genes commence, these transcription factors engage in a series of reciprocal interactions that lead to the stabilisation of this regulatory state and ensure their continued expression (Monsoro-Burq et al., 2005, Sato et al., 2005). For instance, Nikitina and colleagues showed that *Tfap2a* and *Msx1* activate not only each other, but also *Zic1* and *Pax3/7* (Nikitina et al., 2008).

In *Xenopus*, integration of inputs from the BMP, FGF, Wnt, and Notch signalling

pathways activates expression of *Msx1* (Monsoro-Burq et al., 2005, Tribulo et al., 2003). The up-regulation of *Msx1* in the border is essential for formation of *bona fide* NC, as assayed by expression of the NC specifier *Snail2*. This induction of *Snail2* by *Msx1* is indirectly achieved via the induction of two other NPB specifiers, *Pax3* and *Zic1* (Monsoro-Burq et al., 2005). Both *Pax3* and *Zic1* expression require intermediate levels of BMP activity and FGF and/or Wnt signalling to be induced (**Figure 1**). Even though BMP and FGF signals can regulate individual expression of *Pax3* and *Zic1*, both transcription factors need to be activated simultaneously to achieve NC specification (Sato et al., 2005). In *Xenopus*, high levels of either transcription factor, in the absence of the other promotes alternative NPB fates (hatching gland or preplacodal progenitors, respectively) (Hong and Saint-Jeannet, 2007, Litsiou et al., 2005). Recently, *Pax3* and *Zic1* have been implicated in modulating the transcriptional output of multiple signalling pathways involved in NC development (Wnt, Retinoic Acid) through the induction of key pathway regulators such as *Axin2* and *Cyp26c1* (Plouhinec et al., 2014).

### **1.1.1. Challenging the working model of neural crest cell induction**

Until recently, this has been the established model of NC induction. However, in 2015, Buitrago-Delgado and colleagues published a fundamental paper that has questioned this working model of NC (Buitrago-Delgado et al., 2015, Hoppler and Wheeler, 2015). They demonstrated that the previous model (described above) in which the NC could be described as an endogenous population of induced pluripotent stem cells (from ectodermal tissue) was incorrect. This work provided insight into how NC cells retain pluripotency rather than gain it and that this is selectively inherited from the embryonic stem cells from which they are derived (Buitrago-Delgado et al., 2015) (for a more detailed analysis of this paper see section 13.4.3). This study raises questions about the identity of what we conventionally call the ectoderm (Hoppler and Wheeler, 2015). Moreover, the question arises as to how these cells at the NPB region selectively retain pluripotency while cells all around them become restricted in their developmental potential. The work in this PhD research project addresses one potential way in which this process could occur, that being through miRNAs.

## 1.2. Specification of the neural crest

Once the competence of the NPB territory is established by the synergistic activity of NPB specifiers, the prospective NC cells will integrate new signalling inputs and commence the process of specification into the *bona fide* NC. This occurs because of spatial-temporal expression of another set of transcription factors named “neural crest specifier genes”. These include, but are not limited to, *FoxD3*, *Snail2*, *Tfap2a*, *c-Myc*, *Id*, and members of the SoxE family (*Sox9/10*) (Khudyakov and Bronner-Fraser, 2009). These genes are either directly or indirectly regulated by NPB genes as well as receiving various signalling pathway inputs and intricate cross-regulatory activity with other NC specifiers. These transcription factors work together to define a new regulatory state of these cells and guide a complex sequence of developmental events to specify their NC fates (Sauka-Spengler and Bronner-Fraser, 2008a). These events involve substantial changes in the adhesive properties, shape, motility and signalling capacity of NC cell precursors. This allows them to segregate and delaminate from the neuroepithelium, migrate away from the neural tube along precise tracks and settle at distant territories and differentiate. NC specifiers achieve this by directly regulating various downstream targets. Despite working collaboratively to define this regulatory state, the NC specifiers display alternative expression profiles. Some specifiers are present only at the onset of the specification, prior to their migration (such as *Snail2*). Others, such as *Sox10*, persist in migrating and differentiating NC cells. Furthermore, some NC specifiers have a biphasic expression pattern in which they are present, first in NC progenitors and later again in specific differentiating derivatives (e.g., *Sox9*). A subgroup of transcription factors such as *Tfap2a*, *Snail1*, *Id*, *c-Myc*, and *Twist* are expressed even before NC progenitors become apparent, though the timing of their onset and presence within the NPB varies among different vertebrates (Betancur et al., 2010, Nikitina et al., 2008, Sauka-Spengler et al., 2007).

NC specifiers can be separated into two groups: early NC specifiers and late NC specifiers. The expression of early NC specifiers is first identified at the NPB. These include *c-Myc*, *Id3* and *Snail1* (Khudyakov and Bronner-Fraser, 2009, Liu and Harland, 2003). It has been suggested that early NC specifiers such as *c-Myc* and *Id3* may have a role within the NC gene regulatory network (GRN) to

maintain NC cells in a multipotent state, mediating critical cell cycle and/or cell fate decisions by controlling the expression of genes involved in cell division and downregulating factors involved in the onset of terminal differentiation (Bellmeyer et al., 2003, Kee and Bronner-Fraser, 2005, Light et al., 2005, Hatch et al., 2016). *Id* is a small transcriptional regulator that, in *Xenopus*, acts directly downstream of *c-Myc* (**Figure 1**). It functions as a repressor and possesses a helix-loop-helix (HLH) domain for dimerization, but lacks a basic domain for DNA binding. *Id* proteins interfere with gene expression by binding to transcriptional activators from bHLH families and preventing them from activating their direct targets (Ruzinova and Benezra, 2003). Depletion of *Id3*, like depletion of *c-Myc*, leads to the loss of NC progenitors and excess formation of central nervous system progenitors (Light et al., 2005). Conversely, overexpression of *Id3* maintains the NC in a prolonged multipotent progenitor state (Kee and Bronner-Fraser, 2005). Thus, *Id3* has a role in maintaining the multipotency of the NC progenitor pool and in mediating the decision between proliferation and apoptosis, acting as a cell-cycle-control switch (Nikitina et al., 2008).

The expression of late NC specifiers is first seen in pre-migratory NC cells of which some continue expression throughout migration. These include *Snail2*, *FoxD3* and members of the SoxE family (*Sox9* and *Sox10*) (Khudyakov and Bronner-Fraser, 2009). *Snail2*, the zinc finger transcription factor, was one of the first genes shown to affect NC formation in a cell autonomous manner. Its knockdown or overexpression suppresses or expands, respectively, NC cell migration from the neural tube (LaBonne and Bronner-Fraser, 2000). The expression of *Snail2* is directly regulated by intermediate levels of BMP, which is modulated by input from the Wnt pathway. Accordingly, the *Snail2* regulatory region contains binding motifs for Smad1, a transcription factor that mediates BMP signalling (Sakai et al., 2005), and Tcf/Lef1, which mediates the  $\beta$ -catenin-dependent Wnt signal (Vallin et al., 2001). Overexpression of *Hairy2*, a direct downstream effector gene of Notch signalling, causes an expansion of *Snail2* expression in frog (Glavic et al., 2004) and has been proposed as a direct input into the *Snail2* regulatory region. In addition, it has been demonstrated that the NPB specifiers *Zic1*, *Msx1*, and *Pax3/7* are independently necessary and sufficient for the expression of a group of NC specifiers including *Snail1/2*, *Foxd3*, *Twist1*, and *Tfap2b* (Meulemans and Bronner-Fraser, 2004, Sato et al., 2005,

Tribulo et al., 2003, Plouhinec et al., 2014). The winged-helix transcription factor FoxD3 appears to play a role in maintaining NC multipotency by preventing early differentiation (Lister et al., 2006). It has been shown that, the collective activity of Zic1, Msx1 and Pax3/7 complemented with Wnt input induces *FoxD3* expression (Sato et al., 2005).

The SoxE family of transcription factors, most notably *Sox9* and *Sox10*, have well-established roles in NC development. In *Xenopus*, *Sox9* expression is dependent on the activity of Tfap2 $\alpha$  (Lee et al., 2004, Luo et al., 2003). It has been shown that Gbx2 together with Zic1 can induce the expression of NC specifier genes including *Sox9* and *Snail2* while inhibiting preplacodal fate (Li et al., 2009a). Relatively recently, *Ets1* and *cMyb* have been added to the NC GRN as NC specifier genes. It was shown using knockdown experiments that through binding to the promoter region and by inducing the expression of *Ets1*, cMyb both directly and indirectly regulates the onset of *Sox10* expression (Betancur et al., 2014). *Sox10* is expressed in migrating NC cells and later becomes restricted to the glial lineage (Britsch et al., 2001). Inhibition of *Sox10* in *Xenopus* with morpholino antisense oligonucleotides prevents the formation of NC as characterised by a loss of *Snail2* and *FoxD3* (Honore et al., 2003). Mutations of *Sox10* in mice result in a loss of neurons and glia in the peripheral nervous system (Pingault et al., 2013). Similar effects are seen in the zebrafish *Sox10* mutant, colourless (Dutton et al., 2009). *Ets1* however is specific to cranial NC population, it is suggested that it has a unique function of establishing a regulatory state that activates cranial crest-specific effector genes responsible for the transition from the pre-migratory to migratory state (Gao et al., 2010).

Recently, Tfap2a has been described as a pioneer transcription factor in the process of NC specification. Genome-wide profiling of enhancers in NC obtained from human embryonic stem cells showed that this transcription factor, along with NR2F1 and NR2F2 work by reorganising chromatin conformation to provide access to other NPB specifiers, such as Msx1 and Pax3 (Rada-Iglesias et al., 2012). This is consistent with functional studies that show Tfap2a is required for NC specification in Zebrafish, *Xenopus* and Chick (Schorle et al., 1996, de Croze et al., 2011, Wang et al., 2011).

NC specifiers, in general, represent a node point onto which inductive inputs

mediated by or acting in parallel with NPB specifiers converge. Those specifying transcription factors in turn control the expression of effector genes that will give NC cells their unique migratory and multipotent characteristics. Therefore, in the life cycle of a NC cell, it is critical to keep the specifier genes expressed as a unit in the network. For this purpose, in frog, high interdependence among NC specifiers seems to exist (Sauka-Spengler and Bronner-Fraser, 2008a). Gain and loss of function experiments suggest that *Snail2* regulates *FoxD3*, *Twist*, and *Sox10* expression, probably in an indirect fashion (Aoki et al., 2003, Aybar et al., 2003). Ectopic expression of *Tfap2a* in the NP activates the ectopic expression of *Snail2* (Spokony et al., 2002), whereas *Sox10* feeds back to maintain *Snail2*, *Sox9*, and *FoxD3* expression (Honore et al., 2003).

At the same time as NC specification, both the preplacodal region and the hatching gland are also being established. The cranial placodes give rise to the paired sensory organs (olfactory system, lens, inner ear), and contribute to the cranial peripheral nervous system (Saint-Jeannet and Moody, 2014). The hatching gland is a transient structure that produces proteolytic enzymes implicated in the partial digestion of the egg vitelline membrane that protects the embryo early in life (Carroll and Hedrick, 1974, Drysdale and Elinson, 1991, Hong and Saint-Jeannet, 2007). While NC and cranial placode progenitors are derived from the deep layer of the ectoderm, hatching gland cells arise from the outer layer of the ectoderm.

Specification of the preplacodal region is achieved through the expression of the key placodal regulators *Six1*, *Eya1/2* and *Ir1* which are activated by lateral NPB specifiers (*Foxi1/3*, *Gata2/3* and *Dlx5/6*) (Grocott et al., 2012, Sato et al., 2010) (**Figure 2**). In order to molecularly separate the placodal region from the NC both NC and preplacodal genes engage in a number of inhibitory interactions. For instance, in *Xenopus*, *Pax3/7* and *Msx1* repress the expression of *Six1* (Sato et al., 2010). Although these molecular markers suggest a clear division between the NC and preplacodal domain, studies indicate that these two progenitor types are largely intermingled. Labelling of individual cells have shown that, despite their expression of specifier genes, the individual progenitors can give rise to either NC or preplacodal cells (Selleck and Bronner-Fraser, 1995). Conversely, specification of the hatching gland is largely due to the action of the transcription factor *Pax3*. Using a screen designed to identify downstream targets of *Pax3* at

the NPB, Hong and Saint-Jeannet (2014) recently described a molecular marker of the hatching gland, that being the protease *Xenopus* hatching enzyme 2 (*Xhe2*). *Xhe2* is exclusively expressed in hatching gland cells and using gain of function experiments, they showed that *Xhe2* is downstream of *Pax3* and is sufficient to promote digestion of the vitelline membrane (Hong and Saint-Jeannet, 2014).

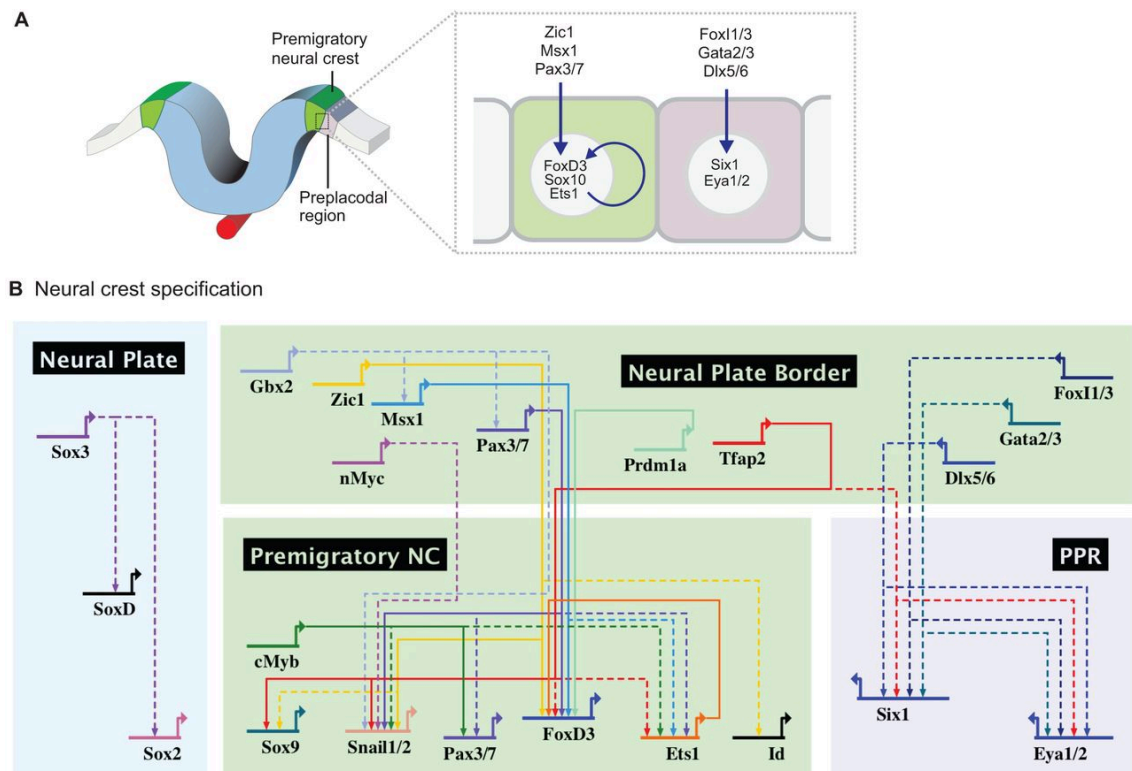


**Figure 2: The gene regulatory network underlying the formation of the various stages of neural crest and the preplacodal region**

As the NP folds during neurulation, the NPB specifier genes *Zic1*, *Msx1* and *Pax3/7* induce the expression of NC specifier genes *FoxD3*, *Sox10* and *Ets1* (green box). Lateral to the NC cells, are the preplacodal cells. They express a distinct set of transcription factors including *Six1* and *Eya1/2*. To stay molecularly separate, the two regions (NC and preplacodal genes) engage in a number of inhibitory interactions (**A**). It is the action of the medially located NPB specifiers that activate the expression of premigratory NC specifiers. The neighbouring preplacodal region (PPR) is defined by expression of *Six1* and *Eya1/2*, the expression of which are activated from the more lateral NPB specifiers. *Six1* and *Eya1/2* identify the progenitor field that will give rise to cranial placodes. Multiple *Sox* genes are expressed in the NP (**B**) (Simoes-Costa and Bronner, 2015).

### 1.3. Neural crest migration

After their specification, premigratory NC precursors reside within the dorsal neural tube. They subsequently undergo EMT and delaminate from the neural tube to undertake their migration and become *bona fide* NC cells. To permit

successful migration, cells are required to become less compact and acquire motility, to achieve this, the EMT induces changes at the cellular level that include switches in cell junctions and adhesion properties as well as major cytoskeletal rearrangements (Simoës-Costa and Bronner, 2015). Initially, the NC cells must lose their apical-basal polarity and tight junctions to permit detachment from the neuroepithelium (Theveneau and Mayor, 2012). To achieve this, a change in cadherin expression is thought to be central to this process. It is reported that *Snail1/2*, *Sox10* and *FoxD3* all play crucial roles in this process which involves upregulation of type II cadherins. These cadherins characterise mesenchymal cells and result in a concomitant downregulation of type I cadherins which are usually associated with stable cell assemblies (Chalpe et al., 2010, Kashef et al., 2009, Cheung et al., 2005). Negative regulation of E-cadherin, which characterise epithelial cells, along with a loss of cell polarity are essential initial steps in NC EMT. This process seems to be directly regulated by *Snail1/2*, which have been shown to bind to the E-cadherin promoter and repress its transcription (Cano et al., 2000, Villarejo et al., 2014). Similarly, *Snail2* and *FoxD3* act directly to negatively regulate the expression of *Cad6B*, a molecule that characterizes cell-cell adhesion among dorsal neural tube cells, most of which are premigratory NC progenitors (Taneyhill et al., 2007). Conversely, as migration is initiated, type II cadherin-7 is upregulated, possibly by the concerted action of *Sox10* and *FoxD3* (Cheung et al., 2005).

*Snail1/2* genes have also been implicated in regulating cell adhesiveness of NC cells through downregulating the expression of structural proteins that constitute tight junctions. Such proteins include occludins, which are transmembrane proteins with possible roles in the regulation of signalling events at the tight junction, and claudins, which mediate calcium-independent cell-cell adhesion and are crucial for the barrier function of tight junctions (Shin et al., 2006, Fishwick et al., 2012). This occurs as the neural tube is fusing and results in an overall decrease in the epithelial character of pre-migratory NC cells, as a part of the EMT initiation. In addition to the downregulation of tight junctions, the concomitant upregulation of gap junction proteins, namely connexin-43 (*Cx43*), is also reported to influence a migratory phenotype. *Cx43* is expressed in mouse NC cells at all axial levels (Lo et al., 1997).

*Sox5*, a member of the *SoxD* family, is another transcription factor proposed to

have a regulatory role during NC delamination. *Sox5* misexpression causes an increase in the number of cranial NC generated. *Sox5* upregulates *Snail2*, *FoxD3*, and *Sox10* in migrating crest cells and cell autonomously upregulates *RhoB*, a member of the Rho family of small GTPases that controls a variety of signal transduction pathways (Groysman et al., 2008, Perez-Alcala et al., 2004). *RhoB* is a well-known regulator of events that change cell morphology such as actin cytoskeleton rearrangements as well as the formation of focal adhesions and stress fibres (Liu and Jessell, 1998). All these cellular changes are necessary for NC delamination (Mackay et al., 1995).

For NC cells to migrate effectively they must remodel and invade the extracellular matrix (ECM). To permit efficient dissemination from the neural tube, NC cells are required to penetrate basement membranes and invade extracellular matrices. This involves migrating through a mesenchyme containing intricate connective tissue barriers that are comprised of collagens, fibronectin, laminins, vitronectin and proteoglycans (Theveneau and Mayor, 2012). To navigate on and through this ECM, NC cells require proteolytic activity of membrane-bound and/or secreted forms of matrix metalloproteases (MMPs), which have been implicated in the invasive behaviour of many forms of metastatic cells (Egeblad and Werb, 2002). NC cells can tightly regulate MMP activity themselves by the release of tissue inhibitors of MMPs (TIMPs) (Cai and Brauer, 2002). MMPs reported to be involved in NC migration include MMP2, MMP14, and the disintegrin and metalloproteinase 10 (ADAM10) (Duong and Erickson, 2004, Schiffmacher et al., 2014, Tomlinson et al., 2009, Harrison et al., 2004, Tan et al., 2016). ADAM metalloproteinases are cell-surface bound glycoproteins that act both by mediating cell–cell adhesion and as ‘sheddasers’, in the remodelling of the ECM. Acting as sheddasers involves facilitating the cleavage of extracellular portions of transmembrane proteins thus producing soluble ectodomains from the cell surface (McCusker and Alfandari, 2009). *Xenopus ADAM13*, which is expressed in both premigratory and migrating cranial NC cells, has several roles in NC cell migration. First, it decreases their adhesion to the ECM and therefore assists in detachment from the neuroepithelium and subsequently, during migration, by cleaving ECM barriers and therefore facilitating the passage of cells (Kee et al., 2007, Abbruzzese et al., 2016). As a result, both the polarity and directionality of the migrating NC are tightly regulated thus permitting colonisation in specific

areas whilst preventing them from invading zones predestined for other cell fates. In the cranial region, such regulatory molecules include Neuropilin-1/2, Roundabout homologs Robo-1/2, and Ephrin receptors (Sauka-Spengler and Bronner-Fraser, 2008a). In addition to interacting with their environment, NC cells have also been shown to communicate with each other. If one NC cell encounters another it will repolarize due to activation of the noncanonical Wnt pathway and migrate in a different direction. This is known as contact inhibition locomotion (CIL) and in *Xenopus* it has been recently shown to be mediated by Cadherin-11 (Becker et al., 2013). Despite this, large numbers of NC cells manage to migrate alongside in a continuous direction. This is because repulsive forces of CIL are balanced with attractive forces between NC cells due to the expression of chemoattractant C3a and the C3a receptor on their cell surface (Carmona-Fontaine et al., 2011).

In summary, the combined regulatory function of NC specifier genes and their downstream effectors endows NC cells with the characteristics that render them mesenchymal, proliferative, and motile. However, out of the many NC downstream effector genes, the direct regulatory inputs and links to upstream NC specifiers are known for only a few, which makes it difficult to assign their precise positions within the NC GRN.

#### **1.4. Neural crest differentiation**

There are two main streams of NC cells; those migrating cranially and those migrating in the trunk, which together give rise to an elaborate list of derivatives (Dupin et al., 2006). Cephalic NC cells which arise from the diencephalon to the third somite, give rise to many cranial structures including the bone and cartilage of the face and neck as well as tendons, muscles and connective tissues of the ear, eye, teeth and blood vessels. They will also form cranial melanophores and give rise to most of the cephalic peripheral nervous system (PNS). A subpopulation of cephalic NC cells, called the cardiac NC, emerge from the otic level to the anterior limit of somite 4. It migrates to the heart and is essential for the septation of the outflow track (Couly et al., 1998). Trunk NC cells, form the dorsal root and sympathetic ganglia of the PNS, pigment cells and endocrine cells of the adrenal gland (Le Douarin and Smith, 1988). Finally, the enteric NC cells delaminate from the neural tube facing somites 1 to 7 and colonise the entire gut

to form the enteric PNS, which controls the digestive track (Mayor and Theveneau, 2013, Le Douarin and Teillet, 1973).

*Cis*-regulatory analysis combined with functional and binding affinity assays have revealed several subcircuits of direct gene regulatory interactions specific for each of the NC lineages. Each subcircuit comprises of a network of unique transcription factors regulating specific effector genes, which in turn will give the cell its fully differentiated properties and characteristics. NC differentiation is thought to be both spatially and temporally regulated. After NC cells have migrated and reached their final destinations, typically expression of most early NC specifiers, including *Snail1/2*, *FoxD3*, *Id*, and *Tfap2α* are down regulated although the direct regulatory interactions triggering this down-regulation are unclear (Meulemans and Bronner-Fraser, 2004). However, this is not always the case. Down-regulation of *FoxD3* in migrating cells prior to differentiation does not take place in all NC derived lineages. While absent from melanoblasts, *FoxD3* expression persists in neural/glial precursors, where it prevents *Pax3* from binding to the promoter of Microphthalmia-associated transcription factor (*MITF*) and thus protects sensory precursors from adapting a pigment cell fate (Thomas and Erickson, 2009). In addition, SoxE transcription factor family members *Sox9* and *Sox10* also persist in specific subpopulations of NC derivatives and appear to be master regulators of terminal differentiation in the majority of NC derivatives (Kelsh, 2006, Sauka-Spengler and Bronner-Fraser, 2008b). *Sox10* persists in melanoblasts and elements of the PNS, whereas *Sox9* is characteristic of NC derived chondrocytes. Experiments in *Xenopus* suggest that the HLH transcriptional repressor *Id* prevents premature NC differentiation during NC migration. Overexpression of *Id3* in *Sox10*-expressing melanoblasts or *Sox9*-expressing NC-derived cartilage cells inhibits SoxE expression, which affects melanocyte and chondrocyte differentiation (Light et al., 2005). Thus, downregulation of *Id* is necessary for the initial steps of NC differentiation to occur.

NC cells are often referred to as the fourth germ layer and have been central to vertebrate evolution. In addition, defects in NC cell development are associated with several congenital defects, collectively known as neurocristopathies (Shahar and Shinawi, 2003). These include disorders of craniofacial and organ development as well as diseases such as neuroblastoma and melanoma.

Consequently, understanding the normal epigenetic mechanisms of NC cell development will provide important clues regarding errors in regulation that may finally lead to abnormal development or loss of the differentiated state.

## **2. miRNAs and their role in development**

Due to advances in high-throughput transcriptome analyses, several projects have demonstrated that mammalian transcriptomes have a large complement of noncoding RNAs (ncRNAs). In fact, only 1–2% of the genome codes for proteins, while the great majority codes for ncRNAs (Amaral et al., 2008). A specific subgroup of ncRNAs are miRNAs, that are involved in myriad cellular events including but not limited to a number of vital processes during early embryogenesis (Ebert and Sharp, 2012, Goljanek-Whysall et al., 2014). miRNAs are evolutionarily conserved and represent small non-protein-coding RNA gene products that regulate gene expression at the posttranscriptional level (Bartel, 2004, Ambros, 2004). This novel mode of regulating gene expression was first discovered in *C. elegans*. In 2000, two separate groups discovered that a small RNA, let-7, was essential for the development of a later larval stage to adult in *C. elegans* (Reinhart et al., 2000, Slack et al., 2000). Subsequently, homologues of this gene were discovered in many other organisms, including humans (Pasquinelli et al., 2000). Following this pioneering discovery, multiple laboratories worked quickly to clone numerous small RNAs from various model organisms in order to further define their functions.

### **2.1. Biogenesis and mechanism of miRNAs**

This well-defined family of ~19–24 nucleotides (nt), non-coding RNA species is known to regulate translation of specific messenger RNA (mRNA) targets in a wide variety of organisms (Filipowicz et al., 2008). Acting through the recognition of binding sites usually located in the 3' untranslated region (UTR) of mRNAs, miRNAs are suggested to regulate approximately 60% of the genes in humans (Bartel, 2009). Expressed from miRNA genes transcribed from the genome, miRNAs are generated from a primary transcript (termed pri-miRNA). This transcript may contain one or more hairpins as miRNAs can be clustered together to give rise to polycistronic transcriptional units (Davis and Hata, 2009). In the

nucleus, the hairpin is excised from the pri-miRNA by the microprocessor complex, minimally composed by the RNaseIII Drosha and the double-stranded RNA-binding protein DGCR8 (**Figure 3**). The resulting hairpin precursor (pre-miRNA) is usually 60–110 nt long, and is actively exported to the cytoplasm by the nuclear-membrane protein Exportin-5 (Lee et al., 2003, Bohnsack et al., 2004). In the cytoplasm, another protein complex containing the RNaseIII enzyme Dicer further processes the pre-miRNA to the mature miRNA, which is loaded onto the RNA Induced Silencing Complex (RISC) (Gibney and Nolan, 2010). Only one of the two strands of the original pre-miRNA stem remains bound to the RISC (the guide strand) as mature miRNA, whereas the other strand (passenger strand) is usually eliminated. Once incorporated into a silencing complex, the miRNA binds to its target sequences resulting in RNA interference, which results in degradation, translational stop or to other means of inhibition of the respective RNA molecule (**Figure 3**) (He and Hannon, 2004, Bartel, 2004, Meister et al., 2004, Ambros, 2004). The method in which a miRNA binds to its target gene is discussed further in section 13.11.1..

## 2.2. miRNAs in development

Tight spatio-temporal control of miRNAs occur resulting in the distinct expression patterns of many miRNAs (Wienholds et al., 2005, Kloosterman et al., 2006, Ahmed et al., 2015), with levels changing quite dramatically in some contexts such as stem cell differentiation (Gangaraju and Lin, 2009). The ability of miRNAs to alter the expression program of many target mRNAs and their encoded proteins, combined with their tight control suggests that miRNAs may affect phenotypic transitions. The importance of miRNAs in development has been demonstrated using knockout Dicer mutants in various model organisms. Germline deficiency of Dicer in mice and Zebrafish causes lethality early in embryogenesis (by embryonic day 7.5 in mice) characterised by abnormal morphology in almost all organs and result in significant lack of stem cells (Bernstein et al., 2003, Andl et al., 2006, Harfe et al., 2005, Kloosterman and Plasterk, 2006, Giraldez et al., 2005)

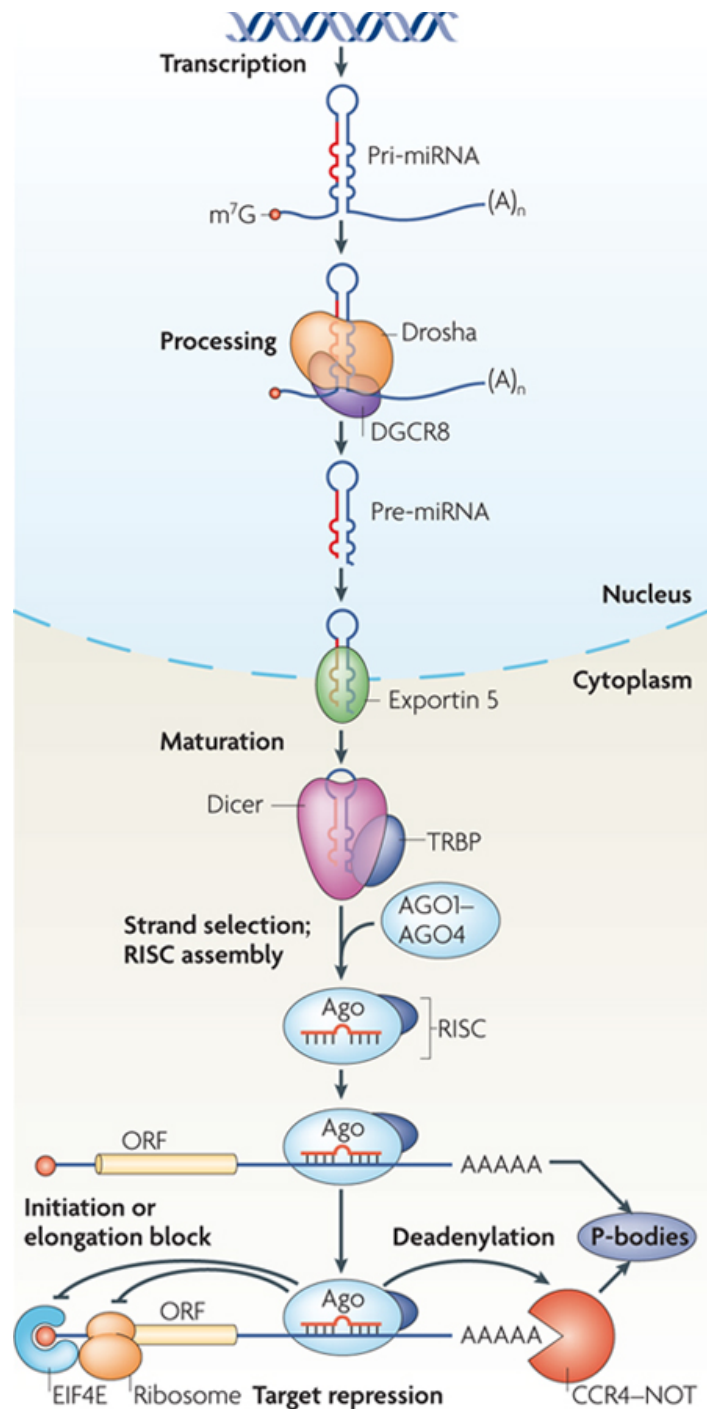


**Figure 3: miRNA biogenesis and mechanism of action**

MiRNAs are transcribed as primary transcripts (pri-miRNAs) by RNA polymerase II. Each pri-miRNA contains at least one hairpin structure that is recognized and processed by the endonuclease, Drosha. This complex generates a stem loop known as the precursor miRNA (pre-miRNA), which is exported to the cytoplasm by exportin 5. In the cytoplasm, the pre-miRNA is recognised by another endonuclease, Dicer. Dicer, along with the RNA-binding protein TRBP binds to the precursor and cleaves the pre-miRNA, generating a 20-nucleotide mature miRNA duplex. Generally, one strand is selected and incorporated into the RNA-induced silencing complex (RISC) which is composed of Argonaute (Ago) protein and the single stranded miRNA, whilst the other strand is degraded. Mature miRNA guides the RISC to its target mRNAs through base pairing between the seed sequence of the miRNA and the seed match sequences in the mRNA. The RISC can inhibit the translation of the target mRNA through multiple mechanisms including removal of the polyA tail (deadenylation) which results in mRNA degradation or through blockage of translation at the initiation step or at the elongation step; for example, by inhibiting eukaryotic initiation factor 4E (EIF4E) (Inui et al., 2010).

Using miRNA specific deletions, the function of individual miRNAs within various aspects of development have been explored. For example, miR-273 is required for establishing left-right asymmetry during neuronal development (Hobert, 2006), and in mice, deletion of miR-1-2 caused severe and irreparable defects in cardiac morphology suggesting critical roles for this miRNA in regulating cardiogenesis (Zhao et al., 2007). In a muscle context, double gene knockout of the muscle-enriched miRNA (myomiR), miR-133a, in mice resulted in increased proliferation and apoptosis of myocytes, ventricular septal defects, and embryonic lethality (Liu et al., 2008). Upregulation of another myomiR – miR-27, along with subsequent downregulation of its target protein, Pax3, were found to be important in reducing myocyte proliferation and facilitating myogenic differentiation (Crist et al., 2009). Together, these studies, along with the spatial and temporal expression patterns of miRNAs in specific organ systems, have unequivocally established the role and relevance of miRNAs as enforcers of the changes in cellular states that occur during development.

### **2.3. miRNAs regulate pluripotency and cell migration in many systems**

Throughout the literature, miRNAs have been described as key players in the regulation of pluripotency in many systems including embryonic stem cells (ESC) and induced pluripotent stem cells (iPSC). Many miRNAs including miR-145, miR-134, miR-296, and miR-470 have been shown to represses the pluripotency of human ESCs by repressing the expression of key transcription factors including Oct4, Sox2, Nanog and Klf4 (Tay et al., 2008, Xu et al., 2009). Another family of miRNAs reported to have roles in the repression of pluripotency is the Let-7 family, more specifically, this family of miRNAs are highly expressed in somatic cells where they function to repress genes involved in self-renewal. Interestingly, the inhibitory effect of let-7c on self-renewal can be rescued by co-transfection of let-7 and miR-294, a member of the ESC specific miR-290 cluster. Introduction of miR-294 indirectly enhances the expression of Lin28 and c-Myc (self-renewal genes). Lin 28 is known to directly block the maturation of let-7 (Viswanathan et al., 2008, Rybak et al., 2008), thereby silencing the Let-7 family and maintaining self-renewal.

In addition to self-renewal, miRNAs have been vastly reported to regulate cell migration in many systems including cancer. Korpál et al. (2008) reported that ectopic expression of the miR-200 family miRNAs significantly increased E-cadherin expression and altered cell morphology to an epithelial phenotype in mouse carcinoma cells. Furthermore, Zhuang et al. (2012b) reported that the tumour secreted miR-9, promotes endothelial cell migration and angiogenesis by activating the JAK-STAT pathway.

## **2.4. The role of miRNAs in neural crest cell development**

miRNAs were first demonstrated to be critical for NC development through work published by a number of groups (Huang et al., 2010, Nie et al., 2011, Zehir et al., 2010). All three groups showed independently using Wnt1-cre-mediated conditional mice knockouts of zygotic *dicer* in NC cells that the differentiation of this cell type is severely impaired resulting in a phenotype consisting of many NC related abnormalities including impaired craniofacial organogenesis. Following on from this work, several groups have shown that miRNAs are central regulators of NC differentiation (Cordes and Srivastava, 2009). Although all three papers found that miRNAs were involved in NC differentiation, they also all claimed that removal of zygotic Dicer did not impair induction, specification or EMT of the NC (Nie et al., 2011, Huang et al., 2010, Zehir et al., 2010). This therefore inadvertently suggested these processes occur independent of miRNA gene regulation. However, there are concerns with the temporal expression of the wnt-1 promoter as it may be too late for early NC development. In addition, in Zebrafish, it is reported that maternal dicer activity has hampered the analysis of the single dicer gene. Mutants for the zygotic function of dicer (Zdicer) retain pre-miRNA processing activity up to 10 days postfertilization as a consequence of maternally contributed dicer (Wienholds et al., 2003). Therefore, it is possible that the presence of maternal Dicer may have allowed for early NC development to occur. Morpholino knockdowns of maternal *Dicer1* result in an earlier developmental arrest than Zdicer mutants (Wienholds et al., 2003) and MZdicer mutants (loss of maternal and zygotic dicer) display abnormal morphogenesis during gastrulation, brain formation, somitogenesis, and heart development

(Giraldez et al., 2005). The effects of these knockdowns are even more prominent in mice whereby a knock down of maternal *dicer* results in the embryo failing to progress through the first cell division (Tang et al., 2007). This therefore demonstrates that although there are differences between species, maternal *Dicer1* plays a pivotal role during early vertebrate embryonic development and therefore possibly during early NC development. To further support this, Gessert et al. (2010) showed that a more targeted Dicer knockdown in the anterior neural tissue of *Xenopus* leads to eye and cranial cartilage defects.

### **3. Rationale**

Since miRNAs are aberrantly expressed in a vast number of embryonic cell types and have been demonstrated to be involved in a number of processes that are vital to NC development including EMT, there is strong reason to believe that miRNAs are key players in early NC development. Functional NC development is key to successful embryogenesis in vertebrates. It is therefore essential to elucidate the mechanisms by which they develop, including the roles miRNAs have in this process.

The aims of this study were:

1. To identify NC enriched miRNAs
2. To explore the function of the candidate miRNAs during *Xenopus* NC development
3. To explore the molecular mechanisms through which these candidate miRNAs are working during *Xenopus* NC development
4. To identify miRNAs that are possibly contributing to NC multipotency

In summary, **Chapter 3** shows results of both the XenmiR and the sRNA sequencing approaches to identify candidate miRNAs. This includes an analysis of the top miRNAs differentially expressed in NC tissue compared to neural tissue. From these results, several candidate miRNAs were identified. The functional role of these miRNAs in relation to NC development is explored in **Chapter 4**. From these candidates, two miRNAs (miR-219 and miR-196a) gave a NC related phenotype. In **Chapter 5** an in-depth analysis using both online target algorithms and RNA sequencing was used to identify the targets of miR-

219 and miR-196a and therefore try and decipher the mechanisms behind these miRNAs in NC development.

# Chapter 2: Materials and methods

---

## 4. Husbandry

### 4.1. Obtaining embryos

All experiments were performed in compliance with the relevant laws and institutional guidelines at the University of East Anglia. The research has been approved by the local ethical review committee according to UK Home Office regulations.

Females are primed 5-10 days prior to the day embryos are required using 100 units of PMSG (pregnant mare serum gonadotropin). To induce ovulation, primed female *Xenopus laevis* were injected with 500 units of human chorionic gonadotrophin (hCG) into their dorsal lymph sac and stored at 18°C. Eggs can then be collected 14-16 h following induction. Testes were isolated from an euthanized male frog and placed in testes buffer. To obtain eggs, the abdomen of the frogs were manually massaged over a clean petri dish. A piece of masticated testes is then crushed with 1ml of high salt solution, 1XMMR, and distributed over the collected eggs and then left for 5 mins at 18°C. 0.1MMR can then be added to the eggs and left for 20 mins at 18°C. After fertilization the jelly coat which encases the eggs is removed. For this they are added to a 250ml beaker containing 2% (w/v) L-cysteine pH 8.0 dissolved in 1XMMR. Swirling the eggs in this solution gently removes the jelly. Eggs are then washed in 1X MMR then 0.1XMMR to remove the cysteine. Embryos can then be left to develop until they reach the required stage according to the Niewkoop and Faber 1967.

Materials:

- 0.1XMMR: 10mM NaCl, 0.2mM KCL, 0.1mM MgCl<sub>2</sub>, 0.2mM CaCl<sub>2</sub>, 0.5mM HEPES (PH7.5)
- 1XMMR: 100mM NaCl, 2mM KCl, 1mM MgCl<sub>2</sub>, 2mM CaCl<sub>2</sub>, 5mM HEPES (PH7.5)

- Testis buffer: 80% (v/v) fetal calf serum, 20% (v/v) 1X MMR, gentamycin (Sigma 1:1000U)
- PMSG (Intervet): 1000U/ml PMSG prepared in solvent and stored at 4°C
- Chorulon (Intervet): 1000U/ml Chorulon prepared in solvent and stored at 4°C.

#### 4.1.1. Fixing embryos

Once *Xenopus* embryos or animal caps reach their desired stage (depicted by Nieuwkoop and Faber, 1967) they were fixed using MEMFA (3.7% (v/v) formaldehyde, 1X MEM salts made up with DEPC H<sub>2</sub>O). They were then left at RT for 1-2 h or overnight at 4°C. The embryos were then washed 2 times in phosphate buffered saline with 0.1% (v/v) Tween-20 (PBST) and then stored at -20°C in 100% EtOH.

## 5. Whole mount *in situ* hybridisation (WISH)

### 5.1. mRNA probe synthesis

#### 5.1.1. Preparation of competent cells

A 5 ml culture of DH5α *E.coli* was grown overnight in Luria Broth (LB) at 37°C and with shaking. 1ml of this culture was added to 200 ml of LB medium and grown at 37°C with shaking until optical density (OD<sub>600</sub>) reached 0.3 to 0.4. At this point the culture was divided into 4x 50ml Falcon tubes and put on ice for 15 mins. The cells were centrifuged at 4°C for 15 mins at 6000 x g. The supernatant was discarded and the bacterial pellet was resuspended in 16 ml filter sterilized TB I buffer. Cells were put on ice for 15 mins, centrifuged at 4°C at 20,000 x g for 30 mins. The supernatant was discarded and the pellet was resuspended in 4ml of sterilized TB II. Aliquots were stored at -80°C.

Materials:

- TB I pH 5.8: RbCl<sub>2</sub> 0.1M, MnCl<sub>2</sub>H<sub>2</sub>O 0.068M, CaCl<sub>2</sub> 0.01M, KAc 1 M pH 7.5, 37.5 ml Glycerol adjust to 250 ml and pH using 0.2 M HAc

- TB II: MOPS 0.5M pH 6.8, RbCL<sub>2</sub> 0.01M, CaCl<sub>2</sub> H<sub>2</sub>O 1.04 M, 37.5 ml Glycerol adjust to 250 ml aliquoted and stored at -80°C

### 5.1.2. Transformation

1 µl of plasmid was added into 100µl of competent *E.coli* cells, left on ice for 30 mins and heat shocked at 42°C for 90 secs. 300 µl of LB media was added and cells were left for one h at 37°C. 200 µl of transformation mix was plated out onto LB agar containing the required antibiotic O/N at 37°C.

### 5.1.3. DNA mini prep

Colonies from the transformation were incubated in 5 ml LB/carbicillin liquid media O/N at 37°C with rocking. The DNA plasmid was then isolated using Qiagen mini plasmid purification kit (Qiagen, UK) according to manufactures instructions. 1µl of the final product was run on an agarose gel by electrophoresis.

### 5.1.4. DNA midi prep

Colonies from the transformation were incubated in 50 ml LB/carbenicillin liquid media O/N at 37°C with rocking. Plasmid DNA was isolated using Qiagen mini plasmid purification kit (Qiagen, UK) according to manufactur's instructions. 1 µl of the final product was analysed by gel electrophoresis.

### 5.1.5. DNA and RNA quantification

DNA was quantified using a standard spectrophotometer; <sup>260</sup>/<sub>280</sub> ratios of 1.8-2.0 indicated good quality DNA.

### 5.1.6. Probe synthesis

Plasmids containing a gene of interest were linearized by by restriction digest downstream/upstream of the sense/ antisense probe, respectively. Linearized DNA was purified before probe synthesis. For probe synthesis, the following reaction mixture was used and in a total volume of 20 µl of nuclease free water (Table 1).

**Table 1: Probe Synthesis**

Reagent	1 reaction
5X transcription buffer (Invitrogen)	4 $\mu$ l
DDT (100mM; Invitrogen)	2 $\mu$ l
1 $\mu$ l Fluorescin labeled UTPs (Roche)	1 $\mu$ l
RNAsin (40 U/ $\mu$ l; Promega)	1 $\mu$ l
linearized DNA	1 $\mu$ g
RNA polymerase (EcoR1 antisense polymerase T3)	2 $\mu$ l
Total volume	20 $\mu$ l

The reaction mix was incubated at 37°C for 3 hrs. Any remaining DNA template was removed by adding 1  $\mu$ l of DNase 1 (2 U/ $\mu$ l; Roche) and incubated for 30 mins at 37°C. 1  $\mu$ l of the probe was verified on a 2% (w/v) agarose gel and visualized in a UV transmitter (BIO-RAD). Plasmids and enzymes used to make probes are displayed in **(Appendix 1)**.

### 5.1.7. Purification of probes

Probes were purified by using Illustra MicroSpin G-50 Columns (GE healthcare life sciences) according to manufacturer's instructions. 5  $\mu$ L of probe was analysed on a 2% (w/v) agarose to confirm probe integrity. 5  $\mu$ g of purified probe was added to approximately 10 ml of hybridisation buffer depending on probe quality (determined on a 2% (w/v) agarose gel) and stored at -20°C.

## 5.2. WISH

Embryos were rehydrated from 100% methanol by using 100%, 75%, 50% 25% (v/v) methanol intermediates (in PBST) for 5 mins each followed by two PBST washes for the same time, all with rocking at RT. Embryos were then treated with 10  $\mu$ g/ml proteinase K (no rocking) for varying times depending on the embryo

stages (e.g. *Xenopus* stage 38 – 10 mins; stage 25 – 4 mins; stage 10.5 – 1 min). *Xenopus* embryos were then subsequently washed twice in PBST for 5 mins and incubated in 3.7% (v/v) formaldehyde/PBST for 45 mins with rocking. The embryos were washed with 50% hybridisation buffer (in PBST) followed by 100% hybridisation buffer both for 10 mins. Following this, embryos were prehybridised in 100% hybridisation buffer for 2-3 h at hybridisation temperature (48°C for LNA probes, 65°C RNA probes)

Probes were removed and stored at -20°C and embryos were washed with fresh hybridisation buffer for 10 mins followed by two 15 min washes with wash solution and one 10 min wash in 50% MABT/ 50% wash buffer. All steps were completed at hybridisation temperature. Embryos then underwent two 30 min washes in maleic acid buffer with 0.1% Tween-20 (1XMABT), a 1 h wash in 2% (w/v) Boehringer Mannheim blocking reagent (BBR) (in MABT) and a 2-3 h wash in 20% (v/v) Goat serum in 2% (w/v) BBR, all at RT. BBR solution was replaced with antibody solution containing anti-Dig antibody (Roche; 150 U) (1:3000) made in 20% (v/v) goat serum and 2% (v/v) BBR at 4°C overnight. All steps with rocking.

Antibody solution was removed and embryos were washed in 1X MABT five times for 60 min each at RT and incubated in a sixth MABT wash overnight at 4°C with rocking. The colour reaction was then carried out by washing the embryos in fresh alkaline phosphate buffer twice for 10 min at RT with rocking. Embryos were then put in NBT/BCIP in alkaline phosphate buffer (4.5 µl/ml NBT, 3.5 µl/ml BCIP) protected from light, until the desired level of colour was noted. Embryos were placed in 5X TBST solution O/N if needed to remove background staining and then imaged.

### **5.2.1. Double WISH:**

Embryos were hybridised overnight with the RNA probe at 65°C, then washed with fresh hybridisation buffer for 10 min followed by two 15 min washes with wash solution and one 10 min wash in 50% MABT/ 50% wash solution. All steps were completed at 65°C. Embryos then underwent two 30 min washes in 1X MABT for 30 min. The embryos were prehybridised for 2-3 h in hybridisation buffer at 48°C (LNA probe hybridisation temperature) and hybridised overnight with the LNA probe. The LNA probe was then detected as described above.

When the colour was developed the embryos were fixed in MEMFA O/N and washed in MABT at 65°C for 1 h to inactivate the anti-DIG antibody. The embryos were then blocked and incubated in anti-Fluorescein antibody (Promega; 150U), 1:1000 dilution. The RNA probe was then detected as described above but using Fast Red solution (Sigma) instead of NBT/BCIP. When the colour reaction was complete, the reaction was stopped with three PBST washes at RT and the embryos were fixed in MEMFA for two h at RT.

Materials for WISH and double WISH:

- PBS – 10X: 2.5 g  $\text{NaH}_2\text{PO}_4\cdot\text{H}_2\text{O}$ , 11.94 g  $\text{NaHPO}_4\cdot\text{H}_2\text{O}$ , 102.2 g NaCl
- PBST – PBS with 0.1% (v/v) Tween-20
- Proteinase K (10  $\mu\text{g}/\text{ml}$ ): 1  $\mu\text{l}$  Proteinase K, 1 ml PBST
- Hybridisation buffer: 50% (v/v) formamide, 5X SSC, 1 mg/ml Torula RNA, 100  $\mu\text{g}/\text{ml}$  Heparin, 1X Denharts solution, 0.1% (v/v) Tween-20, 0.1% (w/v) CHAPS, 10 mM EDTA.
- Washing buffer: 50% (v/v) formamide, 1X SSC, 0.1% (v/v) Tween-20
- MABT (1X): 100 mM Maleic acid, 150 mM NaCl, 0.1% (v/v) Tween-20, (pH 7.5)
- BMB (10%): 10% (w/v) in BMB preheated (50°C), 1X MAB, stirred until dissolved and then autoclaved, aliquoted and stored at -20°C.
- Alkaline phosphatase buffer: 100 mM Tris (pH 9.5), 50 mM  $\text{MgCl}_2$ , 100 mM NaCl, 0.1% (v/v) Tween-20.
- BCIP: 50 mg/ml in 100% DMF
- NBT (Nitro Blue tetrazolium): 75 mg/ml in 70% dimethylformamide (DMF)
- TBST: 125 ml 1M Tris pH 7.5 40 g NaCl, 1 g KCl and 450ml with  $\text{dH}_2\text{O}$ . Autoclaved then add 50 ml of Tween-20.
- MEMFA: 10% (v/v) MEM salts, 10% (v/v) formaldehyde
- MEM salts: 0.1 M MOPS, 2 mM EGTA, 1 mM  $\text{MgSO}_4$ , pH7.4
- Fast Red Solution: SIGMAFAST™ Fast Red TR/Naphthol AS-MX Tablets dissolved in 10 ml alkaline phosphatase buffer

### 5.2.2. Cryosectioning of WISH embryos

Embryos were fixed in MEMFA for 2 h, washed twice for 5 min with PBST and placed in 30% (w/v) sucrose overnight at 4°C. Embryos were transferred to cryo-

moulds filled with optimal cutting temperature (OCT) compound and left for 4 h at RT. Embryos were positioned appropriately for sectioning, frozen on dry ice for 30 min and then left overnight at -20°C. Embryos were sectioned using the LEICA CM 1950 Cryostat and sections were placed on 5% TESPA slides. Slides underwent three 5 min washes in PBS and coverslips were mounted using hydromount. Images were taken using a Zeiss CCD upright microscope with colour camera.

## 6. Alcian blue staining

Embryos were fixed for 1.5 h at RT, dehydrated with five washes of 100% ethanol for 5 min each at RT and then left in Alcian blue staining solution for three nights. Embryos were then washed three times for 15 min in 95% ethanol at RT and gradually rehydrated to 2% KOH using 10 min washes of 75% EtOH in 2% KOH, 50% EtOH in 2% KOH, 25% EtOH in 2% KOH twice and finally 3 x 2% KOH washes. Embryos were then transferred into glycerol using 1 h washes of 20% glycerol in 2% KOH, 40% glycerol in 2% KOH, 60% glycerol in 2% KOH and 80% glycerol in 2% KOH. Craniofacial cartilage was then dissected out prior to imaging.

Solutions:

- Alcian blue solution: 20mg Alcian blue, 15 ml acetic acid, 35ml 100% EtOH
- 2% (w/v) KOH: 1g KOH tablets in 500ml dH<sub>2</sub>O

## 7. Microinjection

Embryos undergoing microinjection were placed in 3% Ficoll PM400 (Sigma, UK) and injected at either the two-cell stage into the animal pole of both blastomeres using a 10 nl calibrated needle or at the four-cell stage in one dorsal blastomere using a 5 nl calibrated needle. Morpholino sequences are listed in **Table 2**. Following a 2 h incubation in Ficol the embryos were transferred into 0.1X MMR and left to develop to the appropriate stage. The injections were completed using a Harvard apparatus injector (Medical Systems Research products) and the

injector was set up at  $P_{out} = 90$ ,  $P_{balance} = 0.6$  and  $P_{inject} = 16$ .

**Table 2: Morpholino sequences**

Morpholino	Sequence
miR-219 MO	5'-AGAATTGCGTTTGGACAATCAAGGG-3'
miR-219 mismatch	5' ACAATTGCCTTTTCGAGAATCAACGG-3'
miR-196a	5'- CAATCCCAACAACATGAAACTACCT-3'
miR-196a mismatch	5'-CATTGCCAAGAACATCAAAGTACCT-3'

Solutions:

3% (w/v) Ficoll: 6 g Ficoll PM400, 60 ml 1X MMR, 140 ml dH<sub>2</sub>O

## **8. Animal cap assay for sRNA sequencing**

### **8.1.1. Capped RNA synthesis**

10 µg of plasmid DNA was digested using 5 µl buffer, 2 µl restriction enzyme in at total volume of 50 µl with RNase free water. This was left at 37°C for 2 h and purified using a Qiagen PCR purification kit according to manufacturer's instructions. The linearized DNA was analysed using a nanodrop to determine the concentration. For capped RNA synthesis 1 µg linearized DNA, 10 µl NTP/CAP, 2 µl buffer, 2 µl SP6/T7 RNA polymerase(20U/ul; Promega) were mixed and made up to 20 µl with RNase free water. This was left for 2 h at 37C. 1µl of DNase-1 (2 U/ul; Roche) was added for 15 min at 37C. 1 µl was analysed by gel electrophoresis. The capped RNA then underwent lithium chloride purification and was split into 1 ng/ 10 nl stocks used to make 5 µl aliquots and stored at -80°C. The plasmids used are displayed in **Table 3**.

**Table 3: Plasmids used for capped RNA synthesis**

Clone name	Sense RE	Sense polymerase	Source
Noggin	Not1	Sp6	Dr Dave Hsu
Wnt1	Xba1	Sp6	Dr Oliver Destree
Lac-Z	Not1	Sp6	Dr Maggie Walmesly
GFP	Not1	Sp6	Dr Maggie Walmesly

At the two-cell stage cRNA was injected into the animal pole of both blastomeres with either Noggin cRNA alone to induce neuroectoderm or Noggin and Wnt cRNA to induce neural crest. Non-injected embryos gave caps with ectoderm cell fate. 2 h following injection Ficoll solution was replaced with 0.1x MMR/gentamycin (1:1000) and the embryos were left to develop until stage 9 when animal caps were cut (**Figure 4**).

Caps were cut in filter-sterilised 1XMMR and the vitelline membrane was removed using sharp forceps and the cap was cut from the centre of the animal hemisphere. Caps were transferred to a 12-well dish containing 0.7MMR, 1mg/ml Bovine serum albumin, 100 µg/ml gentamycin. Caps were kept at a constant temperature until they reached stage 15, when they were harvested for RNA extraction.

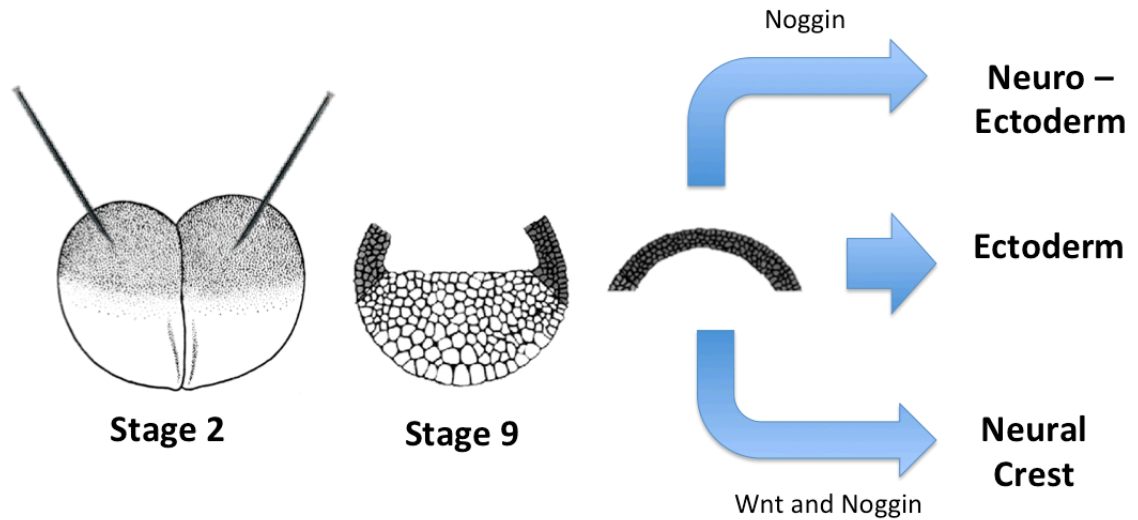


**Figure 4: A schematic drawing of an animal cap assay.**

Embryos are injected at stage 2 with cappedRNA and left to develop until stage 9 when the animal cap was removed. Animal caps were left to develop until stage 15 where they underwent RNA extraction.

## 8.2. RNA extraction for sRNA sequencing

RNA extraction was completed using the miRCURY™ RNA Isolation (for tissue) kit according to manufacturer's instructions. In summary, animal cap tissue was placed in a 2 ml Eppendorf tube and flash frozen in liquid nitrogen. To homogenise the tissue, 300 µl of lysis solution was added to the sample and put through bead homogenization for 1.5 min at 50 shakes per second using TissueLyser (Qiagen). 600 µl of RNase free water and 20 µl of proteinase K was added to the lysate and incubated at 55°C for 15 min and spun for 1 min at 14,000 x g. 450 µl of 95% ethanol was added and the lysate was passed through a column by centrifuging for 1 min at 14,000 x g. 400 µl of wash solution was subsequently passed through the column at 14,000 x g for 1 min to wash the resin. This was repeated a further two times. The resin was then dried by a 2 min spin at 14,000 x g. The RNA was eluted by adding 50 µl of elution buffer to the column and spun for 2 min at 200 x g followed by 1 min at 14,000 x g. The 50 µl was then split into two 25 µl samples (one for sRNA library construction and one for validation of tissue induction). RNA integrity was confirmed by gel-electrophoresis

### 8.2.1. RNA Quantification

RNA was quantified using a standard spectrophotometer;  $^{260}/_{280}$  ratios of 1.8-2.0 indicated good quality RNA.

## 8.3. Semi-quantitative mRNA PCR to validate animal cap tissue induction

### 8.3.1. Reverse Transcription

First strand cDNA Synthesis with SuperScript II Reverse Transcriptase:

For reverse transcription, 500 ng RNA and 1  $\mu$ l Oligo(dT) 12-18 primer were mixed and brought up to 11  $\mu$ l using nuclease-free water. The mixture was heated to 70°C using a PTC- 100 Peltier Thermal Cycler (Bio-Rad) for 10 min before being put back on ice where 4  $\mu$ l 5X First-Strand Buffer (Sigma, UK), 1  $\mu$ l 10mM dNTPs (Roche UK), 1  $\mu$ l RNasin (40U/ $\mu$ l; Roche, UK), 1  $\mu$ l of SuperScript II Reverse Transcriptase (200U/ $\mu$ l; Invitrogen, UK) and 2  $\mu$ l 100mM DTT (Sigma, UK) were added to each tube. The samples were incubated at 42°C for 1 h.

TaqMan RT-PCR:

The reaction mixture was as follows: 12.5  $\mu$ l of Bioline Taq mix (Bioline, UK), 1  $\mu$ l cDNA as a template, 2  $\mu$ l of forward primer, 2  $\mu$ l of reverse primer made up to 25  $\mu$ l with nuclease-free water. The reaction conditions were 95°C for 3 min, 25-35 cycles (specific for each primer set) of 95°C for 30 sec, 50-60°C temp gradient for 1 min (specific for each primer set), 72°C for 2 min and one final 72°C for 10 min. 5  $\mu$ l samples were then analysed by agarose gel electrophoresis.

## 9. sRNA library construction for Next Generation Sequencing

### 9.1.1. HD adapter synthesis

To phosphorylate the adapters, 6  $\mu$ l of 100  $\mu$ M 3' adapter (Sigma), 10  $\mu$ l of 10X T4 polynucleotides kinase buffer, 10  $\mu$ l of 10 mM ATP, 72  $\mu$ l of nuclease free

water and 2  $\mu\text{l}$  of T4 polynucleotide kinase (10 U/ $\mu\text{l}$ ) was mixed and incubated at 37°C on the DNA Engine Dyad Peltier Thermal Cycler (Genetic Technologies) for 30 min. The phosphorylation product was then mixed with 2  $\mu\text{l}$  of 5 mg/ml glycogen, 10  $\mu\text{l}$  of 3 M sodium acetate and 250  $\mu\text{l}$  of ethanol and stored O/N at -20°C. The sample was centrifuged at 20,000 x g for 10 min at 4°C and the supernatant was removed. The pellet was washed in 250  $\mu\text{l}$  of 80% ethanol and centrifuged at 20,000 x g for 5 min at 4°C. The pellet was then air dried and resuspended in 12  $\mu\text{l}$  of water. To adenylate the adapters 2 reaction mixtures (**table 8**) were incubated at 65°C for 1 h on the thermal cycler and then at 85°C for 5 min to inactivate RNA ligase.

**Table 4: Master mix for adapter adenylation**

Reagent	1 Reaction
Phosphorylated DNA oligonucleotide	4.5 $\mu\text{l}$
10X 5' DNA Adenylation reaction buffer	4 $\mu\text{l}$
1 mM ATP	4 $\mu\text{l}$
Mth RNA ligase (NEB)	4 $\mu\text{l}$
Water	23.5 $\mu\text{l}$
Total volume	40 $\mu\text{l}$

Both samples were then combined, added to 200  $\mu\text{l}$  of phenol:chloroform:isoamyl (1:1:1), 120  $\mu\text{l}$  of water and centrifuged at 20,000 x g for 10 min at 4°C. The supernatant was transferred and added to 50  $\mu\text{l}$  of water, 2  $\mu\text{l}$  of 5 mg/ml glycogen, 16  $\mu\text{l}$  of 3M sodium acetate, 400  $\mu\text{l}$  of ethanol and left to precipitate overnight at -20°C. The sample was then centrifuged at 20,000 x g for 15 min at 4°C and the supernatant was removed. The pellet was washed in 500  $\mu\text{l}$  of 80% ethanol, centrifuged at 20,000 x g for 5 min at 4°C and left to air dry. Finally, the pellet was resuspended in 20  $\mu\text{l}$  of water and run on a 16% (w/v) PAGE urea gel (**Table 5**).

**Table 5: Materials required for 16% (w/v) PAGE urea gel synthesis**

Reagent	Amount
Water	2.5 ml
5X TBE	1 ml
Urea (microwave for 20 secs after adding)	4.2 g
40% (w/v) (19:1) acrylamide/bis solution	4 ml
TEMED	5 $\mu$ l
10% (w/v) ammonium persulphate (APS)	100 $\mu$ l
Total volume	10 ml

In order to assess the quality and concentration of the adapter synthesis the samples were run alongside (**Figure 5**):

- 1) 5  $\mu$ l water + 1  $\mu$ l ScriptMiner adapter + 2  $\mu$ l Stop solution loading dye
- 2) 5  $\mu$ l water + 1  $\mu$ l 3' HD adapter + 2  $\mu$ l Stop solution loading dye
- 3) 4  $\mu$ l water + 1  $\mu$ l 3' HD adapter + 1  $\mu$ l non-adenylated adapter + 2  $\mu$ l Stop solution loading
- 4) 5  $\mu$ l water + 1  $\mu$ l non-adenylated adapter + 2  $\mu$ l Stop solution loading dye

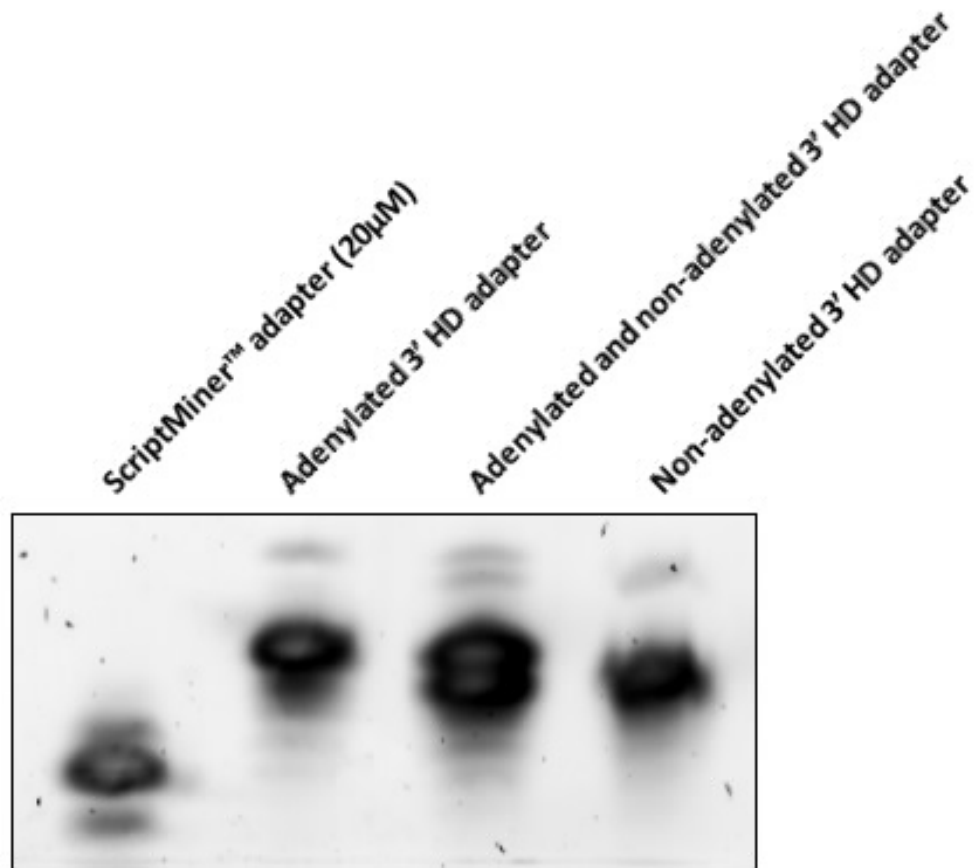


**Figure 5: HD adapter synthesis**

Concentration of adenylylated 3' adapter is 40uM. To assess the concentration of the adenylylated adapter (lane2) it was run next to a 20uM ScriptMiner adapter (lane1) a non adenylylated adapter (lane4) and a combination of both adenylylated and non-adenylylated adapters (lane3). From this it appears that the adenylylated adapter is approximately twice the concentration of the ScriptMiner therefore making it 40 µM/µL

## 9.2. Illumina SRNA preparation

### 9.2.1. 3' adapter ligation

To ligate adapters to RNA, 3 µg of RNA was made up to 11.25 µl with nuclease free water, mixed with 1 µl of 3' HD adapter and incubated at 70°C for 2 min to denature the RNA. Next, a master mix was made (**Table 6**). Following a pulse spin, 4 µl of 50% (w/v) PEG solution (NEB) was added and incubated at 26°C for 2.5h.

**Table 6: Master mix for 3' adapter ligation**

Reagent	1 reaction
T4 RNA ligase 2 (NEB) 10X Buffer	2 µl
RNaseOUT (Invitrogen) 40 U/µL	0.75 µl
T4 RNA Ligase 2 (200U/µL) (NEB)	1 µl
Total volume	20 µl

### 9.2.2. RNA clean up

The RNA was then cleaned using RNA Clean and Concentrator™ -25 (Zymo Research) according to manufacturer's instructions. In summary, 40ml of RNA Binding Buffer and 60ml of ethanol was mixed to each sample and centrifuged through a Zymo-Spin Column at 12,000 x g for 1 min. 800 µl of RNA Wash Buffer was then centrifuged through the column at 12,000 x g for 30 secs. This was repeated using 400 µl RNA Wash Buffer. The column was then centrifuged dry for 2 mins at 12,000 x g. Finally, RNA was eluted using 13.5 µl of RNase-Free water by centrifugation at 12,000 x g for 1 min.

### 9.2.3. Deadenylation and removal of 3' adapters

To deadenylate the adapter, 3.9 µl of a master mix (**Table 7**) was added to each sample, mixed and incubated at 30°C for 30 mins. To stop the reaction, 4 µl of

25mM EDTA was added.

**Table 7: Master mix for deadenylation of adapter**

Reagent	1 reaction
10X deadenylase buffer (Epicentre)	1.6 $\mu$ l
100 mM DTT (Epicentre)	0.8 $\mu$ l
RNaseOUT 40U/ $\mu$ L (Invitrogen)	0.5 $\mu$ l
5' deadenylase (10U/ $\mu$ L (Epigenetics))	1 $\mu$ l
Total volume	3.9 $\mu$ l

To degrade the adapters, a 10  $\mu$ l master mix (**Table 8**) was added to each sample and incubated at 37°C for 30 mins.

**Table 8: Master mix for degradation of adapter of adapter**

Reagent	1 reaction
500 mM Tris-HCl pH 9 (Sigma)	2 $\mu$ l
50 mM MgCl <sub>2</sub> to be determined	7 $\mu$ l
RecJ Exonuclease (10U/ $\mu$ l) (epicentre)	1 $\mu$ l
Total volume	10 $\mu$ l

#### 9.2.4. 5' HD adapter ligation

For ligation, 5  $\mu$ l of a master mix (**Table 9**) was added to each sample. 7  $\mu$ l of 50% (w/v) PEG was then added to each sample and incubated at 26°C for 2 h. Following incubation, 10  $\mu$ l of nuclease free water was added to each sample.

**Table 9: Master mix for 5' adapter ligation**

Reagent	1 reaction
T4 RNA ligase 1 buffer (epicenter)	1 $\mu$ l
10 mM ATP (NEB)	1 $\mu$ l
5' HD adapter (20 $\mu$ M)	2 $\mu$ l
T4 RNA ligase (epicentre) (do 2 mins before end)	1 $\mu$ l
Total volume	5 $\mu$ l

### 9.2.5. Di-Tagged RNA purification

The RNA was then cleaned using RNA Clean and Concentrator™ -25 (Zymo Research) according to manufacturer's instructions. In summary, 100  $\mu$ l of RNA Binding Buffer and 150  $\mu$ l of ethanol was mixed to each sample, and centrifuged through a Zymo-Spin Column at 12,000 x g for 1 min. 400  $\mu$ l of RNA Prep Buffer was then centrifuged at 12,000 x g for 1 min followed by 800  $\mu$ l of RNA Wash Buffer at 12,000 x g for 30 secs. This was repeated using 400  $\mu$ l RNA Wash Buffer. The column is then centrifuged dry for 2 min at 12,000 x g. Finally, RNA was eluted twice using 13.5  $\mu$ l of RNase-Free water by centrifuging at 12,000 x g for 1 min each time. The final eluate was then made up to 30  $\mu$ l using nuclease free water.

### 9.2.6. Reverse transcription

In order to synthesise cDNA 10  $\mu$ l of master mix (**Table 10**) was added to each 30  $\mu$ l sample of purified di-tagged RNA. The samples underwent a pulse spin and were incubated at 37°C for 20 mins followed by 85°C for 15 mins to terminate the reaction.

**Table 10: Master mix for reverse transcription**

Reagent	1 reaction
1X MMLV reverse transcription buffer (epicenter)	4 $\mu$ l
10 mM dNTP premix	2 $\mu$ l
100 mM DTT (epicenter)	2 $\mu$ l
RTP (20 $\mu$ M)	1 $\mu$ l
High performance MMLV reverse transcriptase	1 $\mu$ l
Total volume	10 $\mu$ l

### 9.2.7. Polymerase chain reaction

For PCR amplification 15  $\mu$ l of master mix (**Table 11**) was added to each PCR tube along with 1  $\mu$ l of secondary index primer (alternative primers for alternative samples) and 4  $\mu$ l of cDNA.

**Table 11: Master mix for PCR amplification**

Reagent	1 reaction
Nuclease free water	9.3 $\mu$ l
10 mM dNTPs	0.5 $\mu$ l
5X high fidelity phusion buffer	4 $\mu$ l
Illumina RP-1 primer (10 $\mu$ M)	1 $\mu$ l
Phusion DNA polymerase (2 U/ $\mu$ L)	0.2 $\mu$ l
Total volume	15 $\mu$ l

cDNA was amplified using the following amplification programme: pre-incubation for Phusion DNA polymerase activation at 98°C for 30 s, followed by either 13, 15 or 17 amplification cycles of denaturation at 98°C for 10 secs, annealing at

60°C for 30 secs and extending at 72°C for 15 secs. The programme finished with a final extension at 72°C for 10 mins.

### 9.2.8. 8% PAGE Gel and library band recovery

20 µl of each sample was run on an 8% (w/v) PAGE gel (**Table 12**) at 120V for approximately 2 h and then stained with SYBR gold (in 0.5X TBE). Gels were imaged using a Bio-Rad Molecular Imager FX.

**Table 12: Materials required for 8% PAGE gel synthesis**

Reagent	Amount
Water	20 ml
5X TBE	3 ml
40% (w/v) (19:1) Acrylamide/bis solution	6 ml
TEMED	15 µl
10% (w/v) ammonium persulphate (APS)	300 µl
Total volume	30 ml

## 10. Bioinformatic analysis

Most of the bioinformatic analyses were performed in collaboration with Dr. Janet Higgins and Dr. Leighton Folkes who will be acknowledged where appropriate.

### 10.1.1. Raw sequence mapping and filtering

FASTQ files were converted to FASTA format and adapter sequences were trimmed with custom pearl scripts. Only reads ranging from 16 to 35 nucleotides in length that mapped perfectly by PatMaN v1.2.2 (Prüfer et al., 2008) to the latest version of the *Xenopus laevis* genome assembly (8.0).

### 10.1.2. Profiling of mapped reads to miRBase

Mapped reads were profiled to miRBase release 20 with the UEA SRNA Workbench tool, miRProf. A whole genome annotation of miRNAs was carried out, using all the hairpins in miRBase for BLASTN searches (E-value  $<1e-06$ ) against the *Xenopus laevis* genome assembly 8.0 (removing any hits which have  $\geq 30$  blast hits or hairpin length  $\leq 55$ ). MiRNAs with a low abundance ( $<100$  sequences mapping to the hairpin across all the samples) and miRNAs which did not have a typical hairpin structure, were removed from subsequent analyses (all hairpins were retained for a family if at least one member of the family had alignments).

### 10.1.3. Differential Expression Analysis

Counts were obtained for all the reads aligning to each hairpin for each sample. These counts were used as input for DESeq2\_1.8.2. A Padj value of  $<0.001$  was used to call differential expression. Lists of miRNA which were either up or down regulated between tissues were obtained. Overlap between these lists was used to find miRNAs with a tissue specific expression. A heatmap and PCA plot were generated using the rlog (*regularized-logarithm transformation*) transformed values. Principal components analysis (PCA) was used to visualize sample-to-sample distances. Heat maps were used to show how much each gene deviates in a specific sample from the gene's average across all samples.

### 10.1.4. Novel miRNA predictions

Novel microRNAs were predicted using the three UEA SRNA workbench tools – miRCat, miRCat 2 and miRDeep v.2-0.07 (Stocks et al., 2012, Paicu et al., 2017, An et al., 2013, Friedlander et al., 2008). An intersect bed was used to find hairpins that were predicted by all 3 tools. Those miRNAs predicted by all three tools and those with a good hairpin structure (confirmed manually) were then used for subsequent analyses. These hairpins were clustered using cd-hit-est, hairpins with a sequence similarity  $> 80\%$  were clustered together. The principle behind the novel miRNA predictions was based on their sequence, their genomic location, their abundance and their predicted folded structure of the surrounding genomic sequence.

## **11. Validation of sRNA sequencing**

### **11.1.1. Quantitative miRNA qRT-PCR**

Total RNA was quantified and 10 ng of RNA was reverse transcribed to cDNA using universal cDNA synthesis kit (Exiqon, Vedbæk, Denmark). cDNA was diluted 1:40 and used in the reaction. PCR reactions were set up in triplicates with three biological replicates in ABI one step detection system using SYBR green master mix (Exiqon) following the manufacturer's instructions. The mature miRNA sequence was used to synthesize custom miRNA LNA PCR primer sets (Exiqon) (**Appendix 2**) snU6 was used as a control.

## **12. Experimental evaluation of putative miRNA targets**

### **12.1. Generation of miRNA sensing luciferase construct**

A Luciferase sensor construct for the EYA1-3'UTR was generated by Dr. Camille Viaut from the Münsterberg lab and generously provided for this experiment. Used sequence originated from chicken tissues, however EYA1 is homologous to the *Xenopus laevis* variant (**Figure 6A**).

### **12.2. Generating a mutant pGL3-EYA1 construct**

pGL3 mutant constructs were generated using the FastCloning strategy developed by Li et al. (2011).

#### **12.2.1. Mutagenesis PCR of pGL3-EYA1 construct**

A pair of primers placed in the ampicillin resistance gene were used as universal primers in the mutagenesis cloning. Primers were designed over the miRNA target site which contained mismatched nucleotides chosen to create an enzyme restriction site out of the miRNA target site (**Figure 6A-B**).

The two halves of each pGL3 construct were amplified using phusion High-Fidelity DNA polymerase (Finnzymes, NEB).

### Phusion PCR:

2.5  $\mu$ l Forward primer (10  $\mu$ M), 2.5  $\mu$ l Reverse primer (10 $\mu$ M) and 20ng pDNA were combined in a PCR tube with the mastermix displayed in **Table 13**:

**Table 13: Master mix for phusion PCR**

Reagent	1 reaction
Nuclease free water	31.5 $\mu$ l
10 mM dNTPs	1 $\mu$ l
5X high fidelity phusion buffer	10 $\mu$ l
Phusion DNA polymerase (2 U/ $\mu$ L)	0.5 $\mu$ l
Total volume	43 $\mu$ l

The reaction conditions were 98°C for 30 sec, 22 cycles of 98°C for 10 sec, 59°C temp gradient for 30 sec, 72°C for 2 min (Eya F)/ 4 min (Eya R) and one final 72°C for 10 mins.

Once finished, 5 U Dpn1 restriction enzyme (Promega) was added to the PCR mixture and incubated on a thermocycler at 37°C for 2 h to digest any remaining pDNA. PCR products were verified on an agarose gel.

1  $\mu$ l of each the products were transformed into 200  $\mu$ l of DH5 $\alpha$  competent cells for recombination.

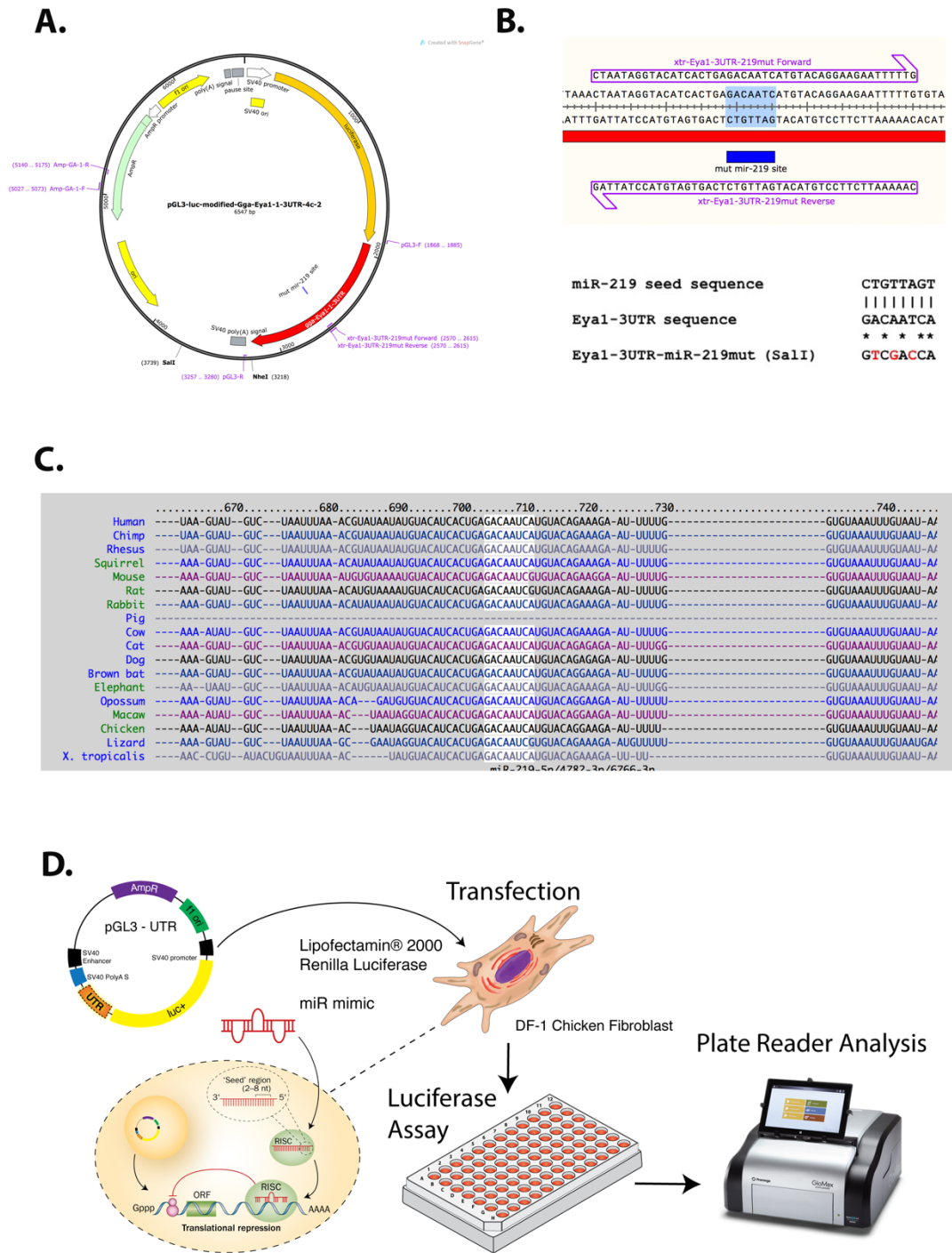


**Figure 6: Luciferase assay protocol used to assess EYA1 as a target of miR-219**

Modified pGL3 plasmid with the region of the 3' UTR of EYA1 incorporated which includes the miR-219 binding site. Forward and Reverse EYA1 primers designed for mutagenesis are labelled in purple (A). A zoomed in version of the primers designed for mutagenesis of EYA1 3'UTR. By mutating three nucleotides the miR-219 target sequence was changed to a SalI restriction site (B). An alignment of the Eya1 3'UTR sequence of various organisms. The region highlighted in white in the target sequence for miR-219 (C). A schematic drawing of the luciferase assay protocol (D).

## 12.3. Luciferase assays of PGL3-EYA1 construct

### 12.3.1. Cell culture

Chicken DF1 fibroblast cells were cultured in Dulbecco's modified Eagle medium (DMEM) containing GutaMAX, 1g/L D-glucose and pyruvate (Life Technologies), with 10% fetal bovine serum (FBS) (Gibco, Life Technologies) and 1% penicillin-streptomycin (Gibco, Life Technologies) added on first use. Cells were passaged every other day by treatment with 1ml 0.25% Trypsin-EDTA (Gibco, Life Technologies) for 30 secs at RT followed by removal of trypsin and further incubation at 37°C for approximately 2 mins. Cells were then transferred to a new flask containing media at a 1:4 dilution. Cells were maintained in a humidified cell culture incubator at 37°C with 5% CO<sub>2</sub>.

### 12.3.2. Cell transfection

Cells were detached from the flask surfaces as described in 9.3.1 and counted using a hemocytometer. Approximately 7,000 cells were added to each well of a 96-well plate and media added to make a volume of 100 µl. Cells were incubated for 24 h to allow re-attachment to the plate surface. The medium was removed and replaced with 50 µl serum-free medium. A transfection mix was prepared as described below.

#### Transfection mix 1:

100 ng pGL3 pDNA

50 nM miRNA mimic

25 ng Renilla pDNA

x µl Serum free media to a total volume of 25 µl

#### Transfection mix 2:

25 µl Serum-free media

0.2 µl Lipofectamine 2000 Transfection reagent (Life Technologies)

Tubes were left at RT for 5 mins. Transfection mixes 1 and 2 were combined and left at RT for 20 mins. 50  $\mu$ l of the combined transfection mix was added to the wells followed by 50 $\mu$ l of serum-free media and cells were left to incubate at 37C for 24 h in a humidified incubator. Custom siRNA oligos (Sigma) were used as miRNA mimics. Each construct was evaluated in the presence of the putative target miRNA mimic, a control miRNA (MISSION siRNA Universal negative control (#1) from Sigma) and without a miRNA mimic.

### **12.3.3. Luciferase assay**

A Dual-Luciferase Reporter Assay System kit was used to assess luciferase activity (Promega). This kit allows *Renilla* Luciferase to serve as an internal control of transfection efficiency.

Cells were washed twice with cold PBS and 60  $\mu$ l 1x Passive Lysis buffer was added to each well and the plate was rocked gently for at least 15 mins. 10  $\mu$ l lysis solution and 50  $\mu$ l luciferase assay reagent II were combined and photo emission was measured at 562 nm using a multi-label counter (Perkin Elmer). 50  $\mu$ l Stop and Glo reagent was added and the *Renilla* Luciferase photo emission measured at 562nm.

### **12.3.4. Normalisation of luciferase assay data**

Three biological replicates, each with four technical replicates, were performed. Each firefly luciferase assay reading was normalized to its *Renilla* luciferase reading. The average activity of the plasmid transfected with control mimic was set to 100%. The activity of the constructs transfected with the putative target miRNA mimic was normalized to the average activity of the plasmid transfected with the control mimic. A Mann-Whitney test was performed using GraphPad Prism version 6 for Mac (GraphPad Software, San Diego California, USA, [www.graphpad.com](http://www.graphpad.com)).

## **13. Microsurgical removal of cranial neural crest tissue for RNA sequencing**

All dissections of neural crest tissue were carried out in collaboration with Prof. Anne-Helene Monsoro-Burq at the Institut Curie (Orsay).

Morpholinos were injected into one dorsal blastomere of a four-cell embryo with the morpholinos at a concentration of 60ng. GFP was co-injected as a tracer. Stage 14 or stage 17 embryos were placed in a 60 mm Petri dish coated with 10ml of 2% agarose in 1/3 MMR. The vitelline envelope was removed manually using forceps. For dissection, depressions were made in the agarose using the forceps and the embryos were placed in the holes dorsal side up. Once secured the first incision was made in the lateral part of the anterior neural fold using an eyebrow knife and an insect pin. The second incision was then made parallel to the first in the more dorsal part of the neural fold using the same instruments. The third incision was then made perpendicular to the first two incisions at the posterior side. Using the side of the eyebrow knife, the NC were then detached from the embryo starting from the third incision. The NC tissue was easy to distinguish as it is rather greyish, while the underlying cephalic mesoderm is white. The two tissues were carefully separated and then the NC was detached anteriorly from the optic vesicle the explant was cut free. Explants were then transferred from the dissection dish into an Eppendorf tube containing 50 µl of TRIzol® using a P20 pipet, immediately vortexed for 30 secs, left for 5 mins at RT and then stored at -20°C prior to extraction.

### **13.1.1. Total RNA purification for RNA seq**

TRIzol® was completed to 400 µl and then all samples were sheared by pipetting up and down with a 25 G needle and a 1 ml syringe. Chloroform was added in a 1/5 volume ration and vortexed for 15 seconds. Samples were left for 4 min at RT and then inverted multiple times to form a homogenous suspension. Pellet Phase Lock Gels were then prepared by centrifuging at 12,000-16,000 x g at 4°C for 20 seconds. Samples were transferred onto the gels and spun at 12,000-16,000 x g at 4°C for 5 min to separate the phases. The nucleic acid phase was then

transferred to a new 1.5 ml Eppendorf tube containing 1 µl linear polyacrylamide (LPA, Ambion) and vortexed. Isopropanol was added at a ½ volume ratio, vortexed, left for 10 min and the samples were left for precipitation O/N at -20°C. Samples were centrifuged for 45 min at 4°C and the supernatant was removed. Freshly prepared 75% EtOH was used to wash the pellet by vortexing before spinning at max RPM for 10 min at 4°C. The supernatant was removed and the pellet air-dried for 10 mins. The pellet was resuspended in 30µl of nuclease free H<sub>2</sub>O (sigma). Of this 30 µl, 10 µl was transferred to a new tube for analysis via nanodrop, bioanlyser and q-PCR. The remaining 20 µl were stored at -80°C for RNA seq analysis.

### 13.1.2. Bioanalyser

RNA quality was examined using the Agilent 2100 Bioanalyser instrument along with the Agilent RNA 6000 Pico Kit (reorder-no 5067-1513). The Agilent 2100 Bioanalyser is a microfluidics based platform that separates RNA molecules depending on their sizes and is able to determine quantities of each molecule. Results can be analyzed with 2100 Expert software (Syngene, Cambridge, UK). Only samples with RNA integrity number (RIN) values of >7 were used for sequencing.

### 13.1.3. Reverse transcription

Following RNA purification, cDNA was synthesized using 4µl of RNA as a template. Samples were normalised using housekeeping genes during PCR.

For cDNA synthesis 4 µl total RNA + 1 µl Random Hexamers (0.05 µg/µl) were incubated at 65°C for 5 mins and then cooled on ice for 15-30 mins. 5 µl of RT mix was added (**Table 14**) and left at 42°C for 30 mins. Two tubes were prepared for each sample; one with Reverse Transcriptase added (RT+) and one without it (RT-) to check whether the RNA was contaminated with DNA.

**Table 14: Master mix for PCR amplification**

Reagent	Amount
5X Buffer	2 $\mu$ l
20 mM DTT	0.5 $\mu$ l
10 mM dNTPs	0.5 $\mu$ l
RNAsin	0.25 $\mu$ l
H <sub>2</sub> O	1.625 $\mu$ l
High performance MMLV reverse transcriptase (Promega)	0.125 $\mu$ l
Total volume	5 $\mu$ l

#### 13.1.4. PCR Amplification

Aliquots from both RT+ and RT- (water control) tubes were amplified for each sample. cDNA was diluted 1/10 and 2  $\mu$ l of the diluted cDNA was added to 5  $\mu$ l of SyberGreen mix (Applied Biosystems, UK), 1  $\mu$ l of 10  $\mu$ M Primer (0.5  $\mu$ l of forward and 0.5  $\mu$ l of reverse) and 2  $\mu$ l of RNase free H<sub>2</sub>O.

#### 13.1.5. RNA sequencing

RNA sequencing was carried out on nine samples all of which contained three replicates each (except miR-219 MO which contained four). The various treatment types can be seen in **Table 15**. All samples were tested prior to sequences using PCR (see sections 13.1.3 and 13.1.4) to detect expected gene expression. RNA samples were sent to Institut Curie (Paris) for library preparation and 50bp paired end sequencing on the HiSeq High Output run mode PE100 for sequencing.

Reads were aligned to the *Xenopus laevis* 9.1 genome reference (James-Zorn et al., 2015, Karpinka et al., 2015) using a topHat2 version 2.0.6 (Kim et al., 2013)

**(Appendix 4).** To carry out exploratory and differential expression analysis, the aligned reads were fed into the Bioconductor (Huber et al., 2015) RNA-seq workflow: gene-level exploratory analysis and differential expression (DE) (Love et al., 2015) which makes use of the DE tool called DEseq2 (Love et al., 2014). Genes with an adjusted p-value of 0.05 or below were considered significant and were reported by the workflow. The gene model used in the DE bioinformatic analysis was *X. laevis* 9.1, annotation version 1.8.3.2 primary gene model (gff3) (James-Zorn et al., 2015, Karpinka et al., 2015). Unannotated genes identified within the DE results were searched against the NCBI nucleotide collection (nr/nt) (Coordinators, 2013) using the local alignment search tool Blastn version 2.6.08 (Camacho et al., 2009) with default search parameters.

**Table 15: Samples collected for RNA sequencing (green boxes). All samples had three replicates except 219MO (stage 14) which had four. 219MO (stage 17) was not sequenced.**

	196a Control	196a MM	196a MO	219 control	219 MM	219 MO
Stage 14	✓	✓	✓	✓	✓	✓  (4 replicates)
Stage 17	✓	✓	✓			

## Chapter 3: Identification of miRNAs in neural crest cells

---

Throughout the literature, it has been shown that miRNAs are key regulators during the differentiation stages of NC, however, the role of miRNAs in NC specification is yet to be investigated. To explore the role of miRNAs during NC specification we first set out to identify candidate miRNAs located within the NC region. To achieve this, two approaches were chosen. The first was a candidate approach which involved looking through a WISH database (XenmiR) and characterising candidate miRNAs expression further. The second was an unbiased sRNA (sRNA) sequencing approach comparing the miRNA profile of induced NC tissue with neural tissue.

### **The XenmiR database; a candidate approach**

#### **13.2. Introduction**

The first approach taken to identify candidate miRNAs in the NC was the 'XenmiR' approach'. The main working aim of this, was to identify miRNAs that are in the developing NC tissue. To achieve this, WISH was completed for 180 mature miRNAs using Locked Nucleic Acid (LNA) probes from Exiqon to detect NC localisation. Here, a summary of the WISHs completed in this project is provided along with the subsequent selection of miRNAs for further investigation.

##### **13.2.1. The XenmiR database**

In recent years, miRNAs have been shown to play a major role in many developmental processes such as early patterning and muscle development (Ebert and Sharp, 2012, Goljanek-Whysall et al., 2014). Although hundreds of miRNAs have been identified and deposited into the miRNA registry miRBase (Kozomara and Griffiths-Jones, 2014), limited data are available on their expression patterns during key developmental stages, including NC development. Such information is important to consider when investigating a

miRNAs potential function in development. To begin to understand the function of miRNAs during embryogenesis, WISH was carried out for 180 miRNAs to characterise their spatiotemporal expression patterns. These expression profiles were then used to locate miRNAs specific to NC regions.

### **13.2.2. Expression analysis using WISH**

The technique used for profiling during this approach was WISH. WISH is a powerful method used to determine expression profiles and has been used extensively over the last 25 years (Hemmati-Brivanlou et al., 1990). Due to the small size of a miRNA, WISH has proved to be a difficult technique for looking at miRNA expression. Initially, probes against the longer, but short-lived, primary transcripts were used (Hubbard et al., 2005). An alternative technique, Northern blot analysis, only provides limited spatial and temporal resolution and is therefore not an ideal alternative. A more recent technology developed by Exiqon, using modified oligos containing miRCURY™ LNA (locked nucleic acid) nucleotides as probes (<http://www.exiqon.com/>), has enabled the clear identification of specific expression patterns of mature miRNAs. LNA probes bind more strongly to complementary sequences and provide the required specificity for detection of mature miRNAs by WISH (Wienholds et al., 2005, Darnell et al., 2006, Sweetman et al., 2006).

## **13.3. Results**

### **13.3.1. Expression profiling of 180 miRNAs reveals diverse expression patterns throughout various developing organs and tissues**

The expression patterns of 180 miRNAs in *Xenopus laevis* were characterised (Ahmed et al., 2015). These have now been made freely available and can be accessed using the XenMARK and Xenbase websites (Karpinka et al., 2015, Gilchrist et al., 2009, Ahmed et al., 2015). At the time of starting this project there were 180 miRNAs identified in *Xenopus laevis* and *tropicalis* as shown in miRBase (Kozomara and Griffiths-Jones, 2014). In collaboration with Exiqon, 174 LNA probes were generated against these miRNAs. The probes were designed to work at the same hybridisation temperature of 50°C. This enabled us to carry

out WISH in a high throughput manner.

Of the 174 miRNAs tested, 140 showed expression at some stages in the developing embryo. Analysis of the expression patterns showed that many of the miRNAs were expressed during development and many of them were also restricted in their expression. **Figure 7** shows examples of some of these miRNAs with very specific expression patterns. Please refer to Ahmed et al. (2015) for more in-depth information about the expression profiles of other miRNAs as this will not be discussed further in this thesis.

### **13.3.2. LNA WISH on potential neural crest miRNAs**

From this dataset, several miRNAs became interesting candidates because their expression was detected in the NP and/or NPB at neurula stages as well as having expression in the branchial arches at tailbud stages. Using these WISH, eight preliminary candidates were selected for further analysis.

For these candidates, a more vigorous investigation of their precise expression profile over the neurula stages was conducted and is summarised in **Figure 8**. WISH was completed at NC specification (stage 15) and later just prior to NC delamination (stage 17-18) for each of the candidates. LNA WISHs were compared to the expression pattern of the neural marker *Sox2* and the NC marker *Sox10* to judge localisation of expression. The results demonstrate that eight of the candidate miRNAs had expression patterns that overlapped with both *Sox2* and *Sox10* therefore indicating that the miRNAs are expressed in the NP tissue and the developing NC tissue. At stage 15/16 the region that is labelled by *Sox10* that gives rise to the NC is named the NPB. Expression in this region was particularly apparent for miR-196a (**Figure 8 E and Ei**).

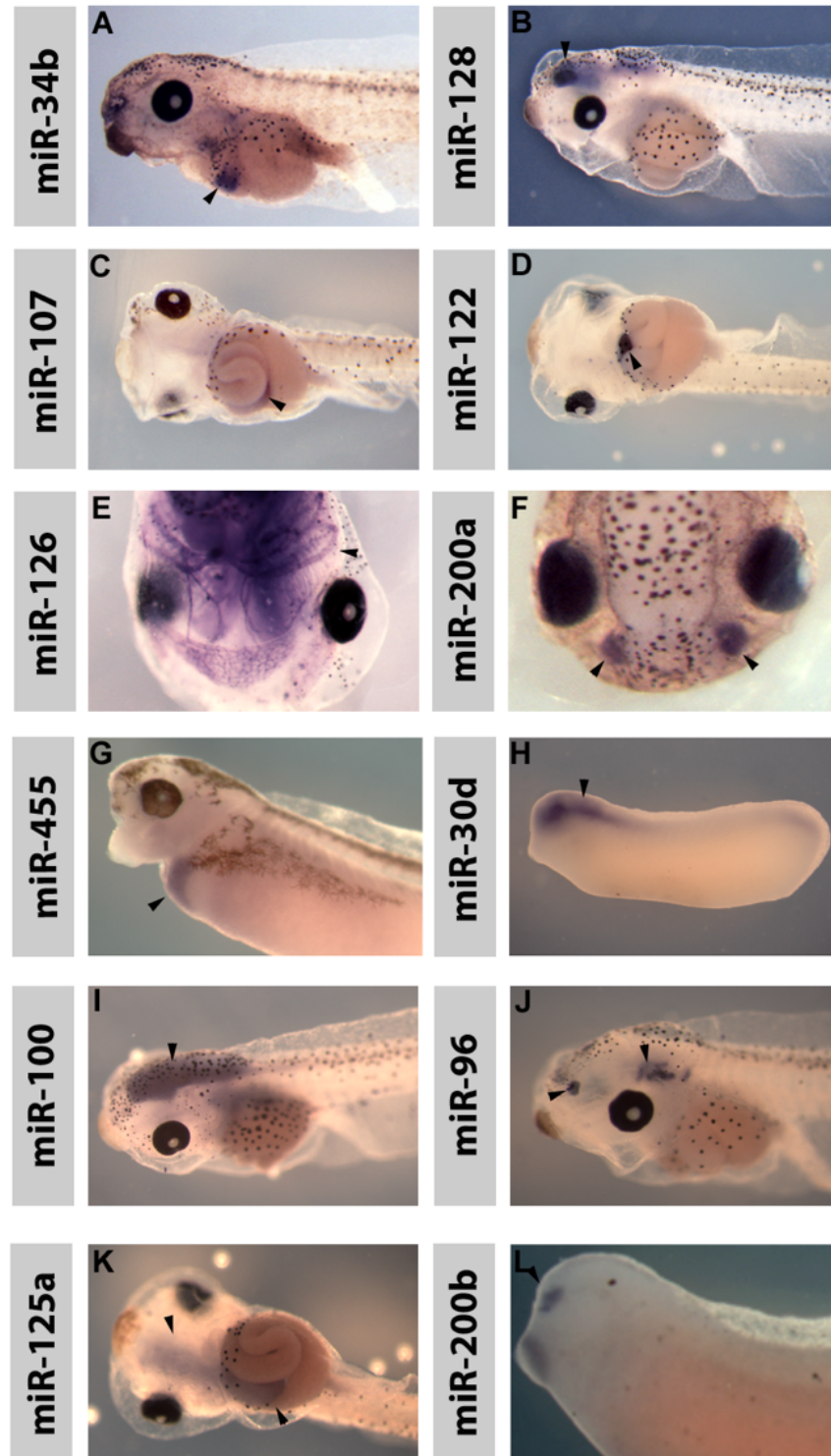


**Figure 7: *Xenopus* miRNA expression in a diverse number of developing organs and cell types.**

Expression patterns of *Xenopus laevis* miRNAs are shown at varying stages. Arrowheads point to relevant expression. Views are lateral with anterior to left except (C, D and K) which is a ventral view with anterior to the left and (E) and (F) which are dorsal views with anterior to the bottom. MiR-34b, pancreas; miR-128, brain; miR-107, gut; miR-122, liver; miR-126, blood vessels; miR-200a, olfactory placodes; miR-455, liver; miR-30d, brain; miR-100, brain; miR-96, brain and olfactory placodes, miR-125, brain and gut, miR-200b, olfactory placode (Ahmed et al., 2015).

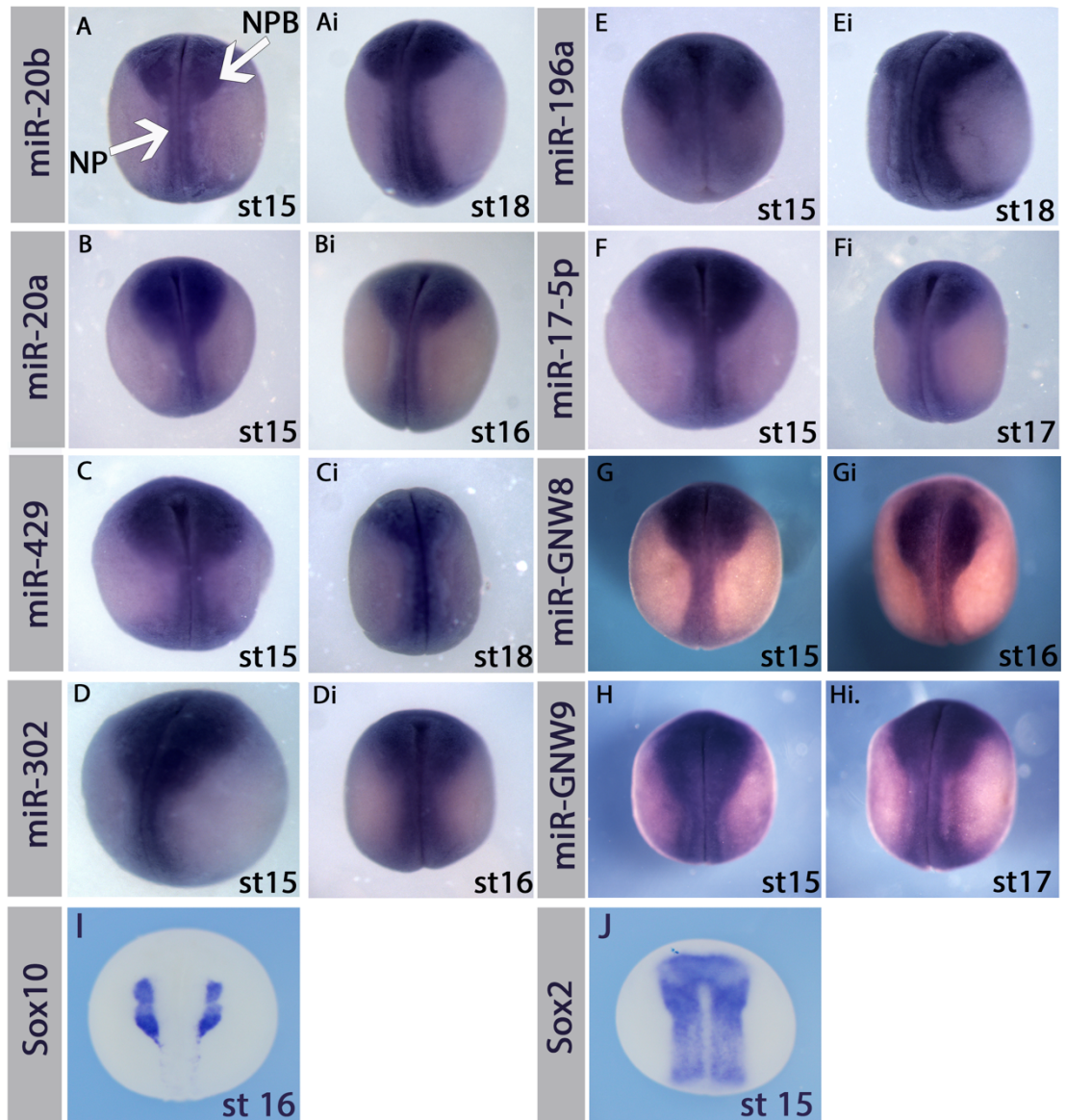


**Figure 8: LNA WISHs on neurula staged embryos show expression in the neural plate and neural plate border for all candidate miRNAs**

Expression patterns of eight *Xenopus laevis* miRNAs are shown at neurula stages. *Sox10* WISH labels the NPB region (I) and *Sox2* staining labels the NP region (J). For all eight miRNAs the expression is noted in the neural plate (NP) and in the neural plate border (NPB), this is indicated with white arrows (A). Views are dorsal with anterior to the top. The most apparent expression of a miRNA in the NPB region is miR-196a (E).

### 13.3.3. Co-expression analysis of candidate miRNAs with the NC marker *Sox10*

#### 13.3.3.1. *miR-196a and miR-302 expression overlaps with the NC marker Sox10*

To see if the expression of these miRNAs truly overlap with that of the NC, double WISH using the NC marker *Sox10* were completed. For this experiment, NBT was used as the substrate for the LNA WISH resulting in a blue precipitate at the location of miRNA expression. Immediately after this, a second WISH, using fast red as a substrate, was carried out for the known NC marker *Sox10* resulting in a red precipitate labelling the NC. These WISH were completed on late neurula stages (stage 17-18).

Of the eight miRNAs that underwent this experiment, two miRNAs came back as being expressed in the same region as the NC marker *Sox10*. This was seen to be true for miR-196a and miR-302 (**Figure 9 A and F**). Another four of the miRNAs (miR-17-5p, miR-30a-3p, miR-429 and GNW8) also appeared to have some overlap with *Sox10* but the overlap was not as evident as with miR-196a and miR-302 (**Figure 10**). Successful double WISH for miR-20a, miR-20b and miR-GNW9 were not produced as the background from the LNA WISH was too high (data not shown).

#### 13.3.3.2. *Sectioned double WISH clearly demonstrate the overlap between miR-196a and miR-302 with the NC marker Sox10*

Often, with double WISH, the dark NBT staining masks the fast-red staining. To overcome this problem, the embryos were subjected to sectioning following WISH and the fast red was visualised with fluorescence to confirm expression localisation.

Sectioning of the embryos revealed that both miR-196a and miR-302 are expressed in both the NP and the NPB. This expression pattern clearly overlapped with the NC marker *Sox10* providing evidence that both miRNAs are co-expressed at the NPB within the developing NC (**Figure 9B-J**).

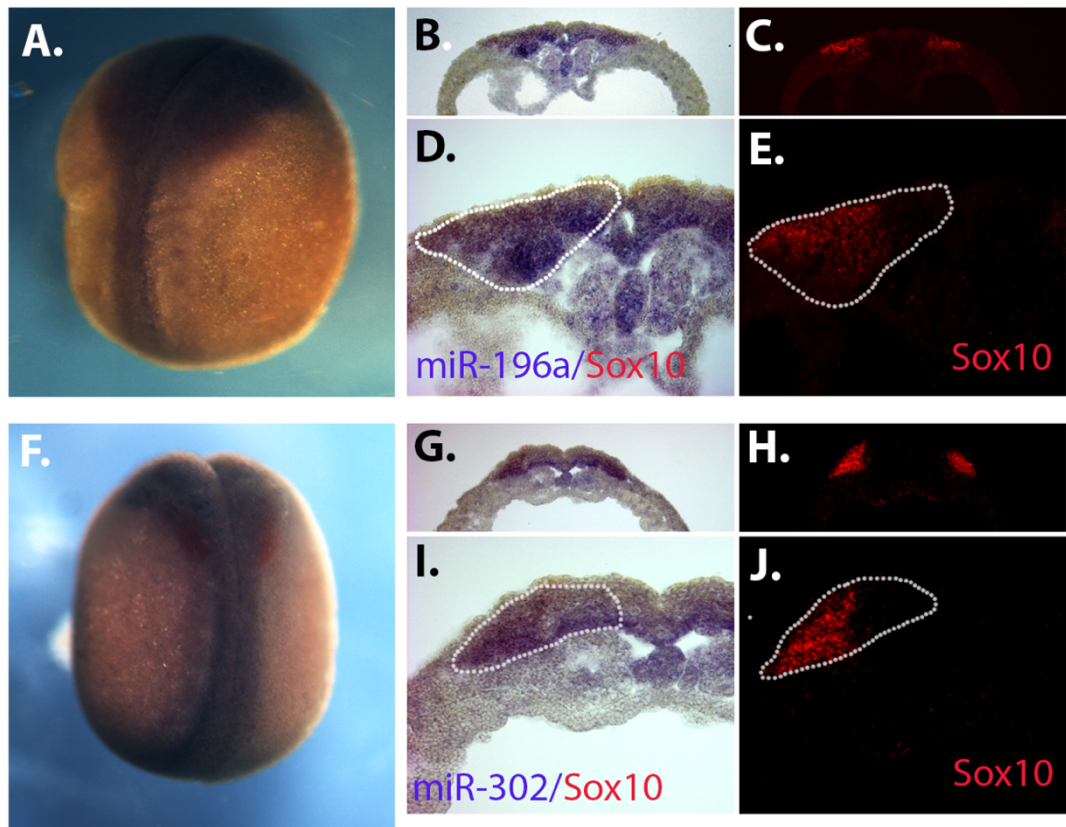


**Figure 9: MiR-302 and miR-196a have clear a overlap in expression with the NC marker *Sox10***

Double WISH of miR-196a (A) and miR-302 (F) with the NC marker *Sox10*. Embryos are at stage 17/18 (late neurula) and are shown with a dorsal view with anterior at the top. Transverse sections show that both miR-196a (B-E) and miR-302 (G-J) are expressed in both the NP and the NPB (indicated with a white dotted line) and have a significant overlap with the expression of *Sox10*.

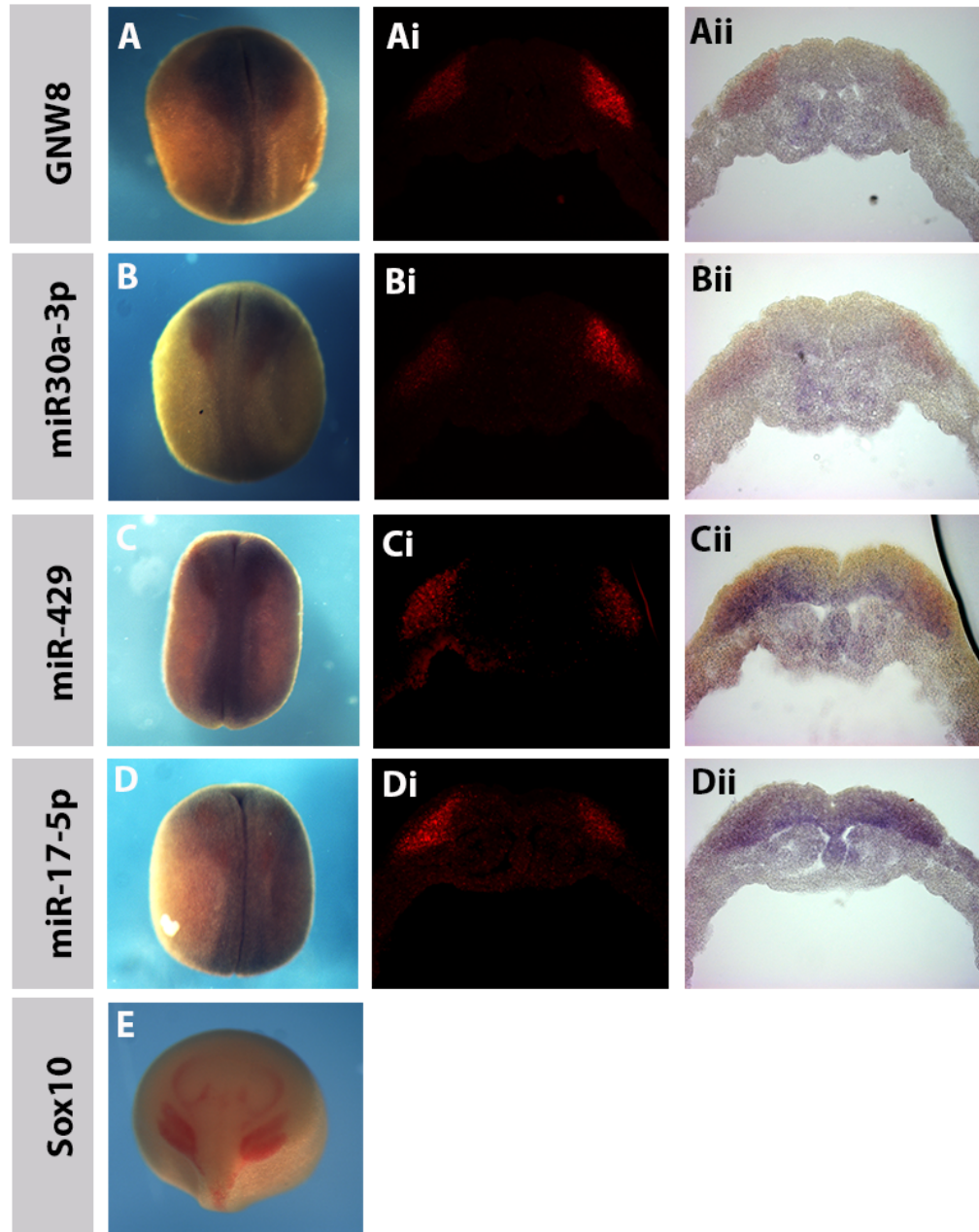


**Figure 10: GNW8, miR-30a-3p, miR-429 and miR-17-5p all show partial overlap in expression with the NC marker *Sox10***

Double WISH of GNW8 (A) miR-30a-3p (B) miR-429 (C) and miR-17-5p with the NC marker *Sox10* (E). Embryos are at stage 17/18 (late neurula) and are shown with a dorsal view with anterior at the top. Sectioning shows that all four of the miRNAs appear to have some overlap with the NC marker *Sox10* but this overlap is not as pronounced as for miR-196a or miR-302 (Figure 9).

# **Next generation sequencing of sRNAs in induced neural crest and neural tissue**

## **13.4. Introduction**

In addition to utilising the XenmiR database, a second, approach was also employed to identify miRNAs within the NC. Whilst designing this experiment, the main working aim was to try and identify both known and novel miRNAs which are specific to the NC tissue when compared to neural tissue. To achieve this, *Xenopus* tissue was induced to become either NC or neural using the animal cap method (see section 13.5.1.1). This tissue was then sequenced for sRNAs along with control ectoderm tissue and blastula tissue. Bioinformatic analysis was performed to identify differentially expressed miRNAs. Here, a summary is provided of the sequence strategy employed in this project along with the bioinformatic analysis of all known and novel miRNAs identified in the samples.

### **13.4.1. Techniques for assessing miRNA expression**

Currently, there are several methods for miRNA expression analysis including hybridisation-based miRNA microarrays, quantitative reverse transcription-PCR (qRT-PCR), and sRNA library sequencing. Microarrays involve the hybridisation of labelled sRNAs to oligonucleotide probes on a platform (Yin et al., 2008). In regard to microarray analysis, the design of miRNA probes is often constrained by the short length of the miRNAs, such that often the entire miRNA sequence must be used as a probe. Consequently, the melting temperatures ( $T_m$ ) of miRNA probes may vary by  $>20^\circ\text{C}$ . Such a large variation in  $T_m$  then results in cross-hybridisation and loss of specificity (Git et al., 2010). In recent years, LNA nucleotides in the probe have overcome this problem by enabling an increase in hybridisation temperature. This increase in hybridisation temperature has also overcome the problem of distinguishing between different members of a miRNA family (which can vary by a little as a single nucleotide) (Tolstrup et al., 2003). Although analysis of microarray data is simple and well established one major flaw is that novel miRNAs are not detected – a key aim of this experiment.

One of the most popular techniques for validating and accurately quantifying

miRNAs is quantitative real time PCR. Once a miRNA has been converted to cDNA, amplification proceeds using a miRNA-specific forward primer and a universal stem-loop/poly-A primer. The  $T_m$  of the forward primer can be adjusted by adding a tail (the length of which will depend on the  $T_m$  of the mature miRNA), (Chen et al., 2005) or by adding LNA nucleotides (Balcells et al., 2011). Following amplification, the PCR product can be assayed using the same methods as a conventional qPCR experiment using either SYBR® Green, TaqMan® or other qPCR variants. However, qPCR has limitations: the design of the miRNA-specific qPCR primers can be costly and identification of good normalisers for each experiment can prove to labour intensive (Git et al., 2010). Unlike conventional qPCR, only one flanking primer can be specific, so care must be taken to ensure only one product is being amplified, especially when using SYBR® Green (Vester and Wengel, 2004). Moreover, as with microarrays, qPCR cannot be used to discover novel miRNAs.

In contrast to both the latter techniques next generation sequencing (NGS) of sRNA libraries does not require prior knowledge of specific miRNAs and therefore provides the opportunity to explore new sRNAs and their corresponding sequence frequencies. Consequently, NGS was selected as the preferred method for this project. The HiSeq 2500 Ultra-High-Throughput Sequencing System (Illumina) was chosen for its sequencing yield and accuracy.

#### 13.4.2. **NGS library preparation and sequencing**

There are several commercially available NGS platforms, the most widely used being Illumina, Applied Biosystems (ABI). The general workflow from biological sample to sequencing result is similar for all platforms: nucleic acid isolation, library preparation, template preparation, sequencing and bioinformatic analysis. Library preparation involves the generation of a pool of cDNA from pure, high quality input RNA. The length of this cDNA will vary depending on the platform and the application, with sequence primers ligated to each end of every strand. A sample of this library is then immobilised on a sequencing slide (in the case of Illumina platforms), amplified and then sequenced by extending primers by synthesis (Metzker, 2010) (Ansorge, 2009).

A fundamental element of the sRNA library preparation for the HiSeq platform

comprises the ligation of alternative sequencing adapters to the 3' and 5' end of a sRNA enriched sample. The Illumina sequencing platform is available as a kit to be used for commercial use. However, the reliability of these kits began to be questioned when large variation was noted between replicate samples when analysed using alternative NGS platforms (Git et al., 2010). It was suggested that one major source of the problem is the RNA ligases used in sRNA library construction (Hafner et al., 2011, Jayaprakash et al., 2011). Within the library construction protocol both T4 RNA ligases (1 and 2) are used in ligating sRNAs to customised adapters. The limiting factor in this ligation reaction is the ability of the sRNA to anneal to the adapter. sRNAs with different sequences have different ligation efficiencies to certain adapters, which consequently lead to variation in representation of different sRNAs. Those sRNAs that can anneal will be ligated to an adapter and therefore sequenced; any sRNAs that cannot be ligated will therefore not be sequenced resulting in bias (Zhuang et al., 2012a). To overcome this problem, we decided to use a new and improved version of these adapters which are modified by adding four degenerate nucleotides at each ligating end of the Illumina adapters. These adapters, named High Definition (HD) adapters have been shown to dramatically reduce the ligation bias previously seen during sRNA sequencing (Sorefan et al., 2012).

### 13.4.3. Are miRNAs the key regulators in the maintenance of NC pluripotency?

Until recently, the model of NC development had been a controversial one. Unlike the typical differentiation pathway of embryonic cell populations (**Figure 11, top panel**), NC were thought of as unique as they could selectively regain pluripotency to increase their differentiation ability (unlike their cellular neighbours) (Waddington, 1959). In 2015, Buitrago-Delgado and colleagues published a fundamental paper that changed this working model of NC so it no longer defied the paradigm of progressive restriction in potential (Buitrago-Delgado et al., 2015). They demonstrated that the previous model whereby the NC could be described as an endogenous population of induced pluripotent stem cells (**Figure 11, middle panel**) was incorrect. This work provided insight into how NC cells retain pluripotency rather than gain it and this is selectively inherited from the embryonic stem cells from which they are derived (**Figure 11, bottom panel**) (Buitrago-Delgado et al., 2015). Although extremely insightful, one question that arose from the results of this paper was; if NC cells can inherit their pluripotent ability from the cells they are derived from, what is the factor that enables them to do so? miRNAs have been shown in many cell populations to be fundamental in the maintenance of pluripotency, so could miRNAs be the key factor in the development of NC?

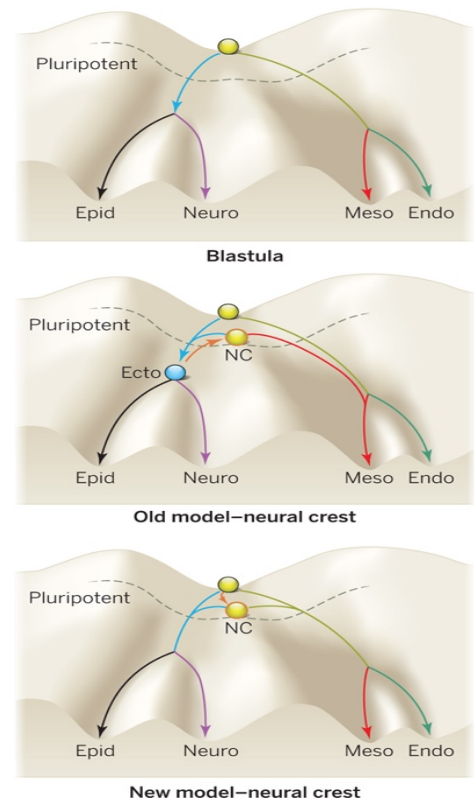


**Figure 11: Models of NC development**

**(Top)** A pluripotent blastula cell “rolls” down one of four differentiation pathways: endoderm (Endo), mesoderm (Meso), neural ectoderm (Neuro), and epidermis (Epid). Once the cell crosses the dashed line, pluripotency is lost. **(Middle)** Previous models implied that the differentiation ability of NCC (orange arrow) was induced from an ectoderm germ layer by “pushing” the NCC back over the dashed line therefore increasing its differentiation potential. **(Bottom)** The new model by Buitrago-Delgado *et al.* shows that NCCs, unlike their cellular neighbours, remain pluripotent before they differentiate, even potentially into endodermal derivatives (Hoppler and Wheeler, 2015).

In light of these results we decided to also complete sRNA sequencing on the tissue that NC derive from, that being the animal pole tissue from blastula cells. From this we aim to identify miRNAs that are present in both blastula and NC

samples and explore the possibility of these miRNAs playing a role in maintaining the pluripotency of the NC cells.

## **13.5. Results:**

### **13.5.1. Induction of both NC and neural animal cap tissue**

#### **13.5.1.1. *Collection of tissue types using the *Xenopus* animal cap assay***

To collect the specific tissue types required for the sRNA sequencing, the *Xenopus* animal cap assay was employed. This assay makes *Xenopus* an excellent model for studying NC development. Through the injection of specific cappedRNA (cRNA) into the animal pole of a one or a two-cell stage embryo we were able to induce various tissue types. To induce neural tissue, the BMP antagonist Noggin cRNA (500pg) was injected, for NC tissue, Noggin (500pg) and Wnt (100pg) were injected and our un-injected control resulted in ectoderm. At stage 8 the induced region of the embryo (animal cap) was removed and left to develop until stage 15 (as judged by sister embryos) at which point RNA was extracted. To ensure correct tissue induction, both WISH and PCR were employed to assess the presence of various tissue markers.

#### **13.5.1.2. *PCR expression profile of neural and NC markers***

To check for NC induction, the NC transcription factor *Snail2* was used as a marker. The results show that only animal caps induced to become NC and the whole embryo control show *Snail2* expression. As expected *Snail2* was not present in neural and ectodermal tissue. *Sox2*, a neural marker was predominantly expressed in the animal caps induced to become neural tissue as well as, to a lesser extent the NC. Epidermal keratin was enriched in the ectodermal sample with a small amount of expression in the neural tissue. Two control genes were used in this experiment, *Histone H4* as a positive control and *Bracyury* for a control of mesoderm contamination. All samples had expression of *Histone H4* and no expression of *Bracyury* indicating that there was no mesoderm contamination in the animal cap tissue and therefore any gene expression was a consequence of prior injections as opposed to mesoderm induction (**Figure 12A**).

### **13.5.1.3. WISH of induced animal cap tissue**

In addition to PCR, WISH for the NC marker *Sox10* was used to further validate the induction of NC tissue. Results from WISH demonstrate that only those animal caps induced to become NC display any expression of *Sox10* (**Figure 12B**). The expression of *Sox10* in the NC animal caps confirms that the NC cell fate has been successfully induced.

### **13.5.1.4. Quality control of sRNA sequencing**

To make libraries, a minimum of 1.5ug of RNA was required. On average, 40 animal caps yielded approximately 4ug of RNA, 0.5ug of this was used for PCR experiments to validate gene expression, 1.5ug was used to synthesis the libraries and any excess was stored for further validation experiments following the sequencing. Following RNA extraction, the quality and quantity of the RNA was tested using a spectrophotometer. The samples selected for library construction and their corresponding spectrophotometer readings are demonstrated in **Figure 12C**.

### **13.5.2. SRNA libraries gave two closely sized bands and minimal adapter-adapter binding**

SRNA libraries were successfully constructed using the Illumina kit and ran on a native 8% polyacrylamide gel. From this gel, the band located at approximately 144bp (miRNA size with adapters) was cut and libraries were extracted ready for sequencing (**Figure 13**). Surprisingly, all samples appeared to have two bands very close to each other in size. This had not been seen previously in the lab on non-*Xenopus* tissue types. For these libraries, both bands were cut out as they were too close to separate with enough accuracy and consistency. As demonstrated with a black arrow (**Figure 13**) all samples had a very minimal degree of adapter-adapter binding meaning that a large proportion of the sample reads will be taken up by sRNAs.

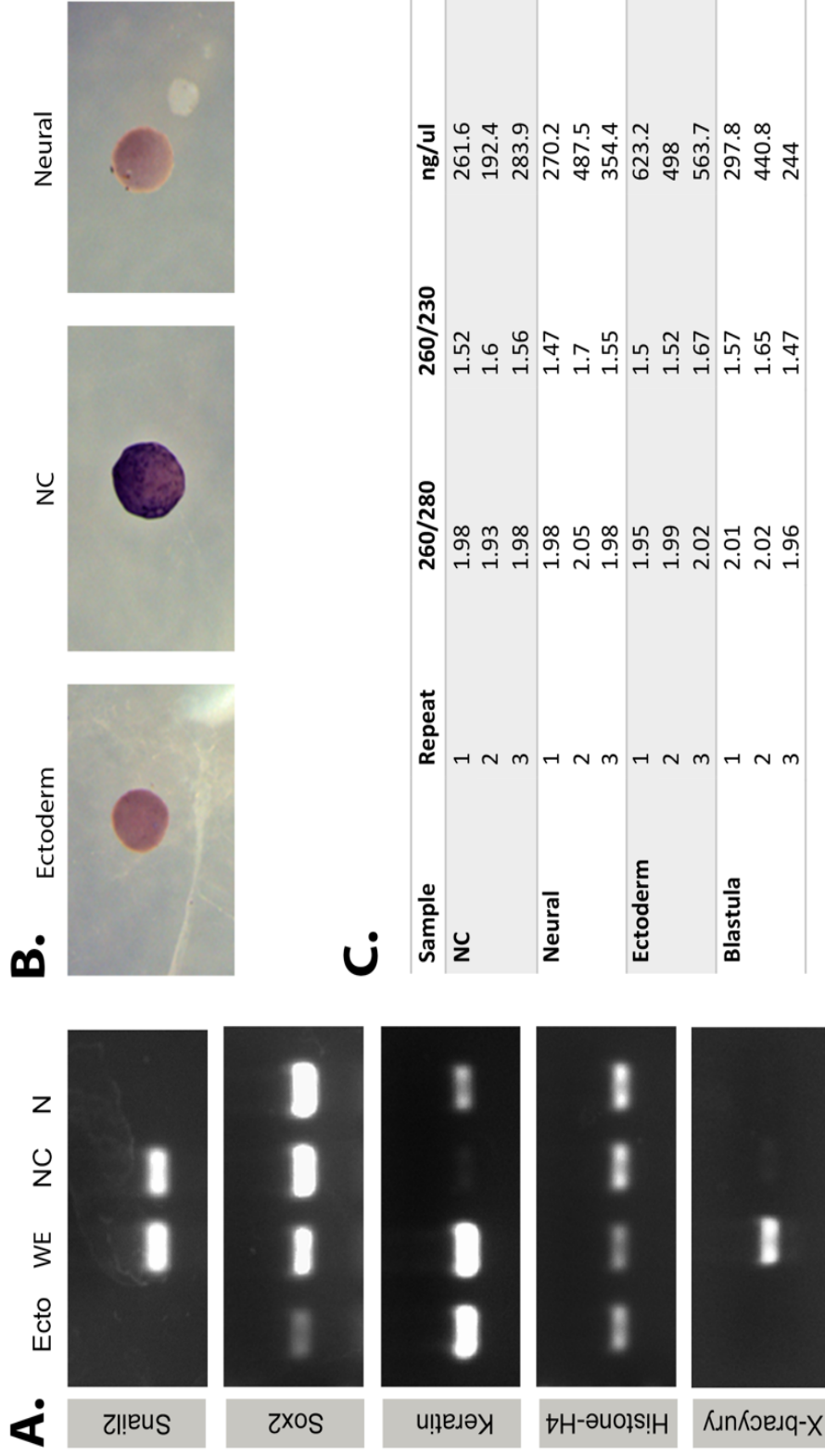


**Figure 12: Neural Crest and neural tissue was sufficiently induced using the animal cap technique**

PCR on RNA extracted from stage 15 animal cap tissue induced to become either neural or NC showed that tissue was induced efficiently. The NC marker *Snail2* was only only expressed in the NC animal cap tissue whilst the neural marker *Sox2* was enriched in the neural tissue and epidermal *keratin* was enriched in the ectoderm (Ecto) sample. *Histone H4* was used as a positive control and *Bracyury* for a control of mesoderm contamination. Whole embryos (WE) were used as a positive controls for all genes (A). *WISH* for the NC marker *Sox10* on stage 15 induced animal caps further confirm induction of NC tissue type with expression only being evident in NC animal caps (B). Nanodrop results demonstrate that all samples sent for sequencing were of good quality (C).

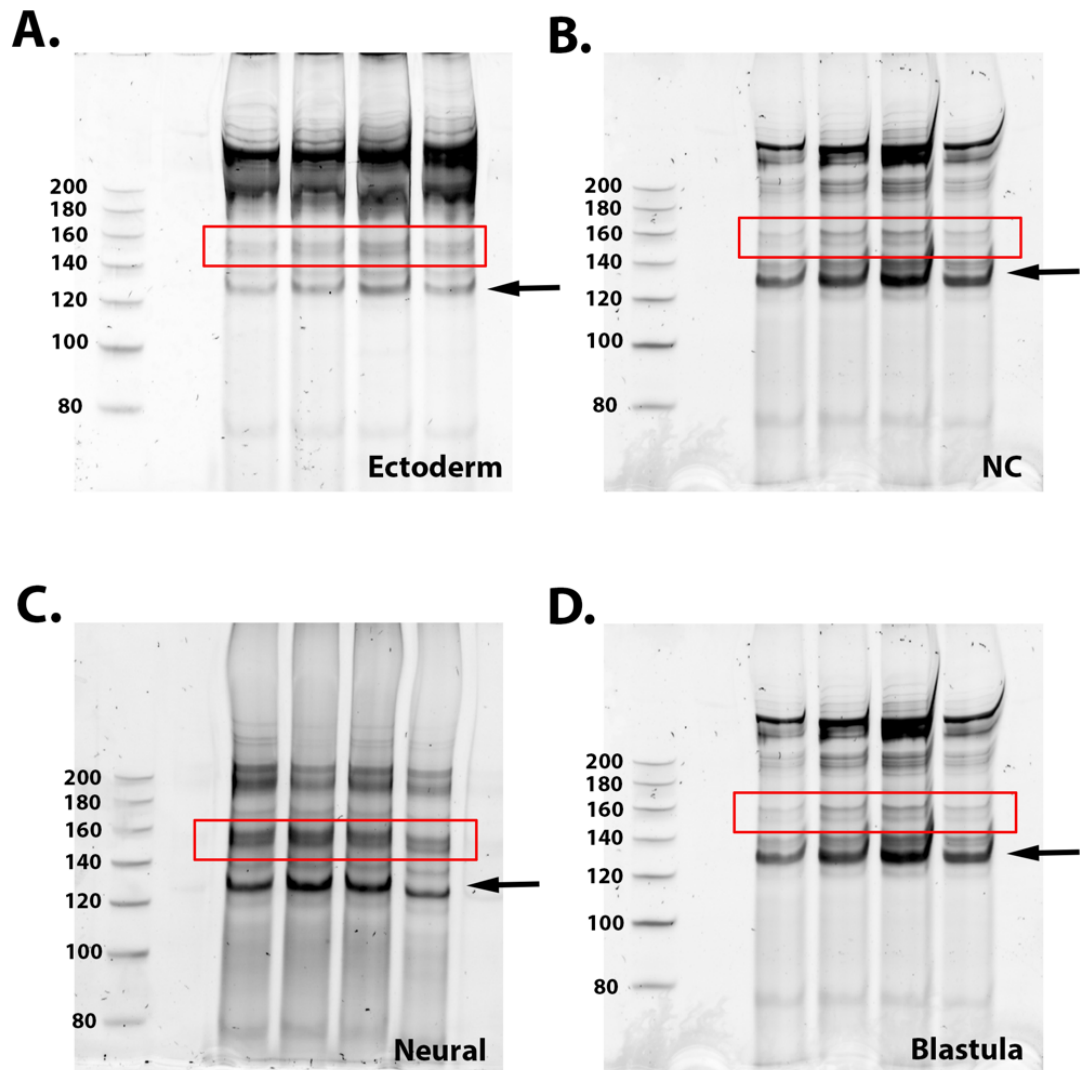


**Figure 13: sRNA libraries gave two closey sized bands and minimal adapter-adapter binding**

SRNA libraries for ectoderm (A), NC (B), neural (C) and blastula (D) tissue were successfully constructed and bands at 144bp in length were cut and extracted. For all samples, two bands very close in size were seen, this is indicated with a red box. All samples had minimal adapter-adapter binding, indicated with a black arrow.

### 13.5.3. Libraries were enriched for both 23 nt and 29 nt sequences

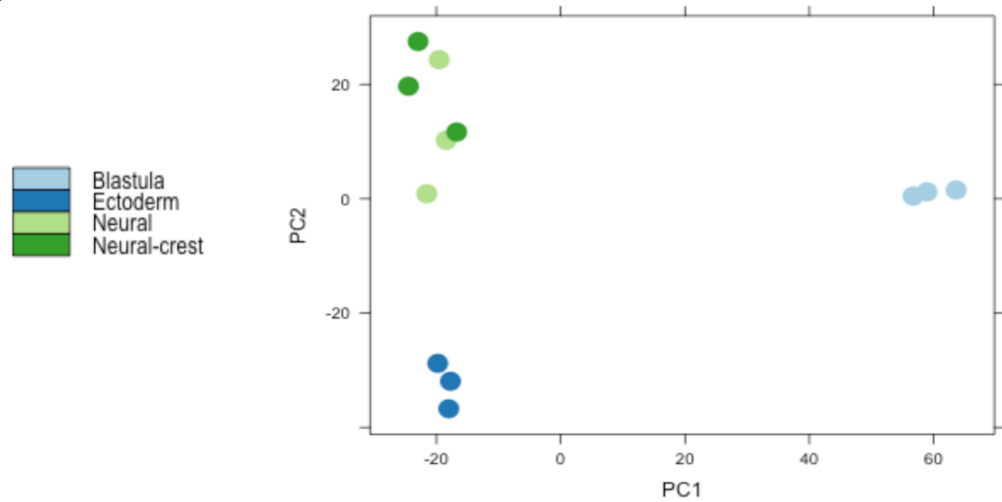
After being sequenced, the raw sequencing FASTQ files were converted to FASTA format and adapter sequences removed with custom Perl scripts. Only reads that mapped perfectly by PatMaN (Prüfer et al., 2008) to the *Xenopus laevis* (V6.1) genome (Meyer et al., 2013) were retained. Between 21-50 million raw reads were obtained per library, of which 49%–70% aligned perfectly to the genome depending on the sample. We sequenced up to 4 million unique aligned sequences per sample (**Table 16**).

Peaks in the length distribution suggest the presence of different classes of sRNAs in the libraries (Armisen et al., 2009). For neural (16.1%), NC (15%) and ectoderm (18%), the majority of reads had a length of 23 nucleotides (nt) indicating that the prepared libraries contained a fraction of RNA corresponding to miRNAs in size (**Figure 14B**). A further peak, approximately 28-29 nt in length (which is indicative of Piwi-interacting RNAs (piRNAs)) also takes up a large proportion of reads for these three tissue types (Armisen et al., 2009). In contrast, the blastula sample has a complete shift in distribution with only 5.6% of the reads being at 23 nt in length and the majority of reads (17.5%) being at 29 nt. This profile is similar to that seen in the literature and therefore confirms that libraries containing mostly miRNA-sized sequences were successfully generated as well as indicating piRNAs in processes occurring between blastula and more specialised tissue in *X.laevis* (Harding et al., 2014). In addition, as demonstrated by the principal component analysis (PCA) plot, replicates cluster well indicating the reproducibility of the experiment. It is clear from the PCA plot that the blastula sample is the most distinct of the four (**Figure 14A**).

**Table 16: A summary of the number of reads obtained from each library and the percentage of these reads that aligned to the genome.**

Sample	Reads	Number of sequences after adaptor removal	Number of unique (non-redundant) sequences	total seqs aligned	% seqs aligned	number of unique seqs aligned	% unique sequences aligned
Neural	40,559,597	27,331,131	3,342,801	13,522,046	49.47	1,777,039	53.16
Neural	46,613,153	41,902,196	4,517,337	28,487,367	67.99	2,623,461	58.08
Neural	21,637,139	20,220,692	1,709,192	13,585,683	67.19	916,889	53.64
NC	50,283,818	24,561,987	3,446,951	13,128,489	53.45	1,902,931	55.21
NC	50,781,624	42,592,632	5,087,921	29,485,739	69.23	2,925,297	57.49
NC	27,794,800	25,358,113	4,780,571	17,920,514	70.67	2,959,732	61.91
Ectoderm	30,983,116	23,443,345	1,762,535	10,938,365	46.66	920,113	52.20
Ectoderm	29,309,332	23,363,917	3,363,699	16,083,931	68.84	1,937,345	57.60
Ectoderm	39,291,438	34,598,996	5,491,787	23,802,575	68.80	3,139,468	57.17
Blastula	29,834,148	24,870,014	5,434,179	15,077,230	60.62	3,052,628	56.17
Blastula	37,848,041	31,246,471	7,063,141	21,636,112	69.24	4,390,081	62.15
Blastula	34,762,275	29,884,479	5,771,754	16,190,680	54.18	2,968,797	51.44

A.



B.

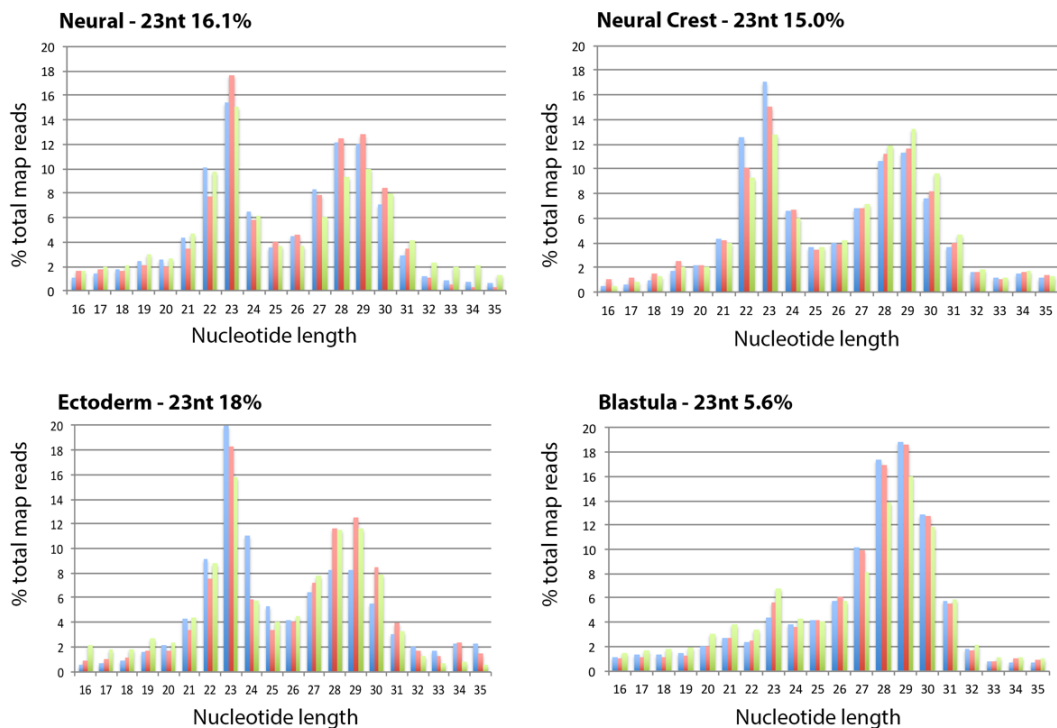


**Figure 14: Size distribution and clustering of sequenced small-RNA enriched total RNA**

The PCA plot of all libraries sent for sequencing demonstrate that samples cluster well and the blastula sample is distinct from the others (A). Bar plots of nucleotide length show that the peak seen at 23 nt corresponds to mature miRNA length. For neural, NC and ectoderm tissue the majority of reads are at 23 nt with a smaller peak at 29 nucleotides. The counter is seen for the blastula sample with the majority of reads being at 29 nt in length. Blue red and green bars represent each of the three replicates for each tissue type (B).

### 13.5.4. Blastula peak shift is not caused by piRNAs

Literature suggests that the peak seen at 29 nt long is indicative of piRNAs (Armisen et al., 2009) but in order to validate this we ran a software which detects and analyses piRNA clusters (proTRAC, probabilistic TRacking and Analysis of Clusters) (Rosenkranz and Zischler, 2012). Surprisingly, we found that, of the four tissue types, blastula had the least percentage of reads that can be assigned to clusters (3.38%) therefore suggesting that the peak seen at 29 nt is not piRNAs and in fact an alternative sRNA (**Table 17**).

During blastula stage the embryo undergoes Mid Blastula Transition (MBT), during this time the maternal RNA products are broken down in preparation for the initiation of zygotic transcription (Mathavan et al., 2005). We therefore decided to run transcriptome analysis to investigate whether this peak was a consequence of degraded maternal transcripts. The results from the transcriptome analysis concluded that there is no increase in the level of sRNAs aligning to genes in the blastula sample when compared to the ectoderm, neural and NC tissues. In fact, as with the proTRAC results there is a decrease (**Table 17**).

**Table 17: piRNA clustering and transcriptome analysis of sequenced animal cap tissue**

ProTRAC analysis on the smallRNA sequences reveals that the large 28/29 nt peak seen in blastula tissue (and not the other tissue types) is not piRNAs. In addition, transcriptome analysis demonstrates that it is not consequence of degraded transcripts during mid blastula transition (MBT).

		Ectoderm	Neural	Blastula	NC
<b>ProTRAC</b>	<b>Predicted piRNA clusters</b>	59	74	56	59
	<b>Total size</b>	0.02%	0.03%	0.02%	0.02%
	<b>Sequence reads that can be assigned to clusters:</b>	5.09%	6.00%	3.38%	4.22%
<b>Transcriptome analysis</b>	<b>Total sequences aligned to transcriptome</b>	1091358	1457080	978399	2074442
	<b>% aligning to genes</b>	6.36%	7.91%	5.54%	10.21%

## 13.5.5. miRNA annotation across the four samples

### 13.5.5.1. *Annotated miRNAs*

In total, over the four tissue types, 106 miRNA families were annotated in *X.laevis* coming from 388 hairpins. Of these, we discovered 15 known animal miRNAs not yet formally identified in *Xenopus*. These will now be added to MiRbase.

### 13.5.5.2. *Novel miRNAs*

Sequencing of the libraries resulted in the discovery of 102 novel miRNAs from 137 hairpins. These miRNAs were detected using the programs mircat (Stocks et al., 2012) and mirdeep2 (Friedlander et al., 2008) and were evaluated for the likelihood of hairpin secondary structure using RNAFold (Gruber et al., 2015). Sequences that met this criterion were designated as new *Xenopus* miRs (Appendix 5).

## 13.5.6. Global miRNA populations within each tissue type are dominated by miR-427

Of the miRNAs annotated, one known miRNA makes up almost 67% of all miRNA reads, this being miR-427. This is the case in all tissue types and is seen most strongly in blastula tissue (74%) (**Figure 15A**). From the sRNA sequencing, five isoforms (homologous miRNAs encoded on different gene loci) of miR-427 hairpins were annotated, all of which had strong conservation in the 5' sequence but poor conservation in the 3' sequence (data not shown). A breakdown of these isoforms by their read number demonstrates that a similar expression profile is seen across all the tissue types with isoform C being the most abundant (**Figure 15B**).

Abundance plots of the mature miRNAs (both sequences) for each isoform clearly demonstrate that although the hairpins may have a similar expression across the tissue types, the profiles of the mature sequences vary greatly (**Figure 15C**). Most of the isoforms have a more abundant 3' sequence which is present in all tissue types at varying degrees. Isoform A proves to have an interesting expression profile with a clear switch occurring between the 3' and 5' sequences. The 3' sequence is abundant in the more specified tissue types (NC, neural and

ectoderm) but absent in the blastula whilst its 5' sequence has the opposing profile being only abundant in the blastula tissue. In isotype C, it is also apparent that the 5' sequence is only apparent in the blastula sample possibly indicating a role for these 5' sequences during the blastula stage of development.

### 13.5.7. miRNA expression profile over the samples

Heatmap analysis of abundant miRNAs across the samples revealed relatively low-level miRNA expression in the blastula tissue when compared to the other tissue types. A small number of miRNAs were found to be abundant in only one tissue type including miR-449c in the ectoderm tissue (**Figure 16E**).

A comparison of the ten most highly detected miRNA hairpins in all four tissue types revealed that NC, neural and ectoderm all have a similar profile of abundant miRNAs with miR-428, miR-200a, miR-141, miR-7, miR-92a and miR-19b being present in all three tissues. In this study, the contributions of the top 10 miRNAs (including miR-427) were found to total 77% in NC, 81.3% in neural 82.6% in ectoderm of the total miRNA hairpin reads sequenced. Following miR-427, the second most abundant miRNA in all three samples is miR-428 taking up 6.4% of the reads in NC, 5.1% in neural and 2.7% in ectoderm (**Figure 16B-D**). In ectoderm, two abundant miRNAs that are not present in the other samples are miR-203 and miR-449. This result was not surprising as these miRNAs have been implicated throughout the literature to be key players in both epithelial development (McKenna et al., 2010) and cilliogenesis (Song et al., 2014) respectively. MiR-26, miR-302 and miR-93 were found to all be uniquely abundant in the neural tissue and the four miRNAs miR-219, miR-17, miR-130b and miR-20b in the NC sample. Although none of these miRNAs have a direct link to NC development, some do have interesting roles in processes during NC development and some interesting potential targets which are discussed further in section 13.6.4.

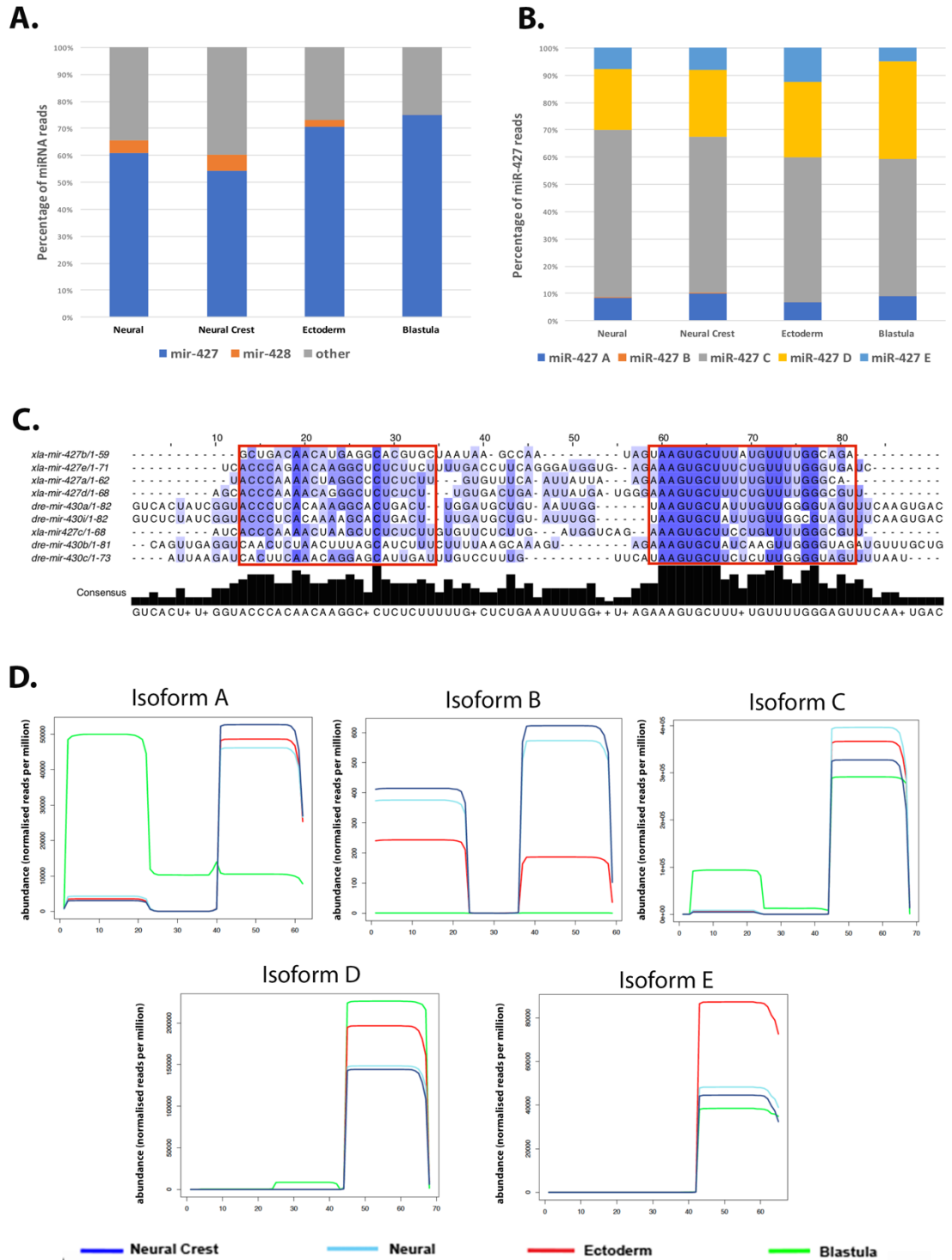


**Figure 15: MiR-427 dominates the miRNA reads in all tissue types.**

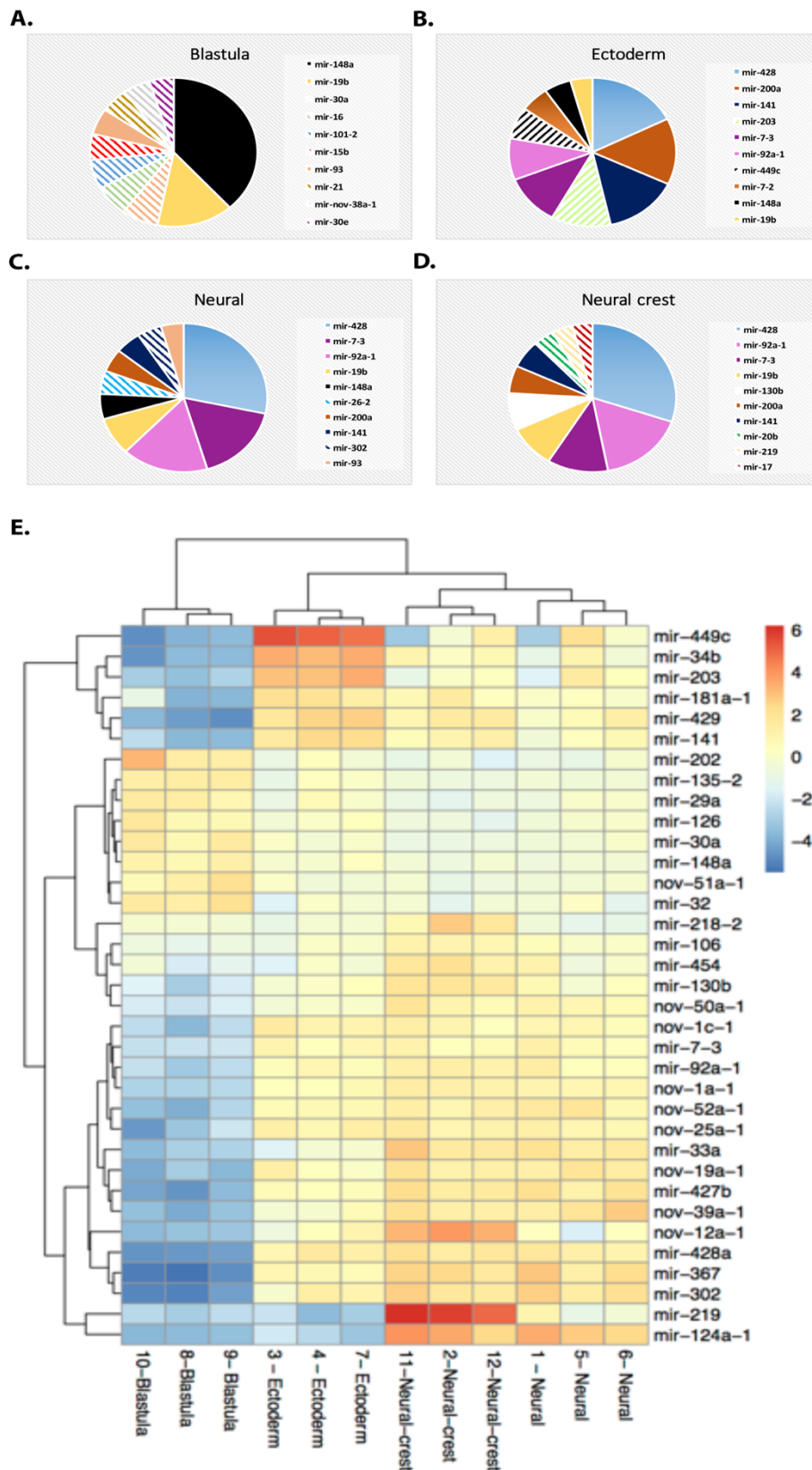
MiR-427 makes up over 67% of all miRNA reads and this saturation is seen in all tissue types (A). In total, five isotypes of miR-427 were sequenced, all of which had a similar hairpin distribution over the tissue types with isotype C being the most abundant (B). Although the hairpins had similar distribution the mature miRNAs had unique profiles across the tissue types. The 3' sequence in all cases is the most abundant. Isoform A has an interesting profile with the 5' sequence being abundant in blastula stage and absent in the other tissues and the counter is seen with the 3' sequence (C).

The blastula sample is very distinct from the other three samples and has a completely unique profile. miR-428 fails to make it into the top 10 most abundant miRNAs, the most abundant miRNA after miR-427 is miR-148a (**Figure 16A**). Interestingly, a novel miRNA (miR-nov-38a-1) is present in the blastula profile. As this miRNA is specific to the blastula sample and is in the top 10 most abundant miRNAs it proves to be a good candidate for a miRNA with an important role in blastula development.

### **13.5.8. Several miRNA hairpins are differentially expressed between neural tissue and NC tissue**

To identify some candidate miRNAs located in the NC, differential expression analysis on neural vs NC tissue was completed using deSEQ2 (**Figure 17B**) (Love et al., 2014). In total, 11 miRNA hairpins were upregulated in NC, all of which are listed in **Figure 17A**. The top miRNA is miR-219 which is abundant in all three replicates of NC and almost absent in all other samples. A similar profile of expression is seen for miR-130C (**Figure 17B,C**). Interestingly, one of the miRNAs upregulated in NC compared to neural tissue was miR-196a - the main candidate that came out of the XenmiR approach. MiR-10b is also in the top 10 differentially expressed miRNAs, as with miR-196a, miR-10b is also located within a HOX cluster (**Figure 20**) (Yekta et al., 2004). One novel miRNA made it into the differentially expressed miRNAs, that being miR-nov-12a (**Figure 17D**).

Two miRNAs that were upregulated in the neural tissue when compared to NC were miR-302 and miR-9 (**Figure 17B**), both of which are implicated to have roles in neural development throughout the literature (Yang et al., 2015, Li et al., 2016).

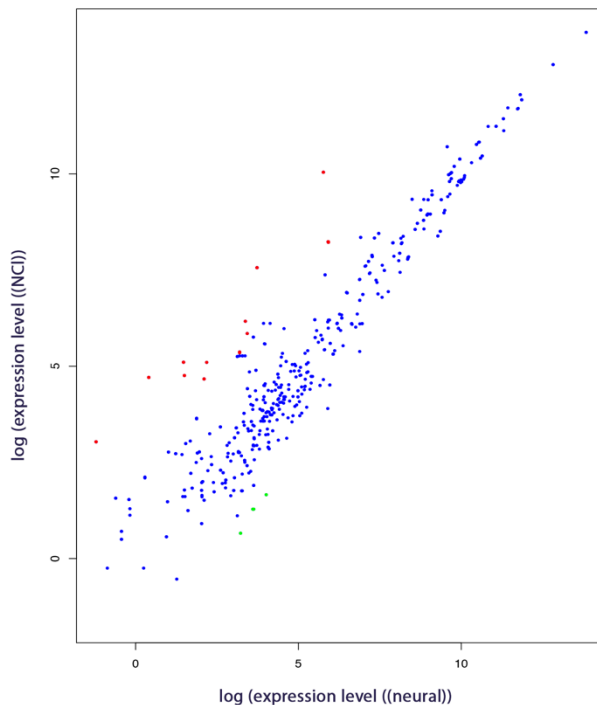
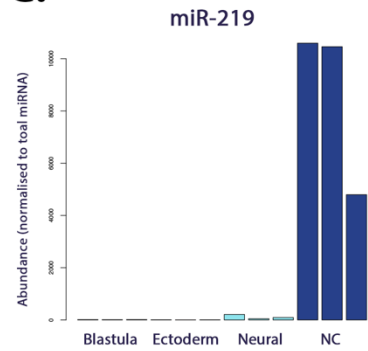
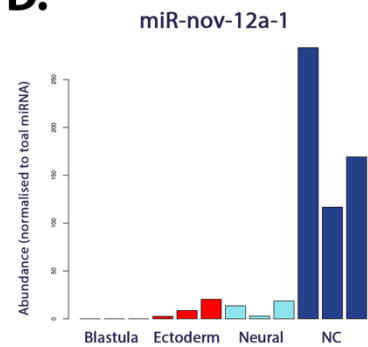
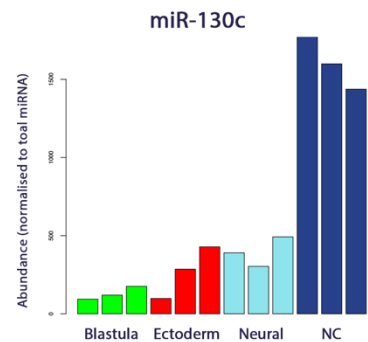


**Figure 16: miRNA expression profiles and heatmap analysis of miRNAs in early *Xenopus* development.**

Pie chart analysis show the distribution of the top 10 most abundant miRNAs across the different tissue types (A, B, C, D). miRNAs were clustered by expression similarity for heatmap analysis. miRNA expression is displayed using a colour key where blue corresponds to low and red to high numbers of miRNA normalized reads. The miRNAs labelled are most abundant in the four libraries (E).

**A.**

MicroRNA	baseMean NC	baseMean Neural	Adjusted p-value
miR-219	22991.56	319.24	3.9E-18
miR-218-2	3726.56	372.31	3.6E-07
miR-nov-12a-1	477.58	29.09	9.5E-07
miR-338-3	1596.34	336.46	2.0E-05
miR-10b	1923.23	41.60	5.6E-05
miR-204a-1	194.31	26.59	0.00018
miR-130c	4227.09	1003.29	0.00024
miR-130b	44651.93	14308.99	0.01007
miR-23a	266.19	52.27	0.01929
miR-24b	394.60	95.31	0.01992
miR-196a-2	106.37	8.19	0.04114
miR-302	8550.08	13297.40	0.64601
miR-9	203.13	430.73	0.35916

**B.****C.****D.****E.**

**Figure 17: Several miRNAs are upregulated in neural crest when compared to neural tissue.**

Differential analysis of miRNA hairpins was completed on neural vs NC samples. In green are miRNAs upregulated in NC. Blue gives two examples of neural specific miRNAs (A). Scatter plot output from DeSEQ2 analysis demonstrates that several miRNAs were upregulated in NC (red dots) and in neural (green dots) (B). miR-219, miR-nov-12a-1 and miR-130C are three examples of miRNAs upregulated in the NC samples when compared to all other tissue types (C, D, E).

### 13.5.9. miR-338 and miR-301a are expressed in both neural crest and blastula samples

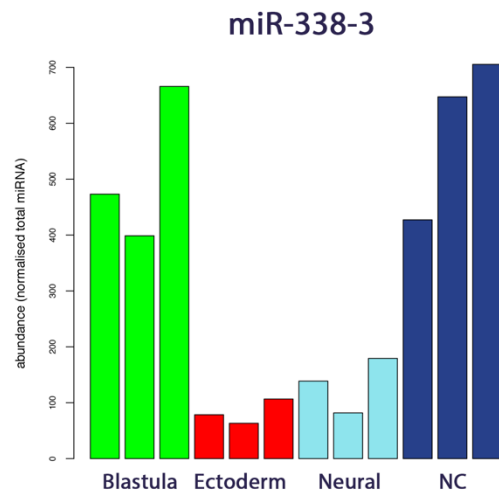
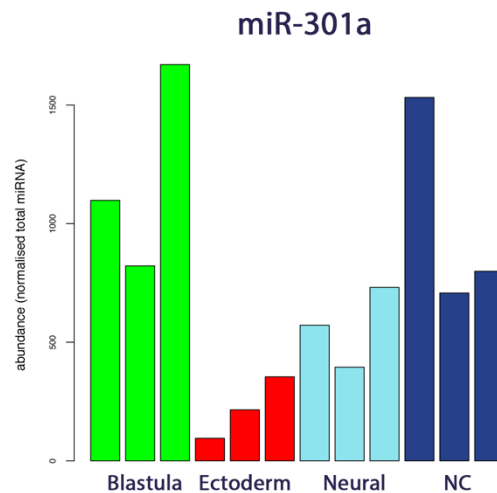
To identify potential candidate miRNAs that are key in maintaining a pluripotent NC population throughout development, miRNAs that were not differentially expressed between blastula tissue and NC as well as being absent in both neural tissue and ectoderm tissue were determined. From this, two miRNAs were identified, these being miR-338 and miR-301a (**Figure 18A**). Both miR-338 and miR-301a were enriched in both the NC and blastula samples (**Figure 18BC**) and have also been linked throughout the literature to being involved with the maintenance of pluripotency (Lin et al., 2009, Li and Belmonte, 2017). This therefore makes them interesting candidates for further investigations.

### 13.5.10. Validation via qRT-PCR

To experimentally validate the sRNA sequencing results qRT-PCR was employed. We used the remaining RNA from the initial library preps to construct cDNA and run qRT-PCR to assess various miRNA expression levels across the tissue types. All miRNA expression levels were normalised to U6 snRNA. As demonstrated in **Figure 19** the miRNAs in question displayed the same expression profile using qRT-PCR as they did in the sRNA sequencing. This includes the novel miRNA, miR-nov-12a that was only expressed in the NC tissue type, two known miRNAs (miR-219 and miR-196a) that were also enriched in the NC sample and a miRNA enriched in the neural tissue (miR-302). From the sRNA sequencing, miR-302 was found to be most abundant in the neural sample, moderately expressed in the NC sample and then low in ectoderm. This profile is replicated in the qRT-PCR with the level of miR-302 in both neural (\*\*\*) and NC (\*) being statistically different from the ectoderm (**Figure 19**). To strengthen these results, validation on dissected NC tissue could be completed. However, due to time constraints these experiments were not completed.

**A.**

microRNA	Base Mean Blastula	Base Mean NC	Adj P Value
miR-338	1716.72	1667.97	0.93
miR-301a	3945.05	2756.40	0.55

**B.****C.**

**Figure 18: MiR-338 and miR-301a are expressed in both neural crest and blastula samples.**

Differential analysis was completed on NC and blastula samples. miR-338 and miR-301 were found to be not differentially expressed between NC and blastula (**A**). miR-338-3 and miR-301a were found to be enriched in both NC and blastula and are therefore candidates for miRNAs which could have a role of maintaining NC pluripotency (**B, C**).

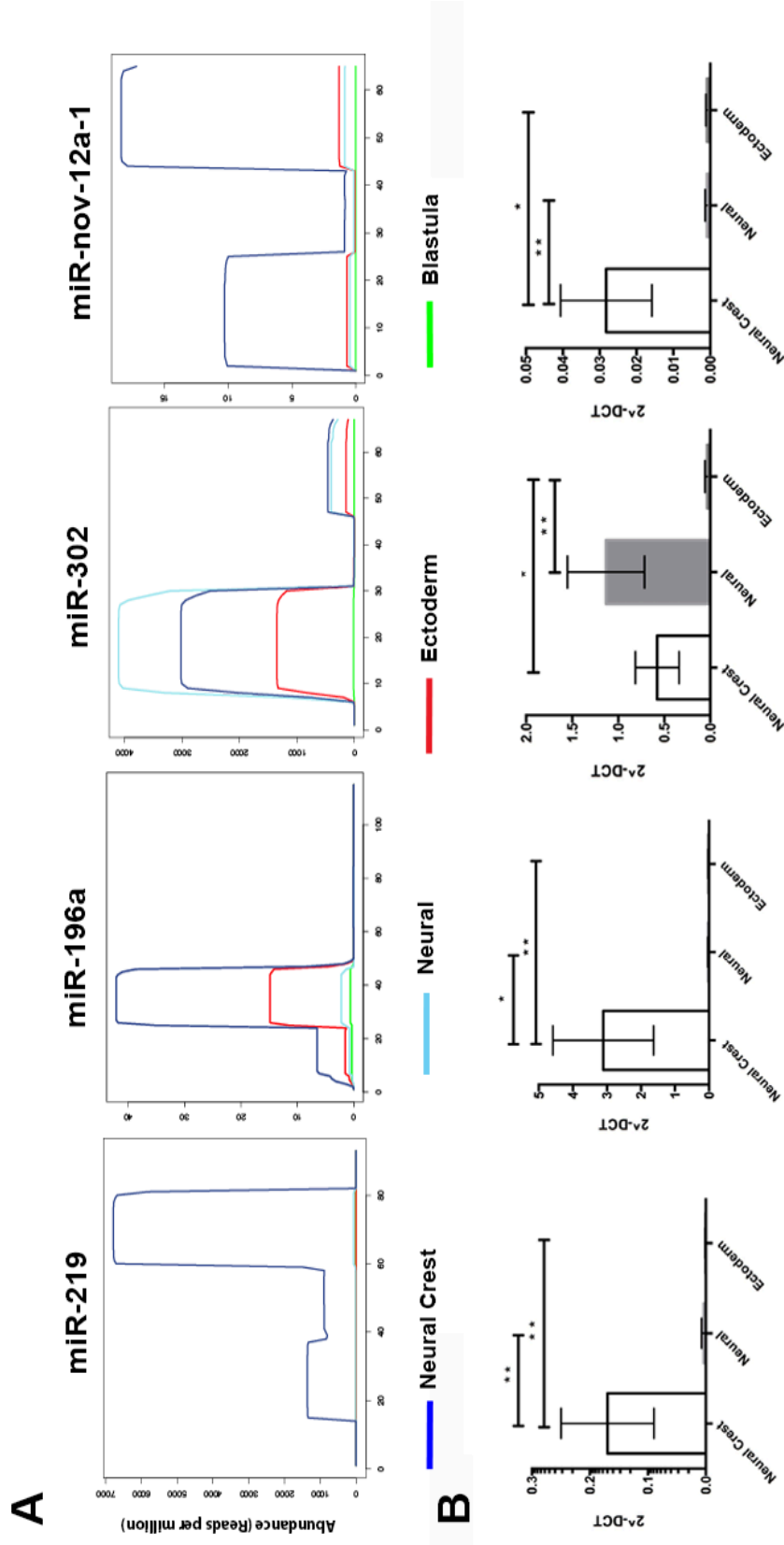


**Figure 19: Neural crest miRNAs identified by small RNA sequencing were validated using qRT-PCR.**

The same RNA was used to make both the small RNA libraries and for qRT-PCR. Abundance plots of various miRNAs following small RNA-seq on blastula and ectoderm animal cap tissue and animal caps induced to form NC and neural (A). qRT-PCR validation of the miRNAs identified from the small RNA-seq in the same order as A (B). One way ANOVA with Tukey post test statistical analyses were performed on the results of each qRT-PCR. For significance:  $P \leq 0.05$ ; \*;  $P \leq 0.01$ ; \*\*;  $P \leq 0.001$ ; \*\*\*;  $P \leq 0.0001$ ; \*\*\*\*.

## 13.6. Discussion

### 13.6.1. miR-196a and miR-302 are co-expressed with Sox10 in the developing NCC

Using the XenmiR approach we found multiple miRNAs to be located in NC tissue. Through WISH and double WISH it can be concluded that miR-196a and miR-302 are expressed in the developing NC as well as in the NP (**Figure 9**). It is also likely that miR-17-5p, miR-30a-3p, miR-429 and GNW8 are expressed in the NC although the staining wasn't quite as strong as for the above miRNAs (**Figure 10**). Potential reasons for the weak staining can be inferior quality of the *in-situ* reaction or a low copy number transcript.

Taking these results, along with literature searches for potential targets the following five miRNAs were chosen for functional analysis:

#### miR-196a:

MiR-196a is a vertebrate specific miRNA that is part of the miR-196 precursor family. MiR-196 is present in three HOX clusters: miR-196b on HOXA, miR-196a-1 on HOXB and miR-196a-2 on HOXC (**Figure 20**). MiR-196a-1 and miR-196a-2 have an identical mature sequence, whereas miR-196b differs by a single nucleotide (Liu et al., 2013). Gessert et al. (2010) showed that KD of miR-196a using MO resulted in abnormal expression of various neural and NC related genes including a reduction in the expression of the NC marker *Snail2*. However, this phenotype was not investigated any further by the authors. MiR-196a has been shown to target several HOX genes, including *HOXA5*, *HOXB7*, *HOXB8* and *HOXC8* (Asli and Kessel, 2010, Li et al., 2010, Liu et al., 2012, Braig et al., 2010) and is predicted using computational algorithms to target many more. HOX genes are expressed at the time of NC induction and play a central role in NC patterning (Lumsden and Krumlauf, 1996). There are multiple papers which demonstrate the link between NC development and anterior HOX genes. It was demonstrated using mice that a rhombomere 4 (r4) specific triple HOX loss-of-function mutation resulted in loss of the expression of all r4 NC derived markers and all the structures normally derived from them (Gavalas et al., 2001). Using gain of function experiments, Gouti and colleagues

showed that the NC markers, *Msx1/2* and *Snail1* were upregulated in response to *HOXB1* expression and that when expressed in the neural tube of the trunk region of the developing chick embryo, anterior HOX genes can induce a switch in cell fate from neural to NC (Gouti and Gavalas, 2008, Gouti et al., 2011). In addition, miR-196a has been shown to regulate sonic hedgehog (shh) signalling via the direct targeting of *HOXB8* during limb development (Hornstein et al., 2005). Shh is also involved in NC development (Jeong et al., 2004). These findings clearly indicate that anterior HOX genes are directly involved in NC specification and as a master regulator of HOX gene expression, is miR-196a part of this network?

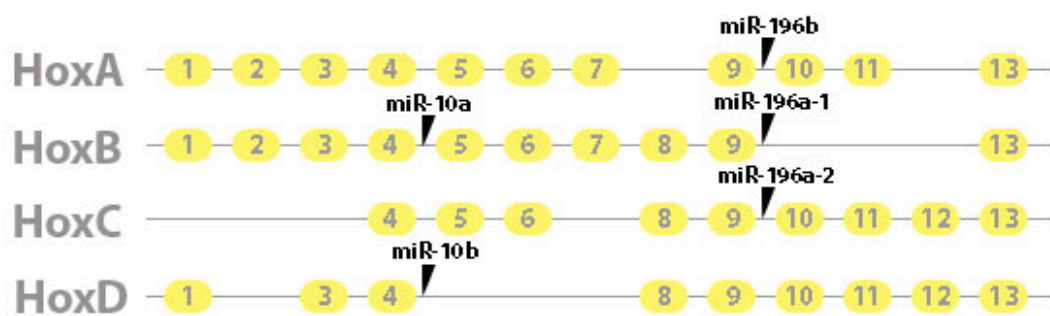


**Figure 20: Schematic representation of the structure of the four mammalian HOX gene clusters with the location of the hosted miRNAs.**

#### miR-302:

The miR-302/367 cluster is highly conserved and is vertebrate-specific. The cluster was initially identified in undifferentiated human embryonic stem cells and was shown to play a role in the maintenance of the pluripotency (Suh et al., 2004). Previous studies in chick have shown using WISH that miR-302 is highly expressed in neural folds, the region where NC arise from (Jeong et al., 2014). The miR-302/367 cluster has been demonstrated to be involved in regulation of various cellular signalling pathways linked with NC development, such as the BMP and TGF- $\beta$  signalling pathway. During development, for the NC lineage to be specified, an intermediate level of BMP signalling is necessary, with a high level required for ectoderm and a low level for neural specification (LaBonne and Bronner-Fraser, 1998). MiR-302 members have been shown to be capable of fine-tuning BMP signalling via regulation of three BMP inhibitors, TOB2, DAZAP2 and SLAIN1 (Lipchina et al., 2011). It is therefore possible that miR-302 is regulating this confined intermediate level of BMP expression required for NC

development. Another key process in NC development is the epithelial to mesenchymal transition (EMT), EMT is the switch to a mesenchymal cell type that enables the NC to delaminate away from the dorsal neural tube and migrate along various axes of the embryo (Theveneau and Mayor, 2012). Using *in vitro* assays, miR-302 has been shown to facilitate the induction of EMT through directly repressing the translation of transforming growth factor beta receptor 2 (*TGFBR2*), and Ras homologue gene family, member C (*RHOC*) genes (O'Connor and Gomez, 2014, Subramanyam et al., 2011). Finally, through targeting of *Lefty1* and *Lefty2* (Nodal inhibitors), and thus modulation of the TGF- $\beta$ /Nodal signalling pathway, miR-302 members have been shown to regulate the balance between a pluripotent state and a differentiated state of a cell - a key aspect of NC development (Barroso-delJesus et al., 2011).

#### **Mir-17-5p:**

miR-17 is part of the miRNA precursor miR-17 family, which includes miR-17, miR-20a/b, miR-93, and miR-106a/b, all of which have the an identical seed sequence (Concepcion et al., 2012). Using computational target algorithms, two interesting predicted targets of miR-17 were identified, these being the BMP inhibitor *BAMBI* and the hypoxia factor *Hif-1 $\alpha$* . As mentioned previously whilst discussing miR-302, an intermediate level of BMP is required for NC specification. It is therefore possible that, as with miR-302, miR-17 is regulating this confined intermediate level of BMP expression required for NC development through regulation of BMP inhibitors. The second interesting predicted target of miR-17 - *Hif-1 $\alpha$* , has previously been demonstrated to be essential for successful EMT and chemotaxis of NCC therefore potentially linking this miRNA into the regulation of NC motility (Barriga et al., 2013). As well as interesting predicted targets, functional analysis has also shown links between miR-17 and NC development. Gokey et al. (2012) demonstrated using microarray analysis on tissue depleted of the NC transcription factor *Sox10* that miR-17 was a *Sox10* dependent miRNA. In addition, data has shown that miR-17 is regulated by the transcription factor c-Myc, an essential regulator of NC formation (Bellmeyer et al., 2003, Hatch et al., 2016).

#### **miR-429:**

miR-429 is a member of the mir-200 family along with miR-200c, miR-200b, miR-

200a, and miR-141. In recent years, the miR-200 family has been extensively studied in the literature in the context of inhibition of EMT and metastasis in various cancer types (Pieraccioli et al., 2013). One gene that multiple members of this family have been shown to target within various biological contexts is *Ets1* (Chan et al., 2011). *Ets1* is a NC regulator, specific to cranial NC population. It is suggested to have a unique function of establishing a regulatory state that activates cranial crest-specific effector genes responsible for the transition from the pre-migratory to migratory state (Gao et al., 2010). This therefore raises the possibility that miR-429 may play a role in inhibiting premature migration through regulation of *Ets1*. To support this potential role of miR-429 in NCC, it is known that members of the miR-200 family inhibit the translation of *ZEB1* and *ZEB2*. These ZEB proteins are transcription factors that promote NC EMT, thus by inhibiting their translation this results in a stabilised epithelial phenotype and E-cadherin expression until the cells are ready to delaminate (Van de Putte et al., 2007) (Christoffersen et al., 2007). Further, in an endothelial cells context, it was shown that the transcription factor Snail (key in NC development) can repress members of the miR-200 family resulting in the promotion of EMT (Gill et al., 2012). Together, this provides a strong potential link between miR-429 and the governance of NC migration.

### **miR-30a-3p:**

miR-30a is a member of the well characterized miR-30 family. This family includes five members (a–e) that are broadly conserved (Rodriguez et al., 2004). Throughout the literature, miR-30a-3p has had links with migration in various cell populations. In endothelial cells, miR-30a-3p targets the methyl CpG binding protein MeCP2 resulting in migratory defects (Volkman et al., 2013). This is interesting in the context of NC development as decreased levels of MeCP2 are associated with Hirschsprung disease, a disease characterised by the absence of the intramural ganglion which itself is associated with impaired proliferation and migration of NCC (Zhou et al., 2013). In addition to this, miR-30a-3p has been demonstrated to upregulate *Hif2a* in renal cell carcinomas (Mathew et al., 2014). *Hif2a* has been shown in various cell types, including NC like tumour cells, to be key in ensuring the maintenance of an undifferentiated/ proliferative state (Pietras et al., 2009). Finally, miR-30a-3p has been demonstrated to target the NC transcription factor *Snail1* and as a result of this regulate EMT in hepatocytes

(Zhang et al., 2012a). Together, this indicates the miR-30a-3p could have a role in the maintenance of a multipotent state and/or inhibition of NC migratory capabilities.

### **13.6.2. Libraries were enriched for both 23 nt and 29 nt sequences**

SRNA sequencing libraries were successfully prepared from samples enriched for sequences of 23 nt, containing mature miRNA transcripts (**Figure 14B**). In the ectoderm, neural and NC samples this peak was the largest with another smaller peak seen at 29 nt. In the blastula sample, the counter was seen with the largest enrichment of sequences being at 29 nt and a smaller one seen at 23 nt. These results are consistent with sequencing results from other experiments, many of which have concluded that this peak is piRNAs (Faunes et al., 2012). PiRNAs are not processed by Dicer during their biogenesis and are largely known for their roles in epigenetic changes and maintenance of the gonads and germ cells of vertebrates (Aravin et al., 2006). PiRNAs are said to be between 26-31 nt long so fit the profile of this large peak in the blastula sample perfectly (Weick and Miska, 2014). However, using proTRAC to analyse this sRNA dataset for piRNA clusters we show that there is not an enrichment of piRNAs in the blastula tissue (3.38%) compared to neural (6%) NC (4.22%) and ectoderm (5.09%) (**Table 16**).

Following this, we used transcriptome analysis to investigate whether the sRNAs in this 29 nt peak are degraded protein coding genes. During blastula stage, the embryo undergoes Mid Blastula Transition (MBT), at this time the maternal RNA products are broken down as zygotic transcription is initiated (Mathavan et al., 2005). Therefore, it would make sense that the blastula embryo had this large peak compared to the more specialised tissue samples. Surprisingly, as with proTRAC we found there was no increase in the number of sRNAs aligning to genes in the blastula sample (5.54%) when compared to the others (6.36%-10.21%) (**Table 16**).

The number of reads at 28/29 nt account for 35% of the total reads in blastula compared to approximately 20% in the other tissue types. This implies that whatever this subset of sRNAs are, it is likely they are playing a key role in the processes during or after MBT. One strong possibility is that this peak is result of

a newly discovered class of sRNAs named site RNAs. Site RNAs are approximately 28 nt in length and are derived from remnants of transposable elements which align in clusters to the introns in protein coding genes (Harding et al., 2014). The focus of this work is the miRNA expression profile of the sequenced tissue so no further analysis was completed, however, this data set could be probed for more information on the origination of this peak and its role in early development.

### **13.6.3. Global miRNA populations within each tissue type are dominated by miR-427**

Our sRNA sequencing reveals a striking dominance of miR-427 in all four of the samples making up over 67% of all the miRNA reads (**Figure 15**). This robust accumulation of one miRNA across the tissue types is likely to be a result of the presence of hundreds of copies of a -1.2kb DNA repeat sequence in the *X. laevis* genome encoding the various isoforms of miR-427 (Lund et al., 2009). Throughout the literature, miR-427 has been implicated in early embryo development, specifically during MBT. As discussed previously in section 13.6.2, just after stage 8 is when MBT occurs and maternal transcripts are broken down as zygotic transcription is initiated. miR-427 has been shown previously to reach maximum levels just after MBT (Watanabe et al., 2005) (Newport and Kirschner, 1982) and to play a key role in the deadenylation and destabilisation of these maternal transcripts. MiR-427 has orthologues in both Zebrafish (miR-430) and humans (miR-302) (Chen et al., 2005) (Rosa et al., 2009), both of which share the same seed sequence and have the same conserved function (Giraldez et al., 2005) (Mishima et al., 2006, Rosa et al., 2009).

In total, five isoforms of miR-427 hairpins were identified across the four tissues (**Figure 15C**). Previous work studying the function of miR-427 in *Xenopus* has reported only four isoforms (A, C, D and E) but this work was completed on the blastula staged embryos and our results demonstrate that the fifth sequence is not expressed in blastula (Lund et al., 2009). Although a similar expression profile is seen for all hairpin isoforms across the samples (**Figure 15B**), abundance plots of the mature miRNA sequences (3' sequence and 5' sequence) clearly demonstrate stage specific expression (**Figure 15C**). It has been shown that for deadenylation of maternal mRNAs the functioning mature sequence of miR-427

is the conserved 3' sequence (Lund et al., 2009). However, which individual isotypes are responsible has yet to be investigated. Although miRNAs primarily bind using their seed sequence (which is identical across the isotypes), often other regions of the miRNA influence binding to its target and ability to complete its function. From this sequencing, two isotypes had abundant expression of the 3' mature miRNA in the blastula sample, that being isotype C and D. It is therefore likely that it is these isotypes that are responsible for deadenylation of maternal transcripts although further investigations need to be carried out.

Whilst analysing the distribution of the mature sequences, isoform A proved to have an interesting expression profile with a clear switch occurring between the 3' and 5' sequences depending on the tissue type. The 3' sequence is abundant in the more specified tissue types (NC, neural and ectoderm) but absent in the blastula whilst its 5' sequence has the opposing profile being only abundant in the blastula tissue (**Figure 15**). This result was surprising as it was expected that the sequence shown to be involved in maternal deadenylation would be abundant in the blastula sample. This point opens two questions; firstly, what is the function of the 5' sequence in the blastula tissue? As there is such an enrichment of this mature sequence at blastula stages it would be interesting to investigate potential targets. Secondly, with such a clear switch in tissue specific expression of the two mature sequences does the 3' sequence in the more specialised tissues play any kind of biological role? Is it the case that the same hairpin plays a different role at different stages of development and if so what controls the processing to permit this? These are all interesting questions which should be investigated but as it is not the aim of the project they will not be discussed any further.

#### **13.6.4. miRNA expression profile over the samples**

Comparisons of miRNAs sequenced in neural, NC and ectodermal tissues revealed several points. First, miRNA diversity over the three tissues is remarkably limited. Just a few miRNAs were found to dominate the sequencing space in all three of these samples (**Figure 16B-D**). In total, the contributions of the top 10 miRNAs were found to total approximately 80% of the total miRNA hairpin reads sequenced across the samples. Following miR-427, the second most abundant miRNA in all three samples is miR-428 taking up between 2.4% and 6.4% of all reads. MiR-428 is a *Xenopus* specific miRNA and although its 5'

region has some similarity to previously identified mammalian miR-302 and miR-20, the function of this miRNA has yet to be investigated (Watanabe et al., 2005).

Despite this limited complexity, we did identify several differentially expressed or tissue-specific miRNAs, some of which are present at high abundance. Examples of these include miR-203 and miR-449, which are expressed in the ectoderm (**Figure 16B**). Both miR-203 and miR-449 have been implicated in epidermal development. MiR-203 is known to target the transcription factor p63 (Nissan et al., 2011), a p53 family member which is known to be critical in the development of stratifying epithelia in both human (Rinne et al., 2007) and mouse (Mills et al., 1999). miR-449 has been shown to play a vital role in ciliogenesis of epithelial tissue in both *Xenopus* and mice (Song et al., 2014). In neural tissue, miR-302 and miR-93 are both highly expressed (**Figure 16C**). MiR-302 has been previously documented to play a role in neural development. Previous studies have shown using WISH that miR-302 is highly expressed in early neuroepithelium (Jeong et al., 2014). In addition, knockout mouse models of miR-302 results in early embryonic lethality characterised by an open neural tube defect (Parchem et al., 2015). Finally, and most interestingly, the four miRNAs miR-219, miR-17, miR-130b and miR-20b are all abundant in the NC sample (**Figure 16D**). None of these miRNAs have previously been linked to NC development but most have indirect links. For example, microarray analysis on tissue depleted of the NC transcription factor *Sox10* demonstrated that both miR-17 and miR-20b were *Sox10* dependent miRNAs (Gokey et al., 2012). In addition, data has shown that miR-17 is regulated by the transcription factor *c-Myc*, an essential regulator of NC formation (Bellmeyer et al., 2003, Hatch et al., 2016). MiR-219 and its link to NC will be discussed more extensively in section 13.6.5.

In contrast to the neural, NC and ectodermal tissue, blastula is more distinct (**Figure 16A**). Unlike the other tissue types, miR-428 is not in the top 10 most abundant miRNAs, the most abundant miRNA after miR-427 is miR-148a which makes up almost 4% of the total reads. Also highly expressed in the blastula sample were miR-30a, miR-16 and miR-101-2. Previous data demonstrates that both miR-148a and miR-101 are abundant in *Xenopus* eggs so it is possible that the expression of these two seen in the blastula is a carry-over from the egg (Armisen et al., 2009). Through targeting of Nodal receptors, miR-16 has been shown to be key in the development of the dorsal signalling centre - Spemann's

organiser (Martello et al., 2007). It is therefore not surprising that this miRNA was relatively highly expressed in the blastula tissue. Interestingly, a novel miRNA (miR-nov-38a-1) is present in blastula profile taking up 2.5% total miRNA reads. With such relatively large read numbers it is possible that this miRNA is playing a role in early development and although it is not the focus of this work it should be followed up further.

### **13.6.5. Several miRNA hairpins are differentially expressed between the neural and NC samples**

In total, 11 miRNA hairpins were differentially upregulated in the NC sample when compared to neural. Of these, the top miRNA which is abundant in all three NC replicates is miR-219 (**Figure 17C**). Although there is no direct link between NC and miR-219 in the literature, miR-219 has some interesting NC related targets (both validated throughout the literature and predicted using target algorithms). One of these is *PDGFR $\alpha$*  (Dugas et al., 2010). *PDGFR $\alpha$*  is a receptor for the ligand PDGF. Once bound, the PDGF ligands exert their function by causing dimerisation and activation of the PDGF receptors. This, in turn, results in activation of a multitude of intracellular signalling cascades. The outcomes of these signalling events are diverse and include proliferation, migration, matrix deposition, survival and EMT (Betsholtz et al., 2001). *PDGFR $\alpha$*  has been demonstrated to be vital for initiation of NC migration through multiple mechanisms such as up-regulation of MMP2 for matrix degradation prior to migration (Robbins et al., 1999) and inhibition of apoptosis (Soriano, 1997). Loss of function experiments for *PDGFR $\alpha$*  result in cleft palatal defects in zebrafish, mice and humans (Roessler et al., 1996) (Tallquist and Soriano, 2003) (Li et al., 2009b). The ligand, PDGF is often used as a marker for migrating NCC. It is therefore possible that miR-219 plays a function in repressing activity in the early pre-migratory NCC to prevent premature migration. In addition, using computational target algorithms multiple interesting targets were recorded for miR-219 including multiple members of the *Pax*, *Six*, *Eya*, *Dach* (PSED) network. Multiple members of this network have been demonstrated to play roles in all derivatives of the NPB (Schlosser, 2007). For an extensive review of these PSED network targets see section 13.12.2.

Interestingly, one of the miRNAs upregulated in NC - miR-196a, was the

strongest candidate that came out of the XenmiR approach (see section 13.6.1). MiR-10b is also in the top 10 differentially expressed miRNAs and as with miR-196a, miR-10b is also located within a HOX cluster (**Figure 20**) (Yekta et al., 2004). As with miR-196a (see section 13.6.1) miR-10b is known to target multiple HOX genes, some of which are implicated in NC development (Woltering and Durston, 2008). In addition, miR-10b has been shown previously *in vitro* to target the histone deacetylase - *HDAC4* (Ahmad et al., 2015). *HDAC4* has been shown to be required for the generation of anterior facial structures in zebrafish by modulating the migration of CNC cells (DeLaurier et al., 2012). Finally, miR-10b has been shown to modulate the TGF $\beta$  pathway by directly targeting *TGF $\beta$*  (Han et al., 2014). TGF-beta ligands and their signalling intermediates have significant roles in patterning and specification of cranial NC cells (Chai et al., 2003). Notably, the miR-130 family had multiple members differentially expressed between neural and NC. This family of miRNAs is vertebrate specific and has recently been shown to be upregulated by the protein YAP (Shen et al., 2015). YAP is an activator of the Hippo pathway, a pathway that has been shown to be key in the establishment of a NC fate (Hindley et al., 2016).

miR-nov-12a was the only novel miRNA to make the top 10 differentially expressed miRNAs (**Figure 17D**). Although the read numbers were not high it is still possible that this miRNA is playing a role in NC development. Due to time restraints, this miRNA was not followed up further but computational target analysis should be performed for this miRNA to investigate potential interesting targets.

### **13.6.6. miR-338 and miR-301a are expressed in both NC and blastula samples**

Two miRNAs were found to have an enriched expression in both NC and blastula tissues when compared to ectoderm and neural (**Figure 18A**). This makes them both candidates for miRNAs that are involved in maintaining this 'pluripotent cell population' of NC cells recently described by Buitrago-Delgado et al that originate in the blastula (Buitrago-Delgado et al., 2015). The first of these miRNAs is miR-338 (**Figure 18B**). miR-338 is an intronic miRNA, transcribed together with a host gene encoding an apoptosis-associated tyrosine kinase (*Aak*) (Barik, 2008). It has been shown that miR-338 is regulated by *Sox10* via the direct regulation of

its host gene, therefore providing a link between this miRNA and NC (Gokey et al., 2012). In addition, miR-338 has been shown in multiple biological contexts to be a negative regulator of differentiation. For example, miR-338 can inhibit the expression of osteoblast differentiation markers such as Osterix (*Osx*), thus reducing osteoblast differentiation (Liu et al., 2014). Finally, and most interestingly, miR-338, is known to be upregulated specifically by c-Myc in embryonic stem cells (Lin et al., 2009). This proves very interesting as Myc proteins are known to have an important function in stem cell maintenance and c-Myc has been demonstrated to be key in NC development (Cartwright et al., 2005, Bellmeyer et al., 2003, Hatch et al., 2016).

The second miRNA found to be enriched in both blastula and NC samples is miR-301a (**Figure 18C**). miR-301a has a strong link to the maintenance of pluripotency as it has been shown to partake in a positive feedback loop essential for human pluripotent stem cell (hPSC) self-renewal and reprogramming (Lu et al., 2014). Lu *et al* demonstrated that miR-301a inhibits the translation of both *SFRS2* and *MBD2*. *SFRS2* is a splicing factor, targeted by *OCT4* and required for pluripotency. *SFRS2* regulates alternative splicing of the methyl-CpG-binding protein *MBD2*, whose isoforms play opposing roles in maintenance of, and reprogramming to, pluripotency (Lu et al., 2014). They concluded that the miR-301 family independently regulate *SFRS2* and *MBD2* to “fine-tune” the expression of *MBD2* isoforms in the favour of self-renewal (Lu et al., 2014). In addition, miR-301 has also been shown to regulate the induction of induced pluripotent stem cells (iPSCs). It was first identified using a miRNA library screen whereby miR-301 was shown to enhance the efficiency of iPSC generation by repressing the homeobox transcription factor *Meox2* (Pfaff et al., 2011).

Clearly, from the results of this sRNA sequencing and through literature searches, both miR-338 and miR-301a are strong candidates for miRNAs that are responsible for maintaining this novel pluripotent cell population which gives rise to NC (Buitrago-Delgado et al., 2015). Unfortunately, it is not the aim of this project so functional analysis will not be performed but the data should be followed up by a future student.

From both the XenmiR approach and the sRNA sequencing presented in this chapter a number of candidate miRNAs that are located in the NC region became

apparent. To explore the possibility of these miRNAs playing a role in NC development, functional analysis using morpholinos (MOs) to knock down the miRNAs of interest was implemented.

# Chapter 4: Functional analysis of candidate miRNAs

---

## 13.7. Introduction

The results obtained from the candidate identification in chapter three suggested that there are six potential miRNAs that could be involved in NC development, those being miR-196a, miR-219, miR-302, miR-429, miR-30a-3p and miR-17-5p. To further investigate this, functional analysis was completed using MOs designed against the miRNAs in question (refer to materials and methods for MO sequences). The working aim of this experiment was to knockdown (KD) the six miRNAs individually and assess the phenotype at both whole embryo and a transcriptome level.

## 13.8. miRNA knockdown

To determine the importance of these candidate miRNAs on NC development the level of expression of each miRNA was depleted individually and the impact of the KD on NC derived structures (i.e. craniofacial cartilage) was assessed along with any changes in the expression of various NC markers. Since it is difficult to obtain a genetic mutant for a miRNA in *Xenopus laevis* we looked for alternative strategies. Antisense molecules such as 2'-O-methyl and locked nucleic acid (LNA) oligonucleotides (oligos) have been used to inhibit miRNAs in cell lines (Hutvagner et al., 2004), *Drosophila* embryos (Leaman et al., 2005), and adult mice (Krutzfeldt et al., 2005). However, they have been reported in multiple model organisms to cause severe toxic effects at the level required for sufficient KDs *in vivo*.

One alternative to the LNA modified oligos are MOs, a different type of oligos. MOs are synthetic molecules usually 25 bases in length, that bind to complementary sequences of RNA by base-pairing. Structurally, the difference between MOs and DNA is that, while DNA bases are bound to deoxyribose rings which are linked through phosphates, whereas the MO structure is based on

nucleic acids that are bound to morphine rings which are linked through phosphorodiamidate groups (Summerton and Weller, 1997). Consequently, the backbone of MOs is no longer charged making it unrecognisable to enzymes or signalling proteins and is therefore more resilient to nucleases and does not trigger an innate immune response. This significantly reduces loss due to oligo degradation, interferon induction and inflammation which are problems commonly encountered with LNA oligonucleotides (Summerton, 1999). MOs do not degrade their target miRNA molecules, instead they act by "steric blocking", binding to a target sequence within an miRNA and simply getting in the way of molecules that might otherwise interact with it (Eisen and Smith, 2008). MOs are commonly used in species such as *Xenopus* and Zebrafish, to study the role of mRNAs and miRNAs in development. For example, in Zebrafish, MOs complementary to miR-214 have revealed that this miRNA regulates expression of *su(fu)*, which encodes a modulator of Hedgehog signalling (Flynt et al., 2007), and MOs complementary to miR-140 have revealed that this miRNA regulates Pdgf signalling during palate formation (Eberhart et al., 2008). In *Xenopus*, the activities of miR-15 and miR-16 have been inhibited by MOs to reveal that these miRNAs target the type II Nodal receptor *Acvr2a* (Martello et al., 2007).

## 13.9. Results

### 13.9.1. Preliminary MO injections

To screen which of the candidate miRNAs may have a functional role in NC development, MOs for all miRNAs were injected at both 40 ng and 60 ng to assess the general phenotype of the developing embryo and the effect on the expression of the NC marker *Sox10* by WISH. MO's were injected into one dorsal blastomere of an eight-cell embryo so only the prospective neural and NC tissue on one half of the embryo would be affected (**Figure 21A**).

Of the six MO's injected, four gave phenotypes in varying degrees. The two MO's that gave no phenotype were those that targeted miR-17-5p and miR-30A-3p. The embryos appeared to develop normally and the expression of *Sox10* was unaltered on the injected side (**Figure 21B**). Although no phenotype was observed, these embryos were treated as useful controls for toxicity. The phenotype of the MO KD of MiR-429 was delayed. Changes were not seen before

embryos reached tadpole stages; they were unable to swim indicating either a neuronal or muscular defect (**Appendix 6**). The KD of the remaining three miRNAs (miR-219, miR-196a and miR-302) gave a phenotype related to NC and/or neural tissue development.

All three MO injections resulted in a reduction and/or loss of the NC marker *Sox10* on the injected side (indicated by red arrow head) (**Figure 21B**). This was most prominent with the miR-219 MO (60ng) with 26% of the injected embryos having a complete loss of *Sox10* expression and 49% with a partial loss. A similar level was seen with miR-196a MO (9% complete loss and 48% reduction) and miR-302 MO (13% loss and 45% reduction) (**Figure 21C**).

In addition to the loss of *Sox10*, multiple alternative phenotypes were observed during the development of the injected embryos. For miR-219 MO, a clear craniofacial deformation was noted in the later embryos (see section 13.9.3.1 for further discussion). As craniofacial cartilage is derived from cranial NC cells, this phenotype is indicative of NC defects. This phenotype was also noted for the miR-196a injected embryos along with an enlarged NP during the neurula stages of development (**Figure 21B**, black bar). During neurulation, the neural tube appeared to close properly on the injected side, however it was substantially wider. Nearly 90% of the embryos injected with 60ng of MO displayed this phenotype (**Figure 21D**). For miR-302 MO injected embryos, a more pronounced phenotype in the neural tissue was observed. As with miR-196a KD there was an enlarged NP in 77% of the embryos. Unlike miR-219 MO and miR-196a MO there was no craniofacial malformations, but instead a clear eye phenotype (see section 13.10.1 for further discussion).

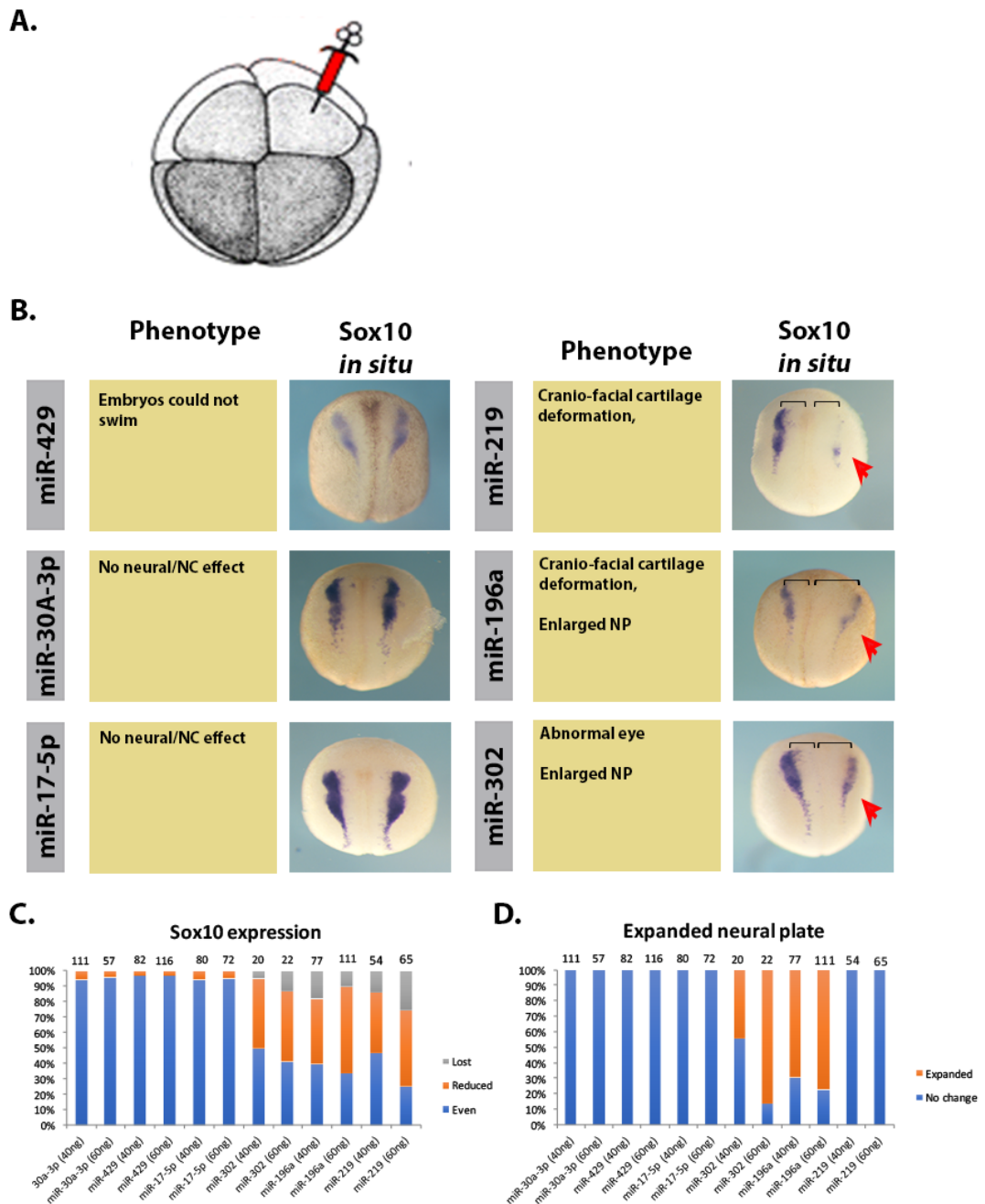


**Figure 21: Preliminary MO screens show miR-219, miR-196a and miR-302 KDs to give a NC phenotype.**

Mos were injected into one dorsal blastomere of an eight cell embryo with 60ng of MO therefore targeting only one half of the embryos prospective neural and neural crest tissue. Injection side is always the right side (A). Embryos with a KD of miR-17-5p and miR-30A-3p gave no altered NC or neural tissue phenotype and the expression of the NC marker *Sox10* was equal on both the injected and uninjected side. miR-429 KD had no change in the levels of *Sox10* but older embryos were unable to swim. KD of miR-302, miR-196a and miR-219 resulted in a reduction and / or loss of the NC marker *Sox10* on the injected side (indicated by red arrow head). MiR-219 and miR-196a KD gave a clear craniofacial deformation in the later embryo and miR-302 KD resulted an abnormal eye. Both miR-196a and miR-302 KD resulted in an enlarged NP (indicated by black bars) (B). Quantification of embryo phenotypes of each treatment, that had either reduced or lost expression of *Sox10* (C). Quantification of embryo phenotypes of each treatment, that had an expanded NP (D). Embryos depicted in dorsal view with anterior at the top.

## qRT-PCR validation of MO knock down

Once it was apparent that miR-196a, miR-219 and miR-302 were likely playing a role in early neural/NC development qRT-PCR was employed to validate that the MO was efficiently knocking down the miRNA in question. As a control for off-target effects, a 5-base pair mismatch (MM) control was designed for each miRNA. MiR-196a, miR-219 and miR-302 were all shown to be knocked down in a dose dependent manner by the appropriate MOs (**Figure 22**).

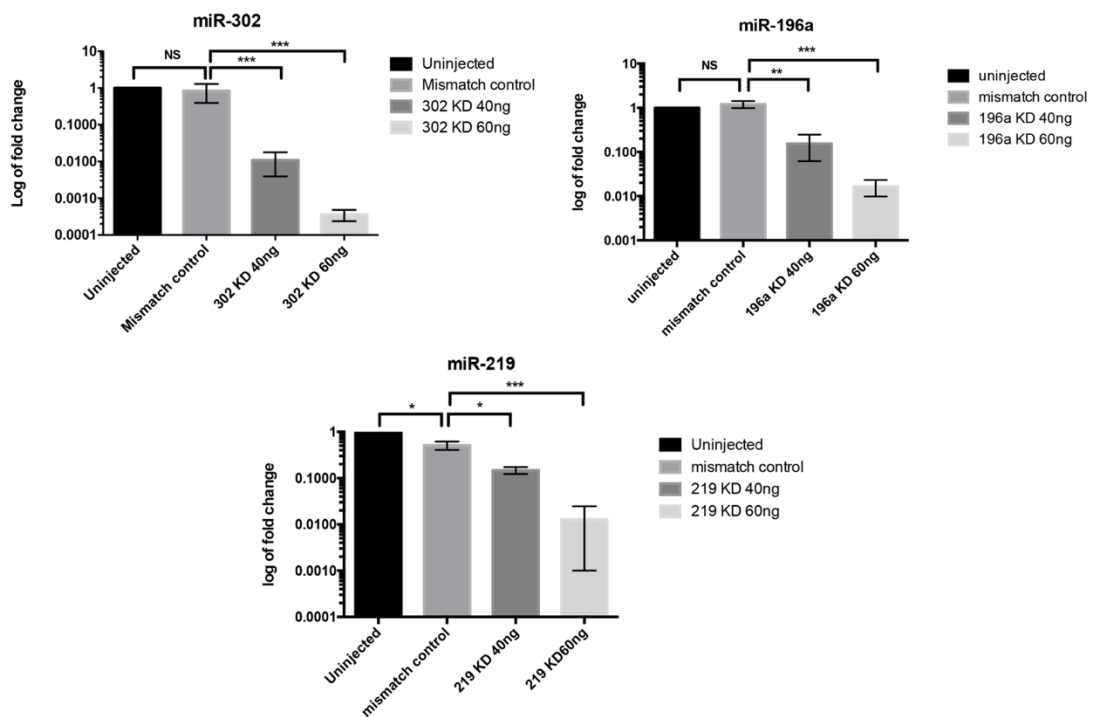


**Figure 22: qRT-PCR confirms that MOs targeting miR-302, miR-219 and miR-196a cause dose dependent knockdown.**

Embryos were injected into both cells of a two cell embryo with either 40ng or 60ng of MO and left to develop until satge 15. RNA was extracted and qRT-PCR was ran. One way ANOVA with Tukey post test statistical analyses were performed on the results of each qRT-PCR. For significance:  $0.05 \geq P > 0.01$ : \*;  $0.01 \geq P > 0.001$ : \*\*;  $0.001 \geq P > 0.0001$ : \*\*\*;  $P \leq 0.0001$ : \*\*\*\*.

### 13.9.2. MiR-302 KD results in defective neural development

As described in section 13.9.1, although miR-302 MO does reduce the expression of the NC marker *Sox10*, the strongest phenotype seems to be neural based. This is not surprising as from the sRNA sequencing results in chapter three we found miR-302 to be expressed in both neural and NC tissue with a higher abundance in the former (**Figure 19**). The phenotype observed following miR-302 MO injection is characterised with an expanded NP and a deformed eye

in the later embryo (**Figure 21**). Although phenotypes in neural tissue are not the main aim of this work, this phenotype was characterised further to generate preliminary data for upcoming projects in the lab.

#### **13.9.2.1. *miR-302 KD results in an abnormal eye development***

MiR-302 MO (60ng) was injected into one dorsal blastomere of an eight-cell embryo to target neural and NC tissue specifically. Embryos were left to develop until stage 37 and then fixed for analysis. The injection of miR-302 MO lead to a smaller, deformed eye (**Figure 23Ai**, black arrow head) which lacked pigment in certain regions. Closer inspection revealed the retinal pigmented epithelium (RPE) had failed to develop fully. Sections showed that although primitive structures were present, retinal lamination was severely disorganised upon miR-302 deficiency (**Figure 23Aii**, black arrow head).

#### **13.9.2.2. *Sox2 is miss-expressed in miR-302KD embryos***

To characterise the eye phenotype further, WISH were completed on miR-302 MO injected embryos (stage 24) for a gene that is key in neural and eye development – Sox2. Interestingly, when miR-302 was knocked down we obtained two separate observations. In the NP tissue, there was an expansion (**Figure 23Bi**, white arrow head), this was confirmed on cryo-sections (**Figure 23Bii**). The second observation made was the loss of expression of Sox2 in the prospective eye region (**Figure 23Bi**, black arrow head). This was seen in 95% of the injected embryos at a whole mount level (**Figure 23Ci**). Surprisingly, following sectioning of these embryos it became clear that the optic vesicle (**Figure 23Cii**) had failed to form and the tissue was poorly organised (**Figure 23Ci**). This was a surprising result as miR-302 KD embryos do go on to develop an eye (albeit primitive).

As this was not the focus of this project, miR-302 was not investigated any further.

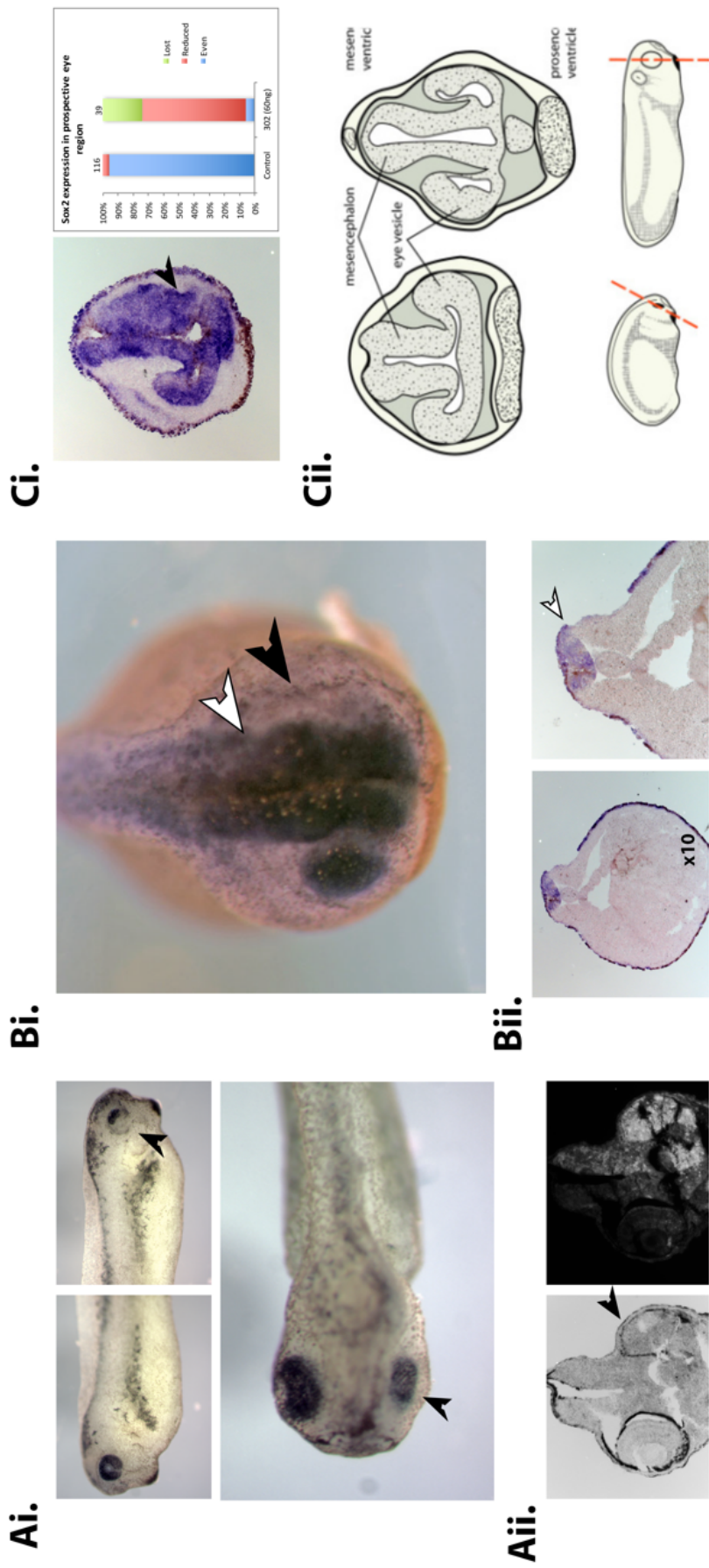


**Figure 23: miR-302 KD results in a neural phenotype characterised by an abnormal eye.**

Embryos were injected into one dorsal blastomere of an eight cell embryo with 60ng of miR-302 MO. The injected side is always the right side. At stage 35 the injected side of the embryo has an abnormal eye (see black arrow head) characterised by an under developed retinal pigmented epithelium (RPE) (28/34 embryos) (Ai). Sectioning demonstrated that although primitive structures were present, retinal lamination was severely disorganised (Aii). Sox2 *WISH* on stage 24 embryos show an expansion in the neural plate domain (see white arrow head) and a loss of Sox2 in the prospective eye region (see black arrow head) (Bi). Sectioning through the neural plate tissue of these embryos clearly demonstrates the expansion of Sox2 in the injected side of the embryo (see black arrow head) (Bii). Sectioning through the eye of the embryos revealed that the optic vesicle had failed to form properly (Ci) (see black arrow head). The percentage of embryos with a reduction or loss of expression of Sox2 in the prospective eye region is quantified in the bar chart. A schematic drawing of how an optic vesicle should look at stage 24 (Cii).

### 13.9.3. Full characterisation of miR-219 and miR-196a knock down

#### 13.9.3.1. *Effect of miRNA KD on craniofacial cartilage development*

As noted previously (**Figure 21B**), embryos with a KD of miR-196a or miR-219 had a craniofacial phenotype indicative of abnormalities in cranial NC development. To fully characterise this phenotype, embryos were injected with 60ng of MO into one dorsal blastomere of an eight-cell embryo and were left to develop until stage 28 for initial observations or stage 45 for alcian blue staining.

By stage 28, both un-injected and MM injected control embryos showed normal craniofacial development characterised by the cement gland being located approximately the same distance away from both eyes of the embryo. In addition to this, clear facial primordia are apparent (**Figure 24A**, white dotted line). This is compared to miR-196a and miR-219 KD embryos where malformations in craniofacial cartilage development was already very clear by this stage. With these embryos, the cement gland is positioned closer to the eye of the injected side of the embryo due to the clear lack of facial primordium (**Figure 24A**, black arrow).

To fully investigate the extent of this malformation, alcian blue staining was conducted on stage 45 embryos. Alcian blue is a stain that will label the glycosaminoglycans whilst leaving the rest of the embryo unstained. The staining worked well for miR-196a KD embryos but unfortunately for miR-219 KD embryos it failed to work. Following staining, cartilage was carefully dissected from the embryos. Analysis of dissected tissue demonstrates that the MM injected embryos showed normal organisation in the injected side when compared to the control side. This was not the case for miR-196a MO injected embryos which displayed much smaller and disorganised cartilage on the injected side despite some primitive structure being present (**Figure 24B**).

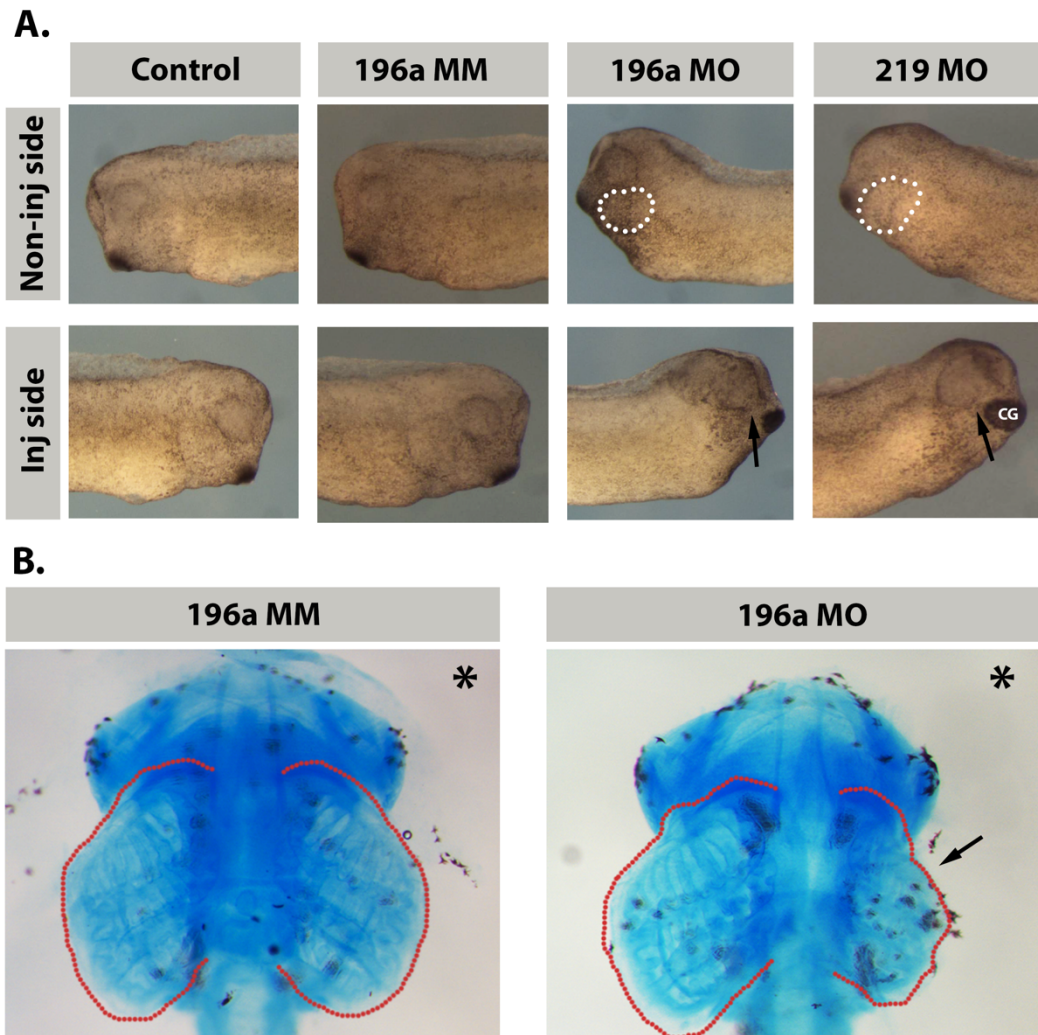


**Figure 24: miR-196a and miR-219 KD results in abnormal craniofacial cartilage development.**

Embryos were injected in one dorsal blastomere of an eight-cell embryo with 60ng of MO and then fixed at stage 28 for initial observations (**A**) and stage 45 for alcian blue staining (**B**). GFP was used as a tracer. Embryos are positioned in lateral view (**A**) and dorsal view (**B**). Downregulation of both miRNAs resulted in reduced facial primordium on the injected side (highlighted in non-injected side with a white dotted line) (n=15/18 embryos for miR-196a and 21/22 embryos for miR-219). As a result of the reduced primordium the cement gland (CG) is positioned closer to the eye on the injected side (indicated with black arrow) (**A**). Alcian blue staining reveals that for miR-196a KD the cartilage was smaller and disorganised although a primitive structure is present (n=7/8). Control MO (196a MM) did not interfere with cartilage development (n=8/8). \* indicates injected side (**B**).

### 13.9.3.2. *Analysis of key NC and NPB genes effected by miRNA knockdowns using WISH*

The results thus far delivered clear evidence that implicate miR-196a and miR-219 in NC development. This is primarily through the loss of the NC marker *Sox10* and abnormalities in the NC derived craniofacial cartilage following MO KD. To further elucidate what is happening at a molecular level, embryos were injected in one dorsal blastomere of an eight-cell embryo with 60ng of MO and then fixed at two neurula stages (stage 14 and stage 17). These embryos then underwent WISH for key NC and NPB markers.

#### *miR-196a*

At stage 14, WISH was completed on whole embryos for *Snail2*, an early transcription factor specific to NC. At stage 14, there a clear loss of the NC marker *Snail2* in the miR-196a MO injected embryos was observed. This loss was not seen in the miR-196a MM or control embryos. Sections of these embryos demonstrated that *Snail2* is completely lost throughout the tissue layers (**Figure 25**).

At stage 17, WISH was carried out for the NC transcription factor *Sox10* and the NPB marker *Pax3*. As with *Snail2*, *Sox10* is decreased in the miR-196a MO injected side of the embryo. Surprisingly, we found the NPB marker *Pax3* to be expanded on the injected side of the embryo. Through closer inspection it became clear that there are two regions of *Pax3* expression, both of which were affected following miR-196a depletion. The dark intense staining on the superficial ectodermal layer of the embryo (indicated on the control side with the black arrow head) is the prospective hatching gland (a gland that releases proteolytic enzymes to enable the tadpole to degrade the vitelline membrane), this staining is lost in the injected side. On the contrary, the *Pax3* positive cells in the NPB zone that go on to become NC cells (indicated with the red arrow head) are expanded (**Figure 25**). As this expansion of the *Pax3* positive NC progenitor field was concomitant with a decrease in genes expressed by specified, pre-migratory NC (*snail2* and *sox10*), this suggests that miR-196a depletion holds these cells in a progenitor, undifferentiated state and prevents them from becoming NC cells.

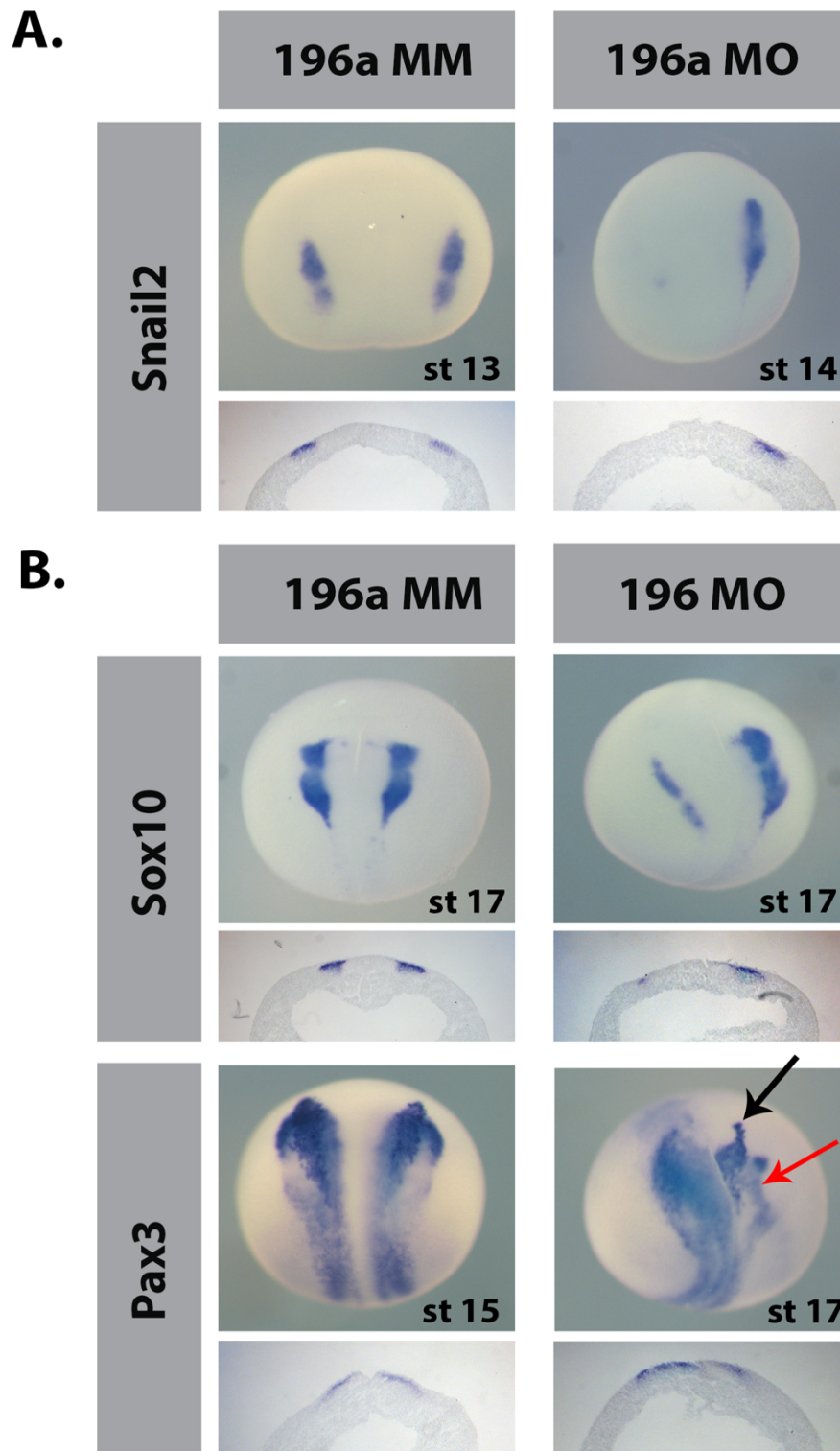


**Figure 25: MiR-196a kd alters expression of neural crest and neural plate border markers.**

Embryos were injected into one dorsal blastomere of an eight-cell embryo with 60ng of MO and then fixed at stage 14 (**A**) or stage 17 (**B**). GFP was used as a tracer. Injection side is always the left side. Embryos are positioned in dorsal view with anterior at the top. At both stage 14 (**A**) and stage 17 (**B**) the NC markers *Snail2* (n= 9/11) and *Sox10* (n=10/11) are lost/reduced in the injected side, this is not seen in the MM injected embryos (11/12). Sectioning of the embryos revealed in both cases that the expression is lost throughout all of the tissue layers. At stage 17 the NPB marker *Pax3* is expanded (n=11/13). The expansion seen is by the underlying NPB zone *Pax3* positive cells (indicated with a red arrow in the control side) whilst the *Pax3* positive hatching gland cells (see black arrow on control side) are lost.

Following the clear effect miR-196a KD is having on both NC and prospective NC cells, WISH was completed for several other markers to further decipher the signalling events at a transcriptional level when miR-196a is depleted.

The first group of genes that were investigated were various NPB markers. These included *Zic1*, *Zic3* and *Msx2*. As indicated with black arrows in **Figure 26A-C**, both *Zic1* and *Zic3* were expanded on the injected side of the embryo which reemphasises that the NPB region of NC progenitor cells is expanded. Interestingly, the NPB marker *Msx2* showed a loss of expression in the most anterior region which is clearly illustrated through sectioning of the embryo (**Figure 26C**).

Expression of the NP marker *Sox2* was broadened in a lateral direction following depletion of miR-196a. This indicates an expansion of the NP. This is true for both the anterior and posterior regions of the NP. In addition, where there is usually a dark concentrated patch of expression towards the more anterior part of the embryo (see control side) this is lost in the injected side (**Figure 26D**, see black arrow). Interestingly, despite an expansion of the *sox2* positive progenitor population being apparent, the neural differentiation markers; *N-tubulin* and *elrC* had reduced expression (**Figure 26H,I**). However, this did seem to be restricted to the more anterior region of the labelled primary neurons. Sectioning of the embryos exemplifies this phenotype. In addition to labelling primary neurons, both *N-tubulin* and *elrC* are also expressed in the trigeminal placodes. Following depletion of miR-196a it became apparent that the expression in this region of the embryo had extended both anteriorly and posteriorly, likely because of the lateral expansion of the NP (**Figure 26H,I**, see white arrow).

It is well documented that increased Notch expression and/or signalling correlates with increased numbers of neural progenitors and decreased differentiated neurons (Imayoshi et al., 2010). Therefore, WISH was completed for *Hairy1* – a downstream target of Notch signalling. Surprisingly, miR-196a KD resulted in a reduction in the mRNA levels of *Hairy1* although the region of expression appears to be expanded laterally along the axis of the NP (**Figure 26F**).

Another neural gene, *Pax6* gave two phenotypes, the first of which was an enlarged expression domain in the anterior neural fold (lens primordia) and the

second was a loss of the forebrain stripe (Li et al., 1997) (**Figure 26E**).

As miR-196a is positioned within a HOX gene the next task was to check expression of *Engrailed2* (*Eng2*), a neuronal regionalisation marker, which is important for patterning. Although *Eng2* had a broader expression pattern and was fainter (as with *Hairy1*) it did not seem to shift in position implying that patterning was not affected (**Figure 26I**).

### miR-219

As with miR-196a KD, both the NC markers *Snail2* (stage 14) and *Sox10* (stage 17) were dramatically reduced following depletion of miR-219. Sectioning of these embryos demonstrated that the markers are lost throughout all tissue layers (**Figure 27**).

Interestingly, the NPB marker *Pax3* was vastly expanded on the injected side at both stage 14 and stage 17 (**Figure 27**). Unlike miR-196a MO injected embryos that had an apparent loss of *pax3* positive hatching gland cells and an expansion of *Pax3* positive NPB zone cells, the inverse was seen in miR-219 depleted embryos. Sectioning revealed that the intense dark staining seen covering the injected side of the embryo is localised to the superficial ectoderm and is therefore likely an expansion of the *Pax3* positive hatching gland cells (see control side, red arrow). Conversely, *Pax3* expression in the deeper layer of tissue where the NC arise from is completely lost (see green arrows, **Figure 27**).

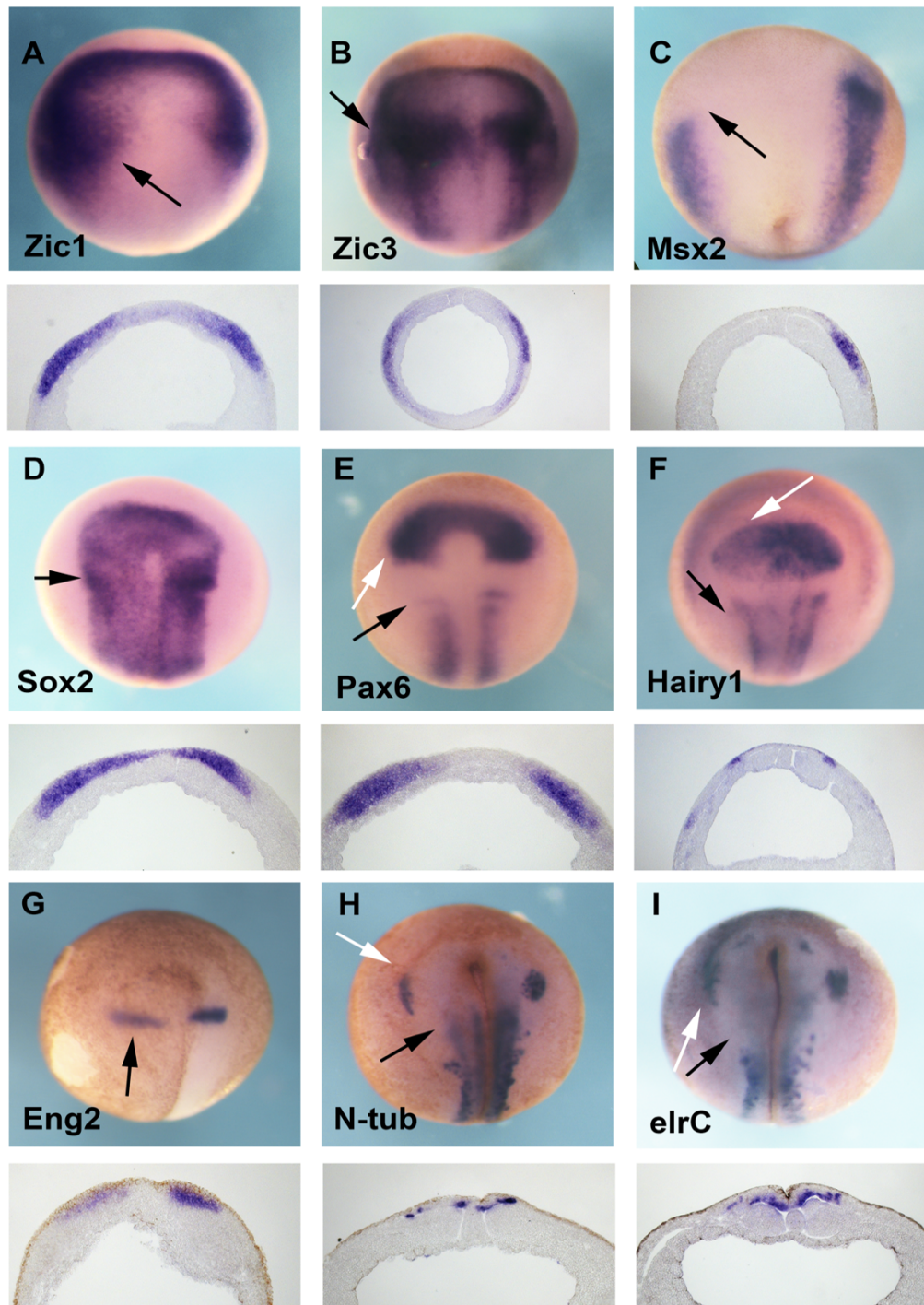


**Figure 26: The effect of miR-196a knock down on various markers.**

Embryos were injected into one dorsal blastomere of an eight-cell embryo with 60ng of miR-196aMO and then fixed at stage 14 (A-E), stage 15 (F-G) or stage 17 (H-I). GFP was used as a tracer. Injection side is always the left side. Embryos are positioned in dorsal view with anterior at the top. Injection of the MO caused an expansion in the NPB markers *Zic1* (n= 28/30) and *Zic3* (n=34/37) but a loss in the anterior region of the NPB marker *MSX2* (n=18/19) (A-C). The neural marker *Sox2* was expanded in a lateral direction and appeared to lose the intense dark region of expression seen in the control side (see black arrow) (n=37/37) (D). Expression of the neural marker *Pax6* was slightly enlarged across the anterior neural fold (lens primordia) (see white arrow) but reduced in the position of the forebrain stripe (see black arrow) (n=18/24) (E). The downstream target of Notch – *Hairy1* had a reduced but broadened expression (n=22/25) (F) and the same phenotype was seen for the neuronal regionalisation marker – *Eng2* (n=19/25) (G). Both neuronal differentiation markers *N-tub* (n=24/30) and *ELRC* (n=23/24) were reduced following miR-196aMO injection although this was restricted to the anterior most part of the NP (see black arrows). The expression of these two markers in the trigeminal placodes had extended in both an anterior and posterior direction (see white arrows) (H,I).

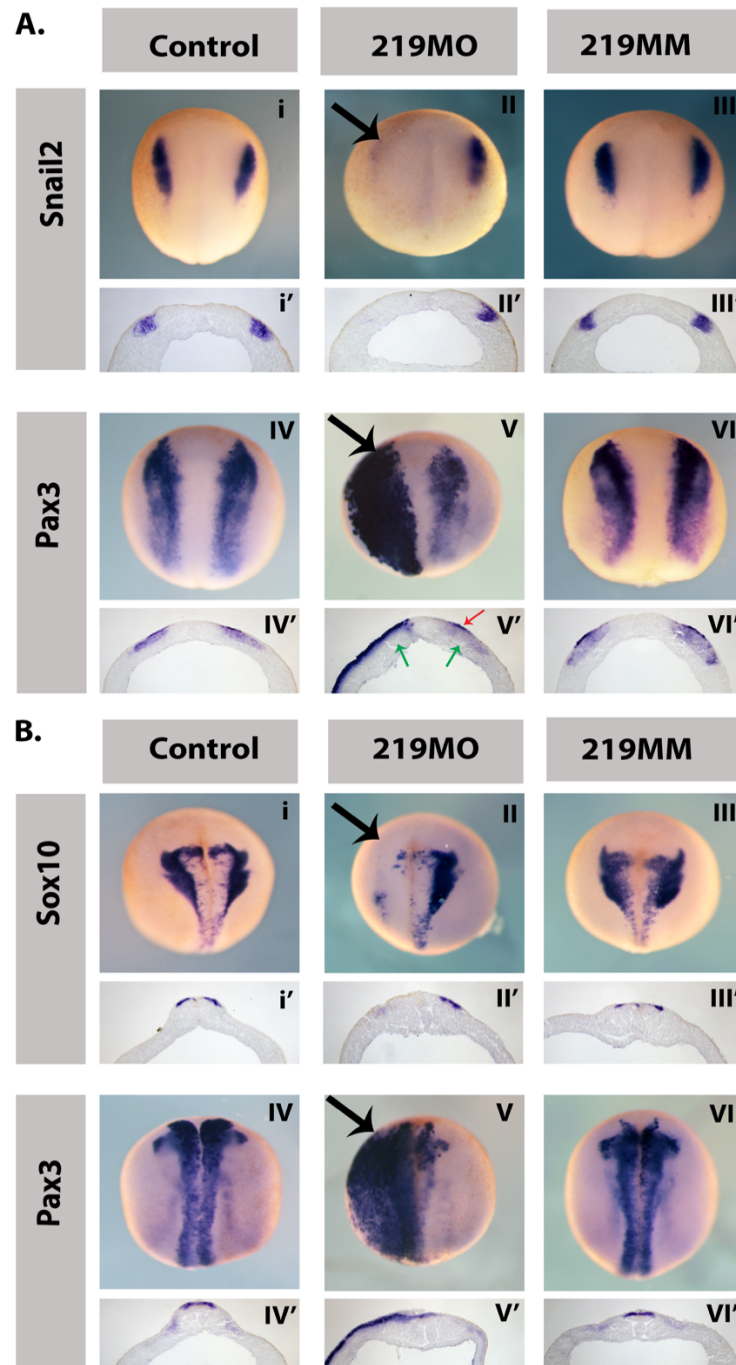


**Figure 27: The effect of miR-219 knock down on both neural plate border and neural crest markers.**

Embryos were injected into one dorsal blastomere of an eight-cell embryo with 60ng of MO and then fixed at stage 14 (**A**) or stage 17 (**B**). GFP was used as a tracer. Injection side is always the left side. Embryos are positioned dorsal view with anterior at the top. Embryos fixed at stage 14 underwent WISH for *Snail2* (n=26/29) and *Pax3* (n=21/21) and embryos fixed at stage 17 underwent WISH for *Sox10* (n=32/37) and *Pax3* (n=24/24). At both stage 14 and stage 17 the NC markers (*Snail2* and *Sox10*) are lost in the injected side (indicated with a black arrow) (**All** and **BII**), this is not seen in either the MM injected or control embryos. Sectioning of the embryos revealed that in both cases the expression is lost throughout all of the tissue layers (**All'** and **BII'**). At both stage 14 and 17 the NPB marker *Pax3* is expanded vastly across the injected side of the embryo (indicated with a black arrow) (**AV** and **BV**). Sectioning revealed that in the uninjected side of the embryo there are two regions of *Pax3* expression; the hatching gland (see red arrow) and the NPB zone cells (see green arrow) (**AV'**). When compared to the injected side it is apparent that the expansion seen at a wholemount level is from the hatching gland region and that in fact those *Pax3* positive NPB zone cells have been lost (**AV'** and **BV'**).

## 13.10. Discussion

Throughout this chapter, the function of six candidate miRNAs in NC development has been assessed using KD experiments. From this approach, one miRNA (miR-302) was found to result in neural defects when depleted and two miRNAs (miR-219 and miR-196a) gave phenotypes indicative of NC defects when depleted. This was evident at both the whole embryo level (abnormal craniofacial cartilage development) and at a transcriptome level (abnormal expression of NC genes using WISH).

### 13.10.1. MiR-302 KD impairs development of neural tissue

Following miR-302 KD a clear phenotype in neural tissue was observed characterised initially by a smaller, deformed eye that lacked a fully developed RPE (**Figure 23Ai, Aii**). To characterise this phenotype further, WISH for the neural marker *Sox2* on miR-302 KD embryos was completed. These ISHs revealed an expansion of *Sox2* in the NP and a loss of expression in the prospective eye region of a whole mount embryo (**Figure 23Bi**). Surprisingly, sectioning of the embryo revealed that the optic vesicle had failed to form by this stage on the injected side despite the embryos eventually forming an eye, albeit primitive (**Figure 23Ci**). One possible reason for this observed eye phenotype could be a perturbation of early neural or eye field induction and differentiation. Although there appears to be no optic vesicle in the earlier embryo, the embryos do go on to form an eye so a vesicle must form at some point. For a more thorough analysis of the time in which this occurs embryos would need to be sectioned at various stages of neural development.

Throughout the literature, miR-302 has been linked to the regulation of a proliferative state in many models (Card et al., 2008, Subramanyam et al., 2011, Parchem et al., 2015). It is possible that the removal of miR-302 encourages a more proliferative state, which causes a delay in development of the optic vesicle. A similar phenotype was observed with the removal of *Sox4* in *Xenopus* (Cizelsky et al., 2013). If the KD of miR-302 does perturb the balance between proliferation and differentiation this also gives a reason as to why we observed an expansion of *Sox2* positive NP tissue in the injected side of the embryo.

As development of neural tissue is not the focus of this project no further work was carried out on miR-302, however, to investigate whether the phenotype seen is due to a lag in development or whether it is in fact a morphological defect, several experiments could be done to test this. To explore the possibility of increased proliferation Bromodeoxyuridine (BRDU) staining could be used. To complement this, a tunel assay could be used to assay the level of apoptosis. Finally, to assess the development of the optic vesicle, embryos could be fixed at various stages and WISH for optic vesicle markers could be used to see if and when one does form.

### **13.10.2. miR-196a and miR-219 KD result in an inhibition of NC development**

Using KD experiments, we show, using WISH on key NC markers, along with analysis of NC derivative structures (craniofacial cartilage) that both miR-196a and miR-219 are playing a role in NC development. Using further WISH on various neural and NC markers we set out to characterise where in the NC network these miRNAs are functioning.

#### **13.10.2.1. *miR-196a***

##### **miR-196a may be involved in the fine tuning of BMP and/or Wnt signalling to enable NC progenitor specification:**

Using WISH for various markers it was observed that at neurula stages, two progenitor populations were expanded (*sox2* positive NP; *pax3* positive NPB), whereas differentiation markers of these tissues (*N-tubulin* positive primary neurons and *Sox10* positive NC) were reduced following depletion of miR-196a (**Figure 24 Figure 25**). This suggests that these cells are being held in a progenitor, undifferentiated state which prevents them from undergoing specification. This is supported by work by Kim et al. (2009) who showed using mesenchymal stem cells that inhibition of miR-196a enhanced proliferation and decreased osteogenic differentiation

Throughout the literature there are strong links between the maintenance of progenitor populations and increased Notch signalling (Imayoshi et al., 2010). To explore whether miR-196a functions in a Notch dependent manner WISH was

carried out for *Hairy1*, a direct Notch signalling target gene (Jouve et al., 2000). Surprisingly, miR-196a KD reduced the mRNA levels of *Hairy1* (**Figure 26F**). These results indicate that the ability of miR-196a to repress differentiation is likely independent of Notch signalling. However, it is possible that there could be a feedback mechanism that is resulting in this phenotype. In addition, Notch signalling has many independent downstream targets (including multiple *Hairy* genes) so more WISH need to be completed on various downstream targets before conclusions can be made.

Along with *Pax3*, multiple other NPB markers were expanded in miR-196a depleted embryos including *Zic1* (**Figure 26A**). *Zic1* expression is induced by low levels of BMP. It is expressed at the same time as *Pax3* and they work synergistically to induce NC fate through the activation of *Snail2* and *Foxd3* in a Wnt dependent manner (Plouhinec et al., 2014). This reiterates the importance of an appropriate balance of BMP and Wnt signalling for induction of NC. The observed changes therefore indicate that the depletion of miR-196a alters this balance enough to prevent induction of NC (Steventon et al., 2009).

One way in which an alteration in this balance may have prevented NC induction is through changes in expression of MSX genes. In contrary to the other NPB genes, the expression of *Msx2* was lost in the anterior most region of the NPB following depletion of miR-196a (**Figure 26C**). Previous studies have shown that MSX genes play a key role in specifying ectodermal cells as NC cells during NC specification. When inhibited, the prospective NC are transformed into NP and epidermis (Khadka et al., 2006). This may account for why a depletion of miR-196a results in an enlarged NP in the injected embryos (**Figure 21A**). *Msx2* has been shown previously to be induced by an intermediate level of BMP and WNT (Tribulo et al., 2003). This therefore further reiterates that miR-196a could play a role in fine tuning the balance of BMP and/or Wnt signalling. Further experiments could be used to test this hypothesis including BMP and Wnt reporters (Faure et al., 2000) to assess the changes in the level of BMP/Wnt following miR-196a KD.

#### **Depletion of miR-196a does not alter neural patterning:**

Despite miR-196a being positioned within a HOX gene there was no shift in position of the neuronal regionalisation marker – *Eng2* suggesting that the depletion of miR-196a does not alter neural patterning (**Figure 26G**). This

expression of *Eng2* however was broader and fainter again reiterating that there appears to be more neural tissue.

### 13.10.2.2. *miR-219*

#### **Depletion of miR-219 upregulates Pax3 positive hatching gland cells whilst Pax3 positive NC cells are lost**

As with miR-196a KD, depletion of miR-219 resulted in a loss of NC markers and deformations in craniofacial cartilage clearly demonstrating that this miRNA plays a role in NC development (**Figure 21**). Surprisingly, in contrary to the NC markers, the NPB marker *Pax3* was expanded vastly following miR-219 KD. Through sectioning of the embryo, it became clear that this expansion is isolated to the *Pax3* positive hatching gland cells. The *Pax3* positive cells that give rise to NC cells (*Pax3* positive NPB zone cells) had been lost (**Figure 27**). This suggests that miR-219 is playing a role early in NC development, before even the NC precursor cells (NPB cells) are formed.

The expansion of the *Pax3* positive hatching gland cells in conjunction with the loss of NC is a phenotype seen previously in the literature. Hong and Saint-Jeannet (2007) show that the specification of cells into hatching gland and NC is a consequence of distinct thresholds of *Pax3*. They show that for both cell populations, *Pax3* expression is required, however, both NC and hatching gland fate can only coexist in the embryo up to a certain amount of *Pax3*. At high levels of *Pax3* activity the entire ectoderm is converted into hatching gland precursor cells and NC are lost. This appears to be the phenotype seen here following miR-219 KD but to validate this, a WISH for hatching gland markers such as *Xhe2* needs to be completed. Evidently the loss of NC through the KD of miR-219 is *Pax3* dependent. *Pax3* is however not a target of miR-219 as there are no potential binding sites in the 3' UTR, therefore the effect we see on *Pax3* is indirect. To investigate this further, direct targets of miR-219 which feed into the *Pax3* gene network should be explored.

To conclude this chapter, KD of both miR-196a and miR-219 result in aberrant NC development. Thus far we can speculate that KD of miR-196a triggers this phenotype because of an extension of the time the progenitor pools stay in an undifferentiated state resulting in a failure of differentiation. This contrasts with

miR-219 where we speculate that the NC fail to form in these embryos because of a loss of the NC progenitor pool. To investigate how these phenotypes are achieved at a transcriptional level target analysis was employed.

## Chapter 5: Downstream target analysis of miR-196a and miR-219

---

Results obtained from the miR-219 and miR-196a KD experiments demonstrate that both miRNAs have key roles in NC development. However, the specific roles for miR-219 and miR-196a in NC development remains unknown. To elucidate this, potential targets of both miRNAs were analysed using two approaches. The first approach was using computational miRNA target prediction followed by validation using luciferase assays (for direct targets) and the second approach was a transcriptome analysis of NC tissue following KD of the miRNAs in question (for both direct and indirect targets).

### **Approach one – Computational miRNA target prediction**

#### **13.11. Introduction**

The first approach used to decipher the targets of both miR-219 and miR-196a was computational miRNA target prediction. Luciferase assays were used to validate predicted targets *in vitro*.

##### **13.11.1. miRNA-mRNA interactions**

In order for miRNAs to downregulate gene expression, they use imperfect binding to complementary sites within transcript sequences (usually in the 3'UTR) and result in either suppression of translation, deadenylation and degradation or induced cleavage of their target transcript (Chekulaeva and Filipowicz, 2009). The sites that the miRNAs bind to are named target sites, in animals, these target sites are usually found clustered at both ends of the 3'UTR as opposed to being evenly distributed (Hon and Zhang, 2007). Many mRNAs have multiple predicted binding sites for the same miRNA, which can enhance the degree of downregulation (Grimson et al., 2007, Doench et al., 2003). Located at the 5' end

of the miRNA is a region called the “seed”, (positions 2-7) which is characterised by complementary base pairing between miRNA and its target site (Lim et al., 2003). The classification of miRNA target sites is based on the complementarity within the seed region and its target site. To date, the effect of different types of seed matches has been assessed by means of signal-to-noise ratio, the degree of mRNA or protein repression (Lewis et al., 2005) (Grimson et al., 2007) (Baek et al., 2008). Based on these experiments, a set of seed matches that differ in abundance and intensity of the regulatory effect have been defined including: (1) canonical, (2) 3'-supplementary and (3) 3'-compensatory sites (Bartel, 2009) (**Figure 28**).

The majority of miRNAs target confirmed mRNA sites via canonical sites (summarised in **Figure 28**). Canonical sites have alternative pairing within the seed region which determines the certainty of the interaction. There are three types of canonical sites: the 7mer1A that has an adenine in position 1 at the 5' end of miRNA (the presence of which acts as an anchor for RISC and therefore improves the degree of gene silencing (Nielsen et al., 2007), the 8mer having matched adenine in position 1 and an additional match in position 8 and the 7mer-m8 that has a match in position 8 (Lewis et al., 2005). In addition to seed binding, many miRNA-mRNA interactions have additional pairing within the 3' part of a miRNA and the 5' part of the mRNA transcript. It has been reported that consecutive pairing in positions 13-16 of at least 3-4 of miRNAs are usually required to enhance the efficacy of the interaction (Grimson et al., 2007).

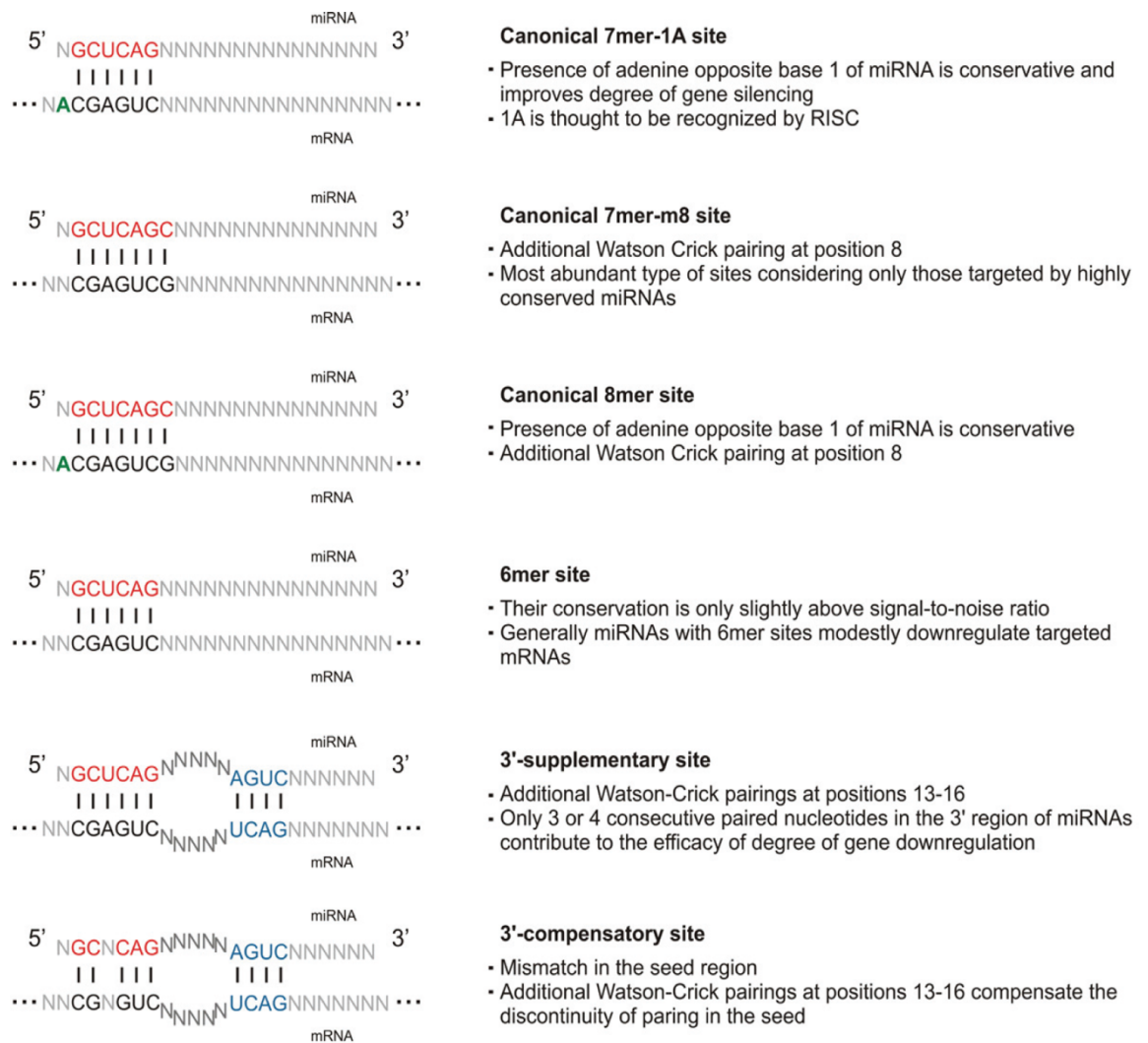


**Figure 28: A schematic representation of various miRNA interactions**

Seed regions of miRNAs are marked in red and the adenine at binding position one in green. In the case of 3'-supplementary and 3'-compensatory sites two regions of pairing (in blue) result in the formation of a loop structure (Witkos et al., 2011).

### 13.11.2. Computational miRNA target prediction

For any given miRNA, an extremely large number of potential target sites exists and the process of validating a potential miRNA target in the laboratory is time consuming and costly. To narrow down the list of candidates, a computational approach for miRNA target prediction is often used. Computational approaches model how miRNAs interact with specific mRNAs for which an increasing collection of tools is available. Each of these has a distinct approach to miRNA target prediction. To assess the probability of a potential target these various algorithms use their own unique set of parameters which will include a measure of conservation level (the maintenance of a sequence across species), free energy (a measure of the hybridization stability) and site accessibility (a measure of the ease with which a miRNA can locate and hybridize with an mRNA target). Two of the most commonly used computational algorithms in the scientific community are miRanda and TargetScan, both of which take different approaches to predicting targets and will briefly be described below:

#### 13.11.2.1. *miRanda*

The main parameters the miRanda algorithm focuses on when predicting targets include the binding energy of the duplex structure, evolutionary conservation of the whole target site and its position within 3'UTR (John et al., 2004). Together, along with the level of seed sequence base pairing these factors are scored. miRanda allows for one wobble pairing in the seed region that is compensated by matches in the 3' end of miRNA. This strategy incorporates different natures of miRNA-mRNA interactions and is therefore beneficial for predicting sites with imperfect binding within the seed region, but it has been criticised for underestimating miRNAs with single but perfect base pairing. As a consequence, this algorithm often results in a large number of false positives (Witkos et al., 2011). Even though still widely accepted, updates for this prediction algorithm have stopped in 2010.

#### 13.11.2.2. *TargetScan*

In contrast to miRanda, TargetScan uses a more precise search that puts emphasis on the sites that have full complementarity in the miRNA seed region (Lewis et al., 2005). In addition to a precise seed match, several parameters

determined in a previous experimentally validated dataset contribute to TargetScan's outcome score including: (1) pairing contribution outside the seed region (2) AU content of the region surrounding the predicted site and (3) the distance to the nearest end of the annotated UTR of the target gene (Grimson et al., 2007). Importantly, the conservation of target sites among orthologous 3'UTRs has a fundamental importance for an outcome score in TargetScan (Friedman et al., 2009). As a result of the number of stringent parameters used by TargetScan, it is seen as more precise than some alternative target prediction algorithms, however, as full complementarity is needed in the seed sequence those sites with poor seed pairing are omitted.

### 13.12. Results and discussion

To investigate the potential targets of both miR-219 and miR-196a computational miRNA target prediction was employed. As a result of poor genome annotation in *X.laevis*, algorithms were run using the *H.sapiens* genome and strongly predicted targets were manually checked for conservation within *X.laevis*. Due to the vast number of predicted targets which are omitted from these various algorithms, multiple algorithms were used and potential target output results were collated to identify strongly predicted common targets.

Initially, target prediction was carried out manually using the following algorithms: TargetScan (Lewis et al., 2005), DIANA (Paraskevopoulou et al., 2013), PicTar (Krek et al., 2005), miRanda (John et al., 2004) and miRDB (Wong and Wang, 2015). Interesting targets that came up across multiple result outputs were then further investigated using literature searches. In addition to manual analysis another integrated programme was used alongside, this being miR-system (Lu et al., 2012). When running the algorithm sites manually, challenges began to arise when predictions were inconsistent due to the different modelling formulas. miR-system is able to overcome this problem by integrating the results of various algorithms ranging from ones that consider seed-matching (TargetScan) to those who focus on other parameters such as affinity (DIANA). miR-system uses a voting scheme and establishes a statistical threshold based on existing data to identify the optimal cutting point. In addition to this, following identification, this system provides information on pathway analyses of the target mRNA therefore facilitating the understanding of the biological functions regulated by the miRNA

(Lu et al., 2012).

### 13.12.1. Predicted targets for miR-196a include various HOX genes

Results from both the manual target analysis (**Figure 29**) and miR-system (**Appendix 8**) show that across various algorithm sites, a number of HOX genes are strongly predicted targets for miR-196a (**Figure 29**). Interestingly, miR-196 is located in the intronic regions of three HOX gene clusters: miR-196b on HOXA, miR-196a-1 on HOXB and miR-196a-2 on HOXC. miR-196a-1 and miR-196a-2 have an identical mature sequence, whereas miR-196b differs by a single nucleotide (Liu et al., 2013). These miRNAs target HOX genes located 5' of their locus, supporting the theory of posterior prevalence (Yekta et al., 2004, McGlenn et al., 2009). miR-196a targets several HOX genes, including *HOXA5*, *HOXB7*, *HOXB8* and *HOXC8* (Liu et al., 2012, Braig et al., 2010, Asli and Kessel, 2010, Li et al., 2010), and is predicted to target many more (**Figure 29**).

HOX genes are expressed at the time of NC induction and play a central role in NC patterning (Trainor and Krumlauf, 2001). Studies in mouse have shown an important link between NC development and HOX genes. For example, Gouti et al. (2011) showed that multiple HOX genes play a central role in NC cell specification by inducing the expression of *Snail2* and *Msx1/2* and that simultaneous loss of HOXA1 and HOXB1 function resulted in NC specification defects. They reported a neural progenitor to NC cell fate switch characterised by cell adhesion changes and an epithelial-to-mesenchymal transition.

For us, the most interesting HOX gene that was predicted (but not experimentally validated) to be a target of miR-196a was *HOXB1*. This HOX gene is of particular interest because it has direct links with NC development. Gouti et al. (2011) showed that, in chick, *HOXB1* functions to induce NC cells through mediating an optimal level of Notch signalling. This was achieved through repression of the downstream effector Hes5. In chapter four we showed that the downstream Notch target *hairy1* had a broader expression but was fainter following miR-196a KD (**Figure 26**). This contradicts the idea that the phenotype we observe is mediated through Notch signalling. However, it is possible that the effect could be mediated by other Notch downstream effectors (i.e. Hes-5) and therefore

further WISH using other markers of Notch signalling and other means of experimental confirmation should be employed.

### 13.12.2. Predicted targets for miR-219 include the co-factor *Eya1*

Results from both the manual target analysis (**Figure 30**) and miR-system (**Appendix 7**) show that across various algorithms, a number of genes from the PSED (Pax-Six-Eya-Dach) network were predicted to be targeted by miR-219 (**Figure 30A,B**). The PSED network is a group of proteins that are connected by protein-protein interactions. They have been shown to be involved in a variety of developmental processes including muscle development and sensory placodal development (Donner and Maas, 2004, Friedrich, 2006, Kozmik et al., 2007). This is interesting for multiple reasons in the context of miR-219 and NC development, firstly because as with NC, the cranial sensory placodes are also derived from the NPB zone (Saint-Jeannet and Moody, 2014). Classic histological descriptions of cranial sensory placode formation identified the origin of all cranial placodes from a common precursor region called the pre-placodal ectoderm (PPE) which is a U-shaped band of ectoderm that surrounds the anterior margin of the NP lateral to the NC (**Figure 31**) (Moody and LaMantia, 2015). The second reason is that some of the genes within this network have been shown to act upstream of *Pax3* in alternative systems which could account for why we get expanded *Pax3* expression (**Figure 27**) following KD of miR-219 (Grifone et al., 2007, Lagutin et al., 2003). One of the PSED genes predicted to be targeted by miR-219 but not yet experimentally validated in any system is the coactivator, *Eya1*.

The EYA proteins are components of a conserved regulatory network involved in cell-fate determination in organisms ranging from insects to humans. Together, along with the other members of the PSED network they play a key regulatory role in the development of multiple organs including but not limited to the eye, muscle, ears, heart and craniofacial skeleton (Tadjuidje and Hegde, 2013). Vertebrates encode four EYA proteins (EYA1-4) that are characterised by a conserved C-terminal 271 amino-acid domain commonly referred to as the EYA domain (Ohto et al., 1999). Early studies in *Drosophila* characterised the transcriptional role of EYA through genetic and/or biochemical interaction with the SIX (Pignoni et al., 1997) and DACH (Chen et al., 1997) classes of

transcription factors. In vertebrates, SIX proteins (SIX1 and SIX4) binds to and translocate EYA1 to the nucleus, where they act as cofactors to activate SIX genes including *Pax3*. The presence of EYA1 converts SIX which is usually a weak activator of transcription into a strong transcriptional activator (Li et al., 2003, Patrick et al., 2013). In the context of somitogenesis Eya1 has been shown to act upstream of *Pax3* with Eya1 null embryos losing all expression of *Pax3* in the dermamyotome (Grifone et al., 2007).

*Eya1* is predicted to be a miR-219 target by all five of the online algorithms and through miR-system (**Appendix 7**) making it a very strong candidate. The seed binding is classified as an 8-mer meaning there is an adenine in position 1 and an additional match in position 8 (**Figure 30C**). As a result of being such a strong potential target of miR-219, *Eya1* was chosen to be validated as a direct target using luciferase assays.

### **13.12.3. Validation of Eya1 as a target of miR-219 using luciferase assays**

Validation of *Eya1* as a direct target was done by luciferase assays of modified pGL3 reporter constructs containing the 3'UTR of *Eya1*. This bioluminescence assay is a quantitative method based on sequential measurements of Firefly and Renilla luciferase activities in a single sample. The 3'UTR of *Eya1* contains one conserved predicted miR-219 binding site which was mutated to show that repression is mediated specifically through the predicted target site.

In summary, WT or mutant constructs (100ng) were co-transfected, into chicken DF1 fibroblast cells, with Renilla vector (25ng) and either with or without the miR-219 siRNA (si-219). This siRNA is used to mimic the action of miR-219. A universal negative control siRNA (siC; Sigma) was used as a negative control.

**A.**

TargetScan	DIANA	PicTar	miRanda	miRDB
HOXC8	HAND1	HOXC8	HOXA7	ZMYND11
HOXA7	HOXA7	ZMYND11	HOXC8	SLC9A6
HOXB8	WIPF2	CCNJ	SMC3	AQP4
NR6A1	SLC9A6	MLR2	SLC9A6	NR2C2
RP1-170019.20	CCDC47	KIAA0685	HOXA9	HOXB7
HOXA9	CASK	HMGA2	HMGA2	GATA6
HMGA2	HOXA9	PPP1R15B	CTBS	PBX1
HOXB7	LRP1B	FLJ46247	GPBP1	ERI2
LCOR	NR6A1	SLC9A6	ZMYND11	DENND6A
SLC9A6	HOXA5	FLJ20232	C1orf88	HOXC8
HAND1	HOXB7	DDX19	C3orf38	RDX
ZMYND11	PSMD11	TRERF1	COL15A1	CCDC47
NRAS	GATA6	SORCS1	ELMO2	MAP3K1
EPC2	ZBTB26	GAN	CCNJ	ELAVL4
HOXA5		GGA3	MAP3K1	CEP350

**B.**

TargetScan	DIANA	PicTar	miRanda	miRDB
HOXC8	HOXC8	HOXC8	HOXA7	HOXB7
HOXA7	HOXA9	HOXB6	HOXC8	HOXC8
HOXB8	HOXA5	HOXB7	HOXA9	HOXA7
HOXA9	HOXB7	HOXA1	HOXD8	HOXA5
HOXA5	HOXB6		HOXA5	HOXA9
HOXB6	HOXB1			HOXB6
HOXB1				

**Figure 29: Multiple HOX genes are predicted to be targeted by miR-196a.**

The top fifteen genes predicted to be targeted by miR-196a using five different computational tools (TargetScan, DIANA, PicTar, miRanda and miRDB) **(A)**. Multiple HOX genes were predicted to be targeted by miR-196a **(B)**.

**A.**

TargetScan	DIANA	PicTar	miRanda	miRDB
ZBTB18	SOX5	FLJ20241	ZNF238	GXYLT1
RORB	XPR1	PI4KII	CD164	CD164
GXYLT1	CAMK1D	NUMB	SMC4	TRHDE
CD164	SIX3	ZNF238	FBX030	KCNA4
RASSF3	CXXC4	SNRK	MYH10	RASSF3
RBM24	LEF1	DKF2p566M1046	MCOLN3	CGNL1
CTD-2330K9.3	DOK6	RBM34	LAPTM4A	CLOCK
<b>EYA1</b>	<b>EYA1</b>	ING3	CXCL11	GLTSCR1L
T	YTHDF3	RARS	ADCYAP1	ELOVL7
FOXJ3	MIER3	MEF2D	EMR2	RAB17
CC2D1A	S100PBP	PIB5PA	PGR4	SLC31A1
TMEM98	TRHDE	SDK1	C20orf108	<b>EYA1</b>
SNRK	CTD-2330K9.3	ZNRF1	EXOC4	INPP5J
DOK6	GLMN	LAPTM4A	TRDN	RECK
CCDC28A	KCNH8	FBXW2	KLHL5	DDAH1

**B.**

TargetScan	Diana	PicTar	miRanda	miRDB
<b>EYA1</b>	SIX3	<b>EYA2</b>	<b>EYA1</b>	<b>EYA1</b>
SIX3	<b>EYA1</b>	<b>EYA1</b>		
EYA2	EYA2			
SKIDA1	EYA3			
EYA3				
PAX2				

**C.**

	Predicted consequential pairing of target region (top) and miRNA (bottom)	Site type
Position 705-712 of EYA1 3' UTR	5' ...UAUGUACAUCACUGAGACAAUCA...	8mer
hsa-miR-219a-5p	3' UCUUAACGCAAACUGUUAGU	

**Figure 30: Multiple members of the PSED network are predicted to be targeted by miR-219.**

The top fifteen genes predicted to be targeted by miR-219 using five different computational tools (TargetScan, DIANA, PicTar, miRanda and miRDB) (**A**). (Multiple members of the PSED network were predicted to be targeted by miR-219, one that was predicted by all computational tools is *Eya1* (indicated with black box) (**B**). The predicted pairing region of miR-219 seed sequence (bottom row) with *Eya1* 3'UTR (**C**).

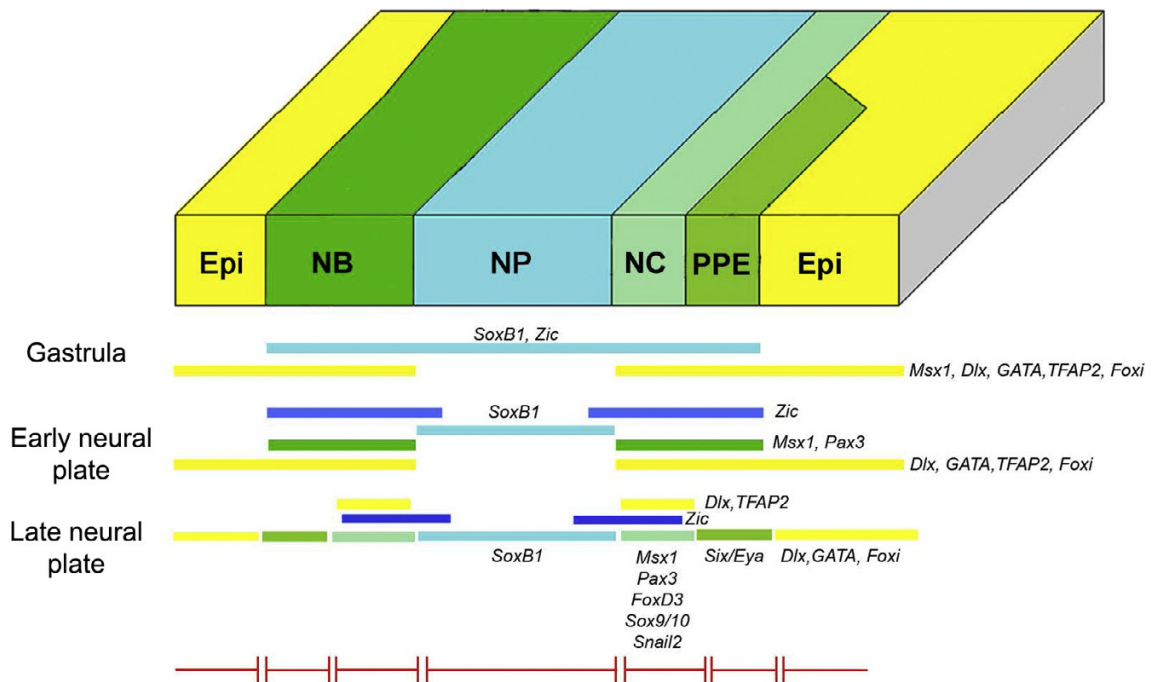


**Figure 31: Schematic drawing of the various regions induced during early neural plate development.**

**Top:** The embryonic ectoderm of a neurula stage has been flattened into a sheet. The left represents the fields apparent at early NP stages: epidermis (Epi), neural border zone (NB) and neural plate (NP). On the right the NB has divided into its neural crest (NC) and pre-placodal ectoderm (PPE) derivatives.

**Bottom:** Different sets of transcription factors are differentially expressed in these ectodermal domains over developmental time (Moody and LaMantia, 2015).

### 13.12.3.1. miR-219 targets *Eya1* 3'UTR

Luciferase reporter assays showed that miR-219 targets the *Eya1* 3'UTR, leading to a decrease in luciferase activity by approximately 50% (Mann Whitney test:  $p < 0.0001$ ). This reduction was rescued by mutating the predicted miR-219 binding site (**Figure 32**). This validates that *Eya1* is a direct target of miR-219 *in vitro*. A future experiment that needs to be completed is to investigate whether the NC phenotype observed is a consequence of miR-219 targeting *Eya1* and not a result of alternative miR-219 interactions. To investigate this, several experiments could be employed. One example would be to inject custom MOs (also known as target protectors) that bind the miR-219 target site on the *Eya1* 3'UTR *in vitro* and then assess the embryo for the various NC phenotypes. This MO would work by preventing any interactions between the miRNA and *Eya1*. If the same phenotype as miR-219 KD is observed then using the appropriate rescues it could be speculated that it is the inhibition of this interaction specifically that prohibits NC development.

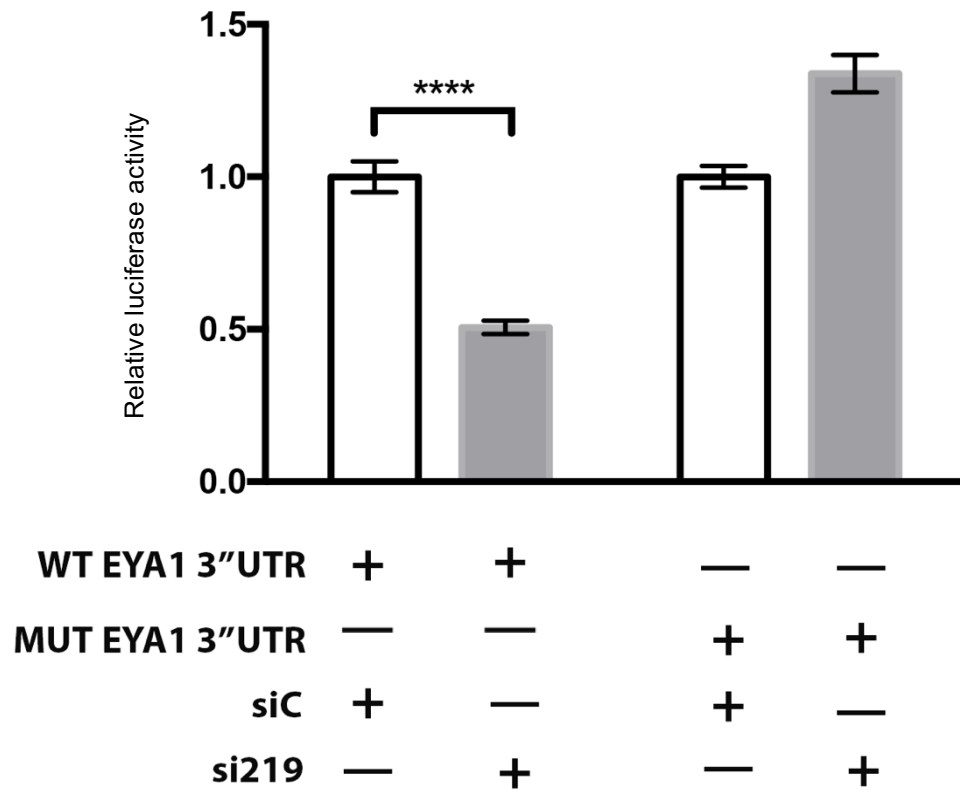


**Figure 32: EYA1 is a target of miR-219 *in vitro*.**

The unmodified 3'UTR and the 3'UTR with the miR-219 target site mutated were assayed using chicken DF1 cells with the miRNA mimics indicated below the graph. MiR-219 reduced luciferase activity by over 50% and this was rescued when the target site was mutated. For statistical analyses, a Mann-Whitney test was performed. For significance:  $P \leq 0.05$ : \*;  $P \leq 0.01$ : \*\*;  $P \leq 0.001$ : \*\*\*;  $P \leq 0.0001$ : \*\*\*\*

## **Approach two: Transcriptomic analysis of neural crest tissue following knockdown of miR-219 and miR196a**

### **13.13.Introduction**

The second approach that was used to gain a global overview of what gene changes were occurring following miR-219 or miR-196a KD was RNA sequencing. The main aim of this experiment was to complete RNA sequencing on NC dissections which had been injected with MO for either miR-196a or miR-219 and compare the gene expression to controls. This would enable us to assess any pathways or NC specific genes that have been altered as a result of a KD of the two miRNAs. These experiments were carried out at the Institut Curie (Orsay) in collaboration with Professor Anne-Helene Monsoro-Burq. She is a pioneer in the technique of NC dissection and therefore her expertise was valuable for obtaining carefully dissected NC tissue.

#### **13.13.1. Experimental pipeline**

At 4-cell stage, embryos were injected with 60ng of one of four MO's (miR-219, miR-219MM, miR-196a or miR-196aMM) into one dorsal blastomere to target neural and NC tissue in one side of the embryo only. Embryos were left to develop until stage 14, 17 and 28. Stage 14 and 17 for dissections and stage 28 for craniofacial cartilage deformations. Those embryos left to develop until stage 14/17 were split into two groups. One group underwent WISH to check NC genes were knocked down and the other group underwent NC dissections. During dissections, the NC region was dissected, mesoderm was removed and RNA was extracted. Three replicates were collected for each condition (MO, MM and non-injected control) at both stage 14 and 17 for each miRNA KD. RNA samples underwent quality control using a Bioanalyser and qRT-PCR was used to further validate the KD of NC specific genes in MO injected samples. Samples were then processed to illumina sequencing. A summary of the protocol used is shown in **Figure 33.**

## 13.14. Results and discussion

### 13.14.1. Validation of knockdowns using qRT-PCR

Prior to sending the samples for sequencing, multiple techniques were used to confirm successful miRNA KD. These include an analysis of the craniofacial cartilage in stage 28 embryos, WISH for various NC markers and qRT-PCR.

Following injections, both miR-196a and miR-219 KD embryos had the abnormal craniofacial cartilage phenotype as described previously in section 13.9.3.1. In addition, they also showed loss of key NC genes (*Snail2* and *Sox10*) as shown by WISH (as previously described in section 13.9.3.2). These experiments were completed on sister embryos of those that had been dissected. To ensure that the dissected tissue had the NC KD seen in the sisters embryos, qRT-PCR was employed. qRT-PCR was completed on several different genes including NPB markers (*Pax3* and *Six1*) NC markers (*Snail2* and *Sox10*) neural markers (*Sox2*) and ectodermal markers (*Keratin*).

qRT-PCR results for all dissections are shown in **Appendix 9** and **Appendix 10**. For some of the results, interpretation of the data was inconclusive so these genes will not be discussed any further (*Six1* and *Sox10*). In addition, miR-219 (stage 17) showed an inconsistent gene expression profile with some NC genes increasing in expression following miR-219 KD (**Appendix 9**). As a result, it was decided that miR-219 (stage 17) samples would not be sequenced.

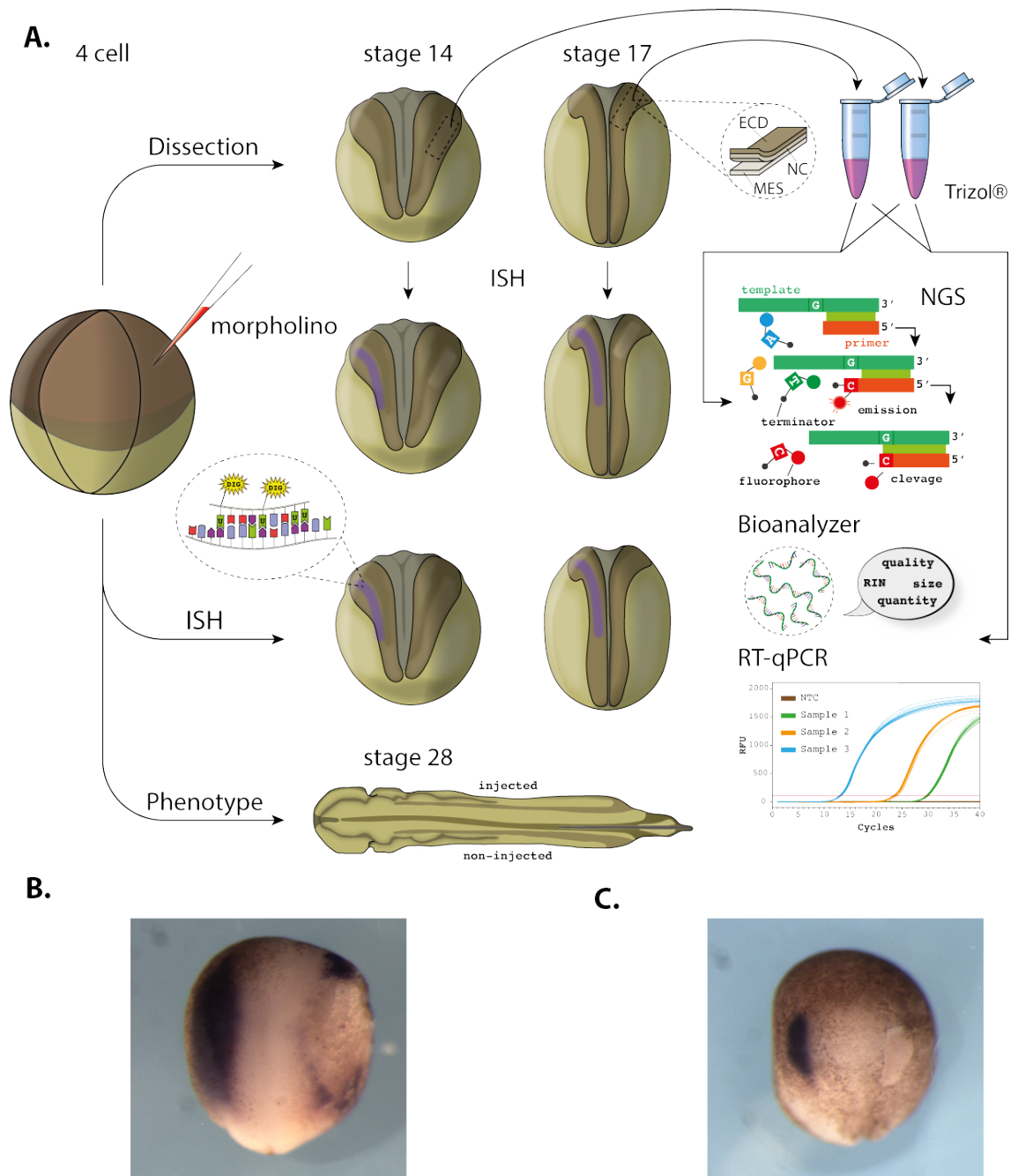


**Figure 33: Schematic drawing of the steps taken for the RNA sequencing of dissected neural crest (NC) tissue.**

At 4-cell stage, embryos were injected with 60ng of one of four MO's (miR-219, miR-219MM, miR-196a or miR-196aMM) into one dorsal blastomere to target only neural and NC tissue in one side of the embryo. GFP was co-injected and used as a tracer. Embryos were left to develop until stage 14, 17 and 28. Stage 14 and 17 for dissections and stage 28 for craniofacial cartilage deformations. Those embryos left to develop until stage 14/17 were split into two groups. Half underwent WISH to check NC genes were knocked down and the other half underwent NC dissections. During dissections, the NC region was dissected, mesoderm was removed and RNA was extracted. Three replicates were collected for each condition (MO, MM and non-injected control) at both stage 14 and 17 for each miRNA. RNA samples underwent quality control using a Bioanalyser and qRT-PCR was used to further validate the knockdown of NC genes in MO injected samples. Samples then underwent RNA sequencing (A). WISH were completed on dissected embryos to check dissection accuracy for *Pax3* (stage 14) (B) and *Snai2* (stage 14). (C)

After miR-196a KD (stage 14) the NC specific gene *Snail2* was reduced in the three biological replicates indicating a loss of NC. In addition, the epidermal marker *Keratin* was also lost indicating a loss of epidermis. In contrast, the neural marker *Sox2* had increased expression in two of the three biological replicates. The expression of the NPB marker *Pax3* varies between the biological replicates with two showing a downregulation compared to the controls and one showing an up regulation (**Figure 34A**). A similar expression profile was seen with miR-196a KD (stage 17) which also showed the loss of both the NC marker *Snail2* and the epidermal marker *Keratin* (**Figure 34B**). In contrast to stage 14, the expression of the NPB marker *Pax3* increased compared to the control in all three MO injected samples.

For miR-219 (stage 14) the results were not quite as clear. Consequently, four MO samples were sent for sequencing. Of these four samples, three had a downregulation of the NC marker *Snail2*. The NPB marker *Pax3* showed no significant changes in expression but the neural marker *Sox2* was increased in three of the samples (**Figure 34C**). A possible explanation for no change being seen in *Pax3* expression is because although using WISH an expansion is seen in the surface ectoderm of the embryo there is also a loss in the prospective NC region (**Figure 27**). This therefore may balance the expression levels so that although there has been a shift in *Pax3* localisation the overall expression levels within the whole explant are not significantly altered.

## 13.14.2. RNA sequencing results

### 13.14.2.1. Quality control of RNA sequencing

To assess the quality of the RNA sequencing results, clustering of replicates was assessed using both PCA plots (**Figure 35**) and sample distance heat maps (**Figure 36**). MO injected samples were analysed against MM injected samples to ensure any gene changes are consequence of the miRNA KD as opposed to just the injection. When replicates were clustered the results demonstrate that for miR-219 KD (stage 14) (**Figure 35A and Figure 36A**) miR-196a KD (stage 14) (**Figure 35B and Figure 36B**) and miR-196a KD (stage 17) (**Figure 35C and Figure 36C**) all replicates for each condition cluster consistently therefore validating the reproducibility of the replicates. The two conditions are also distinct

from one another on the PCA plot confirming that there are gene changes which separate the two groups that can be attributed to the miRNA KD. This is compared to PCA plots (**Appendix 11**) and sample distance heat maps (**Appendix 12**) for MM injected embryos vs control (non-injected) embryos where the replicates do not show any clustering and thus no clear separation between the two groups. For miR-219 MO samples, one of the four replicates deviated substantially from the rest and so this replicate was removed from any further analysis.

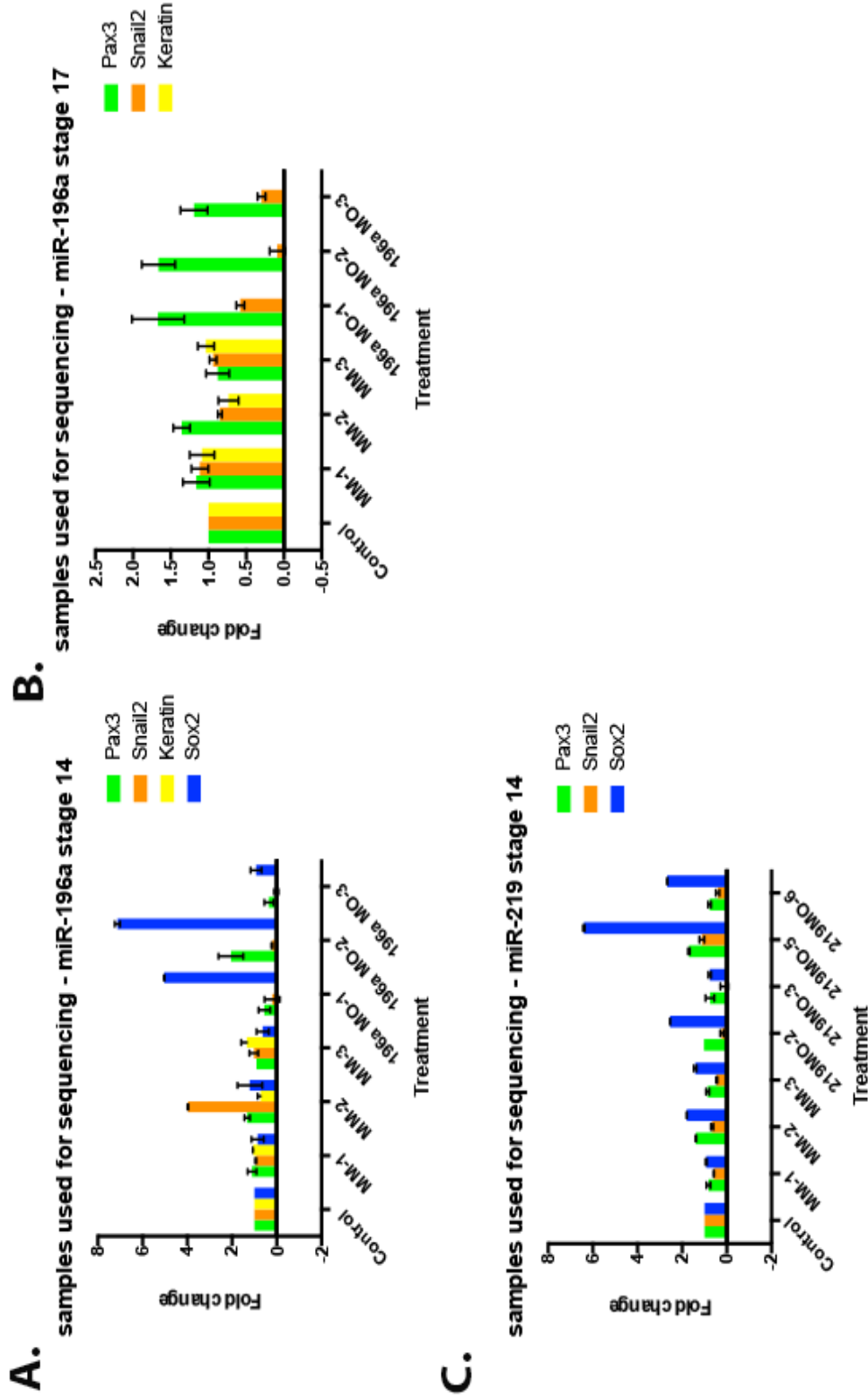


**Figure 34: Expression profile of various genes in dissected samples sent for sequencing following KD of miR-196a or miR-219.**

Embryos were injected into one dorsal blastomere of a four-cell embryo with 60ng of one of four MOs (miR-196a MO, miR-196a MM, miR-219 MO or miR-219MM). GFP was used as a tracer. Once at the appropriate stage (14 or 17) the neural crest region was dissected, RNA extracted and qRT-PCR was used to check gene expression. A non-injected control was used as a reference. ODC was used to normalise gene expression. Dissections with a KD of miR-196a (stage 14) showed a downregulation of the NC marker *Snail2* and the ectodermal marker *Keratin* whilst the neural marker *Sox2* was upregulated (A). As with stage 14, dissections with a KD of miR-196a (stage 17) showed a downregulation of the NC marker *Snail2* and the ectodermal marker *Keratin*, however, the NPB marker *Pax3* was upregulated slightly in all MO samples (B). Dissections with a KD of miR-219 (stage 14) were not as consistent. A downregulation of *Snail2* was seen in three out of four of the MO dissections (Mo-2,3 and 5) and an upregulation of *Sox2* was seen in three out of four of the MO samples (Mo-2,5 and 6) (C).

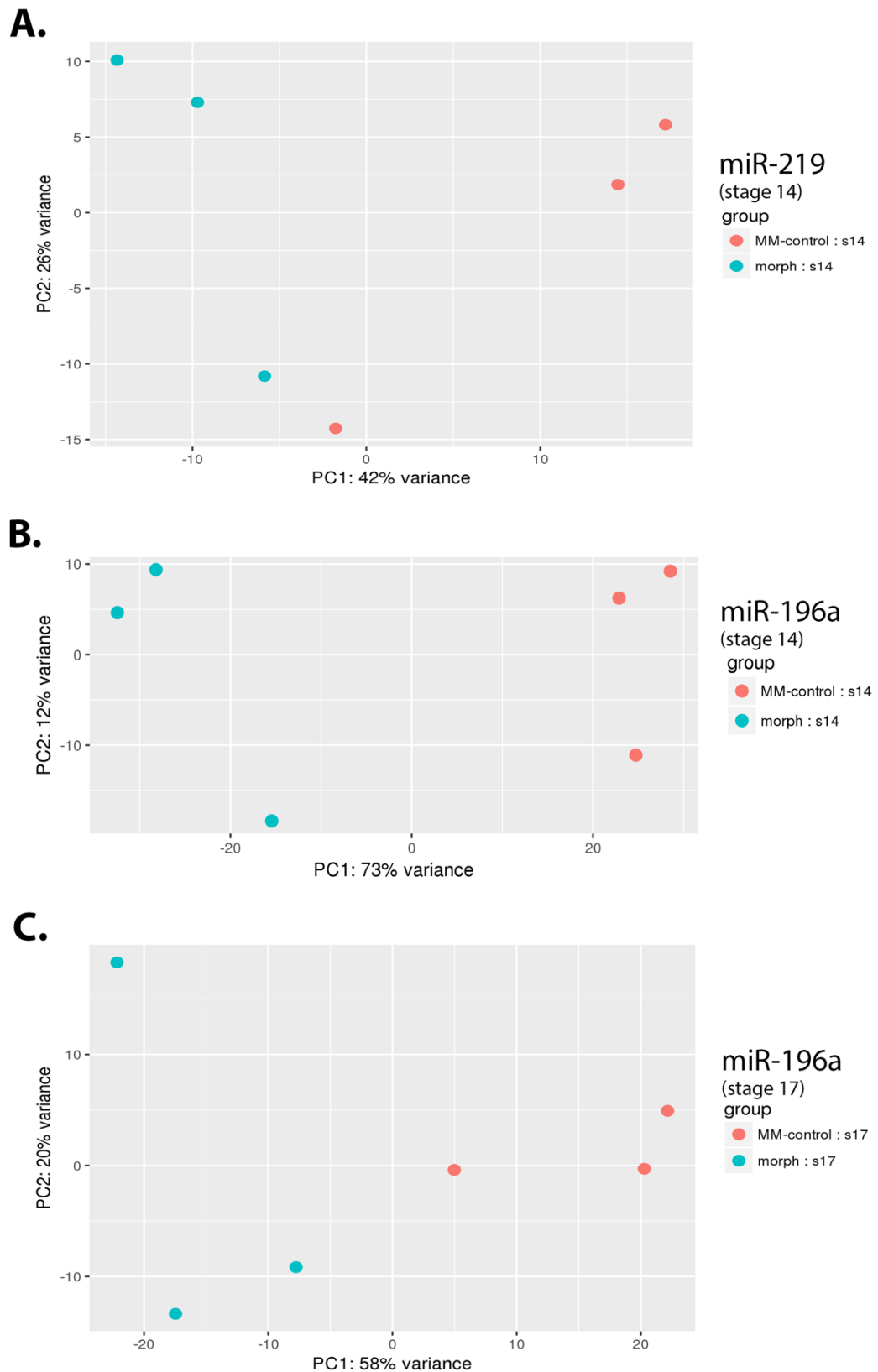


**Figure 35: PCA plot showing clustering of replicates between MO injected embryos and MM control.**

PCA plots of MO samples (blue dots) vs MM controls (red dots) demonstrated that for miR219 (stage 14), (A) miR-196a (stage 14) (B) and miR-196a (stage 17) (C) the replicates cluster and the two treatment types are distinct from one another.

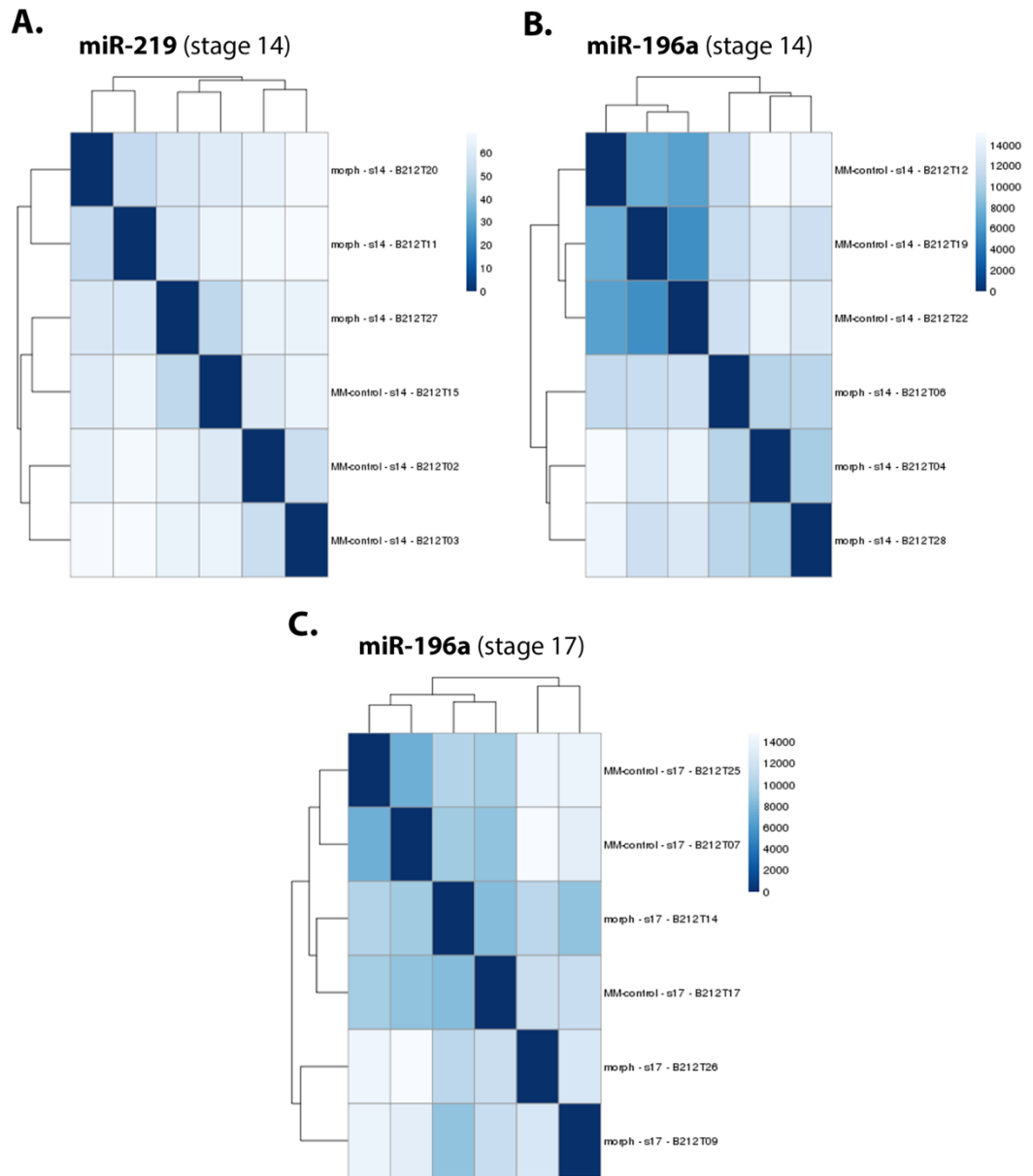


**Figure 36: Sample distance heat map showing clustering of replicates between MO injected embryos and MM control**

Sample distance heat maps of MO samples vs MM controls demonstrated that for miR-219 (stage 14) **(A)**, miR-196a (stage 14) **(B)** and miR-196a (stage 17) **(C)** the replicates cluster with the MO samples being distinct from the MM control.

### **13.14.2.2. miR-219 stage 14**

As mentioned previously, RNA sequencing for miR-219 KD was only completed for stage 14 because of poor quality qRT-PCR results for stage 17. Comparative expression analysis between miR-219 KD with miR-219 MM reveals multiple transcripts that are both upregulated and downregulated in the miR-219 KD tissue (**Appendix 14**). In total, 110 genes were significantly ( $P < 0.05$ ) upregulated whilst 104 genes were downregulated (**Figure 37**). This is compared to MM vs non-injected control tissue where only five genes were differentially expressed (**Appendix 13**).

#### ***GO Analysis of miR-219KD transcriptome***

To gain an overview of the molecular processes operational in the miR-219 KD transcriptome, gene ontology enrichment analysis (GO analysis) using the programme DAVID (v.6.8), along with manual literature searches, were completed on differentially expressed gene sets.

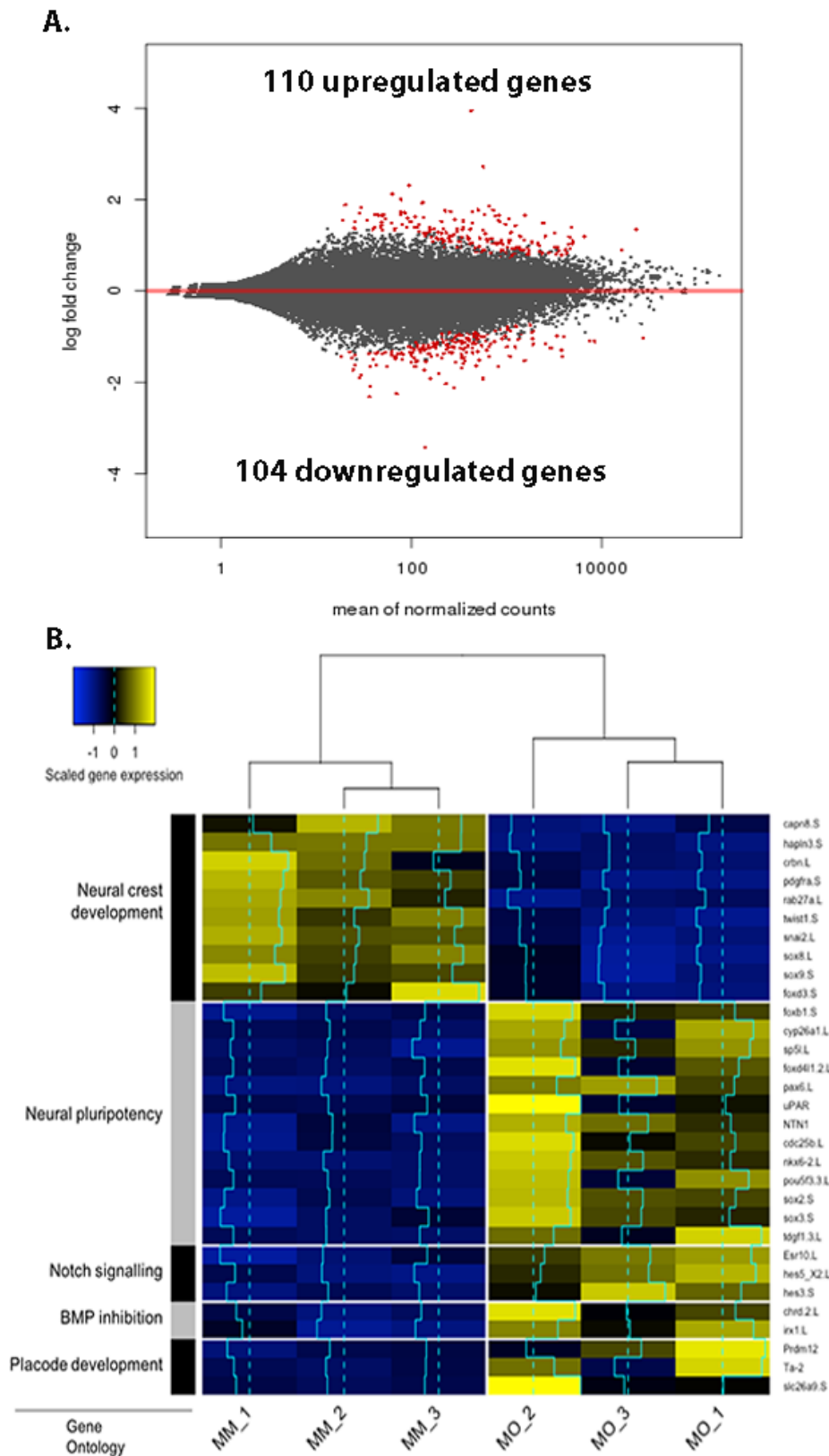


**Figure 37: Gene changes following miR-219 KD.**

Scatter plot comparing global gene expression profiles between miR-196a KD and miR-196a MM samples. Differentially expressed genes ( $P < 0.05$ ) are represented as red dots (A). Heatmap for selected differentially expressed genes (miR-196aMO vs miR-196a MM). Colour depicts gene expression where yellow represents overexpression and blue underexpression. The blue line running throughout the boxes is a histogram representing the level of either upregulation or downregulation against the dotted midline (no change) (B).

### 13.14.2.3. **NC is lost following miR-219 KD**

Unsurprisingly, for the downregulated gene set, GO analysis only identified 'neural crest development' as an output. Manually, the expression of *bona fide* NC transcription factors was assessed and as expected, many were significantly downregulated in the miR-219 KD sample (**Figure 37**). *Snail2*, *Foxd3*, *Twist1*, *Sox8* and *Sox9* are all key NC specifier genes (Rogers et al., 2012) and were among the most downregulated genes following miR-219 KD. In addition to NC specifiers, genes known to play important roles in various alternative aspects of NC development were also found to be significantly downregulated. *Capn8*, *Pdgfra*, *Pcdh8* and *Anxa2* are four examples of these, all of which have roles in the promotion of NC cell migration (Cousin et al., 2011, Smith and Tallquist, 2010, Lumb et al., 2017, Rangarajan et al., 2006). Interestingly, the cell adhesion protein - *Hapln3*, was the fifth most downregulated gene following miR-219 KD (**Figure 38**). Although no functional analysis has been completed on this gene in a NC context, it has recently been put forward as a novel potential member of the NC gene network following transcriptome analysis of dissected pre-migratory NC (Plouhinec et al., 2014). Together this clearly demonstrates that following KD of miR-219, NC tissue is either lost or never forms. Interestingly, although the expression levels were reduced, NPB specifiers (including *Msx1/2*, *Dlx5/6*, *Gbx2*) were not significantly downregulated. This therefore suggests that the NPB does form but the NC fail to do so from the NPB.

The expression of many placodal genes were also not significantly altered following miR-219 KD (i.e *six1*, *six4*, *pax8*, *gata2/3*). This implies that placode tissue developed efficiently and supports the hypothesis the NPB does form. However, some less well-established placodal genes were found to be significantly upregulated following miR-219 KD one of which being the histone-modifying factor *Prdm12* (**Figure 37**). *Prdm12* is expressed in the lateral pre-placodal ectoderm during neurula development, and has recently been shown to be key in separating the placodal tissue from NC (Matsukawa et al., 2015). PRDM12 represses the expression of NC specifier genes in the placodal region via methylation of histone H3K9. CHIP-qPCR analyses showed that PRDM12 promoted the occupancy of the trimethylated histone H3K9 (H3K9me3) on the *Foxd3*, *Snail2*, and *Sox8* promoters specifically (Matsukawa et al., 2015). All three of the latter genes were shown to be significantly downregulated in this

dataset. Another placodal related gene upregulated in miR-219 KD tissue is the transmembrane protein, *Ta-2*. Although the function of this protein is yet to be fully elucidated its expression is restricted to the superficial ectoderm which is where the expansion of *Pax3* is localised to following miR-219 KD (**Figure 27**) (Chalmers et al., 2006).

**13.14.2.4. *Pax3* expansion in the superficial ectoderm does not induce expression of its downstream hatching gland specific target *Xhe2***

Whilst analysing the list of enhanced genes following miR-219 KD the expression of *Pax3*, *Eya1* and *Xhe2* were assessed manually to investigate whether the results supported earlier hypotheses formulated in previous chapters (see section 13.10.2.2). Although *Pax3* and *Eya1* do increase in expression levels following miR-219 KD, this is not significant. For *Pax3* this supports the qRT-PCR results discussed in section 13.14.1. One explanation could be because both genes are already expressed in that region rather than been induced from a region in which it is not usually expressed. Alternatively, it could be that because *Pax3* expression was expanded across the surface ectoderm but also lost in prospective NC region (**Figure 27**) the overall number of transcripts may not have changed. To make this assumption for *Eya1*, WISH needs to be completed on miR-219 KD embryos to assess if the same changes in expression are seen for *Eya1* as they are for *Pax3*. As *Pax3* acts upstream of *Xhe2* in the superficial layer of the ectoderm it was postulated that because of the severe expansion of *Pax3* in this region following miR-219 KD we would predict the same expansion for *Xhe2*. In fact, the opposite was seen with a significant decrease in expression being observed (**Figure 38**). As with *Eya1*, WISH needs to be completed to confirm this result.

**13.14.2.5. *Multiple genes involved in neural pluripotency were upregulated following miR-219 KD***

Unexpectedly, the top upregulated gene following miR-219 KD corresponded to the miR-219 primary miRNA transcript (**Figure 38**). The reason for this is likely because when designing the MO against miR-219, GeneTools designed it so it works by binding to the primary transcript and stops it from being processed by Drosha. Therefore, in miR-219 KD tissue there is an accumulation of primary

transcript which in the control tissue has been processed into the mature transcript. This was not the case for miR-196a KD as the MO against miR-196a binds to the dicer cleavage site following further processing of the miRNA (not to the primary transcript as is the case for miR-219 MO). The results from GO analysis along with manual analysis on upregulated genes resulted in three main outputs including regulation of neural pluripotency and two signalling pathways (Notch and BMP). In total, there were 13 upregulated genes identified as being linked with neural pluripotency including the *bona fide* neural transcription factors *Pax6*, *Sox2* and *Sox3* (**Figure 37**). Interestingly, the previously discussed placodal gene *Eya1* also has links with increased pluripotency. Previous studies have shown *Eya1* to be involved in placodal neurogenesis. Neurogenic placodes express many of the same genes that regulate neurogenesis in the NP including *Sox2* and *Sox3* (Abu-Elmagd et al., 2001, Schlosser and Ahrens, 2004). Schlosser et al. (2008) showed that through activation of *Sox2* and *Sox3*, an increase in expression of *Eya1* results in a promotion of proliferating neural progenitors. Therefore, this could explain why following miR-219 KD, an expansion of neural progenitors is seen.

Another upregulated neural gene included the forkhead transcription factor *FoxB1*. *FoxB1* has been shown previously to be upregulated by POU class V transcription factors (*Pou5f3*) and to be a key factor in the patterning of the dorso-ventral axis of the ectoderm during neurulation (Takebayashi-Suzuki et al., 2007). *FoxB1* promotes neural induction and inhibits epidermal differentiation by suppressing BMP signalling (Takebayashi-Suzuki et al., 2011). As discussed previously in section 1.1 it is the level of BMP signalling (along with other signalling pathways) that determines the fate of embryonic ectodermal stem cells as either epidermal, NC or neural (Liem et al., 1995). Analysis of changes in expression levels of BMP signalling molecules and their downstream signalling transducers such as SMADS showed no significant difference in this data set. However, this was not an unexpected result as *Foxb1* mediates BMP signalling at a protein level. For future investigations, experiments using BMP reporters should identify any changes in the level of BMP signalling at a protein level following miR-219 KD (discussed in section 13.18.5).

Of the 13 upregulated neural genes, many have been shown to have roles in the maintenance of an immature neural state whilst inhibiting differentiation.

*FoxD4L1* is a forkhead transcription factor that expands the neural ectoderm by down-regulating genes that promote the onset of neural differentiation and up-regulating genes that maintain proliferative neural precursors in an immature state (Yan et al., 2009). Overexpression of *FoxD4L1* results in an expansion of the expression domain for *Sox2* and *Sox3* (both of which are also significantly upregulated in this data set) in NP stem cell stages (Yan et al., 2009). Another upregulated gene which is linked to maintaining a neural stem cell population and has previously been mentioned as an upregulator of *FoxB1* is *Pou5f3.3*. It is a member of the *Pou5f3* genes (*Pou5f3.1 Pou5f3.2 Pou5f3.3*), all of which have been shown to have a conserved role in the maintenance of pluripotency (Morrison and Brickman, 2006, Cao et al., 2007). Recently, Young et al. (2014) found that ectopic expression of *Pou5f3* resulted in an increase in pluripotency and a failure of the neuroectoderm to differentiate in response to transforming signals. Together, this upregulation of pluripotent neural factors strongly suggests that the region that has been dissected is mainly composed of neural precursors following miR-219 KD.

#### **13.14.2.6. *Notch signalling is increased further promoting neural pluripotency***

Notch signalling, which is highly conserved from *Drosophila* to humans, plays essential roles in many processes during development including neurogenesis (Artavanis-Tsakonas et al., 1999, Lai, 2004, Bray, 2006). When the Notch transmembrane receptor on the cell surface is activated by its ligands, downstream target genes are activated which mainly include members of the HES (Hairy/ Enhancer of Split) family of basic helix-loop-helix (bHLH) transcriptional regulators (Mumm and Kopan, 2000, Weinmaster, 2000). During early vertebrate development, Notch is expressed broadly throughout the NP, and its signalling pathway plays an essential role in maintaining the neural progenitor state and regulating the diversification of cell fate (Yoon and Gaiano, 2005, Louvi and Artavanis-Tsakonas, 2006). The classical view is that increasing Notch signalling within a cell up-regulates HES genes that subsequently repress neural differentiation bHLH genes (such as *ngn* and *neuroD*) (Sullivan et al., 2001). In addition to neural development, Notch has also been shown to play multiple roles during NC development, although its importance and mode of action has been controversial. Results obtained in chick and frog indicate that

Notch regulates NC through modulation of BMPs. In *Xenopus*, Notch signalling induces NC cell-autonomously by downregulation of BMP4 at the NPB (Glavic et al., 2004). In chick, both gain and loss of function of Notch signalling inhibit BMP4 and Notch induces NC non-cell-autonomously (Endo et al., 2002). From this data set, after miR-219 KD, an increase in expression was seen for multiple members of the Notch signalling network including the downstream targets of Notch - *Hes3* and *Hes5* (**Figure 37**). Using a triple knock-out of *Hes1; Hes3; Hes5* in mice, Hatakeyama et al. (2004) showed that in the absence of these genes, neuroepithelial cells are not properly maintained and prematurely differentiate into neurons at the NP stage. Another upregulated Notch related gene is the Hes5-like gene *Esr10*. This gene is upregulated by the pro-neural protein *Xngnr1* and as with the HES genes has been shown to be key in regulating the differentiation of neural precursors. Of these upregulated Notch genes, *Hes5* is of particular interest as it has been implicated in NC development as discussed previously in section 13.12.1. Gouti et al. (2011) showed that for NC to be induced, an optimum level of *Hes5* is required. Within NC, a repressor of *Hes5* and therefore a regulator of this optimum level is *Hoxb1* (Gouti et al., 2011). Misexpression of *Hoxb1* in the trunk neural tube results in a repression of *Hes5* and a neural to NC cell fate switch which is accompanied by a reduction in proliferation (Gouti et al., 2011). Within this dataset, *Hoxb1* is in the top 50 most downregulated genes (**Figure 38**) which may explain why we get (1) the loss of NC and (2) the upregulation of *Hes5* resulting in a clear increase in a neural progenitor population.

#### **13.14.2.7. *BMP antagonists are upregulated indicating that BMP signalling is decreased***

In addition to members of Notch signalling pathway there was also an upregulation of members of BMP signalling, specifically, genes linked to an inhibition of BMP signalling (**Figure 37**). As a downregulation of BMP signalling (through BMP antagonists) is required for neural induction this fits with the upregulation of neural genes previously discussed. Two key BMP antagonists, *Chrd* and *Ir1*, were significantly upregulated following KD of miR-219. Chordin is a well-established BMP antagonist which has been shown to be key in the establishment of the dorsal ventral axis of the embryo during development. Using loss of function experiments, it has been shown that KD of Chordin inhibits neural

formation (Oelgeschlager et al., 2003, Kuroda et al., 2004). The second BMP antagonist, *Irx1* (*Xiro1*) is a member of the Iroquois family of Iroquois (iro) genes. The iro genes, which encode evolutionary conserved homeoproteins, participate in neurogenesis and in many other developmental processes (reviewed in (Cavodeassi et al., 2001). So far, five iro genes have been identified in *Xenopus* (Bellefroid et al., 1998, Garriock et al., 2001, Gomez-Skarmeta et al., 1998). Among them, *Iro1*, *Iro2* and *Iro3* have very similar patterns of expression and participate, as their *Drosophila* counterparts do, in proneural gene activation (Bellefroid et al., 1998, Gomez-Skarmeta et al., 1998, Gomez-Skarmeta et al., 1996, Leyns et al., 1996). *Irx1* acts early in NP development to induce expression of proneural genes, and specifies a neural precursor state (Bellefroid et al., 1998, Gomez-Skarmeta et al., 1998). In addition, it has been shown that *Irx1* is a repressor that is also required for patterning of the dorso-ventral axis of the embryo including specification of the NP, NC and preplacodal field. This is at least in part by downregulating BMP-4 (Gomez-Skarmeta et al., 2001).

To conclude, from these results it is apparent that following miR-219 KD NC tissue is either lost or never generated (characterised by a decrease in expression of NC specifier genes) and the tissue that has replaced it is an early neural progenitor population (characterised by an increase in expression of multiple neural genes). As GFP is still seen in the injected embryos prior to dissection and as there is no apparent expression of apoptotic or necrotic genes it can be deduced that the tissue is not dead. Instead it appears the NC never formed and changes in gene expression following miR-219 KD has caused a cell fate switch to neural.

In addition to giving us information regarding the fate of the sequenced tissue, this data also gives clues to several potential mechanisms behind this switch in tissue types. These potential mechanisms have been discussed previously in this section but for clarity they have been summarised in **Figure 39**. To fully elucidate the mechanism behind miR-219, the 3' UTR of any potential direct targets (indicated by a dashed line in **Figure 39**) need to be assessed for a miR-219 binding site and then validated using luciferase assays.

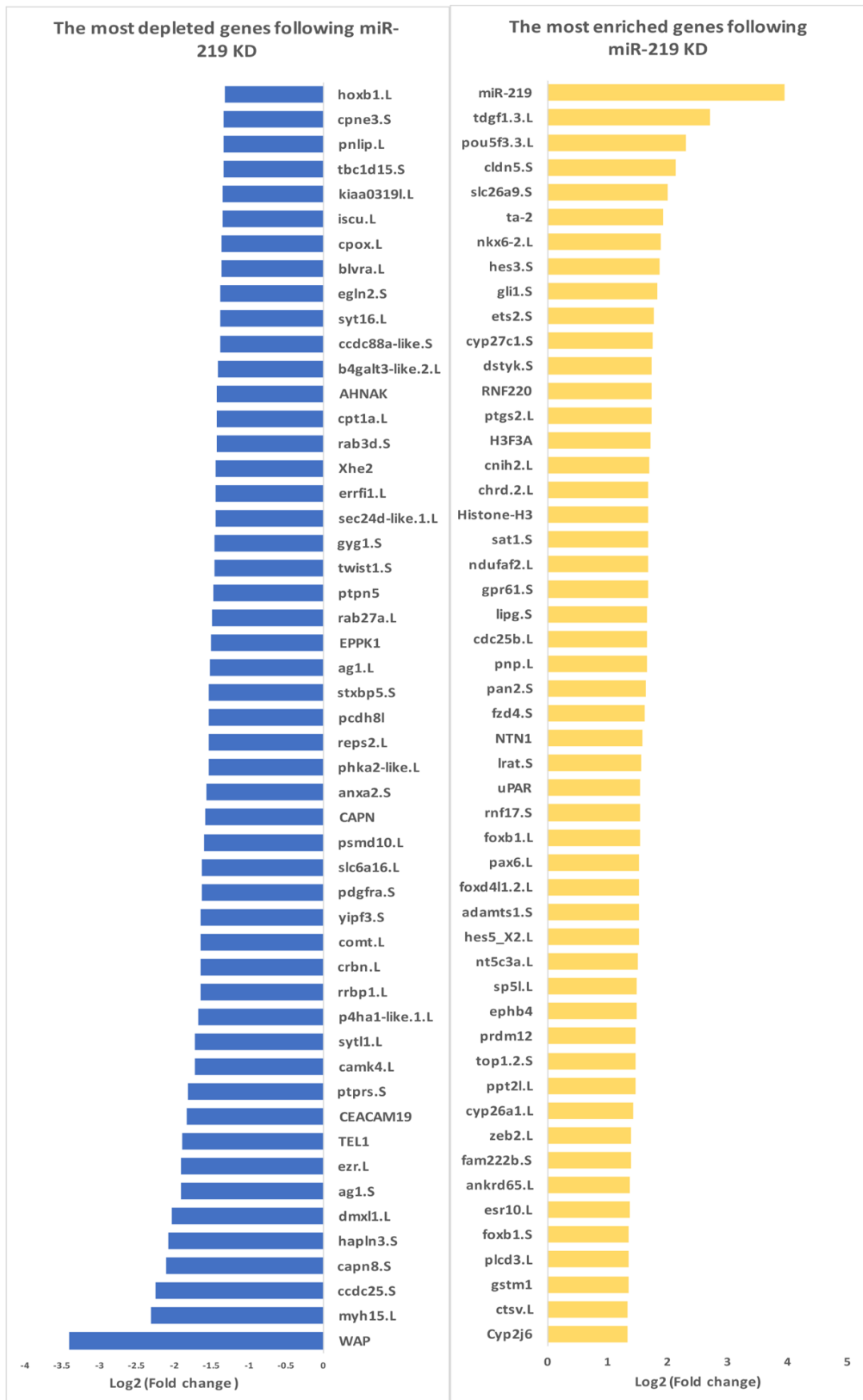


**Figure 38: The top 50 downregulated and upregulated genes following miR-219 KD.**

RNA was sequenced for miR-219MO NC tissue and miR-219MM NC tissue. Differential analysis was completed on miR-219KD vs the MM control to find the top 50 significantly ( $P < 0.05$ ) downregulated genes (blue) and the top 50 significantly ( $P < 0.05$ ) upregulated genes (yellow) following KD of miR-219.

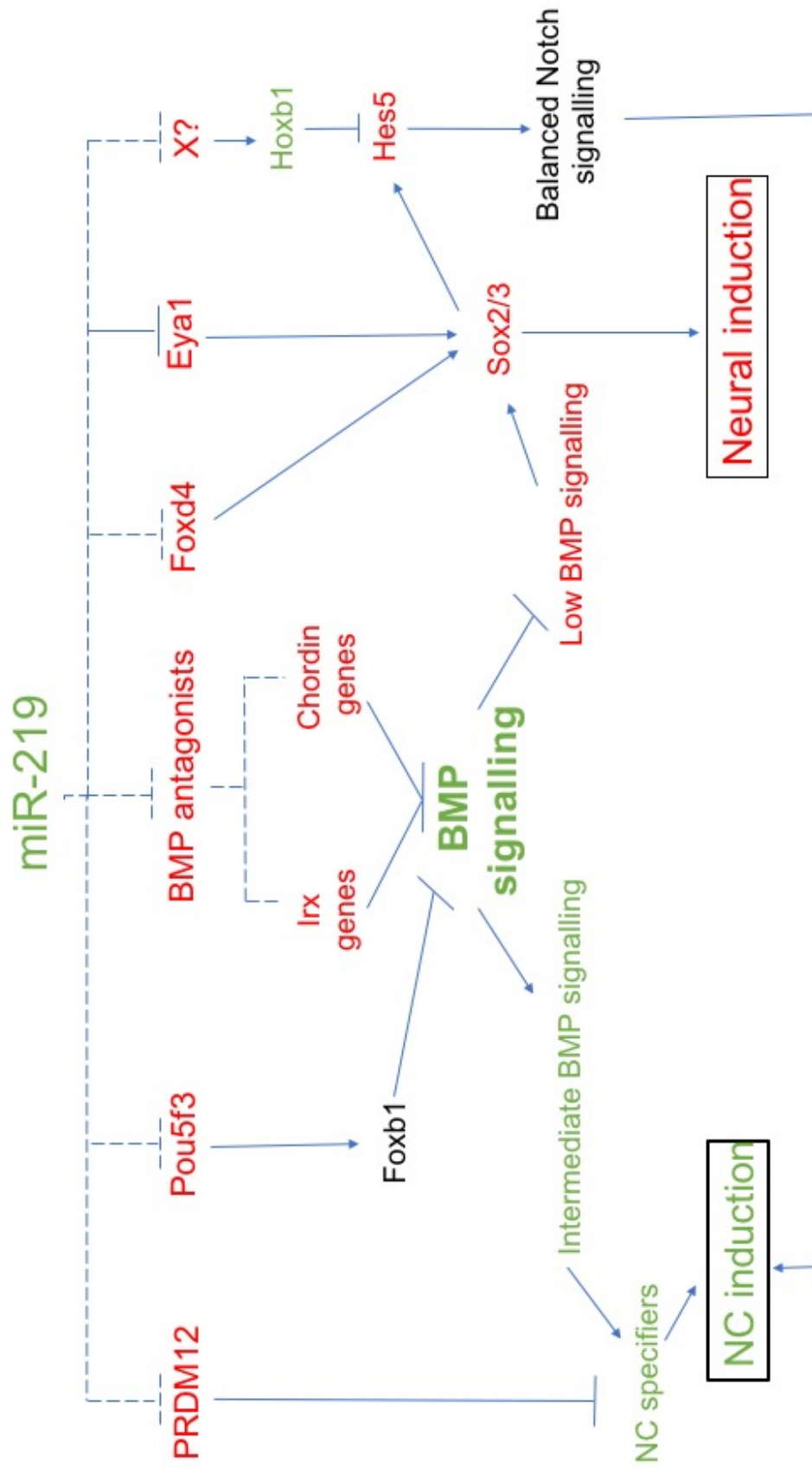


Figure 39: Model of the potential molecular mechanisms miR-219 uses to prevent neural induction and control neural pluripotency during *Xenopus* neuroectoderm patterning.

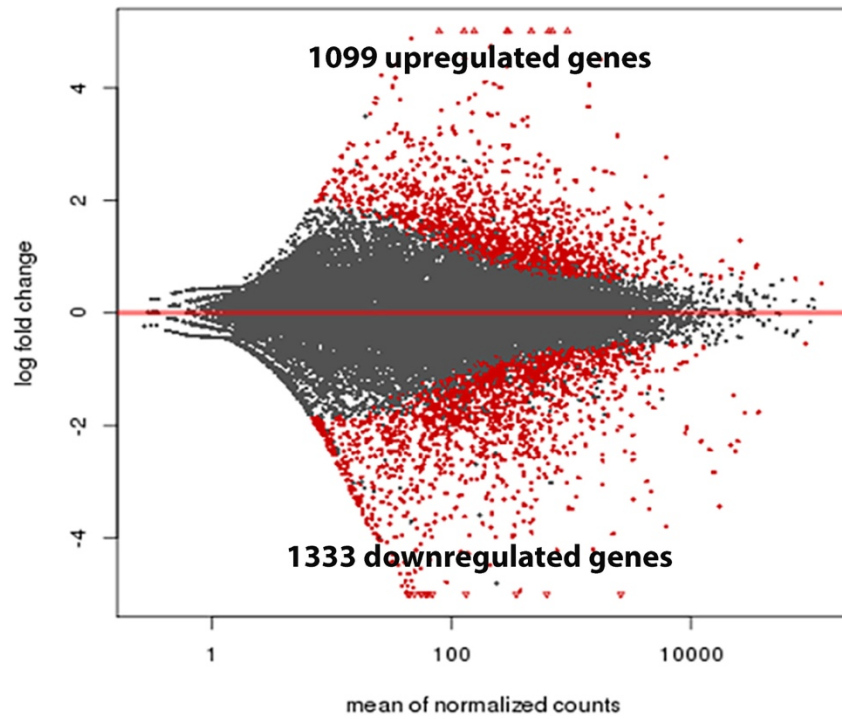
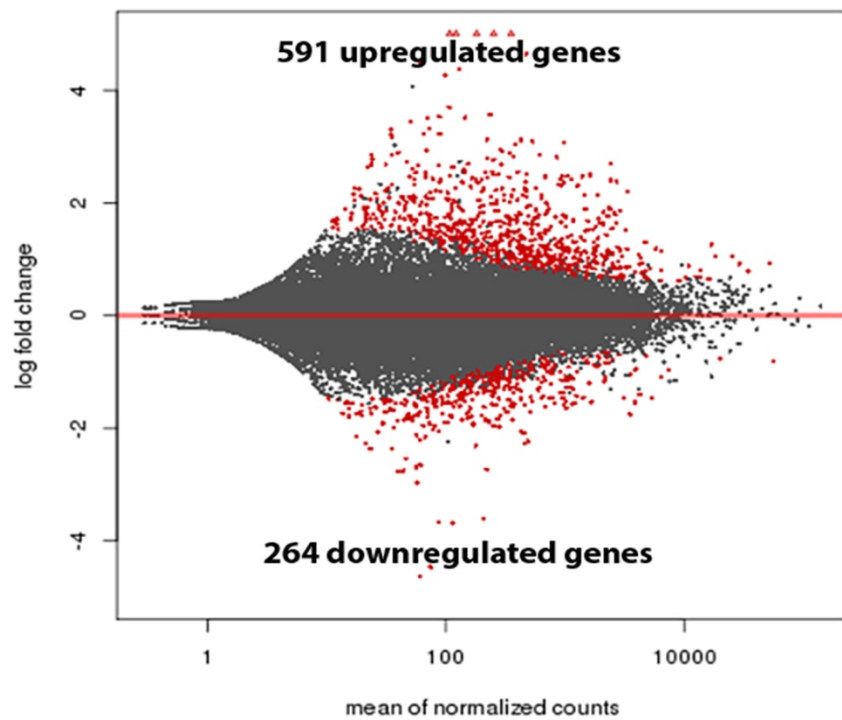
Red represents repression, green represents expression and black represents balanced. Solid and dashed lines are the verified and predicted regulatory relationships, respectively

### **13.14.2.8. miR-196a**

Comparative expression analysis between miR-196a KD with miR-196a MM (stage 14 and stage 17) revealed multiple transcripts that are both upregulated and downregulated in the miR-196a KD tissue (**Appendix 14**). For stage 14, 1099 genes were significantly upregulated whilst 1333 genes were downregulated and for stage 17, 591 genes were significantly upregulated whilst 264 genes were downregulated (**Figure 40**).

### **13.14.2.9. miR-196a KD results in impaired induction of the NPB and a loss of NC specification**

As with the miR-219 KD dataset, the expression of multiple *bona fide* NC transcription factors were significantly reduced following miR-196a KD. Some were noted at both stage 14 and stage 17 (*Snail2*, *Tfap2e*, *Sox8*) whilst others were specific to either stage 14 (*Snail1*, *Ets1*, *c-myc*, *Tfap2a/b/c*, *Foxd3*, *Sox9*, *Twist1*, *Msx1/2*) or stage 17 (*Foxi1*, *Foxi2*, *Sox10*). In addition to these TF, various other genes which have recently been shown to be part of the NC transcriptome signature were also found to be significantly downregulated including the metalloproteinase *Mmp28* (stage 14 and 17), the ECM component, *Hapln3* and the membrane component, *Greb1* (stage 14) (Plouhinec et al., 2014) (**Figure 41 Figure 42**).

**A.****B.**

**Figure 40: Gene changes following miR-196a KD.**

Scatter plot comparing global gene expression profiles between miR-196a KD and miR-196a MM samples. Differentially expressed genes ( $P < 0.05$ ) are represented as red dots for stages 14 (**A**) and stage 17 (**B**).

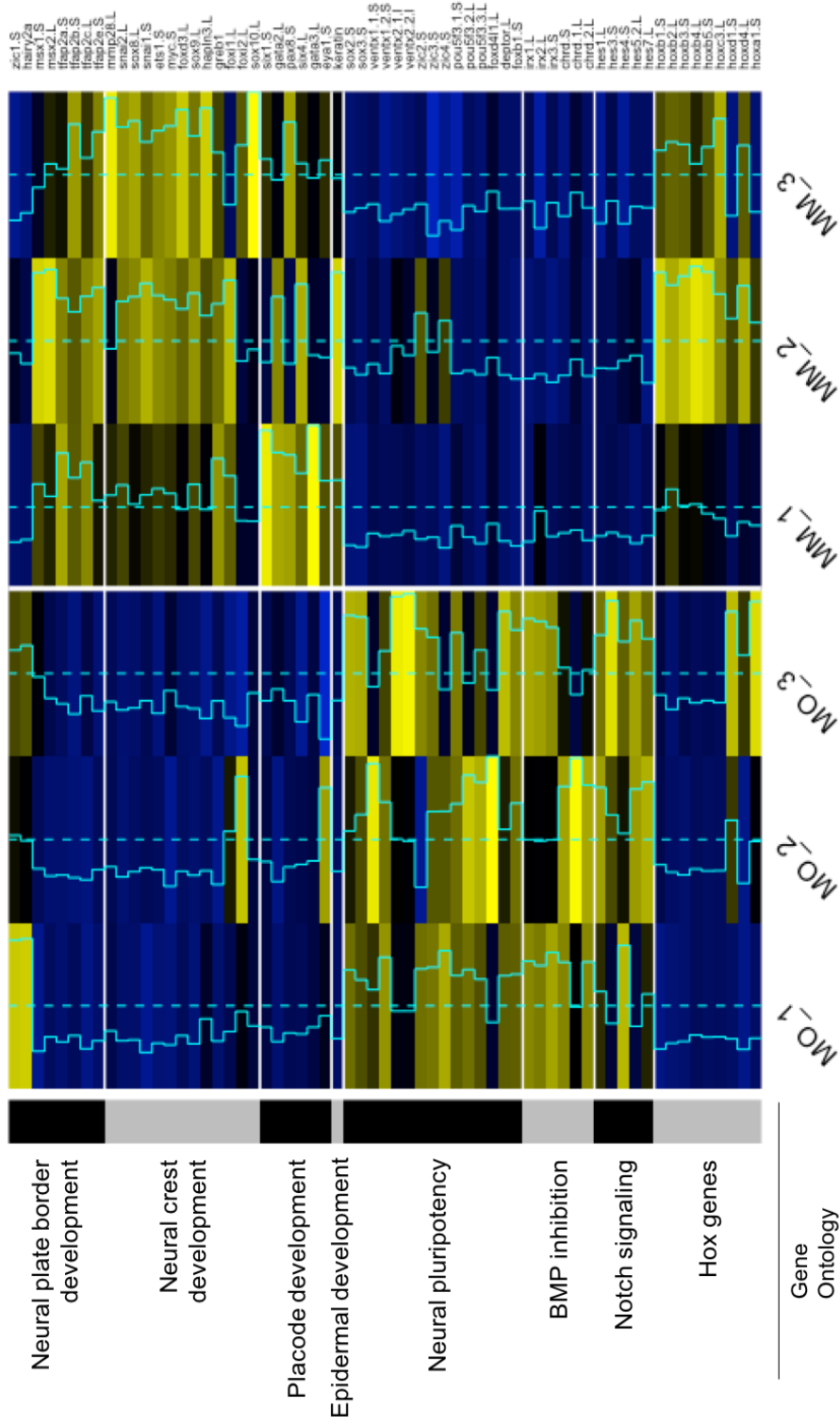
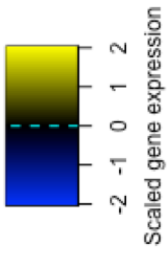


**Figure 41: Heat map of gene changes following miR-196a (stage 14)**

Heat map for selected differentially expressed genes (miR-196aMO vs miR-196a MM). Colour depicts gene expression where yellow represents overexpression and blue under expression. The blue line running throughout the boxes is a histogram representing the level of either upregulation or downregulation against the dotted midline (no change). At stage 14, NC, placode, epidermal and HOX genes are lost in MO samples whilst genes involved in BMP inhibition, neural pluripotency and Notch signalling are

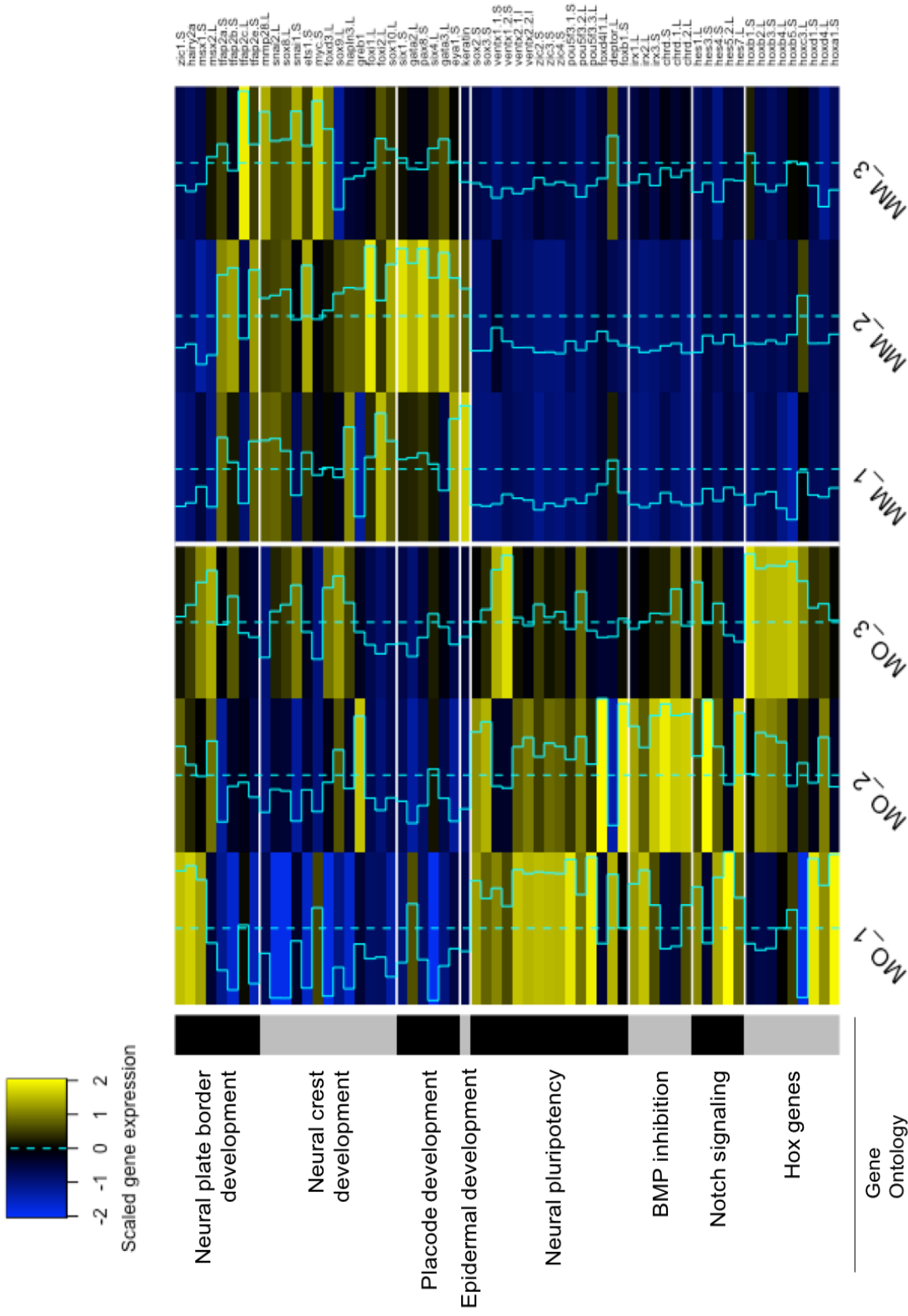


**Figure 42: Heat map of gene changes following miR-196a (stage 17) KD.**

Heat map for selected differentially expressed genes (miR-196aMO vs miR-196a MM). Colour depicts gene expression where yellow represents overexpression and blue under expression. The blue line running throughout the boxes is a histogram representing the level of either upregulation or downregulation against the dotted midline (no change). At stage 17, NC, placode and epidermal genes are lost in MO samples whilst genes involved in BMP inhibition, neural pluripotency, HOX and Notch signalling are upregulated.

Interestingly, despite the expression of almost all known NC specifiers being reduced following miR-196a KD the general changes in expression of NPB specifiers were not clear. The TFs *Pax3/7*, *Dlx5/6* and *Gbx2* had no significant change in expression whilst *Zic1* and *Hairy2a* were both significantly upregulated. The only NPB specifier genes to have significantly reduced expression were *Msx1/2* and *Tfap2a*. The expansion of *Zic1* in combination with a loss of *Tfap2a* has been described previously. de Croze et al. (2011) concluded using loss of function experiments that TFAP2A is essential in initiating the induction of the NPB. They showed that when *Tfap2a* is lost, the NPB is impaired (characterised by a loss of *Msx1*, *Pax3* and *Hairy2a*) and instead it is specified as NP (characterised by an upregulation of *Sox2* and *Zic1*). *Hairy2a* has been shown using overexpression experiments to lie downstream of *Zic1* so this may explain the upregulation of *Hairy2a* (Nichane et al., 2008a). Although the upregulation of both *Zic1* and *Hairy2a* may be accounted for, how and why *Pax3* expression remained unaltered following a loss of *tfap2a* remains unanswered. One possible explanation is that *Tfap2a* expression may have been induced prior to stage 14 and then lost. This would give *Tfap2a* enough time to initiate the transcription of *Pax3* which subsequently has been shown to auto-regulate its own expression (Plouhinec et al., 2014). The second possible explanation is that although the expression is significantly reduced (base mean MM: 5363, base mean MO: 2649) the gene is still expressed. Therefore, the level of expression in the KD sample could still be sufficient to induce expression of downstream targets. Finally, *Tfap2a* is one of five isoforms (a-e) all of which have been shown to have highly conserved functions in the development of the NC (Hilger-Eversheim et al., 2000, Hoffman et al., 2007). Although four out of five of these isoforms have significantly reduced expression following miR-196a KD, it is possible that there is enough redundancy between the isoforms to induce the expression of *Pax3* and possibly *Hairy2a*.

#### **13.14.2.10. Induction of all NPB derivatives are lost**

From this dataset, it is clear that following miR-196a KD, NC specifiers are lost and the formation of the NPB is impaired. Further support for impaired NPB formation comes from the apparent loss of the placodal region following miR-196a KD which would usually lie lateral to the NC and is also derived from the NPB. In this dataset, all *bona fide* placodal genes are significantly reduced in at

least one of the stages following miR-196a KD. These include; *Eya1*, *Six1*, *Six4*, *Gata2*, *Gata3* and *Pax8* (**Figure 41 Figure 42**).

**13.14.2.11. Cell fate has been changed to neural and this appears to be mediated by an upregulation of the zinc finger protein *zic1***

*Zic1*, is a zinc finger protein which has been shown to play a key role in causing the embryonic ectoderm to be more sensitive to neural inductive signals (Kuo et al., 1998). As a result of the upregulation of this gene, other neural related genes were assessed for changes in expression. As expected, multiple *bona fide* neural related genes were upregulated in the miR-196a KD tissue including *Sox2/3* and *Zic1/2/3* (**Figure 41 Figure 42**). The expression of these genes reiterated that there had been a change in tissue fate from NC / placode to neural tissue. As *Zic1* is a regulator of ectodermal sensitivity to neural tissue induction and is upstream of these other definitive neural markers (ie *Sox2*) it is possible that this gene is key in the cell fate change (Kuo et al., 1998, Marchal et al., 2009). The regulation of *Zic1* was next to be addressed. *Zic1* has been shown previously to be an immediate early target of BMP inhibition (Marchal et al., 2009). In fact, within the *Zic1* promoter is a BMP inhibition responding module, that is sufficient for expression in response to BMP inhibition (Tropepe et al., 2006). Therefore, in future experiments it needs to be determined whether it is changes in BMP signalling that is resulting in the loss of NC/ placodal tissue and an increase in neural tissue (possibly via induction of *Zic1*)?

**13.14.2.12. BMP signalling is attenuated following miR-196a KD which potentially regulates *Zic1* induction**

Following miR-196a KD two key families of BMP antagonists were significantly upregulated, that being three chordin genes; *Chrd*, *Chrd.1* and *Chrd.2* and multiple members of the iroquois family including; *lrx1*, *lrx2* and *lrx3* (**Figure 41 Figure 42**). As described previously in section 13.14.2.2 both these families of genes are well-established BMP antagonists that are key players in proneural gene activation (Bellefroid et al., 1998, Gomez-Skarmeta et al., 1998, Gomez-Skarmeta et al., 1996, Leyns et al., 1996). Importantly, *lrx* genes act early in NP development to induce expression of proneural genes, and specify a neural precursor state (Bellefroid et al., 1998, Gomez-Skarmeta et al., 1998). They have been shown to act as repressors that are required for patterning of the dorso-

ventral axis of the embryo including specification of the NP, NC and pre-placodal field. This is at least in part by downregulating BMP-4 (Gomez-Skarmeta et al., 2001). Interestingly, following miR-196a KD the mRNA levels of BMP4 (at stage 14 and 17) was significantly increased which would imply an increase in BMP signalling. However, as these BMP antagonists act at a protein level, the increase in the level of mRNA could be compensatory and does not show if BMP signalling is active or not. To fully assess the changes in BMP signalling a reporter construct would need to be used (as described in 13.14.2.2). Another upregulated gene linked to BMP signalling is *FoxB1*. *FoxB1* is upregulated by the POU class V transcription factors (*Pou5f3.1 Pou5f3.2 Pou5f3.3*), all of which are also upregulated following miR-196a KD. *FoxB1* is of particular interest as it is a key factor in the patterning of the dorso-ventral axis of the ectoderm during neurulation via inhibition of BMP signalling (Takebayashi-Suzuki et al., 2011). More specifically this is through reducing the levels of pSmad1/5/8 and it is a reduction in pSmad that results in expression of *Zic1* (Tropepe et al., 2006). As a result of this clear expansion of neural tissue (likely by altering BMP levels), one may expect a decrease in epidermal tissue. Levels of the expression of *epidermal type I cytokeratin* shows a significant reduction at both stage 14 and stage 17.

#### **13.14.2.13. Notch signalling is increased following miR-196a KD possibly promoting neural pluripotency**

From this data set, an increase in the expression of many downstream members of the Notch signalling pathway was noted. More specifically, there was an increase in the expression of the *hes* genes; *hes1*, *hes3*, *hes4*, *hes5* and *hes7* in at least one of the stages assessed (**Figure 41 Figure 42**). Interestingly, *Zic1* a regulator of *hes* genes has been shown to inhibit neural differentiation through mediating the Notch pathway. Aruga et al. (2002) showed that overexpression of *Zic1* in the spinal cord, expanded the Notch-expressing region and enhanced expression of the pro-pluripotent gene, *Hes1*. This therefore could be yet another way in which *Zic1* acts to expand a neural population. In addition to *Hes1*, multiple other *Hes* genes were upregulated following miR-196a KD. As discussed previously in section 13.14.2.2 it has been shown that a triple knock-out of *Hes1*; *Hes3*; *Hes5* in mice, results in premature differentiation of neuroepithelial cells into neurons at the NP stage. In addition, an optimum level of *Hes5* has been shown to be required to initiate NC development (Gouti et al., 2011). Together,

these studies clearly demonstrate the importance of a tight regulation of Notch signalling during early development, specifically in regard to the maintenance of pluripotency. Interestingly, the repressor of *Hes5*, *Hoxb1* is downregulated in this dataset which may explain the upregulation of *Hes5* in our experiments and therefore possibly as to why NC is absent. The downregulation of *Hoxb1* came as a surprise because as discussed in section 13.12.1 it is a predicted target of miR-196a. Unexpectedly, following miR-196a KD, many of miR-196a target HOX genes were not significantly upregulated. At stage 14, multiple HOX genes (mostly from the HOXB cluster) were actually downregulated (**Table 18**). One explanation for this could be that after miR-196a KD, this interferes with an indirect positive feedback loop between the miRNA and expression of the *Hoxb* genes. This downregulation was not seen at stage 17 and for *Hoxb1* expression was significantly upregulated by that stage. This was also the case for three other HOX genes not located on the HOXB cluster (**Table 18**).

**Table 18: Changes in the expression of various HOX genes following miR-196a KD**

	STAGE 14	STAGE 17
<b>UPREGULATED</b>	-	<i>Hoxa1, Hoxb2, Hoxd1, Hoxd4</i>
<b>DOWNREGULATED</b>	<i>Hoxb1/2/3/4/5</i>  <i>Hoxc3</i>	-

**13.14.2.14. The cell population following miR-196a KD is characterised by high levels of neural ‘stemness factors’**

Whilst analysing the list of enhanced genes following miR-196a KD multiple genes involved with the maintenance of pluripotency and inhibition of differentiation became apparent. For example, the forkhead transcription factor *FoxD4L1* as well as the *Pou5f3* genes are all within the top 50 most upregulated genes at both stage 14 and stage 17 (**Figure 43 Figure 44**). As described previously, all of these genes have been shown to be key in maintaining proliferative neural precursors in an immature state (Yan et al., 2009). In addition

to these, the recently discovered ‘stemness factor’ *deptor* was also significantly upregulated. DEPTOR has been shown to promote pluripotency and self-renewal in ESCs by inhibiting mTOR signalling (Agrawal et al., 2014). Another family of pluripotent linked TFs upregulated following miR-196a KD is the VENTX family. Members of the VENTX family of NKL transcription factors were first identified in *Xenopus* and in total there are 6 ventx paralogs, which can be grouped in 3 subclasses: ventx1s, ventx2s and ventx3s (Scerbo et al., 2012). Of these, *Ventx1.1*, *Ventx1.2*, *Ventx2.1* and *Ventx2.2* are all upregulated in the both stage 14 and stage 17 miR-196a KD. There is a longstanding agreement that all paralogs function in a similar ‘nanog-like’ fashion (Onichtchouk et al., 1998). Previous work has given the VENTX proteins two key functions including bmp4-controlled establishment of dorso-ventral patterning and as guardians of high developmental potential during early *Xenopus* development (Scerbo et al., 2012, Onichtchouk et al., 1998). Scerbo et al. (2012) showed that inactivation of *Ventx1/2* leads to down-regulation of the multipotency marker *Pou5f3.1* (*Oct91*) and premature differentiation of blastula cells. Together, this upregulation of pluripotent factors strongly suggests that the region that has been dissected is mainly composed of neural precursors.

To conclude, from these results it is apparent that following miR-196a KD the NPB formation is impeded and as a result, NPB derivatives (NC and placode) are either lost or do not form. It appears as if the tissue that has replaced it is an early neural progenitor population. We can hypothesise that under wildtype conditions, miR-196a usually controls correct neuroectoderm patterning by modulating two pathways. Firstly, through regulating expression levels of BMP signalling and consequently changes in the expression of key genes such as the neural TF - *Zic1*. Secondly, through modulation of Notch signalling and therefore changes in expression of ‘stemness-like’ genes.

A summary of the potential roles of miR-196a during normal neuroectoderm patterning and NC development is summarised in **Figure 45**. As if with miR-219, any potential direct targets (indicated by a dashed line in **Figure 45**) need to be assessed for a miR-219 binding site and then validated using luciferase assays.

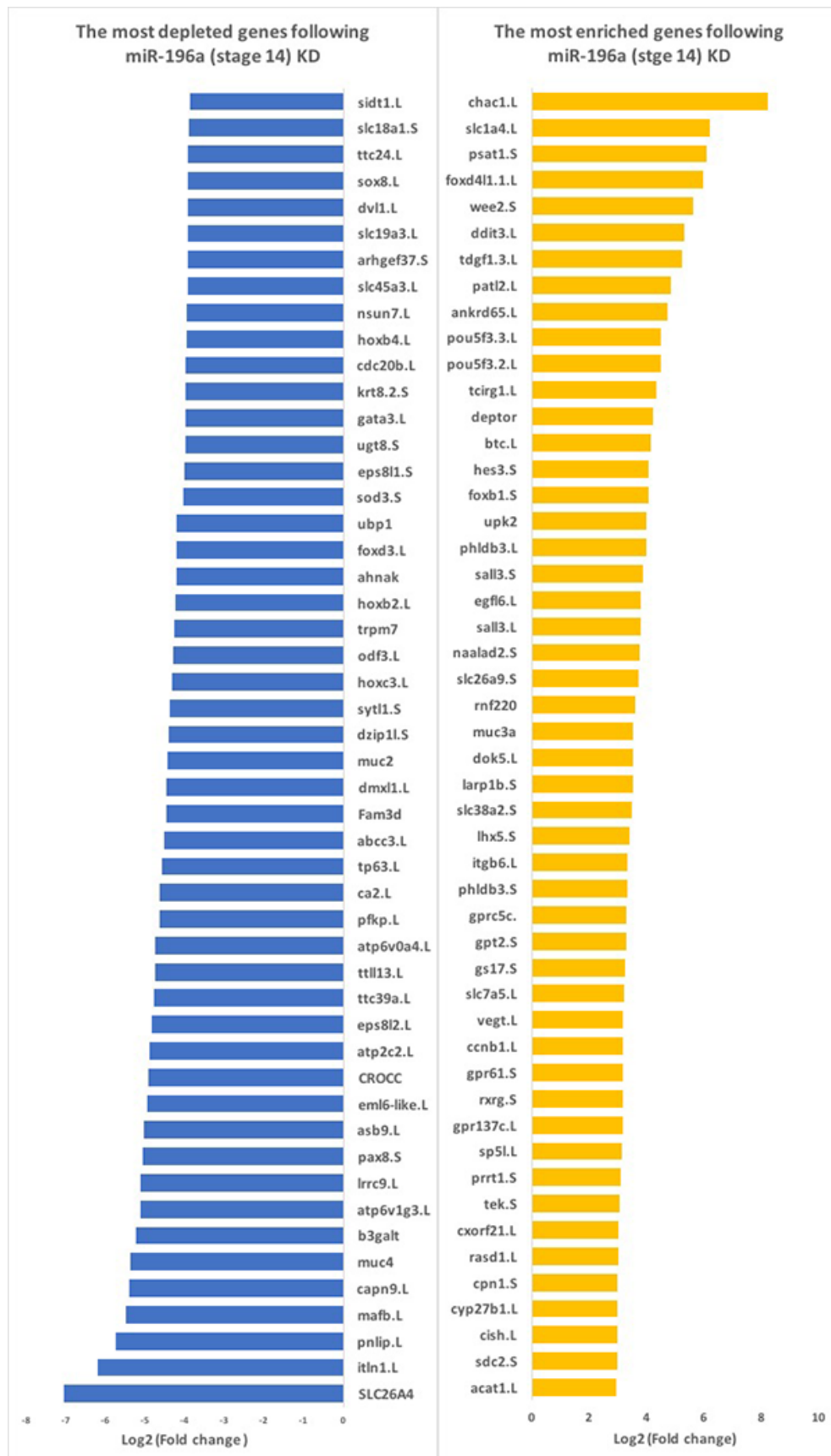


**Figure 43: The top 50 downregulated and upregulated genes following miR-196a (stage 14) KD.**

RNA was sequenced for miR-196a MO NC tissue and miR-196a MM NC tissue. Differential analysis was completed on miR-196aKD vs the MM control to find the top 50 significantly ( $P < 0.05$ ) downregulated genes (blue) and the top 50 significantly ( $P < 0.05$ ) upregulated genes (yellow) following KD of miR-196a.

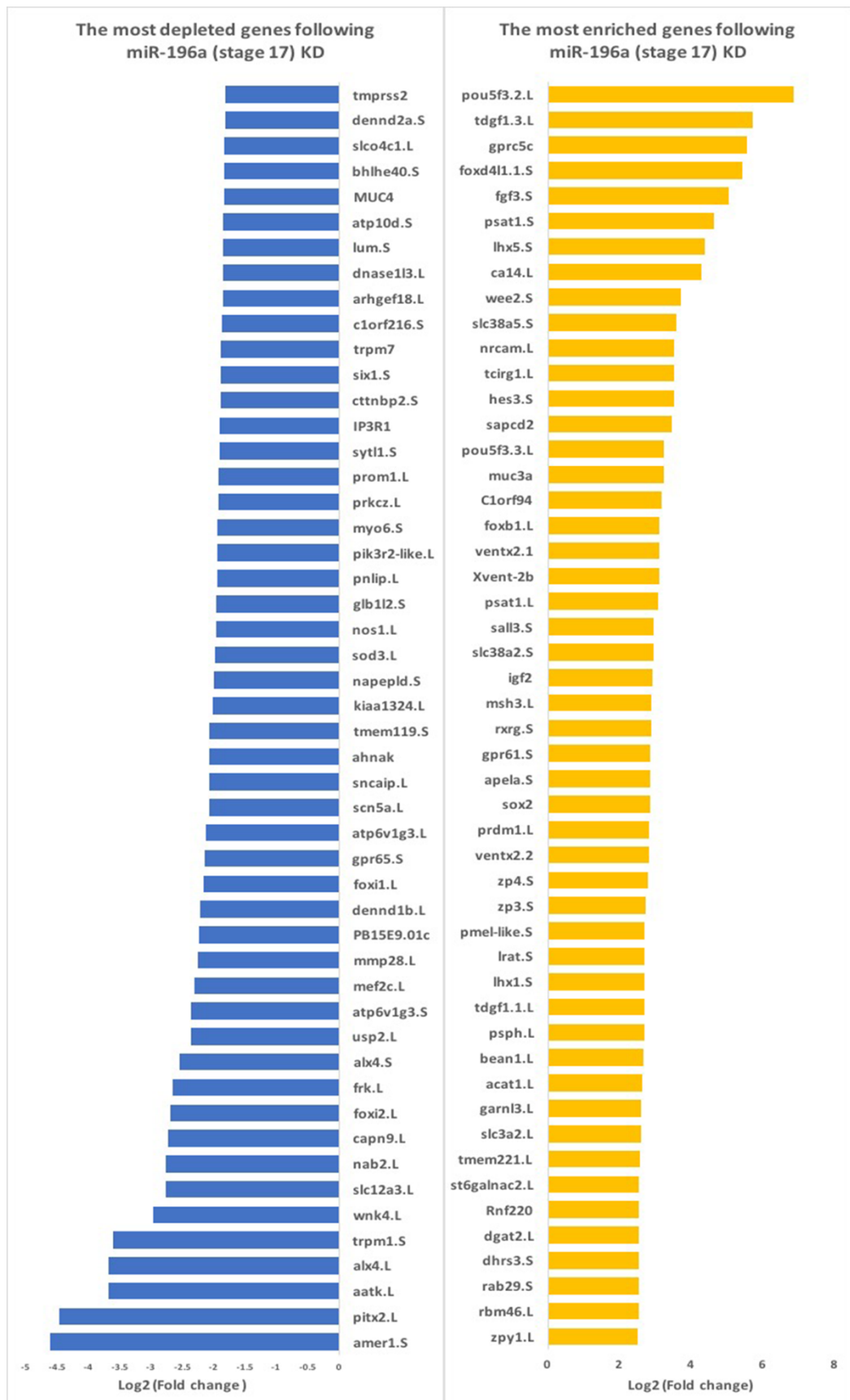


**Figure 44: The top 50 downregulated and upregulated genes following miR-196a (stage 17) KD.**

RNA was sequenced for miR-196a MO NC tissue and miR-196a MM NC tissue. Differential analysis was completed on miR-196aKD vs the MM control to find the top 50 significantly ( $P < 0.05$ ) downregulated genes (blue) and the top 50 significantly ( $P < 0.05$ ) upregulated genes (yellow) following KD of miR-196a.

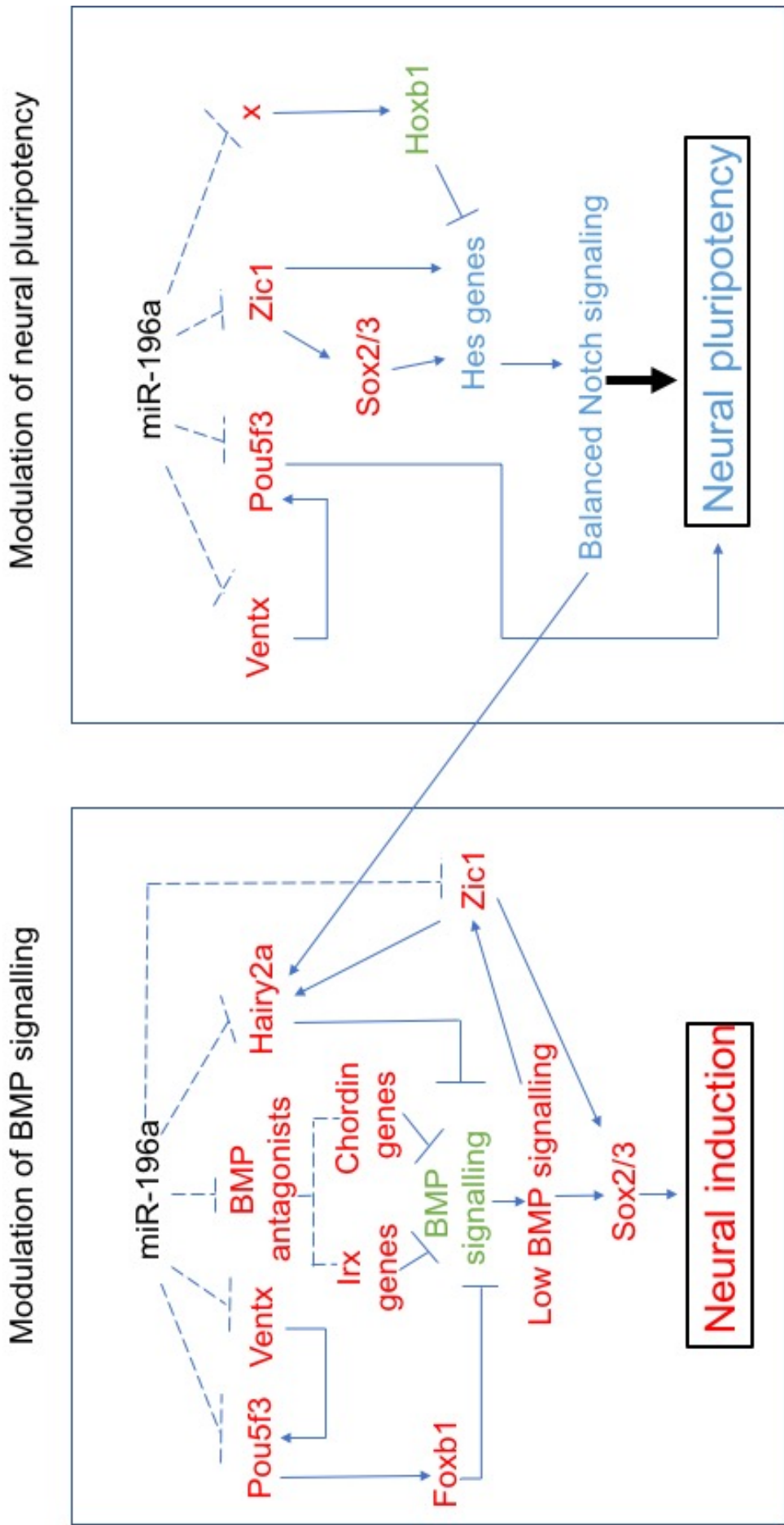


Figure 45: Model of the potential molecular mechanisms miR-196a uses to prevent neural induction and control neural pluripotency during *Xenopus* neuroectoderm patterning.

Red represents repression, green represents expression and blue represents balanced. Solid and dashed lines are the verified and predicted regulatory relationships, respectively.

# Chapter 6: General discussion and concluding remarks

---

## 13.15. Study aims

The aims of this study were:

5. To identify NC enriched miRNAs
6. To explore the function of the candidate miRNAs during *Xenopus* NC development
7. To explore the molecular mechanisms through which these candidate miRNAs are working during *Xenopus* NC development
8. To identify miRNAs that are possibly contributing to NC multipotency

## 13.16. Candidate miRNAs for NC development

Candidate NC miRNAs were identified using two methods; sRNA sequencing on induced NC and the XenmiR approach.

### 13.16.1. Multiple miRNAs are expressed in the developing NC

To identify candidate miRNAs, a NGS miRNA expression profile was generated for induced NC, neural, ectoderm and blastula tissue samples. Bioinformatic analyses of this data revealed expression of 388 known hairpins and 102 novel miRNAs across the four tissue types. Of these, multiple miRNAs were expressed in the NC tissue including miR-219, miR-130C, miR-196a and the novel miRNA miR-Nov-12a (**Figure 17**). In addition to NGS, the XenmiR database was also used to identify candidate miRNAs expressed in NC tissue. Using both approaches and further literature searches six candidates were chosen to undergo functional analysis, those being; miR-219 miR-196a, miR-302, miR-30a-3p, miR-17-5p and miR-429.

## 13.17.miR-219 and miR-196a KD result in aberrant NC development

To determine the importance of the six candidate NC miRNAs, KD experiments using MOs were used. Work from this study has shown that of these six candidates, two miRNA KDs resulted in phenotypes indicative of NC deformations, those being miR-219 and miR-196a. KD of these miRNAs resulted in abnormal craniofacial cartilage development (**Figure 24**) and a loss/reduction of two key NC specification transcription factors - *Snail2* and *Sox10* (**Figure 25** **Figure 27**).

### 13.17.1. miR-219 and its role in NC development

#### 13.17.1.1. *miR-219 KD causes an expansion of Pax3 in the surface ectoderm*

Further characterisation of miR-219 KD phenotype using WISH revealed an unexpected result. KD of miR-219 resulted in a complete shift of expression pattern of the NPB marker *Pax3*. This is characterised by a strong expansion throughout the surface ectoderm (where the *Xenopus* hatching gland forms) and a loss of expression in the underlying prospective NC tissue (**Figure 27**).

#### 13.17.1.2. *miR-219 directly targets Eya1, a placodal gene directly upstream of Pax3*

Using computational target analysis for miR-219, this study shows that the transcription factor *Eya1* is a strong predicted target of miR-219 using various prediction algorithms (**Figure 30**). *Eya1* is a member of the PSED network which is a group of proteins that have been shown to be involved in a variety of developmental processes including sensory placodal development (Donner and Maas, 2004, Friedrich, 2006). miR-219:*Eya1* interaction was chosen to be focused on for three main reasons; (1) it acts upstream of *Pax3* (Grifone et al., 2007) (2) it is expressed in the NPB zone (same as NC) (Moody and LaMantia, 2015) and (3) it is a very strong predicted target of miR-219 (8-mer). Using luciferase reporter assays this work demonstrated for the first time that *Eya1* is a direct target of miR-219 ( $P < 0.0001$ ; control vs miR219 mimic) *in vitro* (**Figure 32**).

As *Eya1* has been shown to act upstream of *Pax3* in other biological processes such as muscle development it would be interesting to explore the possibility of miR-219 playing a similar role in this context (Grifone et al., 2007). As the expansion of *Pax3* is localised to what appears to be the hatching gland (**Figure 27**), one would expect downstream targets of *Pax3* in the hatching gland region to be upregulated. This however was not the case and the opposite was observed. *Xhe2* is a hatching gland specific metalloproteinase that has been shown previously to have an expanded expression domain following an over expression of *Pax3* in the hatching gland region (Hong and Saint-Jeannet, 2014). Surprisingly, in this dataset, *Xhe2* expression was significantly decreased following miR-219 KD (**Figure 38**). To confirm this result, WISH for *Xhe2* on injected embryos needs to be completed.

#### **13.17.1.3. RNA sequencing of miR-219 KD tissue reveals multiple potential models for its role in NC development**

Results from the RNA sequencing data demonstrate that following miR-219 KD, the NC are either lost or never form. This is shown by reduced expression of multiple *bona fide* NC genes (**Figure 37**). This supports the WISH data discussed in chapter 4 where a loss of *Snail2* and *Sox10* is observed following miR-219 KD (**Figure 27**). As a result of an increase in expression of multiple neural genes it appears as if the tissue replacing the NC is a progenitor neural population. Through analysis of the RNA seq data, the role and function of miR-219 can be proposed in several models (summarised in **Figure 39**). Two signalling pathways implicated in nearly all the models are the BMP and Notch signalling pathway. This study indicates that following miR-219 KD there is a decrease in BMP signalling and an increase in Notch signalling. This fits with the upregulation of neural genes following miR-219 KD as low BMP is required for neural induction. These results are supported by several studies in chick whereby an overexpression of Notch signalling impeded NC development whilst a KD of Notch signalling expanded the NC region. This was shown to be via changes in BMP signalling (Endo et al., 2002, Cornell and Eisen, 2005). Conversely, the opposite was observed in *Xenopus* with high Notch signalling (which results in increased BMP signalling) being required for NC induction (Glavic et al., 2004). The role of Notch signalling in NC development is controversial and not fully understood. Conflicting results make it hard to draw final conclusions regarding

its specific role. Overall it can be agreed that for specification of the dorsal-ventral axis of the ectoderm during development there needs to be a gradient of BMP and a fine tuned balanced expression of Notch. miRNAs have been shown in many systems to be key in fine tuning biological signalling pathways and from this data it can be deduced that miR-219 is playing a role in fine tuning the pathways required for NC development. When miR-219 is removed the balance of the signalling molecules is altered and the threshold separating different tissue types is crossed resulting in a change in tissue fate. An overview of the changes induced by miR-219 KD is depicted in **Figure 46**.

### **13.17.2. miR-196a and its role in NC development**

#### **13.17.2.1. *WISH on miR-196a KD embryos revealed a loss of NC specifiers and a gain of neural markers***

Further characterisation of embryos after miR-196a KD using WISH revealed that whilst NC specifiers are reduced and/or lost (*snail2* and *sox10*), the expression of NPB specifiers are more varied. Following miR-196a KD, the expression domain of *Zic1*, *Zic3* and *Pax3* are expanded. Conversely, *Msx2* has reduced expression. The key neural marker – *Sox2* has an expanded domain suggesting there is a cell fate switch from NC to neural (**Figure 26**).

#### **13.17.2.2. *KD of miR-196a results in impeded NPB development, a loss of NPB derivatives and an expansion of NP tissue***

RNA sequencing of miR-196a KD tissue supported previous WISH results as discussed in section 13.17.2.1. Following miR-196a KD, both the NC and placodal tissue are either lost or never developed, whilst the NPB tissue from which they derive from has disrupted gene expression. Some NPB specifiers have increased expression (*Zic1*, *Hairy2a*) whilst others have reduced expression (*Msx1/2*, *Tfap2a*). Using both the WISH data and the RNA seq data together it can be hypothesised that the tissue replacing the absent NC is a neural progenitor population.

### **13.17.2.3. *miR-196a usually maintains a gradient of BMP signalling ensuring correct patterning of the neuroectoderm***

Through analysis of the RNA seq data, the role and function of miR-196a can be proposed in several models (summarised in **Figure 45**). As with miR-219 KD, two signalling pathways implicated in nearly all the models are the BMP and Notch signalling pathway. From this data, it can be hypothesised that miR-196a plays two roles in early *Xenopus* development, the first of which is maintaining a gradient of BMP signalling to ensure correct patterning of the neuroectoderm. This study shows that following miR-196a KD there appears to be a decrease in BMP signalling characterised by an increase in BMP antagonists (**Figure 41 Figure 42**). As discussed previously it is likely that this decrease in BMP signalling resulting in changes in expression of key transcription factors towards a neural fate, one of which being an increase in *Zic1*.

### **13.17.2.4. *Absence of miR-196a alters balances of pluripotency and differentiation (via Notch)***

Previous studies have demonstrated strong links between the maintenance of progenitor populations and increased Notch signalling (Imayoshi et al., 2010). The 'neural population' of cells that replace NC following miR-196a KD is characterised by an increase in downstream Notch effectors as well as many pluripotency related genes including the *Pou5f3* factors (**Figure 41 Figure 42**). This therefore suggests that under wildtype conditions miR-196a is involved in the maintenance of stem cell like properties of cells, possibly via regulating Notch signalling. This is supported by work of Kim and colleagues who showed using mesenchymal stem cells that inhibition of miR-196a enhanced proliferation and decreased osteogenic differentiation (Kim et al., 2009). Throughout the literature, many miRNAs have been described as key players in the regulation of pluripotency in many systems including embryonic stem cells (ESC), induced pluripotent stem cells (iPSC) and cancer (see section 2.3 for a review).

Overall, for specification of the dorsal-ventral axis of the ectoderm during development there needs to be a gradient of BMP and a fine tuned balanced expression of Notch. From these results it is clear that miR-196a plays a role in maintaining both of these and when removed, thresholds are broken resulting in changes in tissue fate. An overview of the changes induced by miR-196a KD is

depicted in **Figure 47**.

### **13.17.3. miR-301 and miR-338 are candidates for the maintenance of NC pluripotency**

Recent work in *Xenopus* has shown that contrary to prior belief, the NC retain their pluripotency from the cells in which they derive from (blastula) rather than selectively regain it (Buitrago-Delgado et al., 2015). Analysis of miRNAs upregulated in both NC and blastula stages in this study revealed two candidates that are maybe involved in the mechanism behind the inheritance of pluripotency, these being miR-301 and miR-338 (**Figure 18**). Both miRNAs have links to pluripotency throughout the literature (see section 13.5.9) and prove to be strong candidates for miRNAs that are responsible for maintaining this pluripotent cell population which gives rise to NC (Buitrago-Delgado et al., 2015). These results provide a good platform for a future project within the lab.

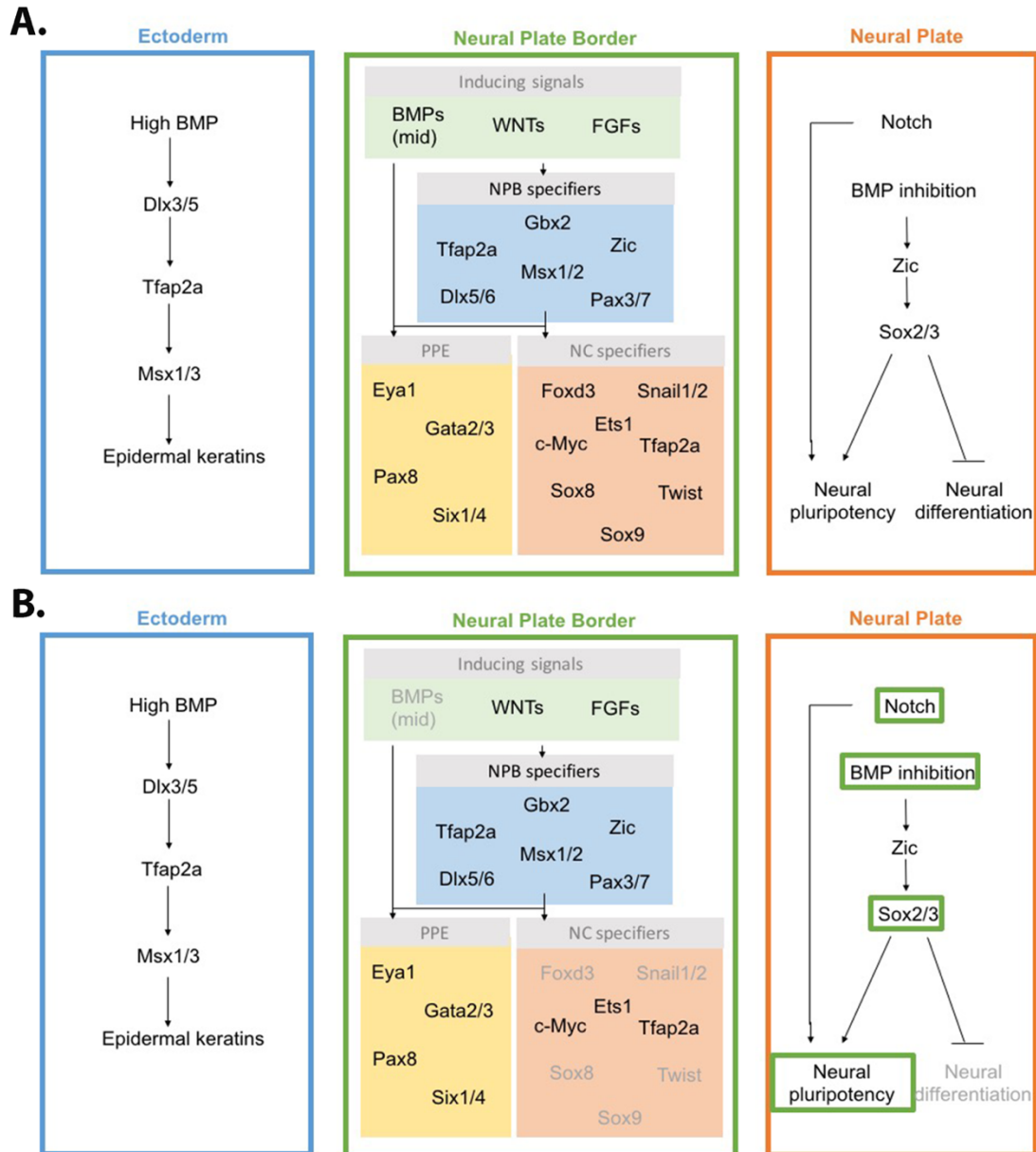


**Figure 46 A summary of the changes in gene expression following miR-219 KD.**

Outline of the GRN controlling neural crest development under normal conditions **(A)** and following miR-219 KD **(B)**. Black words indicate no significant change in expression, grey words indicate a significant decrease in expression and a green box indicates a significant increase in expression. Following miR-219 KD BMP signalling is downregulated whilst Notch signalling is upregulated. This results in increased neural tissue whilst most key NC specifiers are lost or fails to ever form. The NPB and placodal development appears to be unaltered.

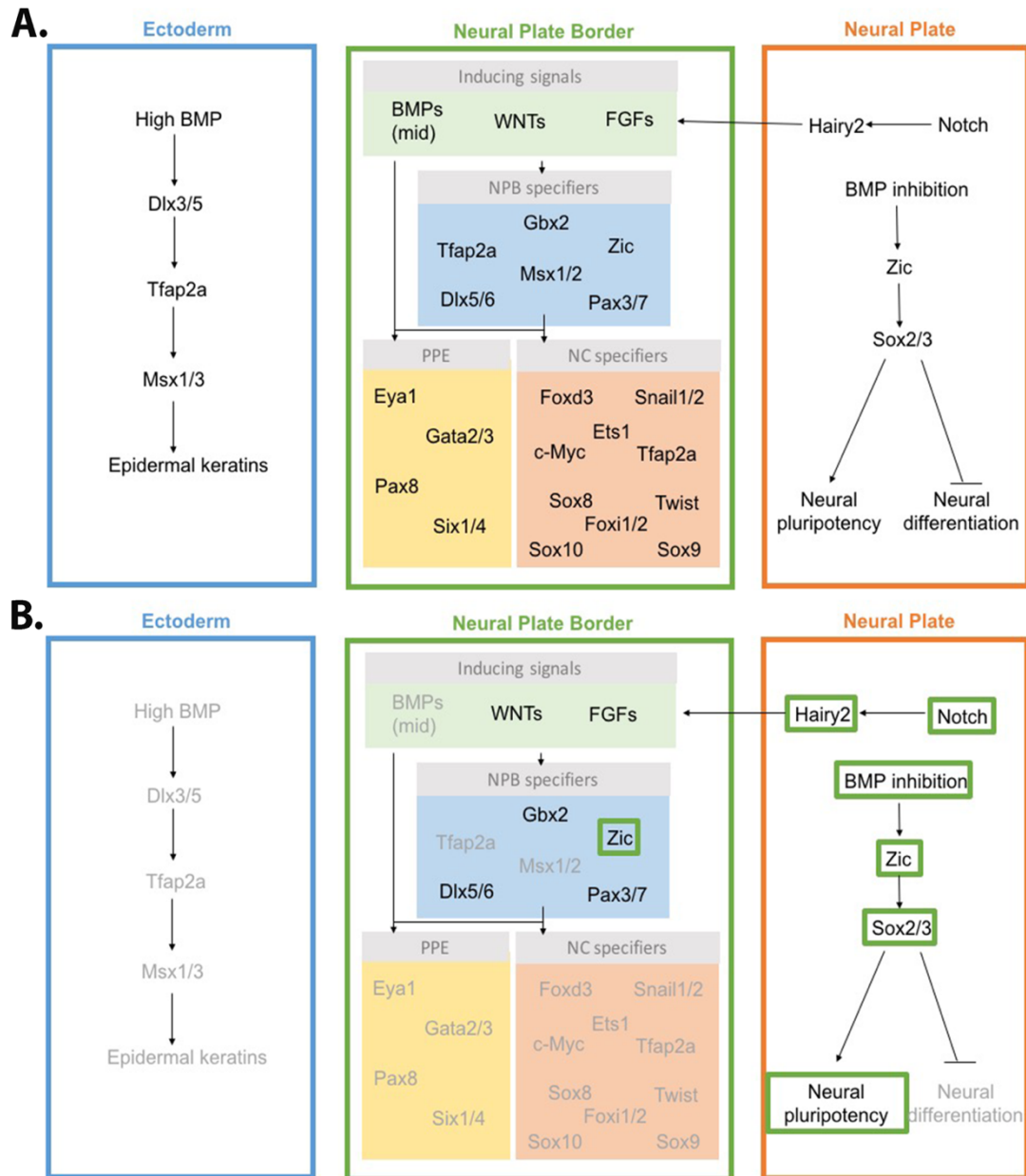


**Figure 47** A summary of the changes in gene expression following miR-196a KD.

Outline of the GRN controlling neural crest development under normal conditions (**A**) and following miR-196a KD (**B**). Black words indicate no significant change in expression, grey words indicate a significant decrease in expression and a green box indicates a significant increase in expression. Following miR-196a KD BMP signalling is downregulated whilst Notch signalling is upregulated. This results in increased neural tissue whilst both NC and placode tissue is lost or fails to ever form. The NPB development is impaired with some genes being downregulated, some upregulated whilst others do not change.

## 13.18.Future work

Despite achieving the overall aim of this project, there are multiple areas that can be developed further in the future in order to consolidate the results presented and to try to validate any proposed models.

### 13.18.1. WISH

#### 13.18.1.1. *miR-219 expression*

A key experiment that needs to be completed to really begin to understand the role miR-219 is playing in NC development is WISH for miR-219. This would enable us to gain both spatial and temporal information regarding the expression of miR-219. WISH using LNA probes against the mature transcript were attempted but only background staining was observed. The reason behind this was unknown. As an alternative, probes should be made against the longer primary transcripts and WISH completed against that.

#### 13.18.1.2. *RNA sequencing validation*

WISH should be completed on KD embryos for various markers to validate the RNA seq results. This has already been completed for some genes including *Msx1*, *Zic1*, *Zic3* (**Figure 26**) but more markers should be validated. As placodal genes were lost following miR-196a KD but not following miR-219 KD WISH for these genes would provide strong evidence supporting the sequencing data.

#### 13.18.1.3. *Changes in expression of Eya1 and Xhe2*

These results show that *Eya1* is a direct target of miR-219 *in vitro* (**Figure 32**) and that following miR-219 KD, *Pax3* is expanded across the surface ectoderm of the embryo (**Figure 27**). As *Eya1* acts upstream of *Pax3* and *Xhe2* is downstream of *Pax3* it could be speculated that one and/or both these genes display the same changes in expression profile. To investigate this, WISH needs to be completed for both genes following miR-219 KD.

### 13.18.2. Can *Eya1* KD rescue the expanded *Pax3* phenotype?

From the results in the study, it has been speculated that following miR-219 KD, *Eya1* is increased and this causes an expansion of *Pax3*. To provide evidence for this, rescue experiments need to be completed. MOs against miR-219 and *Eya1* should be injected both separately and together. If the upregulation of *Eya1* is responsible for the expansion of *Pax3* then the combination of the two MOs should rescue the miR-219 KD phenotype. An alternative way to show this is by using target protectors. These protectors are single stranded modified RNAs that will bind to the miR-219 target site on the 3'UTR of *Eya1* and prevent any miR-219 interactions which would mimic the miR-219 KD phenotype.

### 13.18.3. Validating additional NC candidates

#### 13.18.3.1. *NC specific miRNAs identified from sRNA sequencing*

From the sRNA sequencing results, multiple miRNAs were shown to be upregulated in the NC when compared to neural (**Figure 17**). WISH should be completed for these miRNAs followed by KD experiments using MOs. One miRNA of particular interest is miR-nov-12a. This candidate is a novel miRNA that was expressed specifically in the NC. For this miRNA, target analysis would further enhance these results.

#### 13.18.3.2. *miR-301 and miR-338 and their role in pluripotency*

As discussed in section 13.5.9, from this data set it is clear that miR-301 and miR-338 are strong candidates for miRNAs that could play a role in maintaining the pluripotency of the developing NC. As discussed previously miRNAs have been reported to have roles in regulating pluripotency in many systems making them strong candidates (see section 2.3). To investigate this further WISH should be carried out to assess the spatial and temporal expression of these miRNAs. In addition, functional analysis using MO could be completed followed by WISH for *bona fide* pluripotency markers.

### 13.18.4. Validation of direct targets of miR-219 and miR-196a

From the sequencing results discussed in section 13.14.2, multiple potential direct targets have become apparent for both miR-219 and miR-196a and have

been incorporated into the theoretical models (**Figure 39 Figure 45**). To test that these genes are direct targets, the 3' UTR should be assessed for a target binding site (complementary to the seed of the miRNA) and then luciferase reporter assays can be generated as described previously in section 12.3.3. Alternatively, to test for these targets of both miRNAs (along with others) in an unbiased way the experimental procedure of 'cross-linking, ligation and sequencing of hybrids' (CLASH) could be implemented. The concept of the technique is to stabilize AGO-RNA complexes in live cells using UV and ligate them to form chimeric RNAs. Through sequencing, interacting RNA molecules (bound by AGO) are unambiguously identified as chimeric reads and will be sequenced to give the miRNA and its interacting mRNA target (Helwak et al., 2013).

#### **13.18.5. Measuring changes in BMP activity following miR-219 and miR-196a KD**

From this study, multiple models of how miR-219 and miR-196a regulate correct NC development have been proposed. For both the miRNAs, BMP signalling has been implicated. This is proposed to be in part, via an upregulation of the BMP antagonists; *Chordin* and *Irx1*. As these BMP antagonists work by blocking BMP signalling at a protein level a decrease of BMP signalling could not be observed at a transcriptome level. To assess whether BMP signalling is altered following miR-219 KD a reporter construct should be used like that described in Faure et al. (2000).

#### **13.19. Applying these results to regenerative medicine – 'the bigger picture'**

Stroke and many neurodegenerative disorders such as Parkinson's disease, Alzheimer's disease, amyotrophic lateral sclerosis need cell replacement therapy. Currently, cell-based therapy for treating these diseases is a primary goal in regenerative medicine research that attracts great attention. The successful use of converted neural cells in transplantations has opened a new avenue to treat such diseases (Zhang et al., 2012b). Nevertheless, induced neurons, directly converted from fibroblasts are terminally committed and exhibit very limited proliferative ability (Yang et al., 2011). From the work presented in

this thesis, two miRNAs have been identified which when knocked down result in a cell fate switch to an induced neural progenitor state. These results could have huge implications when applied to regenerative medicine in terms of both clinical applications and disease modelling *in vitro*.

In addition, miR-196a and miR-219 KD result in a loss of NC. This can also have clinical implications in relation to melanoma cancer. Metastatic melanoma is the most aggressive skin cancer and despite tremendous efforts and considerable progress in clinical treatment of melanoma patients within recent years, it remains a deadly disease (Shakhova, 2014). A growing number of publications highlight the existence of phenotypic and functional similarities between embryonic NC cells and melanoma cells. These studies provide compelling evidence that the propagation of melanoma cells critically depends on genes instrumental in NC development (White et al., 2011, Kaufman et al., 2016, Shakhova, 2014). As miR-196a and miR-219 KD resulted in an aberration of NC development they prove to be interesting targets for melanoma treatment. This is particularly true as the recent development of miRNA antisense technology (anti-miR) has shown great promise in the development of novel therapeutics (Stenvang et al., 2012).

## Chapter 7: References

---

**ABBRUZZESE, G., BECKER, S. F., KASHEF, J. & ALFANDARI, D.** 2016. ADAM13 cleavage of cadherin-11 promotes CNC migration independently of the homophilic binding site. *Dev Biol*, 415, 383-90.

**ABU-ELMAGD, M., GARCIA-MORALES, C. & WHEELER, G. N.** 2006. Frizzled7 mediates canonical Wnt signaling in neural crest induction. *Dev Biol*, 298, 285-98.

**ABU-ELMAGD, M., ISHII, Y., CHEUNG, M., REX, M., LE ROUEDEC, D. & SCOTTING, P. J.** 2001. cSox3 expression and neurogenesis in the epibranchial placodes. *Dev Biol*, 237, 258-69.

**AGRAWAL, P., REYNOLDS, J., CHEW, S., LAMBA, D. A. & HUGHES, R. E.** 2014. DEPTOR is a stemness factor that regulates pluripotency of embryonic stem cells. *J Biol Chem*, 289, 31818-26.

**AHMAD, A., GINNEBAUGH, K. R., YIN, S., BOLLIG-FISCHER, A., REDDY, K. B. & SARKAR, F. H.** 2015. Functional role of miR-10b in tamoxifen resistance of ER-positive breast cancer cells through down-regulation of HDAC4. *BMC Cancer*, 15, 540.

**AHMED, A., WARD, N. J., MOXON, S., LOPEZ-GOMOLLON, S., VIAUT, C., TOMLINSON, M. L., PATRUSHEV, I., GILCHRIST, M. J., DALMAY, T., DOTLIC, D., MUNSTERBERG, A. E. & WHEELER, G. N.** 2015. A Database of microRNA Expression Patterns in *Xenopus laevis*. *PLoS One*, 10, e0138313.

**AMARAL, P. P., DINGER, M. E., MERCER, T. R. & MATTICK, J. S.** 2008. The eukaryotic genome as an RNA machine. *Science*, 319, 1787-9.

**AMBROS, V.** 2004. The functions of animal microRNAs. *Nature*, 431, 350-5.

**AN, J., LAI, J., LEHMAN, M. L. & NELSON, C. C.** 2013. miRDeep\*: an integrated application tool for miRNA identification from RNA sequencing data. *Nucleic Acids Res*, 41, 727-37.

**ANDL, T., MURCHISON, E. P., LIU, F., ZHANG, Y., YUNTA-GONZALEZ, M., TOBIAS, J. W., ANDL, C. D., SEYKORA, J. T., HANNON, G. J. & MILLAR, S. E.** 2006. The miRNA-processing enzyme dicer is essential for the morphogenesis and maintenance of hair follicles. *Curr Biol*, 16, 1041-9.

**ANSORGE, W. J.** 2009. Next-generation DNA sequencing techniques. *N Biotechnol*, 25, 195-203.

**AOKI, Y., SAINT-GERMAIN, N., GYDA, M., MAGNER-FINK, E., LEE, Y. H., CREDIDIO, C. & SAINT-JEANNET, J. P.** 2003. Sox10 regulates the development of neural crest-derived melanocytes in *Xenopus*. *Dev Biol*, 259, 19-33.

**ARAVIN, A., GAIDATZIS, D., PFEFFER, S., LAGOS-QUINTANA, M.,**

**LANDGRAF, P., IOVINO, N., MORRIS, P., BROWNSTEIN, M. J., KURAMOCHI-MIYAGAWA, S., NAKANO, T., CHIEN, M., RUSSO, J. J., JU, J., SHERIDAN, R., SANDER, C., ZAVOLAN, M. & TUSCHL, T.** 2006. A novel class of small RNAs bind to MILI protein in mouse testes. *Nature*, 442, 203-7.

**ARMISEN, J., GILCHRIST, M. J., WILCZYNSKA, A., STANDART, N. & MISKA, E. A.** 2009. Abundant and dynamically expressed miRNAs, piRNAs, and other small RNAs in the vertebrate *Xenopus tropicalis*. *Genome Res*, 19, 1766-75.

**ARTAVANIS-TSAKONAS, S., RAND, M. D. & LAKE, R. J.** 1999. Notch signaling: cell fate control and signal integration in development. *Science*, 284, 770-6.

**ARUGA, J., TOHMONDA, T., HOMMA, S. & MIKOSHIBA, K.** 2002. *Zic1* promotes the expansion of dorsal neural progenitors in spinal cord by inhibiting neuronal differentiation. *Dev Biol*, 244, 329-41.

**ASLI, N. S. & KESSEL, M.** 2010. Spatiotemporally restricted regulation of generic motor neuron programs by miR-196-mediated repression of *Hoxb8*. *Dev Biol*, 344, 857-68.

**AYBAR, M. J., NIETO, M. A. & MAYOR, R.** 2003. Snail precedes slug in the genetic cascade required for the specification and migration of the *Xenopus* neural crest. *Development*, 130, 483-94.

**BAEK, D., VILLEN, J., SHIN, C., CAMARGO, F. D., GYGI, S. P. & BARTEL, D. P.** 2008. The impact of microRNAs on protein output. *Nature*, 455, 64-71.

**BALCELLS, I., CIRERA, S. & BUSK, P. K.** 2011. Specific and sensitive quantitative RT-PCR of miRNAs with DNA primers. *BMC Biotechnol*, 11, 70.

**BARIK, S.** 2008. An intronic microRNA silences genes that are functionally antagonistic to its host gene. *Nucleic Acids Res*, 36, 5232-41.

**BARRIGA, E. H., MAXWELL, P. H., REYES, A. E. & MAYOR, R.** 2013. The hypoxia factor Hif-1alpha controls neural crest chemotaxis and epithelial to mesenchymal transition. *J Cell Biol*, 201, 759-76.

**BARROSO-DELJESUS, A., LUCENA-AGUILAR, G., SANCHEZ, L., LIGERO, G., GUTIERREZ-ARANDA, I. & MENENDEZ, P.** 2011. The Nodal inhibitor Lefty is negatively modulated by the microRNA miR-302 in human embryonic stem cells. *FASEB J*, 25, 1497-508.

**BARTEL, D. P.** 2004. MicroRNAs: genomics, biogenesis, mechanism, and function. *Cell*, 116, 281-97.

**BARTEL, D. P.** 2009. MicroRNAs: target recognition and regulatory functions. *Cell*, 136, 215-33.

**BASCH, M. L., BRONNER-FRASER, M. & GARCIA-CASTRO, M. I.** 2006. Specification of the neural crest occurs during gastrulation and requires Pax7. *Nature*, 441, 218-22.

**BECKER, S. F., MAYOR, R. & KASHEF, J.** 2013. Cadherin-11 mediates contact

- inhibition of locomotion during *Xenopus* neural crest cell migration. *PLoS One*, 8, e85717.
- BELLEFRROID, E. J., KOBBE, A., GRUSS, P., PIELER, T., GURDON, J. B. & PAPALOPULU, N.** 1998. Xiro3 encodes a *Xenopus* homolog of the *Drosophila* Iroquois genes and functions in neural specification. *EMBO J*, 17, 191-203.
- BELLMAYER, A., KRASE, J., LINDGREN, J. & LABONNE, C.** 2003. The protooncogene *c-myc* is an essential regulator of neural crest formation in *xenopus*. *Dev Cell*, 4, 827-39.
- BERNSTEIN, E., KIM, S. Y., CARMELL, M. A., MURCHISON, E. P., ALCORN, H., LI, M. Z., MILLS, A. A., ELLEDGE, S. J., ANDERSON, K. V. & HANNON, G. J.** 2003. Dicer is essential for mouse development. *Nat Genet*, 35, 215-7.
- BETANCUR, P., BRONNER-FRASER, M. & SAUKA-SPENGLER, T.** 2010. Assembling neural crest regulatory circuits into a gene regulatory network. *Annu Rev Cell Dev Biol*, 26, 581-603.
- BETANCUR, P., SIMOES-COSTA, M., SAUKA-SPENGLER, T. & BRONNER, M. E.** 2014. Expression and function of transcription factor *cMyb* during cranial neural crest development. *Mech Dev*, 132, 38-43.
- BETSHOLTZ, C., KARLSSON, L. & LINDAHL, P.** 2001. Developmental roles of platelet-derived growth factors. *Bioessays*, 23, 494-507.
- BOHNSACK, M. T., CZAPLINSKI, K. & GORLICH, D.** 2004. Exportin 5 is a RanGTP-dependent dsRNA-binding protein that mediates nuclear export of pre-miRNAs. *RNA*, 10, 185-91.
- BRAIG, S., MUELLER, D. W., ROTHHAMMER, T. & BOSSERHOFF, A. K.** 2010. MicroRNA miR-196a is a central regulator of HOX-B7 and BMP4 expression in malignant melanoma. *Cell Mol Life Sci*, 67, 3535-48.
- BRAY, S. J.** 2006. Notch signalling: a simple pathway becomes complex. *Nat Rev Mol Cell Biol*, 7, 678-89.
- BRITSCH, S., GOERICH, D. E., RIETHMACHER, D., PEIRANO, R. I., ROSSNER, M., NAVE, K. A., BIRCHMEIER, C. & WEGNER, M.** 2001. The transcription factor *Sox10* is a key regulator of peripheral glial development. *Genes Dev*, 15, 66-78.
- BUITRAGO-DELGADO, E., NORDIN, K., RAO, A., GEARY, L. & LABONNE, C.** 2015. NEURODEVELOPMENT. Shared regulatory programs suggest retention of blastula-stage potential in neural crest cells. *Science*, 348, 1332-5.
- CAI, D. H. & BRAUER, P. R.** 2002. Synthetic matrix metalloproteinase inhibitor decreases early cardiac neural crest migration in chicken embryos. *Dev Dyn*, 224, 441-9.
- CAMACHO, C., COULOURIS, G., AVAGYAN, V., MA, N., PAPADOPOULOS, J., BEALER, K. & MADDEN, T. L.** 2009. BLAST+: architecture and applications. *BMC Bioinformatics*, 10, 421.

**CANO, A., PEREZ-MORENO, M. A., RODRIGO, I., LOCASCIO, A., BLANCO, M. J., DEL BARRIO, M. G., PORTILLO, F. & NIETO, M. A.** 2000. The transcription factor snail controls epithelial-mesenchymal transitions by repressing E-cadherin expression. *Nat Cell Biol*, 2, 76-83.

**CAO, Y., SIEGEL, D., DONOW, C., KNOCHER, S., YUAN, L. & KNOCHER, W.** 2007. POU-V factors antagonize maternal VegT activity and beta-Catenin signaling in *Xenopus* embryos. *EMBO J*, 26, 2942-54.

**CARD, D. A., HEBBAR, P. B., LI, L., TROTTER, K. W., KOMATSU, Y., MISHINA, Y. & ARCHER, T. K.** 2008. Oct4/Sox2-regulated miR-302 targets cyclin D1 in human embryonic stem cells. *Mol Cell Biol*, 28, 6426-38.

**CARMONA-FONTAINE, C., THEVENEAU, E., TZEKOU, A., TADA, M., WOODS, M., PAGE, K. M., PARSONS, M., LAMBRIS, J. D. & MAYOR, R.** 2011. Complement fragment C3a controls mutual cell attraction during collective cell migration. *Dev Cell*, 21, 1026-37.

**CARROLL, E. J., JR. & HEDRICK, J. L.** 1974. Hatching in the toad *Xenopus laevis*: morphological events and evidence for a hatching enzyme. *Dev Biol*, 38, 1-13.

**CARTWRIGHT, P., MCLEAN, C., SHEPPARD, A., RIVETT, D., JONES, K. & DALTON, S.** 2005. LIF/STAT3 controls ES cell self-renewal and pluripotency by a Myc-dependent mechanism. *Development*, 132, 885-96.

**CAVODEASSI, F., MODOLELL, J. & GOMEZ-SKARMETA, J. L.** 2001. The Iroquois family of genes: from body building to neural patterning. *Development*, 128, 2847-55.

**CHAI, Y., ITO, Y. & HAN, J.** 2003. TGF-beta signaling and its functional significance in regulating the fate of cranial neural crest cells. *Crit Rev Oral Biol Med*, 14, 78-88.

**CHALMERS, A. D., LACHANI, K., SHIN, Y., SHERWOOD, V., CHO, K. W. & PAPALOPULU, N.** 2006. Grainyhead-like 3, a transcription factor identified in a microarray screen, promotes the specification of the superficial layer of the embryonic epidermis. *Mech Dev*, 123, 702-18.

**CHALPE, A. J., PRASAD, M., HENKE, A. J. & PAULSON, A. F.** 2010. Regulation of cadherin expression in the chicken neural crest by the Wnt/beta-catenin signaling pathway. *Cell Adh Migr*, 4, 431-8.

**CHAN, Y. C., KHANNA, S., ROY, S. & SEN, C. K.** 2011. miR-200b targets Ets-1 and is down-regulated by hypoxia to induce angiogenic response of endothelial cells. *J Biol Chem*, 286, 2047-56.

**CHANG, C. & HEMMATI-BRIVANLOU, A.** 1998. Neural crest induction by Xwnt7B in *Xenopus*. *Dev Biol*, 194, 129-34.

**CHEKULAEVA, M. & FILIPOWICZ, W.** 2009. Mechanisms of miRNA-mediated post-transcriptional regulation in animal cells. *Curr Opin Cell Biol*, 21, 452-60.

**CHEN, C., RIDZON, D. A., BROOMER, A. J., ZHOU, Z., LEE, D. H., NGUYEN,**

**J. T., BARBISIN, M., XU, N. L., MAHUVAKAR, V. R., ANDERSEN, M. R., LAO, K. Q., LIVAK, K. J. & GUEGLER, K. J.** 2005. Real-time quantification of microRNAs by stem-loop RT-PCR. *Nucleic Acids Res*, 33, e179.

**CHEN, R., AMOUI, M., ZHANG, Z. & MARDON, G.** 1997. Dachshund and eyes absent proteins form a complex and function synergistically to induce ectopic eye development in *Drosophila*. *Cell*, 91, 893-903.

**CHEUNG, M., CHABOISSIER, M. C., MYNETT, A., HIRST, E., SCHEDL, A. & BRISCOE, J.** 2005. The transcriptional control of trunk neural crest induction, survival, and delamination. *Dev Cell*, 8, 179-92.

**CHRISTIAN, J. L., MCMAHON, J. A., MCMAHON, A. P. & MOON, R. T.** 1991. Xwnt-8, a *Xenopus* Wnt-1/int-1-related gene responsive to mesoderm-inducing growth factors, may play a role in ventral mesodermal patterning during embryogenesis. *Development*, 111, 1045-55.

**CHRISTOFFERSEN, N. R., SILAHTAROGLU, A., OROM, U. A., KAUPPINEN, S. & LUND, A. H.** 2007. miR-200b mediates post-transcriptional repression of ZFHX1B. *RNA*, 13, 1172-8.

**CIZELSKY, W., HEMPEL, A., METZIG, M., TAO, S., HOLLEMANN, T., KUHLM, M. & KUHLM, S. J.** 2013. sox4 and sox11 function during *Xenopus laevis* eye development. *PLoS One*, 8, e69372.

**CONCEPCION, C. P., BONETTI, C. & VENTURA, A.** 2012. The microRNA-17-92 family of microRNA clusters in development and disease. *Cancer J*, 18, 262-7.

**COORDINATORS, N. R.** 2013. Database resources of the National Center for Biotechnology Information. *Nucleic Acids Res*, 41, D8-D20.

**CORDES, K. R. & SRIVASTAVA, D.** 2009. MicroRNA regulation of cardiovascular development. *Circ Res*, 104, 724-32.

**CORNELL, R. A. & EISEN, J. S.** 2005. Notch in the pathway: the roles of Notch signaling in neural crest development. *Semin Cell Dev Biol*, 16, 663-72.

**COULY, G., GRAPIN-BOTTON, A., COLTEY, P., RUHIN, B. & LE DOUARIN, N. M.** 1998. Determination of the identity of the derivatives of the cephalic neural crest: incompatibility between Hox gene expression and lower jaw development. *Development*, 125, 3445-59.

**COUSIN, H., ABBRUZZESE, G., KERDAVID, E., GAULTIER, A. & ALFANDARI, D.** 2011. Translocation of the cytoplasmic domain of ADAM13 to the nucleus is essential for Calpain8-a expression and cranial neural crest cell migration. *Dev Cell*, 20, 256-63.

**CRANE, J. F. & TRAINOR, P. A.** 2006. Neural crest stem and progenitor cells. *Annu Rev Cell Dev Biol*, 22, 267-86.

**CREAZZO, T. L., GODT, R. E., LEATHERBURY, L., CONWAY, S. J. & KIRBY, M. L.** 1998. Role of cardiac neural crest cells in cardiovascular development. *Annu Rev Physiol*, 60, 267-86.

- CRIST, C. G., MONTARRAS, D., PALLAFACCHINA, G., ROCANCOURT, D., CUMANO, A., CONWAY, S. J. & BUCKINGHAM, M.** 2009. Muscle stem cell behavior is modified by microRNA-27 regulation of Pax3 expression. *Proc Natl Acad Sci U S A*, 106, 13383-7.
- CROCE, C. M.** 2009. Causes and consequences of microRNA dysregulation in cancer. *Nat Rev Genet*, 10, 704-14.
- DARNELL, D. K., KAUR, S., STANISLAW, S., KONIECZKA, J. H., YATSKIEVYCH, T. A. & ANTIN, P. B.** 2006. MicroRNA expression during chick embryo development. *Dev Dyn*, 235, 3156-65.
- DAVIS, B. N. & HATA, A.** 2009. Regulation of MicroRNA Biogenesis: A miRiad of mechanisms. *Cell Commun Signal*, 7, 18.
- DE CROZE, N., MACZKOWIAK, F. & MONSORO-BURQ, A. H.** 2011. Reiterative AP2a activity controls sequential steps in the neural crest gene regulatory network. *Proc Natl Acad Sci U S A*, 108, 155-60.
- DEARDORFF, M. A., TAN, C., SAINT-JEANNET, J. P. & KLEIN, P. S.** 2001. A role for frizzled 3 in neural crest development. *Development*, 128, 3655-63.
- DELAURIER, A., NAKAMURA, Y., BRAASCH, I., KHANNA, V., KATO, H., WAKITANI, S., POSTLETHWAIT, J. H. & KIMMEL, C. B.** 2012. Histone deacetylase-4 is required during early cranial neural crest development for generation of the zebrafish palatal skeleton. *BMC Dev Biol*, 12, 16.
- DOENCH, J. G., PETERSEN, C. P. & SHARP, P. A.** 2003. siRNAs can function as miRNAs. *Genes Dev*, 17, 438-42.
- DONNER, A. L. & MAAS, R. L.** 2004. Conservation and non-conservation of genetic pathways in eye specification. *Int J Dev Biol*, 48, 743-53.
- DRYSDALE, T. A. & ELINSON, R. P.** 1991. Development of the *Xenopus laevis* hatching gland and its relationship to surface ectoderm patterning. *Development*, 111, 469-78.
- DUGAS, J. C., CUELLAR, T. L., SCHOLZE, A., ASON, B., IBRAHIM, A., EMERY, B., ZAMANIAN, J. L., FOO, L. C., MCMANUS, M. T. & BARRES, B. A.** 2010. Dicer1 and miR-219 Are required for normal oligodendrocyte differentiation and myelination. *Neuron*, 65, 597-611.
- DUONG, T. D. & ERICKSON, C. A.** 2004. MMP-2 plays an essential role in producing epithelial-mesenchymal transformations in the avian embryo. *Dev Dyn*, 229, 42-53.
- DUPIN, E., CREUZET, S. & LE DOUARIN, N. M.** 2006. The contribution of the neural crest to the vertebrate body. *Adv Exp Med Biol*, 589, 96-119.
- DUTTON, K., ABBAS, L., SPENCER, J., BRANNON, C., MOWBRAY, C., NIKAIIDO, M., KELSH, R. N. & WHITFIELD, T. T.** 2009. A zebrafish model for Waardenburg syndrome type IV reveals diverse roles for Sox10 in the otic vesicle. *Dis Model Mech*, 2, 68-83.

- EBERHART, J. K., HE, X., SWARTZ, M. E., YAN, Y. L., SONG, H., BOLING, T. C., KUNERTH, A. K., WALKER, M. B., KIMMEL, C. B. & POSTLETHWAIT, J. H.** 2008. MicroRNA Mirn140 modulates Pdgf signaling during palatogenesis. *Nat Genet*, 40, 290-8.
- EBERT, M. S. & SHARP, P. A.** 2012. Roles for microRNAs in conferring robustness to biological processes. *Cell*, 149, 515-24.
- EGEBLAD, M. & WERB, Z.** 2002. New functions for the matrix metalloproteinases in cancer progression. *Nat Rev Cancer*, 2, 161-74.
- EISEN, J. S. & SMITH, J. C.** 2008. Controlling morpholino experiments: don't stop making antisense. *Development*, 135, 1735-43.
- ENDO, Y., OSUMI, N. & WAKAMATSU, Y.** 2002. Bimodal functions of Notch-mediated signaling are involved in neural crest formation during avian ectoderm development. *Development*, 129, 863-73.
- FAUNES, F., ALMONACID, L. I., MELO, F. & LARRAIN, J.** 2012. Characterization of small RNAs in *X. tropicalis* gastrulae. *Genesis*, 50, 572-83.
- FAURE, S., LEE, M. A., KELLER, T., TEN DIJKE, P. & WHITMAN, M.** 2000. Endogenous patterns of TGFbeta superfamily signaling during early *Xenopus* development. *Development*, 127, 2917-31.
- FILIPOWICZ, W., BHATTACHARYYA, S. N. & SONENBERG, N.** 2008. Mechanisms of post-transcriptional regulation by microRNAs: are the answers in sight? *Nat Rev Genet*, 9, 102-14.
- FISHWICK, K. J., NEIDERER, T. E., JHINGORY, S., BRONNER, M. E. & TANEYHILL, L. A.** 2012. The tight junction protein claudin-1 influences cranial neural crest cell emigration. *Mech Dev*, 129, 275-83.
- FLYNT, A. S., LI, N., THATCHER, E. J., SOLNICA-KREZEL, L. & PATTON, J. G.** 2007. Zebrafish miR-214 modulates Hedgehog signaling to specify muscle cell fate. *Nat Genet*, 39, 259-63.
- FRIEDLANDER, M. R., CHEN, W., ADAMIDI, C., MAASKOLA, J., EINSPANIER, R., KNESPEL, S. & RAJEWSKY, N.** 2008. Discovering microRNAs from deep sequencing data using miRDeep. *Nat Biotechnol*, 26, 407-15.
- FRIEDMAN, R. C., FARH, K. K., BURGE, C. B. & BARTEL, D. P.** 2009. Most mammalian mRNAs are conserved targets of microRNAs. *Genome Res*, 19, 92-105.
- FRIEDRICH, M.** 2006. Ancient mechanisms of visual sense organ development based on comparison of the gene networks controlling larval eye, ocellus, and compound eye specification in *Drosophila*. *Arthropod Struct Dev*, 35, 357-78.
- GANGARAJU, V. K. & LIN, H.** 2009. MicroRNAs: key regulators of stem cells. *Nat Rev Mol Cell Biol*, 10, 116-25.
- GAO, Z., KIM, G. H., MACKINNON, A. C., FLAGG, A. E., BASSETT, B.,**

**EARLEY, J. U. & SVENSSON, E. C.** 2010. Ets1 is required for proper migration and differentiation of the cardiac neural crest. *Development*, 137, 1543-51.

**GARCIA-CASTRO, M. I., MARCELLE, C. & BRONNER-FRASER, M.** 2002. Ectodermal Wnt function as a neural crest inducer. *Science*, 297, 848-51.

**GARRIOCK, R. J., VOKES, S. A., SMALL, E. M., LARSON, R. & KRIEG, P. A.** 2001. Developmental expression of the Xenopus Iroquois-family homeobox genes, *Irx4* and *Irx5*. *Dev Genes Evol*, 211, 257-60.

**GAVALAS, A., TRAINOR, P., ARIZA-MCNAUGHTON, L. & KRUMLAUF, R.** 2001. Synergy between *Hoxa1* and *Hoxb1*: the relationship between arch patterning and the generation of cranial neural crest. *Development*, 128, 3017-27.

**GESSERT, S., BUGNER, V., TECZA, A., PINKER, M. & KUHL, M.** 2010. FMR1/FXR1 and the miRNA pathway are required for eye and neural crest development. *Dev Biol*, 341, 222-35.

**GIBNEY, E. R. & NOLAN, C. M.** 2010. Epigenetics and gene expression. *Heredity (Edinb)*, 105, 4-13.

**GILCHRIST, M. J., CHRISTENSEN, M. B., BRONCHAIN, O., BRUNET, F., CHESNEAU, A., FENGER, U., GEACH, T. J., IRONFIELD, H. V., KAYA, F., KRICHA, S., LEA, R., MASSE, K., NEANT, I., PAILLARD, E., PARAIN, K., PERRON, M., SINZELLE, L., SOUOPGUI, J., THURET, R., YMLAHI-OUAZZANI, Q. & POLLET, N.** 2009. Database of queryable gene expression patterns for Xenopus. *Dev Dyn*, 238, 1379-88.

**GILL, J. G., LANGER, E. M., LINDSLEY, R. C., CAI, M., MURPHY, T. L. & MURPHY, K. M.** 2012. Snail promotes the cell-autonomous generation of Flk1(+) endothelial cells through the repression of the microRNA-200 family. *Stem Cells Dev*, 21, 167-76.

**GIRALDEZ, A. J., CINALLI, R. M., GLASNER, M. E., ENRIGHT, A. J., THOMSON, J. M., BASKERVILLE, S., HAMMOND, S. M., BARTEL, D. P. & SCHIER, A. F.** 2005. MicroRNAs regulate brain morphogenesis in zebrafish. *Science*, 308, 833-8.

**GIT, A., DVINGE, H., SALMON-DIVON, M., OSBORNE, M., KUTTER, C., HADFIELD, J., BERTONE, P. & CALDAS, C.** 2010. Systematic comparison of microarray profiling, real-time PCR, and next-generation sequencing technologies for measuring differential microRNA expression. *RNA*, 16, 991-1006.

**GLAVIC, A., SILVA, F., AYBAR, M. J., BASTIDAS, F. & MAYOR, R.** 2004. Interplay between Notch signaling and the homeoprotein Xiro1 is required for neural crest induction in Xenopus embryos. *Development*, 131, 347-59.

**GOKEY, N. G., SRINIVASAN, R., LOPEZ-ANIDO, C., KRUEGER, C. & SVAREN, J.** 2012. Developmental regulation of microRNA expression in Schwann cells. *Molecular and cellular biology*, 32, 558-568.

**GOLJANEK-WHYSALL, K., MOK, G. F., FAHAD ALREFAEI, A., KENNERLEY,**

**N., WHEELER, G. N. & MUNSTERBERG, A.** 2014. myomiR-dependent switching of BAF60 variant incorporation into Brg1 chromatin remodeling complexes during embryo myogenesis. *Development*, 141, 3378-87.

**GOMEZ-SKARMETA, J., DE LA CALLE-MUSTIENES, E. & MODOLELL, J.** 2001. The Wnt-activated Xiro1 gene encodes a repressor that is essential for neural development and downregulates Bmp4. *Development*, 128, 551-60.

**GOMEZ-SKARMETA, J. L., DIEZ DEL CORRAL, R., DE LA CALLE-MUSTIENES, E., FERRE-MARCO, D. & MODOLELL, J.** 1996. Araucan and caupolican, two members of the novel iroquois complex, encode homeoproteins that control proneural and vein-forming genes. *Cell*, 85, 95-105.

**GOMEZ-SKARMETA, J. L., GLAVIC, A., DE LA CALLE-MUSTIENES, E., MODOLELL, J. & MAYOR, R.** 1998. Xiro, a Xenopus homolog of the Drosophila Iroquois complex genes, controls development at the neural plate. *EMBO J*, 17, 181-90.

**GOUTI, M., BRISCOE, J. & GAVALAS, A.** 2011. Anterior Hox genes interact with components of the neural crest specification network to induce neural crest fates. *Stem Cells*, 29, 858-70.

**GOUTI, M. & GAVALAS, A.** 2008. Hoxb1 controls cell fate specification and proliferative capacity of neural stem and progenitor cells. *Stem Cells*, 26, 1985-97.

**GRIFONE, R., DEMIGNON, J., GIORDANI, J., NIRO, C., SOUIL, E., BERTIN, F., LACLEF, C., XU, P. X. & MAIRE, P.** 2007. Eya1 and Eya2 proteins are required for hypaxial somitic myogenesis in the mouse embryo. *Dev Biol*, 302, 602-16.

**GRIMSON, A., FARH, K. K., JOHNSTON, W. K., GARRETT-ENGELE, P., LIM, L. P. & BARTEL, D. P.** 2007. MicroRNA targeting specificity in mammals: determinants beyond seed pairing. *Mol Cell*, 27, 91-105.

**GROCOTT, T., TAMBALO, M. & STREIT, A.** 2012. The peripheral sensory nervous system in the vertebrate head: a gene regulatory perspective. *Dev Biol*, 370, 3-23.

**GROVES, A. K. & LABONNE, C.** 2014. Setting appropriate boundaries: fate, patterning and competence at the neural plate border. *Dev Biol*, 389, 2-12.

**GROYSMAN, M., SHOVAL, I. & KALCHEIM, C.** 2008. A negative modulatory role for rho and rho-associated kinase signaling in delamination of neural crest cells. *Neural Dev*, 3, 27.

**GRUBER, A. R., BERNHART, S. H. & LORENZ, R.** 2015. The ViennaRNA web services. *Methods Mol Biol*, 1269, 307-26.

**HAFNER, M., RENWICK, N., BROWN, M., MIHAILOVIC, A., HOLOCH, D., LIN, C., PENA, J. T., NUSBAUM, J. D., MOROZOV, P., LUDWIG, J., OJO, T., LUO, S., SCHROTH, G. & TUSCHL, T.** 2011. RNA-ligase-dependent biases in miRNA representation in deep-sequenced small RNA cDNA libraries. *RNA*, 17, 1697-712.

**HALL, B. K.** 2000. The neural crest as a fourth germ layer and vertebrates as quadroblastic not triploblastic. *Evol Dev*, 2, 3-5.

**HAN, X., YAN, S., WEIJIE, Z., FENG, W., LIUXING, W., MENGQUAN, L. & QINGXIA, F.** 2014. Critical role of miR-10b in transforming growth factor-beta1-induced epithelial-mesenchymal transition in breast cancer. *Cancer Gene Ther*, 21, 60-7.

**HARDING, J. L., HORSWELL, S., HELIOT, C., ARMISEN, J., ZIMMERMAN, L. B., LUSCOMBE, N. M., MISKA, E. A. & HILL, C. S.** 2014. Small RNA profiling of *Xenopus* embryos reveals novel miRNAs and a new class of small RNAs derived from intronic transposable elements. *Genome Res*, 24, 96-106.

**HARFE, B. D., MCMANUS, M. T., MANSFIELD, J. H., HORNSTEIN, E. & TABIN, C. J.** 2005. The RNaseIII enzyme Dicer is required for morphogenesis but not patterning of the vertebrate limb. *Proc Natl Acad Sci U S A*, 102, 10898-903.

**HARRISON, M., ABU-ELMAGD, M., GROCCOTT, T., YATES, C., GAVRILOVIC, J. & WHEELER, G. N.** 2004. Matrix metalloproteinase genes in *Xenopus* development. *Dev Dyn*, 231, 214-20.

**HATAKEYAMA, J., BESSHO, Y., KATOH, K., OOKAWARA, S., FUJIOKA, M., GUILLEMOT, F. & KAGEYAMA, R.** 2004. Hes genes regulate size, shape and histogenesis of the nervous system by control of the timing of neural stem cell differentiation. *Development*, 131, 5539-50.

**HATCH, V. L., MARIN-BARBA, M., MOXON, S., FORD, C. T., WARD, N. J., TOMLINSON, M. L., DESANLIS, I., HENDRY, A. E., HONTELEZ, S., VAN KRUIJSBERGEN, I., VEENSTRA, G. J., MUNSTERBERG, A. E. & WHEELER, G. N.** 2016. The positive transcriptional elongation factor (P-TEFb) is required for neural crest specification. *Dev Biol*, 416, 361-72.

**HE, L. & HANNON, G. J.** 2004. MicroRNAs: small RNAs with a big role in gene regulation. *Nat Rev Genet*, 5, 522-31.

**HELWAK, A., KUDLA, G., DUDNAKOVA, T. & TOLLERVEY, D.** 2013. Mapping the Human miRNA Interactome by CLASH Reveals Frequent Noncanonical Binding. *Cell*, 153, 654-665.

**HEMMATI-BRIVANLOU, A., FRANK, D., BOLCE, M. E., BROWN, B. D., SIVE, H. L. & HARLAND, R. M.** 1990. Localization of specific mRNAs in *Xenopus* embryos by whole-mount in situ hybridization. *Development*, 110, 325-30.

**HILGER-EVERSHEIM, K., MOSER, M., SCHORLE, H. & BUETTNER, R.** 2000. Regulatory roles of AP-2 transcription factors in vertebrate development, apoptosis and cell-cycle control. *Gene*, 260, 1-12.

**HINDLEY, C. J., CONDURAT, A. L., MENON, V., THOMAS, R., AZMITIA, L. M., DAVIS, J. A. & PRUSZAK, J.** 2016. The Hippo pathway member YAP enhances human neural crest cell fate and migration. *Sci Rep*, 6, 23208.

**HOBERT, O.** 2006. Architecture of a microRNA-controlled gene regulatory network that diversifies neuronal cell fates. *Cold Spring Harb Symp Quant Biol*,

71, 181-8.

**HOFFMAN, T. L., JAVIER, A. L., CAMPEAU, S. A., KNIGHT, R. D. & SCHILLING, T. F.** 2007. Tfap2 transcription factors in zebrafish neural crest development and ectodermal evolution. *J Exp Zool B Mol Dev Evol*, 308, 679-91.

**HON, L. S. & ZHANG, Z.** 2007. The roles of binding site arrangement and combinatorial targeting in microRNA repression of gene expression. *Genome Biol*, 8, R166.

**HONG, C. S., PARK, B. Y. & SAINT-JEANNET, J. P.** 2008. Fgf8a induces neural crest indirectly through the activation of Wnt8 in the paraxial mesoderm. *Development*, 135, 3903-10.

**HONG, C. S. & SAINT-JEANNET, J. P.** 2007. The activity of Pax3 and Zic1 regulates three distinct cell fates at the neural plate border. *Mol Biol Cell*, 18, 2192-202.

**HONG, C. S. & SAINT-JEANNET, J. P.** 2014. Xhe2 is a member of the astacin family of metalloproteases that promotes *Xenopus* hatching. *Genesis*, 52, 946-51.

**HONORE, S. M., AYBAR, M. J. & MAYOR, R.** 2003. Sox10 is required for the early development of the prospective neural crest in *Xenopus* embryos. *Dev Biol*, 260, 79-96.

**HOPPLER, S. & WHEELER, G. N.** 2015. DEVELOPMENTAL BIOLOGY. It's about time for neural crest. *Science*, 348, 1316-7.

**HORNSTEIN, E., MANSFIELD, J. H., YEKTA, S., HU, J. K., HARFE, B. D., MCMANUS, M. T., BASKERVILLE, S., BARTEL, D. P. & TABIN, C. J.** 2005. The microRNA miR-196 acts upstream of Hoxb8 and Shh in limb development. *Nature*, 438, 671-4.

**HUANG, T., LIU, Y., HUANG, M., ZHAO, X. & CHENG, L.** 2010. Wnt1-cre-mediated conditional loss of Dicer results in malformation of the midbrain and cerebellum and failure of neural crest and dopaminergic differentiation in mice. *Journal of molecular cell biology*, 2, 152-163.

**HUBBARD, S. J., GRAFHAM, D. V., BEATTIE, K. J., OVERTON, I. M., MCLAREN, S. R., CRONING, M. D., BOARDMAN, P. E., BONFIELD, J. K., BURNSIDE, J., DAVIES, R. M., FARRELL, E. R., FRANCIS, M. D., GRIFFITHS-JONES, S., HUMPHRAY, S. J., HYLAND, C., SCOTT, C. E., TANG, H., TAYLOR, R. G., TICKLE, C., BROWN, W. R., BIRNEY, E., ROGERS, J. & WILSON, S. A.** 2005. Transcriptome analysis for the chicken based on 19,626 finished cDNA sequences and 485,337 expressed sequence tags. *Genome Res*, 15, 174-83.

**HUBER, W., CAREY, V. J., GENTLEMAN, R., ANDERS, S., CARLSON, M., CARVALHO, B. S., BRAVO, H. C., DAVIS, S., GATTO, L., GIRKE, T., GOTTARDO, R., HAHNE, F., HANSEN, K. D., IRIZARRY, R. A., LAWRENCE, M., LOVE, M. I., MACDONALD, J., OBENCHAIN, V., OLES, A. K., PAGES, H., REYES, A., SHANNON, P., SMYTH, G. K., TENENBAUM, D., WALDRON, L. & MORGAN, M.** 2015. Orchestrating high-throughput genomic analysis with

Bioconductor. *Nat Methods*, 12, 115-21.

**HUNT, P., FERRETTI, P., KRUMLAUF, R. & THOROGOOD, P.** 1995. Restoration of normal Hox code and branchial arch morphogenesis after extensive deletion of hindbrain neural crest. *Dev Biol*, 168, 584-97.

**HUTVAGNER, G., SIMARD, M. J., MELLO, C. C. & ZAMORE, P. D.** 2004. Sequence-specific inhibition of small RNA function. *PLoS Biol*, 2, E98.

**IMAYOSHI, I., SAKAMOTO, M., YAMAGUCHI, M., MORI, K. & KAGEYAMA, R.** 2010. Essential roles of Notch signaling in maintenance of neural stem cells in developing and adult brains. *J Neurosci*, 30, 3489-98.

**INUI, M., MARTELLO, G. & PICCOLO, S.** 2010. MicroRNA control of signal transduction. *Nat Rev Mol Cell Biol*, 11, 252-63.

**JAMES-ZORN, C., PONFERRADA, V. G., BURNS, K. A., FORTRIEDE, J. D., LOTAY, V. S., LIU, Y., BRAD KARPINKA, J., KARIMI, K., ZORN, A. M. & VIZE, P. D.** 2015. Xenbase: Core features, data acquisition, and data processing. *Genesis*, 53, 486-97.

**JAYAPRAKASH, A. D., JABADO, O., BROWN, B. D. & SACHIDANANDAM, R.** 2011. Identification and remediation of biases in the activity of RNA ligases in small-RNA deep sequencing. *Nucleic Acids Res*, 39, e141.

**JEONG, H. S., LEE, J. M., SURESH, B., CHO, K. W., JUNG, H. S. & KIM, K. S.** 2014. Temporal and Spatial Expression Patterns of miR-302 and miR-367 During Early Embryonic Chick Development. *Int J Stem Cells*, 7, 162-6.

**JEONG, J., MAO, J., TENZEN, T., KOTTMANN, A. H. & MCMAHON, A. P.** 2004. Hedgehog signaling in the neural crest cells regulates the patterning and growth of facial primordia. *Genes Dev*, 18, 937-51.

**JOHN, B., ENRIGHT, A. J., ARAVIN, A., TUSCHL, T., SANDER, C. & MARKS, D. S.** 2004. Human MicroRNA targets. *PLoS Biol*, 2, e363.

**JOUVE, C., PALMEIRIM, I., HENRIQUE, D., BECKERS, J., GOSSLER, A., ISH-HOROWICZ, D. & POURQUIE, O.** 2000. Notch signalling is required for cyclic expression of the hairy-like gene HES1 in the presomitic mesoderm. *Development*, 127, 1421-9.

**KARPINKA, J. B., FORTRIEDE, J. D., BURNS, K. A., JAMES-ZORN, C., PONFERRADA, V. G., LEE, J., KARIMI, K., ZORN, A. M. & VIZE, P. D.** 2015. Xenbase, the *Xenopus* model organism database; new virtualized system, data types and genomes. *Nucleic Acids Res*, 43, D756-63.

**KASHEF, J., KOHLER, A., KURIYAMA, S., ALFANDARI, D., MAYOR, R. & WEDLICH, D.** 2009. Cadherin-11 regulates protrusive activity in *Xenopus* cranial neural crest cells upstream of Trio and the small GTPases. *Genes Dev*, 23, 1393-8.

**KAUFMAN, C. K., MOSIMANN, C., FAN, Z. P., YANG, S., THOMAS, A. J., ABLAIN, J., TAN, J. L., FOGLEY, R. D., VAN ROOIJEN, E., HAGEDORN, E. J., CIARLO, C., WHITE, R. M., MATOS, D. A., PULLER, A. C., SANTORIELLO,**

**C., LIAO, E. C., YOUNG, R. A. & ZON, L. I.** 2016. A zebrafish melanoma model reveals emergence of neural crest identity during melanoma initiation. *Science*, 351, aad2197.

**KEE, Y. & BRONNER-FRASER, M.** 2005. To proliferate or to die: role of Id3 in cell cycle progression and survival of neural crest progenitors. *Genes Dev*, 19, 744-55.

**KEE, Y., HWANG, B. J., STERNBERG, P. W. & BRONNER-FRASER, M.** 2007. Evolutionary conservation of cell migration genes: from nematode neurons to vertebrate neural crest. *Genes Dev*, 21, 391-6.

**KELSH, R. N.** 2006. Sorting out Sox10 functions in neural crest development. *Bioessays*, 28, 788-98.

**KHADKA, D., LUO, T. & SARGENT, T. D.** 2006. Msx1 and Msx2 have shared essential functions in neural crest but may be dispensable in epidermis and axis formation in *Xenopus*. *Int J Dev Biol*, 50, 499-502.

**KHUDYAKOV, J. & BRONNER-FRASER, M.** 2009. Comprehensive spatiotemporal analysis of early chick neural crest network genes. *Dev Dyn*, 238, 716-23.

**KIM, D., PERTEA, G., TRAPNELL, C., PIMENTEL, H., KELLEY, R. & SALZBERG, S. L.** 2013. TopHat2: accurate alignment of transcriptomes in the presence of insertions, deletions and gene fusions. *Genome Biol*, 14, R36.

**KIM, Y. J., BAE, S. W., YU, S. S., BAE, Y. C. & JUNG, J. S.** 2009. miR-196a regulates proliferation and osteogenic differentiation in mesenchymal stem cells derived from human adipose tissue. *J Bone Miner Res*, 24, 816-25.

**KLOOSTERMAN, W. P. & PLASTERK, R. H.** 2006. The diverse functions of microRNAs in animal development and disease. *Dev Cell*, 11, 441-50.

**KLOOSTERMAN, W. P., WIENHOLDS, E., DE BRUIJN, E., KAUPPINEN, S. & PLASTERK, R. H.** 2006. In situ detection of miRNAs in animal embryos using LNA-modified oligonucleotide probes. *Nat Methods*, 3, 27-9.

**KNECHT, A. K. & BRONNER-FRASER, M.** 2002. Induction of the neural crest: a multigene process. *Nat Rev Genet*, 3, 453-61.

**KORPAL, M., LEE, E. S., HU, G. & KANG, Y.** 2008. The miR-200 family inhibits epithelial-mesenchymal transition and cancer cell migration by direct targeting of E-cadherin transcriptional repressors ZEB1 and ZEB2. *J Biol Chem*, 283, 14910-4.

**KOZMIK, Z., HOLLAND, N. D., KRESLOVA, J., OLIVERI, D., SCHUBERT, M., JONASOVA, K., HOLLAND, L. Z., PESTARINO, M., BENES, V. & CANDIANI, S.** 2007. Pax-Six-Eya-Dach network during amphioxus development: conservation in vitro but context specificity in vivo. *Dev Biol*, 306, 143-59.

**KOZOMARA, A. & GRIFFITHS-JONES, S.** 2014. miRBase: annotating high confidence microRNAs using deep sequencing data. *Nucleic Acids Res*, 42, D68-73.

**KREK, A., GRUN, D., POY, M. N., WOLF, R., ROSENBERG, L., EPSTEIN, E. J., MACMENAMIN, P., DA PIEDADE, I., GUNSALUS, K. C., STOFFEL, M. & RAJEWSKY, N.** 2005. Combinatorial microRNA target predictions. *Nat Genet*, 37, 495-500.

**KRUTZFELDT, J., RAJEWSKY, N., BRAICH, R., RAJEEV, K. G., TUSCHL, T., MANOHARAN, M. & STOFFEL, M.** 2005. Silencing of microRNAs in vivo with 'antagomirs'. *Nature*, 438, 685-9.

**KUO, J. S., PATEL, M., GAMSE, J., MERZDORF, C., LIU, X., APEKIN, V. & SIVE, H.** 1998. Opl: a zinc finger protein that regulates neural determination and patterning in *Xenopus*. *Development*, 125, 2867-82.

**KURODA, H., WESSELY, O. & DE ROBERTIS, E. M.** 2004. Neural induction in *Xenopus*: requirement for ectodermal and endomesodermal signals via Chordin, Noggin, beta-Catenin, and Cerberus. *PLoS Biol*, 2, E92.

**LABONNE, C. & BRONNER-FRASER, M.** 1998. Neural crest induction in *Xenopus*: evidence for a two-signal model. *Development*, 125, 2403-14.

**LABONNE, C. & BRONNER-FRASER, M.** 2000. Snail-related transcriptional repressors are required in *Xenopus* for both the induction of the neural crest and its subsequent migration. *Dev Biol*, 221, 195-205.

**LAGUTIN, O. V., ZHU, C. C., KOBAYASHI, D., TOPCZEWSKI, J., SHIMAMURA, K., PUELLES, L., RUSSELL, H. R., MCKINNON, P. J., SOLNICA-KREZEL, L. & OLIVER, G.** 2003. Six3 repression of Wnt signaling in the anterior neuroectoderm is essential for vertebrate forebrain development. *Genes Dev*, 17, 368-79.

**LAI, E. C.** 2004. Notch signaling: control of cell communication and cell fate. *Development*, 131, 965-73.

**LE DOUARIN, N. M. & SMITH, J.** 1988. Development of the peripheral nervous system from the neural crest. *Annu Rev Cell Biol*, 4, 375-404.

**LE DOUARIN, N. M. & TEILLET, M. A.** 1973. The migration of neural crest cells to the wall of the digestive tract in avian embryo. *J Embryol Exp Morphol*, 30, 31-48.

**LE DOUARIN, N. M. & TEILLET, M. A.** 1999. *The Neural Crest*. Cambridge University Press.

**LEAMAN, D., CHEN, P. Y., FAK, J., YALCIN, A., PEARCE, M., UNNERSTALL, U., MARKS, D. S., SANDER, C., TUSCHL, T. & GAUL, U.** 2005. Antisense-mediated depletion reveals essential and specific functions of microRNAs in *Drosophila* development. *Cell*, 121, 1097-108.

**LEE, Y., AHN, C., HAN, J., CHOI, H., KIM, J., YIM, J., LEE, J., PROVOST, P., RADMARK, O., KIM, S. & KIM, V. N.** 2003. The nuclear RNase III Drosha initiates microRNA processing. *Nature*, 425, 415-9.

**LEE, Y. H., AOKI, Y., HONG, C. S., SAINT-GERMAIN, N., CREDIDIO, C. & SAINT-JEANNET, J. P.** 2004. Early requirement of the transcriptional activator

Sox9 for neural crest specification in *Xenopus*. *Dev Biol*, 275, 93-103.

**LEWIS, B. P., BURGE, C. B. & BARTEL, D. P.** 2005. Conserved seed pairing, often flanked by adenosines, indicates that thousands of human genes are microRNA targets. *Cell*, 120, 15-20.

**LEWIS, J. L., BONNER, J., MODRELL, M., RAGLAND, J. W., MOON, R. T., DORSKY, R. I. & RAIBLE, D. W.** 2004. Reiterated Wnt signaling during zebrafish neural crest development. *Development*, 131, 1299-308.

**LEYNS, L., GOMEZ-SKARMETA, J. L. & DAMBLY-CHAUDIERE, C.** 1996. iroquois: a prepattern gene that controls the formation of bristles on the thorax of *Drosophila*. *Mech Dev*, 59, 63-72.

**LI, B., KURIYAMA, S., MORENO, M. & MAYOR, R.** 2009a. The posteriorizing gene *Gbx2* is a direct target of Wnt signalling and the earliest factor in neural crest induction. *Development*, 136, 3267-78.

**LI, C., WEN, A., SHEN, B., LU, J., HUANG, Y. & CHANG, Y.** 2011. FastCloning: a highly simplified, purification-free, sequence- and ligation-independent PCR cloning method. *BMC Biotechnol*, 11, 92.

**LI, H., TIERNEY, C., WEN, L., WU, J. Y. & RAO, Y.** 1997. A single morphogenetic field gives rise to two retina primordia under the influence of the prechordal plate. *Development*, 124, 603-15.

**LI, M. & BELMONTE, J. C.** 2017. Ground rules of the pluripotency gene regulatory network. *Nat Rev Genet*.

**LI, N., FELBER, K., ELKS, P., CROUCHER, P. & ROEHL, H. H.** 2009b. Tracking gene expression during zebrafish osteoblast differentiation. *Dev Dyn*, 238, 459-66.

**LI, S., LIU, Y., LIU, Z. & WANG, R.** 2016. Neural fate decisions mediated by combinatorial regulation of *Hes1* and miR-9. *J Biol Phys*, 42, 53-68.

**LI, X., OGI, K. A., ZHANG, J., KRONES, A., BUSH, K. T., GLASS, C. K., NIGAM, S. K., AGGARWAL, A. K., MAAS, R., ROSE, D. W. & ROSENFELD, M. G.** 2003. Eya protein phosphatase activity regulates Six1-Dach-Eya transcriptional effects in mammalian organogenesis. *Nature*, 426, 247-54.

**LI, Y., ZHANG, M., CHEN, H., DONG, Z., GANAPATHY, V., THANGARAJU, M. & HUANG, S.** 2010. Ratio of miR-196s to HOXC8 messenger RNA correlates with breast cancer cell migration and metastasis. *Cancer Res*, 70, 7894-904.

**LIEM, K. F., JR., TREMML, G., ROELINK, H. & JESSELL, T. M.** 1995. Dorsal differentiation of neural plate cells induced by BMP-mediated signals from epidermal ectoderm. *Cell*, 82, 969-79.

**LIGHT, W., VERNON, A. E., LASORELLA, A., IAVARONE, A. & LABONNE, C.** 2005. *Xenopus* *Id3* is required downstream of *Myc* for the formation of multipotent neural crest progenitor cells. *Development*, 132, 1831-41.

**LIM, L. P., LAU, N. C., WEINSTEIN, E. G., ABDELHAKIM, A., YEKTA, S.,**

- RHOADES, M. W., BURGE, C. B. & BARTEL, D. P.** 2003. The microRNAs of *Caenorhabditis elegans*. *Genes Dev*, 17, 991-1008.
- LIN, C. H., JACKSON, A. L., GUO, J., LINSLEY, P. S. & EISENMAN, R. N.** 2009. Myc-regulated microRNAs attenuate embryonic stem cell differentiation. *EMBO J*, 28, 3157-70.
- LIPCHINA, I., ELKABETZ, Y., HAFNER, M., SHERIDAN, R., MIHAIOVIC, A., TUSCHL, T., SANDER, C., STUDER, L. & BETEL, D.** 2011. Genome-wide identification of microRNA targets in human ES cells reveals a role for miR-302 in modulating BMP response. *Genes Dev*, 25, 2173-86.
- LISTER, J. A., COOPER, C., NGUYEN, K., MODRELL, M., GRANT, K. & RAIBLE, D. W.** 2006. Zebrafish *Foxd3* is required for development of a subset of neural crest derivatives. *Dev Biol*, 290, 92-104.
- LITSIOU, A., HANSON, S. & STREIT, A.** 2005. A balance of FGF, BMP and WNT signalling positions the future placode territory in the head. *Development*, 132, 4051-62.
- LIU, C. J., TSAI, M. M., TU, H. F., LUI, M. T., CHENG, H. W. & LIN, S. C.** 2013. miR-196a overexpression and miR-196a2 gene polymorphism are prognostic predictors of oral carcinomas. *Ann Surg Oncol*, 20 Suppl 3, S406-14.
- LIU, H., SUN, Q., WAN, C., LI, L., ZHANG, L. & CHEN, Z.** 2014. MicroRNA-338-3p regulates osteogenic differentiation of mouse bone marrow stromal stem cells by targeting *Runx2* and *Fgfr2*. *J Cell Physiol*, 229, 1494-502.
- LIU, J. P. & JESSELL, T. M.** 1998. A role for rhoB in the delamination of neural crest cells from the dorsal neural tube. *Development*, 125, 5055-67.
- LIU, K. J. & HARLAND, R. M.** 2003. Cloning and characterization of *Xenopus* *Id4* reveals differing roles for *Id* genes. *Dev Biol*, 264, 339-51.
- LIU, N., BEZPROZVANNAYA, S., WILLIAMS, A. H., QI, X., RICHARDSON, J. A., BASSEL-DUBY, R. & OLSON, E. N.** 2008. microRNA-133a regulates cardiomyocyte proliferation and suppresses smooth muscle gene expression in the heart. *Genes Dev*, 22, 3242-54.
- LIU, X. H., LU, K. H., WANG, K. M., SUN, M., ZHANG, E. B., YANG, J. S., YIN, D. D., LIU, Z. L., ZHOU, J., LIU, Z. J., DE, W. & WANG, Z. X.** 2012. MicroRNA-196a promotes non-small cell lung cancer cell proliferation and invasion through targeting *HOXA5*. *BMC Cancer*, 12, 348.
- LO, C. W., COHEN, M. F., HUANG, G. Y., LAZATIN, B. O., PATEL, N., SULLIVAN, R., PAUKEN, C. & PARK, S. M.** 1997. *Cx43* gap junction gene expression and gap junctional communication in mouse neural crest cells. *Dev Genet*, 20, 119-32.
- LOUVI, A. & ARTAVANIS-TSAKONAS, S.** 2006. Notch signalling in vertebrate neural development. *Nat Rev Neurosci*, 7, 93-102.
- LOVE, M. I., ANDERS, S., KIM, V. & HUBER, W.** 2015. RNA-Seq workflow: gene-level exploratory analysis and differential expression. *F1000Res*, 4, 1070.

- LOVE, M. I., HUBER, W. & ANDERS, S.** 2014. Moderated estimation of fold change and dispersion for RNA-seq data with DESeq2. *Genome Biol*, 15, 550.
- LU, T. P., LEE, C. Y., TSAI, M. H., CHIU, Y. C., HSIAO, C. K., LAI, L. C. & CHUANG, E. Y.** 2012. miRSystem: an integrated system for characterizing enriched functions and pathways of microRNA targets. *PLoS One*, 7, e42390.
- LU, Y., LOH, Y. H., LI, H., CESANA, M., FICARRO, S. B., PARIKH, J. R., SALOMONIS, N., TOH, C. X., ANDREADIS, S. T., LUCKEY, C. J., COLLINS, J. J., DALEY, G. Q. & MARTO, J. A.** 2014. Alternative splicing of MBD2 supports self-renewal in human pluripotent stem cells. *Cell Stem Cell*, 15, 92-101.
- LUMB, R., BUCKBERRY, S., SECKER, G., LAWRENCE, D. & SCHWARZ, Q.** 2017. Transcriptome profiling reveals expression signatures of cranial neural crest cells arising from different axial levels. *BMC Dev Biol*, 17, 5.
- LUMSDEN, A. & KRUMLAUF, R.** 1996. Patterning the vertebrate neuraxis. *Science*, 274, 1109-15.
- LUND, E., LIU, M., HARTLEY, R. S., SHEETS, M. D. & DAHLBERG, J. E.** 2009. Deadenylation of maternal mRNAs mediated by miR-427 in *Xenopus laevis* embryos. *RNA*, 15, 2351-63.
- LUO, T., LEE, Y. H., SAINT-JEANNET, J. P. & SARGENT, T. D.** 2003. Induction of neural crest in *Xenopus* by transcription factor AP2alpha. *Proc Natl Acad Sci U S A*, 100, 532-7.
- MACKAY, D. J., NOBES, C. D. & HALL, A.** 1995. The Rho's progress: a potential role during neuritogenesis for the Rho family of GTPases. *Trends Neurosci*, 18, 496-501.
- MANCILLA, A. & MAYOR, R.** 1996. Neural crest formation in *Xenopus laevis*: mechanisms of Xslug induction. *Dev Biol*, 177, 580-9.
- MARCHAL, L., LUXARDI, G., THOME, V. & KODJABACHIAN, L.** 2009. BMP inhibition initiates neural induction via FGF signaling and Zic genes. *Proc Natl Acad Sci U S A*, 106, 17437-42.
- MARCHANT, L., LINKER, C., RUIZ, P., GUERRERO, N. & MAYOR, R.** 1998. The inductive properties of mesoderm suggest that the neural crest cells are specified by a BMP gradient. *Dev Biol*, 198, 319-29.
- MARTELLO, G., ZACCHIGNA, L., INUI, M., MONTAGNER, M., ADORNO, M., MAMIDI, A., MORSUT, L., SOLIGO, S., TRAN, U., DUPONT, S., CORDENONSI, M., WESSELY, O. & PICCOLO, S.** 2007. MicroRNA control of Nodal signalling. *Nature*, 449, 183-8.
- MATHAVAN, S., LEE, S. G., MAK, A., MILLER, L. D., MURTHY, K. R., GOVINDARAJAN, K. R., TONG, Y., WU, Y. L., LAM, S. H., YANG, H., RUAN, Y., KORZH, V., GONG, Z., LIU, E. T. & LUFKIN, T.** 2005. Transcriptome analysis of zebrafish embryogenesis using microarrays. *PLoS Genet*, 1, 260-76.
- MATHEW, L. K., LEE, S. S., SKULI, N., RAO, S., KEITH, B., NATHANSON, K. L., LAL, P. & SIMON, M. C.** 2014. Restricted expression of miR-30c-2-3p and

miR-30a-3p in clear cell renal cell carcinomas enhances HIF2alpha activity. *Cancer Discov*, 4, 53-60.

**MATSUKAWA, S., MIWATA, K., ASASHIMA, M. & MICHIEU, T.** 2015. The requirement of histone modification by PRDM12 and Kdm4a for the development of pre-placodal ectoderm and neural crest in *Xenopus*. *Dev Biol*, 399, 164-76.

**MAYOR, R. & THEVENEAU, E.** 2013. The neural crest. *Development*, 140, 2247-51.

**MCCUSKER, C. D. & ALFANDARI, D.** 2009. Life after proteolysis: Exploring the signaling capabilities of classical cadherin cleavage fragments. *Commun Integr Biol*, 2, 155-7.

**MCGLINN, E., YEKTA, S., MANSFIELD, J. H., SOUTSCHEK, J., BARTEL, D. P. & TABIN, C. J.** 2009. In ovo application of antagomiRs indicates a role for miR-196 in patterning the chick axial skeleton through Hox gene regulation. *Proc Natl Acad Sci U S A*, 106, 18610-5.

**MCKENNA, D. J., MCDADE, S. S., PATEL, D. & MCCANCE, D. J.** 2010. MicroRNA 203 expression in keratinocytes is dependent on regulation of p53 levels by E6. *J Virol*, 84, 10644-52.

**MEISTER, G., LANDTHALER, M., DORSETT, Y. & TUSCHL, T.** 2004. Sequence-specific inhibition of microRNA- and siRNA-induced RNA silencing. *RNA*, 10, 544-50.

**MELO, S. A. & ESTELLER, M.** 2011. Dysregulation of microRNAs in cancer: playing with fire. *FEBS Lett*, 585, 2087-99.

**METZKER, M. L.** 2010. Sequencing technologies - the next generation. *Nat Rev Genet*, 11, 31-46.

**MEULEMANS, D. & BRONNER-FRASER, M.** 2004. Gene-regulatory interactions in neural crest evolution and development. *Dev Cell*, 7, 291-9.

**MEYER, L. R., ZWEIG, A. S., HINRICHS, A. S., KAROLCHIK, D., KUHN, R. M., WONG, M., SLOAN, C. A., ROSENBLUM, K. R., ROE, G., RHEAD, B., RANEY, B. J., POHL, A., MALLADI, V. S., LI, C. H., LEE, B. T., LEARNED, K., KIRKUP, V., HSU, F., HEITNER, S., HARTE, R. A., HAEUSSLER, M., GURUVADOO, L., GOLDMAN, M., GIARDINE, B. M., FUJITA, P. A., DRESZER, T. R., DIEKHANS, M., CLINE, M. S., CLAWSON, H., BARBER, G. P., HAUSSLER, D. & KENT, W. J.** 2013. The UCSC Genome Browser database: extensions and updates 2013. *Nucleic Acids Res*, 41, D64-9.

**MILLS, A. A., ZHENG, B., WANG, X. J., VOGEL, H., ROOP, D. R. & BRADLEY, A.** 1999. p63 is a p53 homologue required for limb and epidermal morphogenesis. *Nature*, 398, 708-13.

**MISHIMA, Y., GIRALDEZ, A. J., TAKEDA, Y., FUJIWARA, T., SAKAMOTO, H., SCHIER, A. F. & INOUE, K.** 2006. Differential regulation of germline mRNAs in soma and germ cells by zebrafish miR-430. *Curr Biol*, 16, 2135-42.

**MONSORO-BURQ, A. H., FLETCHER, R. B. & HARLAND, R. M.** 2003. Neural

crest induction by paraxial mesoderm in *Xenopus* embryos requires FGF signals. *Development*, 130, 3111-24.

**MONSORO-BURQ, A. H., WANG, E. & HARLAND, R.** 2005. Msx1 and Pax3 cooperate to mediate FGF8 and WNT signals during *Xenopus* neural crest induction. *Dev Cell*, 8, 167-78.

**MOODY, S. A. & LAMANTIA, A. S.** 2015. Transcriptional regulation of cranial sensory placode development. *Curr Top Dev Biol*, 111, 301-50.

**MORRISON, G. M. & BRICKMAN, J. M.** 2006. Conserved roles for Oct4 homologues in maintaining multipotency during early vertebrate development. *Development*, 133, 2011-22.

**MUMM, J. S. & KOPAN, R.** 2000. Notch signaling: from the outside in. *Dev Biol*, 228, 151-65.

**NEWPORT, J. & KIRSCHNER, M.** 1982. A major developmental transition in early *Xenopus* embryos: II. Control of the onset of transcription. *Cell*, 30, 687-96.

**NGUYEN, V. H., SCHMID, B., TROUT, J., CONNORS, S. A., EKKER, M. & MULLINS, M. C.** 1998. Ventral and lateral regions of the zebrafish gastrula, including the neural crest progenitors, are established by a bmp2b/swirl pathway of genes. *Dev Biol*, 199, 93-110.

**NICHANE, M., DE CROZE, N., REN, X., SOUOPGUI, J., MONSORO-BURQ, A. H. & BELLEFROID, E. J.** 2008a. Hairy2-I $\delta$ 3 interactions play an essential role in *Xenopus* neural crest progenitor specification. *Dev Biol*, 322, 355-67.

**NICHANE, M., REN, X. & BELLEFROID, E. J.** 2010. Self-regulation of Stat3 activity coordinates cell-cycle progression and neural crest specification. *EMBO J*, 29, 55-67.

**NICHANE, M., REN, X., SOUOPGUI, J. & BELLEFROID, E. J.** 2008b. Hairy2 functions through both DNA-binding and non DNA-binding mechanisms at the neural plate border in *Xenopus*. *Dev Biol*, 322, 368-80.

**NIE, X., WANG, Q. & JIAO, K.** 2011. *Dicer* activity in neural crest cells is essential for craniofacial organogenesis and pharyngeal arch artery morphogenesis. *Mechanisms of development*, 128, 200-207.

**NIELSEN, C. B., SHOMRON, N., SANDBERG, R., HORNSTEIN, E., KITZMAN, J. & BURGE, C. B.** 2007. Determinants of targeting by endogenous and exogenous microRNAs and siRNAs. *RNA*, 13, 1894-910.

**NIKITINA, N., SAUKA-SPENGLER, T. & BRONNER-FRASER, M.** 2008. Dissecting early regulatory relationships in the lamprey neural crest gene network. *Proc Natl Acad Sci U S A*, 105, 20083-8.

**NISSAN, X., DENIS, J. A., SAIDANI, M., LEMAITRE, G., PESCHANSKI, M. & BALDESCHI, C.** 2011. miR-203 modulates epithelial differentiation of human embryonic stem cells towards epidermal stratification. *Dev Biol*, 356, 506-15.

**O'CONNOR, J. W. & GOMEZ, E. W.** 2014. Biomechanics of TGF $\beta$ -induced

epithelial-mesenchymal transition: implications for fibrosis and cancer. *Clin Transl Med*, 3, 23.

**OELGESCHLAGER, M., KURODA, H., REVERSADE, B. & DE ROBERTIS, E. M.** 2003. Chordin is required for the Spemann organizer transplantation phenomenon in *Xenopus* embryos. *Dev Cell*, 4, 219-30.

**OHTO, H., KAMADA, S., TAGO, K., TOMINAGA, S. I., OZAKI, H., SATO, S. & KAWAKAMI, K.** 1999. Cooperation of six and *eya* in activation of their target genes through nuclear translocation of *Eya*. *Mol Cell Biol*, 19, 6815-24.

**ONICHTCHOUK, D., GLINKA, A. & NIEHRS, C.** 1998. Requirement for *Xvent-1* and *Xvent-2* gene function in dorsoventral patterning of *Xenopus* mesoderm. *Development*, 125, 1447-56.

**PAICU, C., MOHORIANU, I., STOCKS, M., XU, P., COINCE, A., BILLMEIER, M., DALMAY, T., MOULTON, V. & MOXON, S.** 2017. miRCat2: Accurate prediction of plant and animal microRNAs from next-generation sequencing datasets. *Bioinformatics*.

**PARASKEVOPOULOU, M. D., GEORGAKILAS, G., KOSTOULAS, N., VLACHOS, I. S., VERGOULIS, T., RECZKO, M., FILIPPIDIS, C., DALAMAGAS, T. & HATZIGEORGIOU, A. G.** 2013. DIANA-microT web server v5.0: service integration into miRNA functional analysis workflows. *Nucleic Acids Res*, 41, W169-73.

**PARCHEM, R. J., MOORE, N., FISH, J. L., PARCHEM, J. G., BRAGA, T. T., SHENOY, A., OLDHAM, M. C., RUBENSTEIN, J. L., SCHNEIDER, R. A. & BLELLOCH, R.** 2015. miR-302 Is Required for Timing of Neural Differentiation, Neural Tube Closure, and Embryonic Viability. *Cell Rep*, 12, 760-73.

**PASQUINELLI, A. E., REINHART, B. J., SLACK, F., MARTINDALE, M. Q., KURODA, M. I., MALLER, B., HAYWARD, D. C., BALL, E. E., DEGNAN, B., MULLER, P., SPRING, J., SRINIVASAN, A., FISHMAN, M., FINNERTY, J., CORBO, J., LEVINE, M., LEAHY, P., DAVIDSON, E. & RUVKUN, G.** 2000. Conservation of the sequence and temporal expression of *let-7* heterochronic regulatory RNA. *Nature*, 408, 86-9.

**PATRICK, A. N., CABRERA, J. H., SMITH, A. L., CHEN, X. S., FORD, H. L. & ZHAO, R.** 2013. Structure-function analyses of the human SIX1-EYA2 complex reveal insights into metastasis and BOR syndrome. *Nat Struct Mol Biol*, 20, 447-53.

**PEREZ-ALCALA, S., NIETO, M. A. & BARBAS, J. A.** 2004. *LSox5* regulates *RhoB* expression in the neural tube and promotes generation of the neural crest. *Development*, 131, 4455-65.

**PFUFF, N., FIEDLER, J., HOLZMANN, A., SCHAMBACH, A., MORITZ, T., CANTZ, T. & THUM, T.** 2011. miRNA screening reveals a new miRNA family stimulating iPS cell generation via regulation of *Meox2*. *EMBO Rep*, 12, 1153-9.

**PIERACCIOLI, M., IMBASTARI, F., ANTONOV, A., MELINO, G. & RASCHELLA, G.** 2013. Activation of miR200 by c-Myb depends on ZEB1 expression and miR200 promoter methylation. *Cell Cycle*, 12, 2309-20.

**PIETRAS, A., HANSFORD, L. M., JOHNSON, A. S., BRIDGES, E., SJOLUND, J., GISSELSSON, D., REHN, M., BECKMAN, S., NOGUERA, R., NAVARRO, S., CAMMENGA, J., FREDLUND, E., KAPLAN, D. R. & PAHLMAN, S.** 2009. HIF-2 $\alpha$  maintains an undifferentiated state in neural crest-like human neuroblastoma tumor-initiating cells. *Proc Natl Acad Sci U S A*, 106, 16805-10.

**PIGNONI, F., HU, B., ZAVITZ, K. H., XIAO, J., GARRITY, P. A. & ZIPURSKY, S. L.** 1997. The eye-specification proteins So and Eya form a complex and regulate multiple steps in Drosophila eye development. *Cell*, 91, 881-91.

**PINGAULT, V., BODEREAU, V., BARAL, V., MARCOS, S., WATANABE, Y., CHAOUI, A., FOUVEAUT, C., LEROY, C., VERIER-MINE, O., FRANCANNET, C., DUPIN-DEGUINE, D., ARCHAMBEAUD, F., KURTZ, F. J., YOUNG, J., BERTHERAT, J., MARLIN, S., GOOSSENS, M., HARDELIN, J. P., DODE, C. & BONDURAND, N.** 2013. Loss-of-function mutations in SOX10 cause Kallmann syndrome with deafness. *Am J Hum Genet*, 92, 707-24.

**PLOUHINEC, J. L., ROCHE, D. D., PEGORARO, C., FIGUEIREDO, A. L., MACZKOWIAK, F., BRUNET, L. J., MILET, C., VERT, J. P., POLLET, N., HARLAND, R. M. & MONSORO-BURQ, A. H.** 2014. Pax3 and Zic1 trigger the early neural crest gene regulatory network by the direct activation of multiple key neural crest specifiers. *Dev Biol*, 386, 461-72.

**PRUFER, K., STENZEL, U., DANNEMANN, M., GREEN, R. E., LACHMANN, M. & KELSO, J.** 2008. PatMaN: rapid alignment of short sequences to large databases. *Bioinformatics*, 24, 1530-1.

**RADA-IGLESIAS, A., BAJPAI, R., PRESCOTT, S., BRUGMANN, S. A., SWIGUT, T. & WYSOCKA, J.** 2012. Epigenomic annotation of enhancers predicts transcriptional regulators of human neural crest. *Cell Stem Cell*, 11, 633-48.

**RANGARAJAN, J., LUO, T. & SARGENT, T. D.** 2006. PCNS: a novel protocadherin required for cranial neural crest migration and somite morphogenesis in Xenopus. *Dev Biol*, 295, 206-18.

**REINHART, B. J., SLACK, F. J., BASSON, M., PASQUINELLI, A. E., BETTINGER, J. C., ROUGVIE, A. E., HORVITZ, H. R. & RUVKUN, G.** 2000. The 21-nucleotide let-7 RNA regulates developmental timing in *Caenorhabditis elegans*. *Nature*, 403, 901-6.

**RINNE, T., BRUNNER, H. G. & VAN BOKHOVEN, H.** 2007. p63-associated disorders. *Cell Cycle*, 6, 262-8.

**ROBBINS, J. R., MCGUIRE, P. G., WEHRLE-HALLER, B. & ROGERS, S. L.** 1999. Diminished matrix metalloproteinase 2 (MMP-2) in ectomesenchyme-derived tissues of the Patch mutant mouse: regulation of MMP-2 by PDGF and effects on mesenchymal cell migration. *Dev Biol*, 212, 255-63.

**RODRIGUEZ, A., GRIFFITHS-JONES, S., ASHURST, J. L. & BRADLEY, A.** 2004. Identification of mammalian microRNA host genes and transcription units. *Genome Res*, 14, 1902-10.

**ROESSLER, E., BELLONI, E., GAUDENZ, K., JAY, P., BERTA, P., SCHERER, S. W., TSUI, L. C. & MUENKE, M.** 1996. Mutations in the human Sonic Hedgehog gene cause holoprosencephaly. *Nat Genet*, 14, 357-60.

**ROGERS, C. D., JAYASENA, C. S., NIE, S. & BRONNER, M. E.** 2012. Neural crest specification: tissues, signals, and transcription factors. *Wiley Interdiscip Rev Dev Biol*, 1, 52-68.

**ROSA, A., SPAGNOLI, F. M. & BRIVANLOU, A. H.** 2009. The miR-430/427/302 family controls mesendodermal fate specification via species-specific target selection. *Dev Cell*, 16, 517-27.

**ROSENKRANZ, D. & ZISCHLER, H.** 2012. proTRAC--a software for probabilistic piRNA cluster detection, visualization and analysis. *BMC Bioinformatics*, 13, 5.

**RUZINOVA, M. B. & BENEZRA, R.** 2003. Id proteins in development, cell cycle and cancer. *Trends Cell Biol*, 13, 410-8.

**RYBAK, A., FUCHS, H., SMIRNOVA, L., BRANDT, C., POHL, E. E., NITSCH, R. & WULCZYN, F. G.** 2008. A feedback loop comprising lin-28 and let-7 controls pre-let-7 maturation during neural stem-cell commitment. *Nat Cell Biol*, 10, 987-93.

**SAINT-JEANNET, J. P., HE, X., VARMUS, H. E. & DAWID, I. B.** 1997. Regulation of dorsal fate in the neuraxis by Wnt-1 and Wnt-3a. *Proc Natl Acad Sci U S A*, 94, 13713-8.

**SAINT-JEANNET, J. P. & MOODY, S. A.** 2014. Establishing the pre-placodal region and breaking it into placodes with distinct identities. *Dev Biol*, 389, 13-27.

**SAKAI, D., TANAKA, Y., ENDO, Y., OSUMI, N., OKAMOTO, H. & WAKAMATSU, Y.** 2005. Regulation of Slug transcription in embryonic ectoderm by beta-catenin-Lef/Tcf and BMP-Smad signaling. *Dev Growth Differ*, 47, 471-82.

**SATO, S., IKEDA, K., SHIOI, G., OCHI, H., OGINO, H., YAJIMA, H. & KAWAKAMI, K.** 2010. Conserved expression of mouse Six1 in the pre-placodal region (PPR) and identification of an enhancer for the rostral PPR. *Dev Biol*, 344, 158-71.

**SATO, T., SASAI, N. & SASAI, Y.** 2005. Neural crest determination by co-activation of Pax3 and Zic1 genes in *Xenopus* ectoderm. *Development*, 132, 2355-63.

**SAUKA-SPENGLER, T. & BRONNER-FRASER, M.** 2008a. A gene regulatory network orchestrates neural crest formation. *Nat Rev Mol Cell Biol*, 9, 557-68.

**SAUKA-SPENGLER, T. & BRONNER-FRASER, M.** 2008b. Insights from a sea lamprey into the evolution of neural crest gene regulatory network. *Biol Bull*, 214, 303-14.

**SAUKA-SPENGLER, T., MEULEMANS, D., JONES, M. & BRONNER-FRASER, M.** 2007. Ancient evolutionary origin of the neural crest gene regulatory network. *Dev Cell*, 13, 405-20.

**SCERBO, P., GIRARDOT, F., VIVIEN, C., MARKOV, G. V., LUXARDI, G., DEMENEIX, B., KODJABACHIAN, L. & COEN, L.** 2012. Ventx factors function as Nanog-like guardians of developmental potential in *Xenopus*. *PLoS One*, 7, e36855.

**SCHERSON, T., SERBEDZIJA, G., FRASER, S. & BRONNER-FRASER, M.** 1993. Regulative capacity of the cranial neural tube to form neural crest. *Development*, 118, 1049-62.

**SCHIFFMACHER, A. T., PADMANABHAN, R., JHINGORY, S. & TANEYHILL, L. A.** 2014. Cadherin-6B is proteolytically processed during epithelial-to-mesenchymal transitions of the cranial neural crest. *Mol Biol Cell*, 25, 41-54.

**SCHLOSSER, G.** 2007. How old genes make a new head: redeployment of Six and Eya genes during the evolution of vertebrate cranial placodes. *Integr Comp Biol*, 47, 343-59.

**SCHLOSSER, G. & AHRENS, K.** 2004. Molecular anatomy of placode development in *Xenopus laevis*. *Dev Biol*, 271, 439-66.

**SCHLOSSER, G., AWTRY, T., BRUGMANN, S. A., JENSEN, E. D., NEILSON, K., RUAN, G., STAMMLER, A., VOELKER, D., YAN, B., ZHANG, C., KLYMKOWSKY, M. W. & MOODY, S. A.** 2008. Eya1 and Six1 promote neurogenesis in the cranial placodes in a SoxB1-dependent fashion. *Dev Biol*, 320, 199-214.

**SCHMID, B., FURTHAUER, M., CONNORS, S. A., TROUT, J., THISSE, B., THISSE, C. & MULLINS, M. C.** 2000. Equivalent genetic roles for *bmp7/snailhouse* and *bmp2b/swirl* in dorsoventral pattern formation. *Development*, 127, 957-67.

**SCHMIDT, C., MCGONNELL, I. M., ALLEN, S., OTTO, A. & PATEL, K.** 2007. Wnt6 controls amniote neural crest induction through the non-canonical signaling pathway. *Dev Dyn*, 236, 2502-11.

**SCHORLE, H., MEIER, P., BUCHERT, M., JAENISCH, R. & MITCHELL, P. J.** 1996. Transcription factor AP-2 essential for cranial closure and craniofacial development. *Nature*, 381, 235-8.

**SELLECK, M. A. & BRONNER-FRASER, M.** 1995. Origins of the avian neural crest: the role of neural plate-epidermal interactions. *Development*, 121, 525-38.

**SHAHAR, E. & SHINAWI, M.** 2003. Neurocristopathies presenting with neurologic abnormalities associated with Hirschsprung's disease. *Pediatr Neurol*, 28, 385-91.

**SHAKHOVA, O.** 2014. Neural crest stem cells in melanoma development. *Curr Opin Oncol*, 26, 215-21.

**SHEN, S., GUO, X., YAN, H., LU, Y., JI, X., LI, L., LIANG, T., ZHOU, D., FENG, X. H., ZHAO, J. C., YU, J., GONG, X. G., ZHANG, L. & ZHAO, B.** 2015. A miR-130a-YAP positive feedback loop promotes organ size and tumorigenesis. *Cell Res*, 25, 997-1012.

**SHIN, K., FOGG, V. C. & MARGOLIS, B.** 2006. Tight junctions and cell polarity. *Annu Rev Cell Dev Biol*, 22, 207-35.

**SIMOES-COSTA, M. & BRONNER, M. E.** 2015. Establishing neural crest identity: a gene regulatory recipe. *Development*, 142, 242-57.

**SLACK, F. J., BASSON, M., LIU, Z., AMBROS, V., HORVITZ, H. R. & RUVKUN, G.** 2000. The lin-41 RBCC gene acts in the *C. elegans* heterochronic pathway between the let-7 regulatory RNA and the LIN-29 transcription factor. *Mol Cell*, 5, 659-69.

**SMITH, C. L. & TALLQUIST, M. D.** 2010. PDGF function in diverse neural crest cell populations. *Cell Adh Migr*, 4, 561-6.

**SONG, R., WALENTEK, P., SPONER, N., KLIMKE, A., LEE, J. S., DIXON, G., HARLAND, R., WAN, Y., LISHKO, P., LIZE, M., KESSEL, M. & HE, L.** 2014. miR-34/449 miRNAs are required for motile ciliogenesis by repressing cp110. *Nature*, 510, 115-20.

**SOREFAN, K., PAIS, H., HALL, A. E., KOZOMARA, A., GRIFFITHS-JONES, S., MOULTON, V. & DALMAY, T.** 2012. Reducing ligation bias of small RNAs in libraries for next generation sequencing. *Silence*, 3, 4.

**SORIANO, P.** 1997. The PDGF alpha receptor is required for neural crest cell development and for normal patterning of the somites. *Development*, 124, 2691-700.

**SPOKONY, R. F., AOKI, Y., SAINT-GERMAIN, N., MAGNER-FINK, E. & SAINT-JEANNET, J. P.** 2002. The transcription factor Sox9 is required for cranial neural crest development in *Xenopus*. *Development*, 129, 421-32.

**STENVANG, J., PETRI, A., LINDOW, M., OBAD, S. & KAUPPINEN, S.** 2012. Inhibition of microRNA function by antimiR oligonucleotides. *Silence*, 3, 1.

**STEVENTON, B., ARAYA, C., LINKER, C., KURIYAMA, S. & MAYOR, R.** 2009. Differential requirements of BMP and Wnt signalling during gastrulation and neurulation define two steps in neural crest induction. *Development*, 136, 771-9.

**STOCKS, M. B., MOXON, S., MAPLESON, D., WOOLFENDEN, H. C., MOHORIANU, I., FOLKES, L., SCHWACH, F., DALMAY, T. & MOULTON, V.** 2012. The UEA sRNA workbench: a suite of tools for analysing and visualizing next generation sequencing microRNA and small RNA datasets. *Bioinformatics*, 28, 2059-61.

**STUHLMILLER, T. J. & GARCIA-CASTRO, M. I.** 2012. Current perspectives of the signaling pathways directing neural crest induction. *Cell Mol Life Sci*, 69, 3715-37.

**SUBRAMANYAM, D., LAMOUILLE, S., JUDSON, R. L., LIU, J. Y., BUCAY, N., DERYNCK, R. & BLELLOCH, R.** 2011. Multiple targets of miR-302 and miR-372 promote reprogramming of human fibroblasts to induced pluripotent stem cells. *Nat Biotechnol*, 29, 443-8.

**SUH, M. R., LEE, Y., KIM, J. Y., KIM, S. K., MOON, S. H., LEE, J. Y., CHA, K.**

- Y., CHUNG, H. M., YOON, H. S., MOON, S. Y., KIM, V. N. & KIM, K. S.** 2004. Human embryonic stem cells express a unique set of microRNAs. *Dev Biol*, 270, 488-98.
- SULLIVAN, S. A., AKERS, L. & MOODY, S. A.** 2001. foxD5a, a Xenopus winged helix gene, maintains an immature neural ectoderm via transcriptional repression that is dependent on the C-terminal domain. *Dev Biol*, 232, 439-57.
- SUMMERTON, J.** 1999. Morpholino antisense oligomers: the case for an RNase H-independent structural type. *Biochim Biophys Acta*, 1489, 141-58.
- SUMMERTON, J. & WELLER, D.** 1997. Morpholino antisense oligomers: design, preparation, and properties. *Antisense Nucleic Acid Drug Dev*, 7, 187-95.
- SWEETMAN, D., RATHJEN, T., JEFFERSON, M., WHEELER, G., SMITH, T. G., WHEELER, G. N., MUNSTERBERG, A. & DALMAY, T.** 2006. FGF-4 signaling is involved in mir-206 expression in developing somites of chicken embryos. *Dev Dyn*, 235, 2185-91.
- TADJUIDJE, E. & HEGDE, R. S.** 2013. The Eyes Absent proteins in development and disease. *Cell Mol Life Sci*, 70, 1897-913.
- TAKEBAYASHI-SUZUKI, K., ARITA, N., MURASAKI, E. & SUZUKI, A.** 2007. The Xenopus POU class V transcription factor XOct-25 inhibits ectodermal competence to respond to bone morphogenetic protein-mediated embryonic induction. *Mech Dev*, 124, 840-55.
- TAKEBAYASHI-SUZUKI, K., KITAYAMA, A., TERASAKA-IIOKA, C., UENO, N. & SUZUKI, A.** 2011. The forkhead transcription factor FoxB1 regulates the dorsal-ventral and anterior-posterior patterning of the ectoderm during early Xenopus embryogenesis. *Dev Biol*, 360, 11-29.
- TALLQUIST, M. D. & SORIANO, P.** 2003. Cell autonomous requirement for PDGFRalpha in populations of cranial and cardiac neural crest cells. *Development*, 130, 507-18.
- TAMAI, K., SEMENOV, M., KATO, Y., SPOKONY, R., LIU, C., KATSUYAMA, Y., HESS, F., SAINT-JEANNET, J. P. & HE, X.** 2000. LDL-receptor-related proteins in Wnt signal transduction. *Nature*, 407, 530-5.
- TAN, Y., FU, R., LIU, J., WU, Y., WANG, B., JIANG, N., NIE, P., CAO, H., YANG, Z. & FANG, B.** 2016. ADAM10 is essential for cranial neural crest-derived maxillofacial bone development. *Biochem Biophys Res Commun*, 475, 308-14.
- TANEYHILL, L. A., COLES, E. G. & BRONNER-FRASER, M.** 2007. Snail2 directly represses cadherin6B during epithelial-to-mesenchymal transitions of the neural crest. *Development*, 134, 1481-90.
- TANG, F., KANEDA, M., O'CARROLL, D., HAJKOVA, P., BARTON, S. C., SUN, Y. A., LEE, C., TARAKHOVSKY, A., LAO, K. & SURANI, M. A.** 2007. Maternal microRNAs are essential for mouse zygotic development. *Genes Dev*, 21, 644-8.
- TAY, Y., ZHANG, J., THOMSON, A. M., LIM, B. & RIGOUTSOS, I.** 2008.

MicroRNAs to Nanog, Oct4 and Sox2 coding regions modulate embryonic stem cell differentiation. *Nature*, 455, 1124-8.

**THEVENEAU, E. & MAYOR, R.** 2012. Neural crest delamination and migration: from epithelium-to-mesenchyme transition to collective cell migration. *Dev Biol*, 366, 34-54.

**THOMAS, A. J. & ERICKSON, C. A.** 2009. FOXD3 regulates the lineage switch between neural crest-derived glial cells and pigment cells by repressing MITF through a non-canonical mechanism. *Development*, 136, 1849-58.

**TOLSTRUP, N., NIELSEN, P. S., KOLBERG, J. G., FRANKEL, A. M., VISSING, H. & KAUPPINEN, S.** 2003. OligoDesign: Optimal design of LNA (locked nucleic acid) oligonucleotide capture probes for gene expression profiling. *Nucleic Acids Res*, 31, 3758-62.

**TOMLINSON, M. L., GUAN, P., MORRIS, R. J., FIDOCK, M. D., REJZEK, M., GARCIA-MORALES, C., FIELD, R. A. & WHEELER, G. N.** 2009. A chemical genomic approach identifies matrix metalloproteinases as playing an essential and specific role in *Xenopus* melanophore migration. *Chem Biol*, 16, 93-104.

**TRAINOR, P. A. & KRUMLAUF, R.** 2001. Hox genes, neural crest cells and branchial arch patterning. *Curr Opin Cell Biol*, 13, 698-705.

**TRIBULO, C., AYBAR, M. J., NGUYEN, V. H., MULLINS, M. C. & MAYOR, R.** 2003. Regulation of Msx genes by a Bmp gradient is essential for neural crest specification. *Development*, 130, 6441-52.

**TROPEPE, V., LI, S., DICKINSON, A., GAMSE, J. T. & SIVE, H. L.** 2006. Identification of a BMP inhibitor-responsive promoter module required for expression of the early neural gene *zic1*. *Dev Biol*, 289, 517-29.

**VALLIN, J., THURET, R., GIACOMELLO, E., FARALDO, M. M., THIERY, J. P. & BRODERS, F.** 2001. Cloning and characterization of three *Xenopus* slug promoters reveal direct regulation by Lef/beta-catenin signaling. *J Biol Chem*, 276, 30350-8.

**VAN DE PUTTE, T., FRANCIS, A., NELLES, L., VAN GRUNSVEN, L. A. & HUYLEBROECK, D.** 2007. Neural crest-specific removal of *Zfhx1b* in mouse leads to a wide range of neurocristopathies reminiscent of Mowat-Wilson syndrome. *Hum Mol Genet*, 16, 1423-36.

**VESTER, B. & WENGEL, J.** 2004. LNA (locked nucleic acid): high-affinity targeting of complementary RNA and DNA. *Biochemistry*, 43, 13233-41.

**VILLAREJO, A., CORTES-CABRERA, A., MOLINA-ORTIZ, P., PORTILLO, F. & CANO, A.** 2014. Differential role of Snail1 and Snail2 zinc fingers in E-cadherin repression and epithelial to mesenchymal transition. *J Biol Chem*, 289, 930-41.

**VISWANATHAN, S. R., DALEY, G. Q. & GREGORY, R. I.** 2008. Selective blockade of microRNA processing by Lin28. *Science*, 320, 97-100.

**VOLKMANN, I., KUMARSWAMY, R., PFAFF, N., FIEDLER, J., DANGWAL, S., HOLZMANN, A., BATKAI, S., GEFFERS, R., LOTHER, A., HEIN, L. & THUM,**

T. 2013. MicroRNA-mediated epigenetic silencing of sirtuin1 contributes to impaired angiogenic responses. *Circ Res*, 113, 997-1003.

WADDINGTON, C. H. 1959. Canalization of development and genetic assimilation of acquired characters. *Nature*, 183, 1654-5.

WANG, W. D., MELVILLE, D. B., MONTERO-BALAGUER, M., HATZOPOULOS, A. K. & KNAPIK, E. W. 2011. Tfp2a and Foxd3 regulate early steps in the development of the neural crest progenitor population. *Dev Biol*, 360, 173-85.

WATANABE, T., TAKEDA, A., MISE, K., OKUNO, T., SUZUKI, T., MINAMI, N. & IMAI, H. 2005. Stage-specific expression of microRNAs during *Xenopus* development. *FEBS Lett*, 579, 318-24.

WEICK, E. M. & MISKA, E. A. 2014. piRNAs: from biogenesis to function. *Development*, 141, 3458-71.

WEINMASTER, G. 2000. Notch signal transduction: a real rip and more. *Curr Opin Genet Dev*, 10, 363-9.

WHITE, R. M., CECH, J., RATANASIRINTRAWOOT, S., LIN, C. Y., RAHL, P. B., BURKE, C. J., LANGDON, E., TOMLINSON, M. L., MOSHER, J., KAUFMAN, C., CHEN, F., LONG, H. K., KRAMER, M., DATTA, S., NEUBERG, D., GRANTER, S., YOUNG, R. A., MORRISON, S., WHEELER, G. N. & ZON, L. I. 2011. DHODH modulates transcriptional elongation in the neural crest and melanoma. *Nature*, 471, 518-22.

WIENHOLDS, E., KLOOSTERMAN, W. P., MISKA, E., ALVAREZ-SAAVEDRA, E., BEREZIKOV, E., DE BRUIJN, E., HORVITZ, H. R., KAUPPINEN, S. & PLASTERK, R. H. 2005. MicroRNA expression in zebrafish embryonic development. *Science*, 309, 310-1.

WIENHOLDS, E., KOUDIJS, M. J., VAN EEDEN, F. J., CUPPEN, E. & PLASTERK, R. H. 2003. The microRNA-producing enzyme Dicer1 is essential for zebrafish development. *Nat Genet*, 35, 217-8.

WILSON, P. A., LAGNA, G., SUZUKI, A. & HEMMATI-BRIVANLOU, A. 1997. Concentration-dependent patterning of the *Xenopus* ectoderm by BMP4 and its signal transducer Smad1. *Development*, 124, 3177-84.

WITKOS, T. M., KOSCIANSKA, E. & KRZYZOSIAK, W. J. 2011. Practical Aspects of microRNA Target Prediction. *Curr Mol Med*, 11, 93-109.

WOLTERING, J. M. & DURSTON, A. J. 2008. MiR-10 represses HoxB1a and HoxB3a in zebrafish. *PLoS One*, 3, e1396.

WONG, N. & WANG, X. 2015. miRDB: an online resource for microRNA target prediction and functional annotations. *Nucleic Acids Res*, 43, D146-52.

XU, N., PAPAGIANNAKOPOULOS, T., PAN, G., THOMSON, J. A. & KOSIK, K. S. 2009. MicroRNA-145 regulates OCT4, SOX2, and KLF4 and represses pluripotency in human embryonic stem cells. *Cell*, 137, 647-58.

- YAN, B., NEILSON, K. M. & MOODY, S. A.** 2009. foxD5 plays a critical upstream role in regulating neural ectodermal fate and the onset of neural differentiation. *Dev Biol*, 329, 80-95.
- YANG, N., NG, Y. H., PANG, Z. P., SUDHOF, T. C. & WERNIG, M.** 2011. Induced neuronal cells: how to make and define a neuron. *Cell Stem Cell*, 9, 517-25.
- YANG, S. L., YANG, M., HERRLINGER, S., LIANG, C., LAI, F. & CHEN, J. F.** 2015. MiR-302/367 regulate neural progenitor proliferation, differentiation timing, and survival in neurulation. *Dev Biol*, 408, 140-50.
- YARDLEY, N. & GARCIA-CASTRO, M. I.** 2012. FGF signaling transforms non-neural ectoderm into neural crest. *Dev Biol*, 372, 166-77.
- YEKTA, S., SHIH, I. H. & BARTEL, D. P.** 2004. MicroRNA-directed cleavage of HOXB8 mRNA. *Science*, 304, 594-6.
- YIN, J. Q., ZHAO, R. C. & MORRIS, K. V.** 2008. Profiling microRNA expression with microarrays. *Trends Biotechnol*, 26, 70-6.
- YOON, K. & GAIANO, N.** 2005. Notch signaling in the mammalian central nervous system: insights from mouse mutants. *Nat Neurosci*, 8, 709-15.
- YOUNG, J. J., KJOLBY, R. A., KONG, N. R., MONICA, S. D. & HARLAND, R. M.** 2014. Spalt-like 4 promotes posterior neural fates via repression of pou5f3 family members in *Xenopus*. *Development*, 141, 1683-93.
- ZEHIR, A., HUA, L. L., MASKA, E. L., MORIKAWA, Y. & CSERJESI, P.** 2010. Dicer is required for survival of differentiating neural crest cells. *Developmental biology*, 340, 459-467.
- ZHANG, J., ZHANG, H., LIU, J., TU, X., ZANG, Y., ZHU, J., CHEN, J., DONG, L. & ZHANG, J.** 2012a. miR-30 inhibits TGF-beta1-induced epithelial-to-mesenchymal transition in hepatocyte by targeting Snail1. *Biochem Biophys Res Commun*, 417, 1100-5.
- ZHANG, W., DUAN, S., LI, Y., XU, X., QU, J., ZHANG, W. & LIU, G. H.** 2012b. Converted neural cells: induced to a cure? *Protein Cell*, 3, 91-7.
- ZHAO, Y., RANSOM, J. F., LI, A., VEDANTHAM, V., VON DREHLE, M., MUTH, A. N., TSUCHIHASHI, T., MCMANUS, M. T., SCHWARTZ, R. J. & SRIVASTAVA, D.** 2007. Dysregulation of cardiogenesis, cardiac conduction, and cell cycle in mice lacking miRNA-1-2. *Cell*, 129, 303-17.
- ZHOU, Z., QIN, J., TANG, J., LI, B., GENG, Q., JIANG, W., WU, W., REHAN, V., TANG, W., XU, X. & XIA, Y.** 2013. Down-regulation of MeCP2 in Hirschsprung's disease. *J Pediatr Surg*, 48, 2099-105.
- ZHUANG, F., FUCHS, R. T., SUN, Z., ZHENG, Y. & ROBB, G. B.** 2012a. Structural bias in T4 RNA ligase-mediated 3'-adapter ligation. *Nucleic Acids Res*, 40, e54.
- ZHUANG, G., WU, X., JIANG, Z., KASMAN, I., YAO, J., GUAN, Y., OEH, J.,**

**MODRUSAN, Z., BAIS, C., SAMPATH, D. & FERRARA, N.** 2012b. Tumour-secreted miR-9 promotes endothelial cell migration and angiogenesis by activating the JAK-STAT pathway. *EMBO J*, 31, 3513-23.

## Appendices

As some documents are very large or are videos they have been placed on an 'electronic appendix'. To access this please use the following link:

<https://drive.google.com/open?id=0B8k6eLrrbmlGNlg4aHoydW9ZSk0>

## Chapter 2 - Materials and methods:

### Appendix 1: plasmids used to make RNA probes

Clone name	Antisense RE	Antisense polymerase	Source
<b>Sox2</b>	EcoR1	T7	Prof Yoshiki Sasai
<b>Snail2</b>	Bgl2	Sp6	Dr Michael Sargent
<b>Sox10</b>	EcoR1	T3	Prof Jean-Pierre Saint-Jeannet
<b>Pax6</b>	Xbal		
<b>FoxD3</b>	BamH1	T7	Prof Yoshiki Sasai
<b>Zic1</b>	EcoR1	T3	Dr Jung Aruga
<b>Zic3</b>	BamH1	T3	Dr Jung Aruga
<b>Twist</b>	BamH1		Michael G. Sargent
<b>Hairy1</b>	ASP718		Michael G. Sargent
<b>Snail1</b>	Clal	SP6	Prof Jean-Pierre Saint-Jeannet
<b>Hairy2</b>	BamH1	T7	Michael G. Sargent
<b>MSX1</b>	EcoR1	T7	Jean Illes and Harv Isaacs
<b>MSX2</b>	Sal1	T7	Michael G. Sargent

<b>DLX5</b>	Xbal	T3	Thomas Sargent
<b>PAX3</b>	BglII	SP6	Prof Anne-Helene-Monsoro
<b>ENG2</b>	Xbal	T3	Nancy Papalopoulos
<b>N-tubulin</b>	NcoI	T3	Nancy Papalopoulos
<b>ELRC</b>	Hind3	T7	Nancy Papalopoulos

### Appendix 2: miRNA primers used for smallRNA sequencing validation

Name	Primer
Xtr-miR-196a	UAGGUAGUUUCAUGUUGUUGG
Ipu-miR-219a	AGAAUUGUGCCUGGACAUCUGU
Xtr-miR-302	UAAGUGCUCCAAUGUUUUAGUGG
Dps-miR-219	UGAUUGUCCAAACGCAAUUCUUG

### Appendix 3: mRNA primers used for qRT-PCR prior to RNA sequencing

gene	Forward primer	Reverse primer
Snail2	CACACGTTACCCTGCGTATG	TCTGTCTGCGAATGCTCTGT
ODC	CATGGCATTCTCCCTGAAGT	TGGTCCCAAGGCTAAAGTTG
Pax3	CAAGCTCACAGAGGCGCGAGT	AGCTGGCATAGCTGCAGGAGG
MyoD	TACTGACAGCCCCAATGA	TGCAGAGGAGAACAGGGACT
EF1	ACACTGCTCACATTGCTTGC	AGAAGCTCTCCACGCACATT
SOX10	CTATTACTGACACACGACGGAGC	ACCTCTCATCCTCTGAATCCTGC
XHE	CATGTCTAATGGCGGTTGTG	TGCTGGATGATCCCATATT
Six1	TGGTTCAAGAACAGGAGGCA	CGACTTCCCTCCGTCTAGGG

#### **Appendix 4: Number of reads and percentage of mapped reads following RNA sequencing**

**Document number 1 on electronic appendix:** An excel sheet containing information regarding total number of reads, total number of mapped reads and percentage of mapped reads for each sample following RNA sequencing of miR-219 and miR-196a KD NC tissue

## **Chapter 3 – Identification of miRNAs in neural crest cells**

#### **Appendix 5: Structure of novel miRNA hairpins.:**

**Document number 2 of electronic appendix:** Novel miRNAs were detected using the programs mircat (Stocks et al., 2012) and mirdeep2 (Friedlander et al., 2008) and were evaluated for the likelihood of hairpin secondary structure using RNAFold (Gruber et al., 2015).

## **Chapter 4 – functional analysis of candidate miRNAs**

#### **Appendix 6: miR-429 KD embryos do not respond during the ‘poke and stroke’ assay.**

**Document number 3 of the electronic appendix:** The first embryo ‘poked’ is a control non-injected embryo. This embryo responds immediately and swims off. This is compared to miR-429 KD embryo (injected with 60ng of miR-429 MO into a one-cell staged embryo) which does not respond at all to being ‘poked’.

## Chapter 5: Downstream target analysis of miRNAs miR-196a and miR-219

TARGET_GENE	DIANA	MIRANDA	MIRBRIDGE	PICTAR	PITA	RNA22	TARGETSCAN	TOTAL_HIT
PRDM16	V	V	V	V	V	V	V	7
BCL11A	V	V	V		V	V	V	6
CD164	V	V	V	V	V		V	6
CPEB3	V	V		V	V	V	V	6
DCP2	V	V	V	V	V		V	6
DDAH1	V	V	V	V	V		V	6
EGR3	V	V	V	V	V		V	6
ERG	V	V	V	V	V		V	6
ESR1	V	V	V	V	V		V	6
EYA1	V	V	V	V	V		V	6
FAM120C	V	V		V	V	V	V	6
FOXJ3	V	V		V	V	V	V	6
FZD4	V	V	V	V	V		V	6
INPP5J	V	V	V	V	V		V	6
ISL1	V	V	V	V	V		V	6
KBTBD8	V	V	V	V	V		V	6
LPP	V	V	V	V	V		V	6
MEF2D	V	V	V	V	V		V	6
OCRL	V	V	V	V	V		V	6
PDE4D	V	V	V	V	V		V	6
PDGFRA	V	V	V	V	V		V	6
PPARGC1A	V	V	V	V	V		V	6
RORB	V	V	V	V	V		V	6
SHC1	V	V	V	V	V		V	6
SNRK	V	V	V	V	V		V	6
SOX6	V	V	V	V	V		V	6
T	V	V	V	V	V		V	6
TRHDE	V	V	V	V	V		V	6
TSC22D2	V	V	V	V	V		V	6
UBE2N	V	V	V	V	V		V	6
ZNF238	V	V	V	V	V		V	6

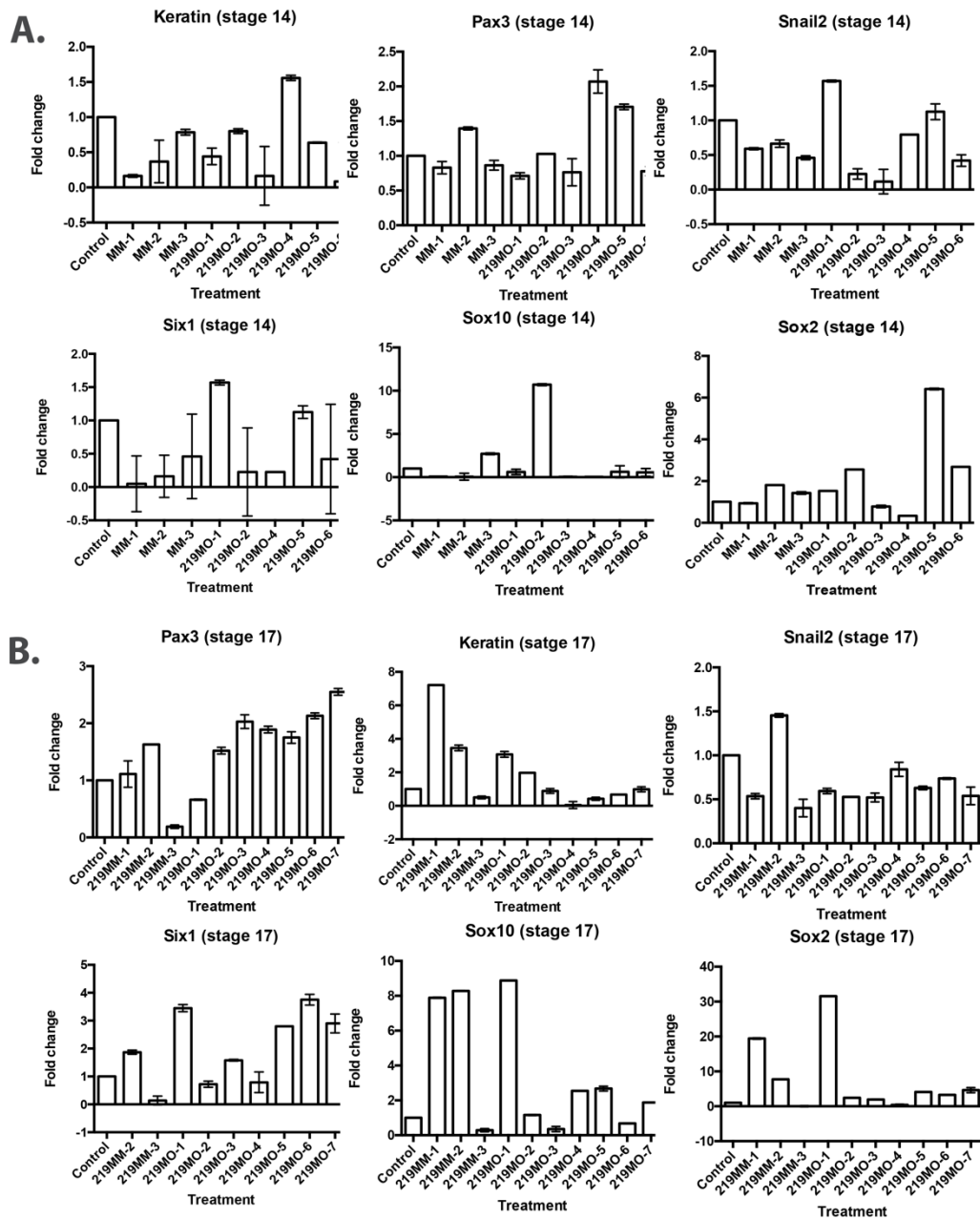
### Appendix 7: Top predicted targets of miR-219 using miR-system

MiR-system was used to find targets of miR-219. Analysis was completed using human genes and any interesting targets were checked for conservation by the author. Only genes predicted to be targets by at least 6 of the algorithm sites are displayed in the table (last column).

TARGET_GENE	DIANA	MIRANDA	MIRBRIDGE	PICTAR	PITA	RNA22	TARGETSCAN	TOTAL_HIT
HOXC8	V	V	V	V	V	V	V	8
GATA6	V	V	V	V	V	V	V	7
HOXB6	V	V	V	V	V	V	V	7
BACH1	V	V	V	V	V		V	6
BCAT1	V	V	V		V	V	V	6
CALM3	V	V	V	V	V		V	6
CBFA2T3	V	V	V	V	V		V	6
CCDC47	V	V		V	V	V	V	6
CCNJ	V	V	V	V	V		V	6
CDV3	V	V	V	V	V		V	6
CDYL	V	V	V	V	V		V	6
COL1A2	V	V	V	V	V		V	6
COL3A1	V	V	V	V	V		V	6
CPM	V		V	V	V	V	V	6
DDX19B	V	V	V	V	V		V	6
EPC2	V	V	V	V	V		V	6
EPS15	V	V	V	V	V		V	6
GAN	V	V		V	V	V	V	6
HOXB7	V	V	V	V	V		V	6
IGF2BP3	V	V		V	V	V	V	6
LRP1B	V	V	V	V	V		V	6
MECP2	V	V	V	V	V		V	6
NRAS	V	V	V	V	V		V	6
NRK	V	V		V	V	V	V	6
RANBP10	V	V		V	V	V	V	6
RIOK3	V	V		V	V	V	V	6
SLC9A6	V	V	V	V	V		V	6
SMARCC1	V	V	V	V	V		V	6
UHRF2	V	V	V	V	V		V	6
ZMYND11	V	V	V	V	V		V	6

### Appendix 8: Top predicted targets of miR-196a using miR-system.

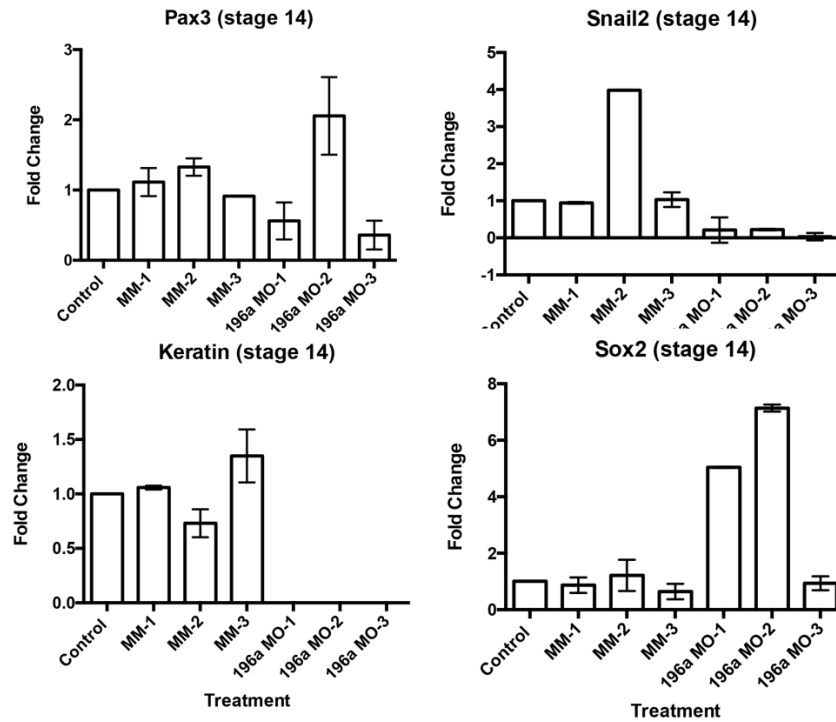
MiR-system was used to find targets of miR-196a. Analysis was completed using human genes and any interesting targets were checked for conservation by the author. . Only genes predicted to be targets by at least 6 of the algorithm sites are displayed in the table (last column).



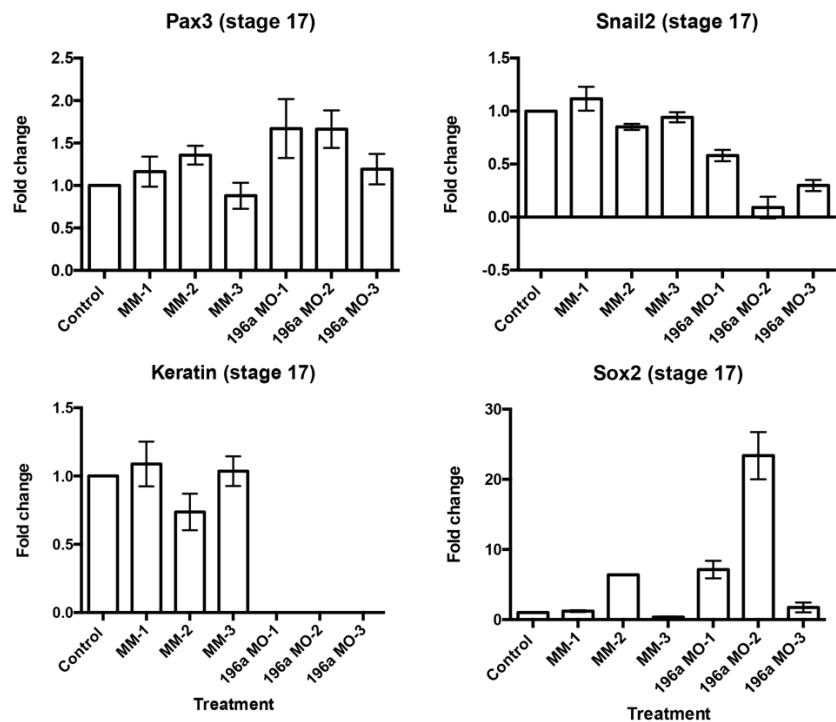
## Appendix 9: Expression profile of various genes detected by qRT-PCR in dissected samples following KD of miR-219.

The aim of this experiment was to use qRT-PCR to select the best samples to send to sequencing (those with a clear KD of neural crest genes). Embryos were injected into one dorsal blastomere of a four-cell embryo with 60ng of one of two MOs (miR-219 MO or miR-219MM). GFP was used as a tracer. Once at the appropriate stage (14 or 17) the neural crest region was dissected, RNA extracted and qRT-PCR was run to check gene expression. A non-injected control was used as a reference. *ODC* was used to normalise gene expression. Genes that were investigated include the NPB markers (*Six1* and *Pax3*), the NC markers (*Snail2* and *Sox10*), the neural marker (*Sox2*) and the ectodermal markers (*Keratin*) (A) Expression of various genes at stage 14 dissections. Focusing mainly on the expression levels of *Snail2* and *Sox2* the samples chosen to be sent for sequencing were 2, 3, 5 and 6. Four samples were chosen (instead of three) so one could be excluded from analysis if it did not cluster with the other replicates. (B) Expression of various genes at stage 17 dissections. As the gene expression looked abnormal (not biologically reproducible) and no KD of the NC marker *Snail2* was seen no samples were sent for sequencing

A.

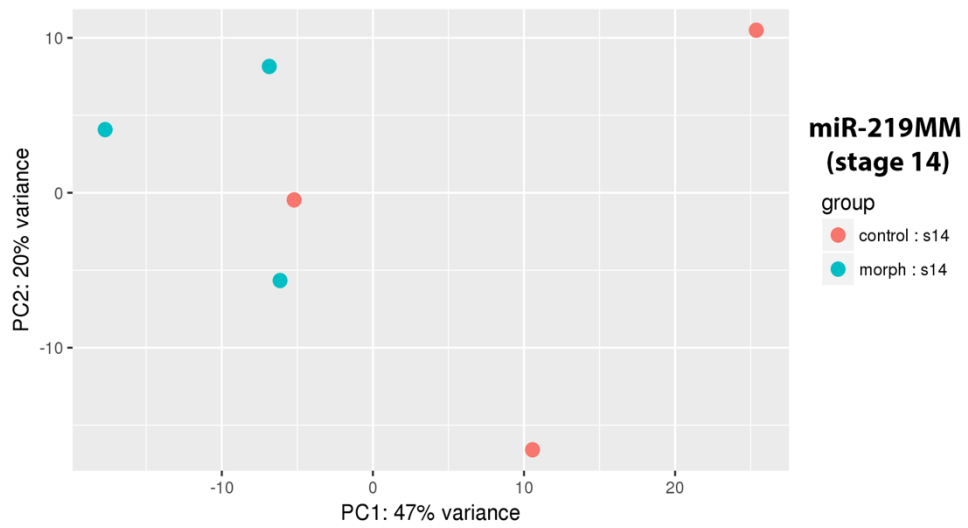
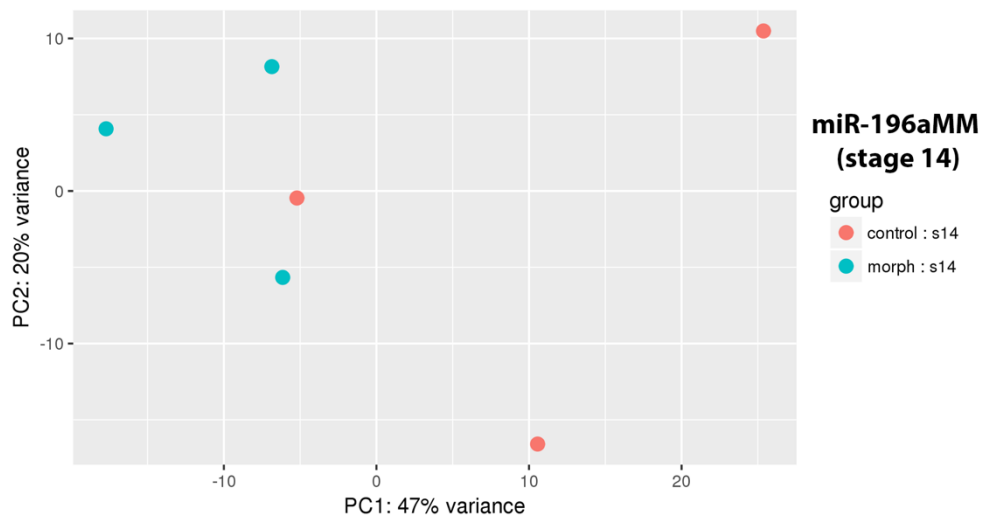
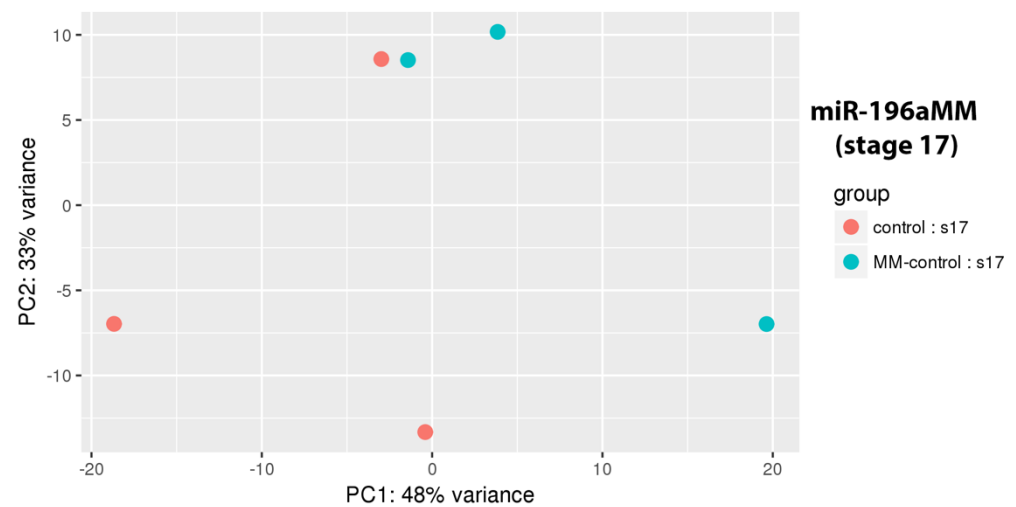


B.



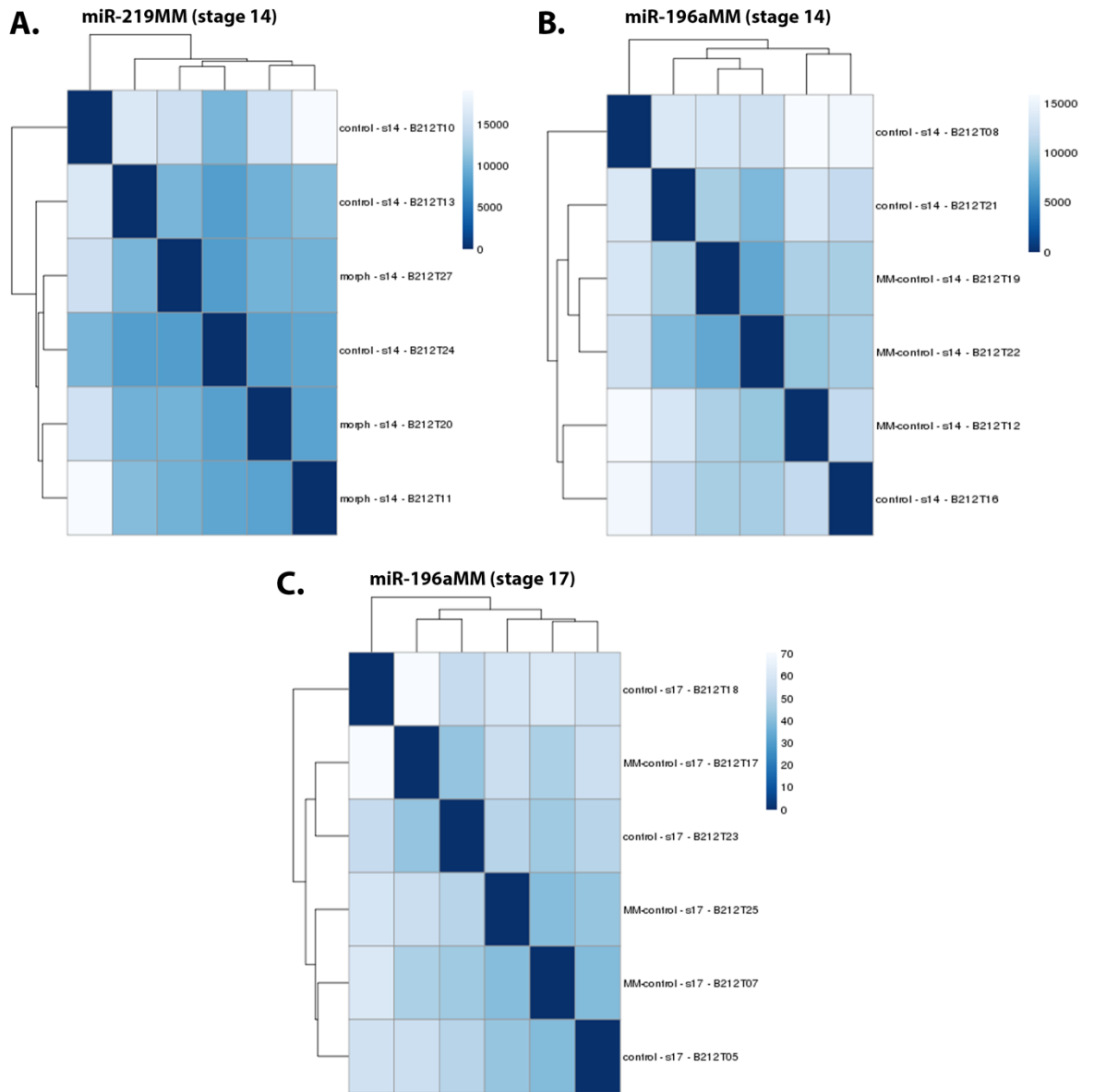
### Appendix 10: Expression profile of various genes detected by qRT-PCR in dissected samples following KD of miR-196a.

The aim of this experiment was to use qRT-PCR to select the best samples to send to sequencing (those with a clear KD of neural crest genes). As the first three samples tested all had the appropriate gene expression, no further samples were tested (unlike for miR-219). Therefore, all the samples displayed here were sent for sequencing. Embryos were injected into one dorsal blastomere of a four-cell embryo with 60ng of one of two MOs (miR-196a MO or miR-196aMM). GFP was used as a tracer. Once at the appropriate stage (14 or 17) the neural crest region was dissected, RNA extracted and qRT-PCR was ran to check gene expression. A non-injected control was used as a reference. *ODC* was used to normalise gene expression. Genes that were investigated include the NPB marker (*Pax3*), the NC marker (*Snail2*), the neural marker (*Sox2*) and the ectodermal markers (*Keratin*) (A) Expression of various genes at stage 14 dissections (B) Expression of various genes at stage 17 dissections.

**A.****B.****C.**

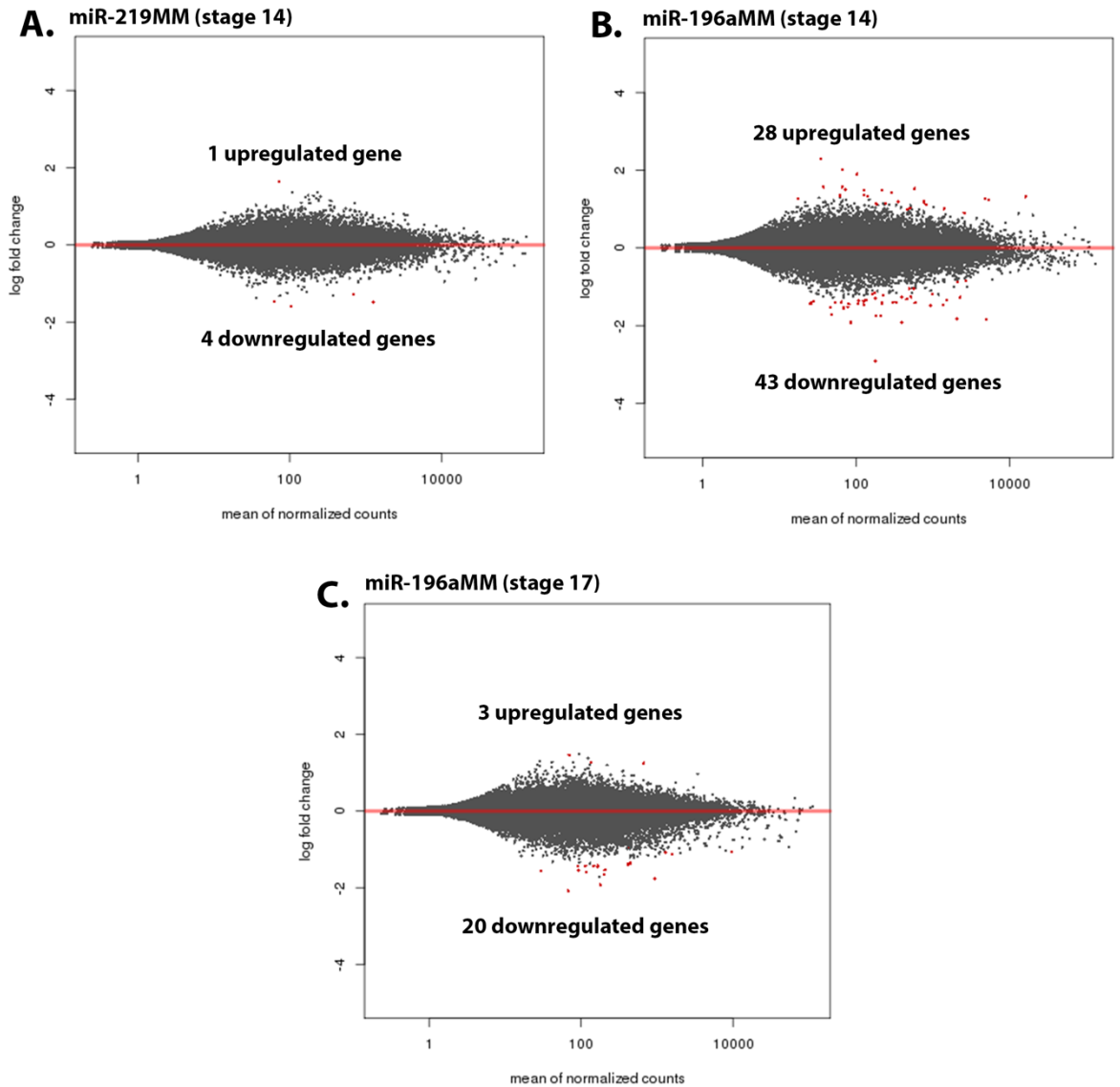
### Appendix 11: PCA plot showing clustering of replicates between MO injected embryos and MM control.

PCA plots of MM controls (blue dots) vs non-injected controls (red dots) demonstrated that for **(A)** miR219MM (stage 14), **(B)** miR-196aMM (stage 14) and **(C)** miR-196aMM (stage 17) there is no clustering between the two treatment types and they are not distinct from one another.



**Appendix 12: Sample distance heat map showing clustering of replicates between MM control and control.**

Sample distance heat maps of MM controls vs non-injected controls demonstrated that for (A) miR219MM (stage 14), (B) miR-196aMM (stage 14) and (C) miR-196aMM (stage 17) the there is no clustering between the two treatment types.



### Appendix 13: An MA-plot of gene changes between MM control and non-injected controls.

Each gene is represented with a dot. Genes with an adjusted p value below a threshold (here 0.1, the default) are shown in red. MA plot of MM controls vs non-injected controls demonstrated that for (A) miR219MM (stage 14), (B) miR-196aMM (stage 14) and (C) miR-196aMM (stage 17) there are very few genes which deviate from the midline meaning there are not many gene changes between the two treatments.

**Appendix 14: Differential expression analysis results following RNA sequencing of MO vs MM samples**

**Document number 3 on electronic appendix:** The excel document has three sheets clearly labelled, one for each of the treatment types. The relevant data used by the author for analysis includes column C (log2fold change) column G (Padj) and column M (BLAST results). Genes were sorted by Padj and those genes with a Padj<0.05 were sorted by log2fold change.

## **Publications**

Ahmed A\*, **Ward NJ\***, Moxon S, Lopez-Gomollon S, Viaut C, et al. (2015) A Database of microRNA Expression Patterns in *Xenopus laevis*. PLOS ONE 10(10): e0138313.

Victoria L. Hatch, Marta Marin-Barba, Simon Moxon, Christopher T. Ford, **Nicole J. Ward**, Matthew L. Tomlinson, Ines Desanlis, Adam E. Hendry, Saartje Hontelez, Ila van Kruijsbergen, Gert Jan C. Veenstra, Andrea E. Münsterberg and Grant N. Wheeler (2016). The Positive Transcriptional Elongation Factor (P-TEFb) is required for Neural Crest Specification. *Developmental Biology*, 416: 361-372